

TEMPERATURE EFFECT ON CALCIUM ALUMINATE CEMENT BASED
COMPOSITE BINDERS

A THESIS SUBMITTED TO
THE GRADUATE SCHOOL OF NATURAL AND APPLIED SCIENCES
OF
MIDDLE EAST TECHNICAL UNIVERSITY

BY

ÖNDER KIRCA

IN PARTIAL FULFILLMENT OF THE REQUIREMENTS
FOR
THE DEGREE OF DOCTOR OF PHILOSOPHY
IN
CIVIL ENGINEERING

JULY 2006

Approval of the Graduate School of Natural and Applied Sciences

Prof. Dr. Canan Özgen
Director

I certify that this thesis satisfies all the requirements as a thesis for the degree of Doctor of Philosophy.

Prof. Dr. Erdal Çokca
Head of Department

This is to certify that we have read this thesis and that in our opinion it is fully adequate, in scope and quality, as a thesis for the degree of Doctor of Philosophy.

Prof. Dr. Mustafa Tokyay
Supervisor

Examining Committee Members

Prof. Dr. Turhan Y. Erdoğan (METU, CE) _____

Prof. Dr. Mustafa Tokyay (METU, CE) _____

Prof. Dr. Abdullah Öztürk (METU, METE) _____

Prof. Dr. Kambiz Ramyar (Ege Uni., CE) _____

Assoc. Prof. Dr. İ. Özgür Yaman (METU, CE) _____

I hereby declare that all information in this document has been obtained and presented in accordance with academic rules and ethical conduct. I also declare that, as required by these rules and conduct, I have fully cited and referenced all material and results that are not original to this work.

Önder Kırca

ABSTRACT

TEMPERATURE EFFECT ON CALCIUM ALUMINATE CEMENT BASED COMPOSITE BINDERS

Kırca, Önder

Ph.D., Department of Civil Engineering

Supervisor: Prof. Dr. Mustafa Tokyay

July 2006, 209 pages

In calcium aluminate cement (CAC) systems the hydration process is different than portland cement (PC) systems. The hydration products of CAC are subjected to conversion depending on temperature, moisture, water-cement ratio, cement content, etc. Consequently, strength of CAC system can be seriously reduced. However, presence of other inorganic binders or additives may alter the hydration process and improve various properties of CAC based composites.

The objective of this study is to investigate the temperature effect on the behaviour of CAC based composite binders. Throughout this research, several combinations of CAC-PC, CAC-gypsum, CAC-lime, CAC-ground granulated blast furnace slag (CAC-GGBFS) were studied. These CAC based composite binders were subjected to seven different curing regimes

and their strength developments were investigated up to 210 days. In addition, the mechanism of strength development was examined by XRD analyses performed at 28 and 210 days. Finally, some empirical relationships between strength-time-curing temperatures were formulated.

Experimental results revealed that the increase in ambient temperature resulted in an increase in the rate of conversion, thereby causing drastic strength reduction, particularly in pure CAC mix. It has been observed that inclusion of small amount of PC, lime, and gypsum in CAC did not induce conversion-free CAC binary systems, rather they resulted in faster conversion by enabling rapid formation of stable C_3AH_6 instead of metastable, high strength inducing CAH_{10} and C_2AH_8 . On the other hand, in CAC-GGBFS mixes, the formation of stable straelingite (C_2ASH_8) instead of calcium aluminate hydrates hindered the conversion reactions. Therefore, CAC-GGBFS mixes, where GGBFS ratio was over 40%, did not exhibit strength loss due to conversion reactions that occurred in pure CAC systems.

Keywords: Calcium Aluminate Cement, CAC Based Composite Binder, Temperature Effect, Conversion, Ground Granulated Blast Furnace Slag.

ÖZ

SICAKLIĞIN KALSİYUM ALUMİNATLI ÇİMENTO ESASLI KOMPOZİT BAĞLAYICILAR ÜZERİNE ETKİSİ

Kırca, Önder

Doktora, İnşaat Mühendisliği Bölümü

Tez Yöneticisi: Prof. Dr. Mustafa Tokyay

Temmuz 2006, 209 sayfa

Kalsiyum alüminatlı çimento (KAÇ) sistemlerinde hidrasyon, portland çimentosununkinden (PÇ) çok farklıdır. KAÇ'nin hidrasyon ürünleri; sıcaklığa, rutubete, su-çimento oranına, çimento miktarına, vb. bağlı olarak dönüşüm reaksiyonlarına maruz kalmaktadır. Sonuç olarak, KAÇ sistemlerinin dayanımı düşmektedir. Fakat başka inorganik bağlayıcıların veya katkıların bulunması, hidrasyon ürünlerini değiştirebilmekte ve KAÇ esaslı kompozitlerin çeşitli özelliklerini iyileştirebilmektedir.

Araştırmanın amacı, sıcaklığın KAÇ esaslı kompozit bağlayıcıların davranışı üzerindeki etkisinin araştırılmasıdır. Araştırma boyunca, KAÇ-PÇ, KAÇ-alçı, KAÇ-kireç, KAÇ-granüle yüksek fırın çürüğü (KAÇ-GYFC) gibi kompozit sistemlerin değişik kombinasyonları incelenmiştir. Bu KAÇ esaslı kompozit bağlayıcılar, yedi farklı kür sıcaklığına maruz bırakılmış ve

210 güne kadar olan dayanım gelişimleri incelenmiştir. Ayrıca; 28. ve 210. günde yapılan XRD analizleriyle dayanım gelişme mekanizması araştırılmıştır. Son olarak; dayanım-zaman-kür sıcaklığı arasında, bazı ampirik ilişkiler kurgulanmıştır.

Sonuçlar; özellikle tekil KAÇ karışımlarında, dış ortam sıcaklığının artmasının, daha hızlı dönüşüme ve buna bağlı olarak önemli dayanım düşüşüne neden olduğunu göstermektedir. KAÇ'ye PÇ, kireç ve alçının az miktarda katılması ise, dönüşüm göstermeyen KAÇ sistemlerinin oluşmasına neden olmamaktadır. Aksine bunlar; yüksek dayanım veren fakat kararsız olan CAH_{10} ve C_2AH_8 yerine, kararlı olan C_3AH_6 'nın daha hızlı oluşmasını sağlayarak, dönüşümün daha hızlı gerçekleşmesine neden olmaktadır. Öte yandan, KAÇ-GYFC karışımlarında, kalsiyum aluminat hidratların yerine kararlı straelingite (C_2ASH_8) oluşumu, dönüşüm reaksiyonlarını engellemektedir. Bu nedenle GYFC oranının %40'ın üzerinde olduğu KAÇ-GYFC karışımları, tekil KAÇ sistemlerinin dönüşüm reaksiyonları dolayısıyla gösterdiği dayanım düşüşünü göstermemektedir.

Anahtar Kelimeler: Kalsiyum Aluminatlı Çimento, KAÇ Esaslı Kompozit Bağlayıcılar, Sıcaklık Etkisi, Dönüşüm, Granüle Yüksek Fırın Cürufu.

To My Daughter

And
To My Wife

ACKNOWLEDGEMENTS

I would like to express my sincere gratitude to my advisor Prof. Dr. Mustafa Tokyay not only for his continuous supervision and suggestions throughout this investigation, but also for his support and encouragement, which I needed to fulfil the requirements of this work faraway from university ambience.

I also wish to thank Assoc. Prof. Dr. İ. Özgür Yaman, and Prof. Dr. Abdullah Öztürk for their valuable comments and contributions through this investigation.

I am also thankful to Prof. Dr. Turhan Y. Erdoğan, and to all my teachers and professors, through whom I am aware of the scientific methodology.

I also want to sincerely acknowledge my company, ÇimSA Cement Production and Trade Company, and its managers, without whose support I could not accomplish such a long-lasting and sophisticated investigation. Special thanks go to my general manager Mr. Yılmaz Külcü, Mr. Mehmet Şahin, Mrs. Müge Yanç, and Mr. Levent Öncel.

The devoted assistance of my work friends Mr. A. Bahadır Öztürk, Mr. Erol Güldoğan, and Mr. Hakkı Dal is also profoundly appreciated.

Special, sincere thanks go to my friend Dr. Tahir Kemal Erdem not only for his inexhaustible support through this research, but also for his endless friendship throughout my life.

Finally, I do not know how to express my gratitude to my parents, who devoted their life for our happiness, and to my daughter and my wife, who are my sole wealth in my life. Thanks God for their existence on me.

TABLE OF CONTENTS

PLAGIARISM.....	iii
ABSTRACT.....	iv
ÖZ.....	vi
DEDICATION.....	viii
ACKNOWLEDGEMENTS.....	ix
TABLE OF CONTENTS.....	xi
LIST OF TABLES.....	xiv
LIST OF FIGURES.....	xviii

CHAPTERS

1. INTRODUCTION.....	1
1.1 General.....	1
1.2 Object and Scope.....	3
2. THEORETICAL CONSIDERATIONS.....	5
2.1 General.....	5
2.2 Physical and Mechanical Properties of CAC.....	8
2.3 Chemical Composition of CAC.....	10
2.4 Mineralogical Composition of CAC.....	12
2.5 Hydration and Conversion of CAC.....	13
2.5.1 Hydration Mechanism of CAC.....	14
2.5.2 Conversion Mechanism of CAC.....	16
2.6 Factors Affecting Conversion.....	19
2.6.1 Temperature Effect.....	19
2.6.2 Effect of Water-Cement (w/c) Ratio and Humidity.....	23
2.7 CAC Based Composite Binders.....	24

2.7.1	CAC-PC Combination.....	25
2.7.2	CAC-Gypsum Combination.....	26
2.7.3	CAC-Lime Combination.....	27
2.7.4	CAC-GGBFS Combination.....	27
3.	REVIEW OF RESEARCH ON HYDRATION, CONVERSION AND STRENGTH DEVELOPMENT OF CALCIUM ALUMINATE CEMENT BASED COMPOSITE BINDERS.....	30
3.1	General.....	30
3.2	Previous Studies on Conversion of Pure CAC and on Factors Affecting Conversion.....	31
3.2.1	Effects of Temperature on Hydration and Conversion.....	33
3.2.2	Effects of Temperature on Strength.....	38
3.2.3	Effects of Temperature and Water-Cement Ratio on Strength.....	40
3.3	Previous Studies on CAC-PC Combinations.....	43
3.4	Previous Studies on CAC-Gypsum Combinations.....	47
3.5	Previous Studies on CAC-Lime Combinations.....	48
3.6	Previous Studies on CAC-GGBFS Combinations.....	48
4.	EXPERIMENTAL STUDY.....	54
4.1	Introduction.....	54
4.2	Materials.....	55
4.3	Types of CAC Based Composite Binders.....	61
4.4	Experimental Program.....	62
5.	TEST RESULTS AND DISCUSSION.....	74
5.1	Determination of Physical Properties of CAC Based Composite Binders.....	74
5.1.1	Setting Time.....	74
5.1.2	Heat of Hydration.....	79
5.2	Effect of Temperature on Strength Development of CAC Based Composite Binders.....	84

5.2.1	Effect of Temperature on Compressive Strength Development of CAC-PC Mixes.....	92
5.2.2	Effect of Temperature on Compressive Strength Development of CAC-Gypsum Mixes.....	116
5.2.3	Effect of Temperature on Compressive Strength Development of CAC-Lime.....	126
5.2.4	Effect of Temperature on Compressive Strength Development of CAC-GGBFS Mixes.....	135
5.3	Statistical Assessment of Temperature Effect on Strength Development of CAC Based Composite Binders.....	151
5.3.1	Statistical Assessment for CAC-PC Mixes.....	153
5.3.2	Statistical Assessment for CAC-Gypsum Mixes.....	159
5.3.3	Statistical Assessment for CAC-Lime Mixes.....	161
5.3.4	Statistical Assessment for CAC-GGBFS Mixes.....	162
6.	CONCLUSIONS.....	168
7.	RECOMMENDATIONS.....	172
	REFERENCES.....	174
	APPENDICES.....	183
	APPENDIX A: Statistical Analysis of CAC-PC Mixes.....	183
	APPENDIX B: Statistical Analysis of CAC-Gypsum Mixes.....	193
	APPENDIX C: Statistical Analysis of CAC-Lime Mixes.....	195
	APPENDIX D: Statistical Analysis of CAC-GGBFS Mixes.....	197
	CURRICULUM VITAE.....	207

LIST OF TABLES

Table 2.1	Types of Calcium Aluminate Cement According to TS 6271.....	6
Table 2.2	Comparison of the Heats of Hydration of Different Cements.....	9
Table 2.3	Chemical Composition of CAC.....	11
Table 2.4	Physical Properties of Calcium Aluminate Hydrates.....	16
Table 2.5	The Rate of Conversion of CAH_{10} and C_2AH_8 to C_3AH_6 Depending on Temperature.....	22
Table 2.6	Effects of Temperature and Humidity on Conversion.....	23
Table 3.1	Types of Hydrates at Different Temperatures.....	36
Table 3.2	Effects of Curing Temperature on Strength of CAC.....	39
Table 3.3	Summary of Compounds Identified by XRD Analysis of CAC-PC Combinations at Different Ages.....	46
Table 3.4	Phases Present in CAC-GGBFS Blends.....	50
Table 3.5	Some Properties of CAC-GGBFS Blends in Different Mix Ratios.....	52
Table 4.1	Chemical Compositions of Binders in Percentage.....	56
Table 4.2	Fineness of Binders.....	56
Table 4.3	Compressive and Flexural Strengths of CAC and PC.....	57
Table 4.4	Curing Regimes Applied.....	63
Table 4.5	Ages and Types of Tests Performed on Samples Cured Continuously at 20°C.....	67

Table 4.6	Ages and Types of Tests Performed on Samples Cured Continuously at 30°C.....	68
Table 4.7	Ages and Types of Tests Performed on Samples Cured 28 days at 20°C then at 30°C.....	69
Table 4.8	Ages and Types of Tests Performed on Samples Cured Continuously at 40°C.....	70
Table 4.9	Ages and Types of Tests Performed on Samples Cured 28 days at 20°C then at 40°C.....	71
Table 4.10	Ages and Types of Tests Performed on Samples Cured Continuously at 50°C.....	72
Table 4.11	Ages and Types of Tests Performed on Samples Cured 28 days at 20°C then at 50°C.....	73
Table 5.1	Setting Times of CAC Based Composite Binders.....	75
Table 5.2	Heat of Hydration of CAC Based Composite Binders.....	80
Table 5.3	Compressive Strengths of CAC Based Composite Binders Cured Continuously at 20°C.....	85
Table 5.4	Compressive Strengths of CAC Based Composite Binders Cured Continuously at 30°C.....	86
Table 5.5	Compressive Strengths of CAC Based Composite Binders Cured 28 days at 20°C then at 30°C.....	87
Table 5.6	Compressive Strengths of CAC Based Composite Binders Cured Continuously at 40°C.....	88
Table 5.7	Compressive Strengths of CAC Based Composite Binders Cured 28 days at 20°C then at 40°C.....	89
Table 5.8	Compressive Strengths of CAC Based Composite Binders Cured Continuously at 50°C.....	90
Table 5.9	Compressive Strengths of CAC Based Composite Binders Cured 28 days at 20°C then at 50°C.....	91
Table 5.10	The Designations Used for Various Phases in XRD Analysis.....	95

Table 5.11	XRD Patterns of Most Common Phases.....	100
Table 5.12	Area under the Peak of the Phases Observed in IP100 at Different Curing Temperatures.....	102
Table 5.13	Area under the Peak of the Phases Observed in IP75 at Different Curing Temperatures.....	103
Table 5.14	Area under the Peak of the Phases Observed in IP25 at Different Curing Temperatures.....	104
Table 5.15	Area under the Peak of the Phases Observed in IP0 at Different Curing Temperatures.....	105
Table 5.16	Phases Formed in the CAC-PC Mixes Depending on Time and Curing Temperatures.....	106
Table 5.17	Area under the Peak of the Phases Observed in IA96 at Different Curing Temperatures.....	121
Table 5.18	Phases Formed in IA96 Depending on Time and Curing Temperatures.....	122
Table 5.19	Area under the Peak of the Phases Observed in IK98 at Different Curing Temperatures.....	131
Table 5.20	Phases Formed in IK98 Depending on Time and Curing Temperatures.....	132
Table 5.21	Area under the Peak of the Phases Observed in IC80 at Different Curing Temperatures.....	142
Table 5.22	Area under the Peak of the Phases Observed in IC60 at Different Curing Temperatures.....	143
Table 5.23	Area under the Peak of the Phases Observed in IC40 at Different Curing Temperatures.....	144
Table 5.24	Phases Formed in the CAC-GGBFS Mixes Depending on Time and Curing Temperatures.....	145
Table 5.25	Variables and Their Low and High-Settings.....	153
Table 5.26	Regression Coefficients and p-Values of Variables in CAC-PC System According to Response Surface Regression Analysis.....	154

Table 5.27	Analysis of Variance for Regression between Compressive Strength and Variables of CAC-PC Mixes.....	155
Table 5.28	Regression Coefficients and p-Values of Variables in CAC-GGBFS System According to Response Surface Regression Analysis.....	162
Table 5.29	Analysis of Variance for Regression between Compressive Strength and Variables of CAC-GGBFS Mixes.....	163

LIST OF FIGURES

Figure 2.1	Composition Range of CAC Compared to Portland Cement in CaO-SiO ₂ -Al ₂ O ₃ Equilibrium Phase Diagram.....	10
Figure 2.2	Summary of Hydration Mechanism of CAC.....	15
Figure 2.3	Hydration and Conversion Behaviour of CA at Different Temperatures.....	17
Figure 2.4	The Formation of Different Hydrate Phases Depending on Time at Ambient Temperature of 20°C.....	20
Figure 2.5	Time to Reach Minimum Strength after Conversion at Different Curing Temperatures.....	21
Figure 3.1	Evolution of the Concentration of CaO and Al ₂ O ₃ in Solution During the Hydration of CA.....	32
Figure 3.2	DTA Diagrams at Different Temperatures.....	34
Figure 3.3	XRD Diagrams at Different Temperatures.....	35
Figure 3.4	28 Days XRD spectra of CAC mortars at Different Temperatures.....	37
Figure 3.5	120 Days XRD spectra of CAC mortars at Different Temperatures.....	37
Figure 3.6	Relationship among Compressive Strength, W/C Ratio and Porosity of CAC at 28 Days and Cured at Different Temperatures.....	40
Figure 3.7	Relationship Among Compressive Strength, Time, and W/C Ratio.....	41
Figure 3.8	Influence of Water-Cement Ratio on the Long-Term Strength of CAC Concrete Stored at 18°C and 38°C.....	42
Figure 3.9	Setting Times of CAC-PC Combinations.....	44

Figure 3.10	Compressive Strength of CAC-PC Combinations.....	45
Figure 3.11	Compressive Strength Development of 50 % CAC-50 % GGBFS Combination at 20°C.....	49
Figure 3.12	Compressive Strength Development of CAC-GGBFS Blend at 20°C and 38°C.....	53
Figure 4.1	XRD Pattern of CAC.....	58
Figure 4.2	XRD Pattern of PC.....	58
Figure 4.3	XRD Pattern of GGBFS.....	59
Figure 4.4	XRD Pattern of Lime.....	59
Figure 4.5	XRD Pattern of Gypsum.....	60
Figure 4.6	Climatic Chamber Where Different Curing Regimes Were Applied.....	64
Figure 5.1	Setting Time and Water Requirement of CAC-PC Mixes.....	76
Figure 5.2	Setting Time and Water Requirement of CAC-Gypsum Combinations.....	76
Figure 5.3	Setting Time and Water Requirement of CAC-GGBFS Mixes.....	77
Figure 5.4	Setting Time and Water Requirement of CAC-Lime Mixes.....	77
Figure 5.5	Heat Evolution Rates of CAC-PC Mixes.....	81
Figure 5.6	Heat Evolution Rates of CAC-Gypsum Mixes.....	81
Figure 5.7	Heat Evolution Rates of CAC-GGBFS Mixes.....	82
Figure 5.8	Heat Evolution Rates of CAC-Lime Mixes.....	82
Figure 5.9	Compressive Strength Development of IP100 at Different Curing Temperatures.....	92
Figure 5.10	Compressive Strength Development of IP75 at Different Curing Temperatures.....	93

Figure 5.11	Compressive Strength Development of IP50 at Different Curing Temperatures.....	93
Figure 5.12	Compressive Strength Development of IP25 at Different Curing Temperatures.....	94
Figure 5.13	Compressive Strength Development of IP0 at Different Curing Temperatures.....	94
Figure 5.14	XRD Patterns of IP100 at 28 days.....	96
Figure 5.15	XRD Patterns of IP100 at 210 days.....	96
Figure 5.16	XRD Patterns of IP0 at 28 days.....	97
Figure 5.17	XRD Patterns of IP0 at 210 days.....	97
Figure 5.18	XRD Patterns of IP75 at 28 days.....	98
Figure 5.19	XRD Patterns of IP75 at 210 days.....	98
Figure 5.20	XRD Patterns of IP25 at 28 days.....	99
Figure 5.21	XRD Patterns of IP25 at 210 days.....	99
Figure 5.22	Compressive Strength Development of IA99.5 at Different Curing Temperatures	117
Figure 5.23	Compressive Strength Development of IA98 at Different Curing Temperatures.....	118
Figure 5.24	Compressive Strength Development of IA96 at Different Curing Temperatures.....	118
Figure 5.25	Compressive Strength Development of IA92 at Different Curing Temperatures.....	119
Figure 5.26	XRD Patterns of IA96 at 28 days.....	120
Figure 5.27	XRD Patterns of IA96 at 210 days.....	120
Figure 5.28	Compressive Strength Development of IK99.5 at Different Curing Temperatures.....	127
Figure 5.29	Compressive Strength Development of IK99 at Different Curing Temperatures.....	127

Figure 5.30	Compressive Strength Development of IK98 at Different Curing Temperatures.....	128
Figure 5.31	Compressive Strength Development of IK96 at Different Curing Temperatures.....	128
Figure 5.32	XRD Patterns of IK98 at 28 days.....	129
Figure 5.33	XRD Patterns of IK98 at 210 days.....	130
Figure 5.34	Compressive Strength Development of IC80 at Different Curing Temperatures.....	136
Figure 5.35	Compressive Strength Development of IC60 at Different Curing Temperatures.ç.....	137
Figure 5.36	Compressive Strength Development of IC40 at Different Curing Temperatures.....	137
Figure 5.37	Compressive Strength Development of IC20 at Different Curing Temperatures.....	138
Figure 5.38	XRD Patterns of IC80 at 28 days.....	139
Figure 5.39	XRD Patterns of IC80 at 210 days.....	139
Figure 5.40	XRD Patterns of IC60 at 28 days.....	140
Figure 5.41	XRD Patterns of IC60 at 210 days.....	140
Figure 5.42	XRD Patterns of IC40 at 28 days.....	141
Figure 5.43	XRD Patterns of IC40 at 210 days.....	141

CHAPTER 1

INTRODUCTION

1.1 General

The term calcium aluminate cement (CAC), also called aluminous cement or high alumina cement covers a range of inorganic binders characterized by the presence of monocalciumaluminate (CA) as their main constituents. The raw materials of CAC are mainly bauxite and calcareous materials. The chemical composition of CAC may vary over a wide range, with Al_2O_3 contents ranging between 40% and 80% [1].

CAC was developed during the later stages of the nineteenth century as a solution to the problem of decomposition of portland cement (PC) under sulphate attack alternatively to it, which differs from CAC by containing calcium silicate phases [2-4].

The inventor of CAC (Jules Bied from France) estimated that CAC is not prone to sulphate attack like PC, due to the absence of calcium silicates. The patent of CAC was obtained in 1908 in France [3].

The first known special property of CAC was its high sulphate resistance. Rapid hardening property and the refractory properties of CAC were realized later. Among these three properties, the rapid hardening property

caused wide usage of CAC in the construction industry particularly in precast applications.

Although CAC became considerably used in many structural applications, its use in load-carrying system was soon limited, after the failures of structures in different countries that were built by CAC [1]. The failures were caused by the conversion reactions of the hydration products of CAC. At low or normal temperatures up to 40°C, the hydration process causes higher strengths. However, these high strength inducing calcium aluminate hydrates convert to stable hydrates having lesser strength within a period lasting several days or many years depending particularly on temperature and humidity [2,4].

Misunderstanding of this conversion process especially during the 1960's and 1970's caused serious failures in several countries. Afterwards, use of calcium aluminate cement in load carrying systems has been forbidden [2,4].

One of the main application areas of calcium aluminate cement is its use as a major or minor constituent in inorganic cementitious systems. In such systems, generally speaking, CAC is blended with one or more inorganic materials such as PC, lime, gypsum, and ground granulated blast furnace slag (GGBFS), etc. to obtain specified properties like rapid hardening, self-stressing, etc. Therefore, it is essential to understand the characteristics of hydration and strength development of these blends as affected by temperature, which is of vital importance in pure CAC application, too.

1.2 Objective and Scope

CAC is a special hydraulic cement, which is distinguished from ordinary PC by its high performance characteristics such as slow setting but very rapid hardening, high chemical resistance, high corrosion resistance, high resistance to acids and high refractory properties. These superiorities of CAC enable it to be used within a wide spectrum in the construction industry as well as in other industries such as the refractory industry.

One of the main application areas of CAC is focused on building chemistry, such as repair mortars, self-levelling compounds, tile adhesives, etc. Generally speaking, in such applications, it is blended with one or more inorganic materials, e.g. PC, GGBFS, lime, gypsum, etc. In such binary or ternary cementitious systems CAC is utilized as either the main constituent or may take place in small amounts in order to modify various properties of such systems. As a result, special properties such as fast setting, rapid hardening, high early strength, shrinkage compensation, etc. may be obtained.

CAC has several advantages over PC particularly through its rapid strength development. However, depending especially upon temperature and humidity, the strength of CAC may decrease significantly with time. In fact, in CAC systems the hydration process is much different than that of ordinary portland cement systems. The initially formed metastable hydration products of CAC may convert to stable hydrates resulting in reduced strength.

The aim of this study is to investigate the temperature effect on the behaviour of CAC based composite binders, which is of vital importance in pure CAC system. During this research, several combinations of CAC-PC, CAC-gypsum, CAC-lime and CAC-GGBFS were examined. These CAC

based composite binders were subjected to different curing regimes. Curing continuously at 20°C, 30°C, 40°C, and 50°C and curing 28 days at 20°C then at 30°C, 40°C, and 50°C were the types of curing regimes studied. All curing regimes had the same 100% RH. By performing compressive strength tests at several ages up to 210 days, strength development of different CAC based composite binders at different temperatures was investigated. In addition, the mechanism of strength development was tried to be explained by XRD analyses performed at 28 and 210 days. Through understanding the hydration and strength development mechanism by the above tests, some empirical relations between strength-time-curing temperatures were formulated. In this way, by estimating formulations within different cementitious systems, several cases in real life may be simulated in a quite accurate manner.

CHAPTER 2

THEORETICAL CONSIDERATIONS

2.1 General

Calcium aluminate cement (CAC) is a hydraulic binder i.e. it is a finely ground inorganic material which, when mixed with water, forms a paste which sets and hardens by means of hydration reactions and processes and which, after the hydration process has produced stable hydrates, retains its strength and stability even under water [2,4]

Main characteristic of CAC is the fact that although its setting is quite slow similar to ordinary portland cements (PC), its strength gain is very rapid compared to ordinary PC. This feature is related with the oxide and compound composition of the cement. As the name implies, CAC is composed of mainly calcium aluminates and the main phase, mono calcium aluminate (CA), sets quite slowly but hardens very rapidly, liberating huge amount of heat of hydration.

The properties of CAC are mainly determined by the alumina content. There are many types of CAC in the world, which are classified and as well as distinguished in terms of brand name according to its alumina content. For instance, the relevant Turkish Standard TS 6271 [5] states

four groups of CAC according to its alumina content. These are given in Table 2.1:

Table 2.1 Types of CAC According to TS 6271 [5]

Properties	1st Class	2nd Class	3rd Class	4th Class
Al ₂ O ₃ (%)	> 77	> 70	> 50	> 38
Fe ₂ O ₃ (%)	< 0,5	< 0,7	< 3,5	< 18
CaO (%)	< 22	< 30	< 40	< 40
Retained on 90 µm sieve (%)	< 5	< 5	< 5	< 5
Initial Set (hr)	> 0,1	> 2	> 1	> 1
Final Set (hr)	< 4	< 12	< 12	< 12
Compressive Strength (MPa)				
6 th Hour	-	-	-	-
24th Hour	> 10	> 25	> 45	> 35

The most frequently used CAC has approximately 40% of alumina. CACs with higher alumina content are used for very specific applications, particularly refractory applications, whereas those with alumina content of especially 40% are used both for refractory and structural applications.

In this investigation the CAC, ISIDAÇ 40 (brand name of CAC) with an alumina content of 40% were examined. That is why, throughout this

investigation CAC is defined as the CAC with an alumina content of almost 40%.

Main properties of CAC can be summarized as follows:

- Working times similar to ordinary PC (can be retarded or accelerated by the use of some chemical and/or mineral admixtures, e.g. lime, PC, Li_2CO_3 , etc.).
- High early strength (according to prEN 1467:2004 compressive strength at 6 hr and 24 hr must be higher than 18 MPa and 40 MPa, respectively [2,4]).
- High abrasion resistance due to its high alumina content.
- High corrosion resistance and high durability under severe environmental effects such as sulphate attack, acid attack, etc. (In the hydration reactions of calcium aluminate cement, unlike ordinary PC, no $\text{Ca}(\text{OH})_2$ is formed. In addition, gypsum used in PC production is not utilized in CAC production. That is why the durability problem of PC mainly due to the presence of $\text{Ca}(\text{OH})_2$ is not experienced in calcium aluminate cements).
- Refractoriness up to 1300°C (the huge amount of Al_2O_3 that possesses refractoriness property by itself causes high heat resistance in calcium aluminate cement).

Depending on these properties, CAC is used throughout a wide spectrum, which can be listed as follows:

- ◆ Applications where rapid hardening and high early strength are required (Highways, airports, repair works, etc.).
- ◆ Applications where high abrasion resistance is required (industrial floors, highways, spillways of dams, etc.).

- ◆ Applications in winter where conventional concreting is not possible (since the hydration rate and heat of hydration of CAC is too high compared to ordinary cements [6]).
- ◆ Applications where heat resistance is required (refractory applications up to 1300°C).
- ◆ Applications where resistance to chemical, biological and acidic attack (pH>4) is required (pipes, sewers, industrial floors, tunnels, applications in soil, coastal application, etc.).
- ◆ Usage as a constituent in building chemistry formulations (rapid hardening repair mortar, self levelling compounds, tile adhesives, etc.).

2.2 Physical and Mechanical Properties of CAC

The colour of CAC is grey-black. In comparison with an ordinary PC it is much darker. The colour mainly depends on the iron content of the cement, which may be up to 18%. In fact, cements, generally speaking, get darker as the iron content is increased.

The CACs with alumina content higher than 40%, particularly those containing 70 to 80% of alumina with only very little silica and iron oxide, are white. The whiteness is related therefore with the alumina and iron oxide content [3].

The specific gravity of CAC is slightly higher than that of PC. It is 3,00 to 3.25 [3,6].

The setting time of CAC is very similar to that of PC. Generally, it is longer than 2 hours but shorter than 5 hours. Unlike PC, hardening and strength

gaining period is too short. Almost within 6 hours, it reaches such a strength that it is higher than 28 days strength value of ordinary PC.

Rapid hardening means that hydration reactions take place fast. As a result, the heat of hydration, i.e. the heat evolved in hydration reaction of calcium aluminate based phases, is high. Heat of hydration of CAC and ordinary PC was compared in previous studies as illustrated in Table 2.2 [3,6].

Table 2.2 Comparison of the Heat of Hydration Values of Different Cements [3,6]

Cements	Heat of Hydration (cal/g) at				
	1 day	3days	7days	28 days	90 days
CAC	77-93	78-94	78-95		
Rapid hardening cement	35-71	45-89	51-91	70-100	
Ordinary PC	23-46	42-65	47-75	66-94	80-105

Main characteristic of CAC, which can be interpreted from the Table 2.2, is the fact that the cement gains its strength very rapidly although the setting is slow, when it is compared with ordinary PC. This feature is related to the oxide and compound composition of the cement. The main phase, which is responsible for this property, is monocalcium aluminate (CA). Its

reaction with water leads to huge amount of heat generation and formation of calcium-aluminate-hydrate (C-A-H).

2.3 Chemical Composition of CAC

CAC clinker is comprised of the same basic oxides as PC clinker. Like PC it contains lime, silica, alumina, and iron oxide, but their proportions are quite different from each other [7,8]. Although PC is defined as calcium silicate based cement due to its high lime and silica content, as the name implies, CAC is based upon calcium oxide and alumina. These differences in chemical composition can clearly be seen in the ternary diagram of the $\text{CaO-SiO}_2\text{-Al}_2\text{O}_3$ system, shown in Figure 2.1[9].

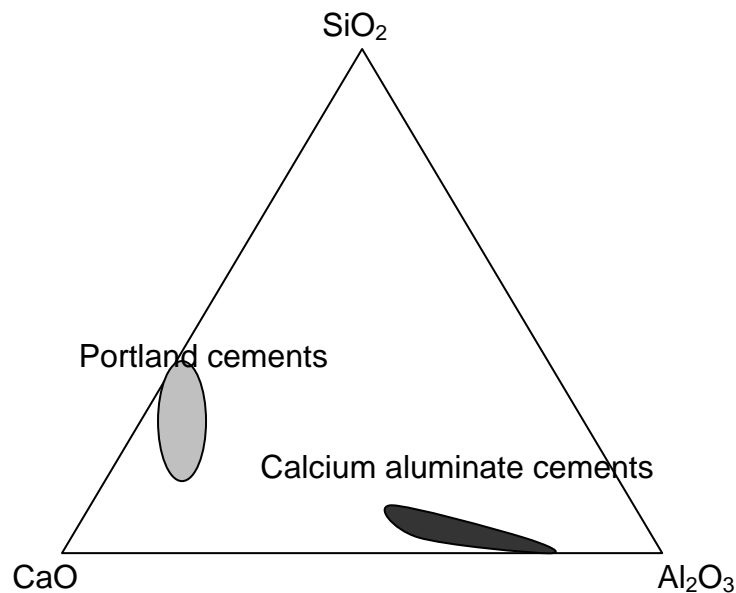


Figure 2.1 Composition Range of CAC Compared to PC in $\text{CaO-SiO}_2\text{-Al}_2\text{O}_3$ Equilibrium Phase Diagram [9]

As seen in Figure 2.1, CAC is composed of mainly alumina and lime whereas PC contains mainly lime and silica.

Table 2.3 [1] shows the range of chemical composition of CAC. The Al_2O_3 content of CAC varies over a wide range, depending mainly on the ratio of raw materials, limestone to bauxite ratio in the mixture. The CaO content may also vary widely and it decreases as the alumina content increases [1].

Table 2.3 Chemical Composition of CAC [1]

Oxides	%
Al_2O_3	38-82
CaO	18-40
Fe_2O_3	0.3-18
SiO_2	0.5-6
TiO_2	0.1-4
MgO	0.2-1.5
$\text{Na}_2\text{O}+\text{K}_2\text{O}$	0.4-7
SO_3	0.2-0.4

Appreciable amount of silica and iron oxide may also be present in CACs with lower alumina contents. The other ingredients, such as TiO_2 , MgO, SO_3 and alkali oxides are only in small amounts and have little effects on CAC properties [1].

The most frequently used CAC has an alumina content of 40%. Cements with higher alumina content are usually used in refractory applications, due to the refractoriness of alumina. The brand names of CAC available in the market are generally followed by the alumina content, since the properties are mainly dominated by it [7]. Higher alumina content means higher refractoriness, higher abrasion resistance and shorter setting time.

2.4 Mineralogical Composition of CAC

As stated previously, the main phase of calcium aluminate cement with an Al_2O_3 content of 40 % is monocalciumaluminate (CA), whereas the minor phases are dodecacalcium heptaaluminate (C_{12}A_7), tetracalcium aluminoferrite (C_4AF), dicalcium silicate (C_2S), and dicalcium aluminosilicate (C_2AS).

Brief information about the mineralogical compounds of CAC is as follows:

Mono calcium aluminate ($\text{CA}=\text{CaO}.\text{Al}_2\text{O}_3$): CA is the main constituent of all types of calcium aluminate cements like CAC with alumina content of 40 %. It is primarily responsible for the particular cementitious behaviour in this type of cement [6]. Its setting is slow, whereas it hardens very rapidly. It is formed by heating equimolar blend of CaO and Al_2O_3 above 800°C . It is monoclinic and pseudo-hexagonal ($a=0.8700$ nm, $b=0.8092$ nm, $c=1.5191$ nm, $\beta=90.3^\circ$, $d=2945$ kg/m³). Moreover, its crystal structure consists of a three dimensional framework of AlO_4 tetrahedra sharing corners with Ca^{2+} ions in between [1, 10-12].

Dodeca calcium heptaaluminate ($\text{C}_{12}\text{A}_7=12\text{CaO}.7\text{Al}_2\text{O}_3$): It is present in the cement in small percentages. Other factors remaining equal, the

amount of $C_{12}A_7$ in the cement rises when C/A ratio is increased. It sets rapidly but it makes no contribution to the strength, therefore it is not regarded as a very desirable constituent of CAC except in minor amounts [6]. It has a cubic atomic structure ($a=1,1983$ nm, $d=2680$ kg/m³) [1].

Tetracalciumaluminoferrite ($C_4AF=4CaO.Al_2O_3.Fe_2O_3$): C_4AF is the second most abundant component of CAC. In spite of this, it makes no or very little contribution to the setting and the strength development [7].

Dicalcium silicate ($C_2S=2CaO.SiO_2$): C_2S behaves as in PC, i.e. its hydration is slow and its contribution to the strength is at later ages rather than at early ages.

Dicalcium aluminosilicate (Gehlenite) ($C_2AS= 2CaO.Al_2O_3.SiO_2$): Generally speaking CAC with alumina content of 40% contains limited amount of SiO_2 , mostly less than 5%. That is why; both C_2S and C_2AS are in limited amount in such types of CAC. Like C_2S , C_2AS sets slowly and contributes to the strength after a considerable period [6].

2.5 Hydration and Conversion of CAC

Hydration is the reaction between cement and water. In the case of CAC, this reaction proceeds very differently than in PC. Generally in PC 60-80% of hydration occurs in 28 days depending on the type of PC, and the hydration reactions proceed even behind 28 days but in a slower manner [7]. However, in CAC most of the hydration occurs only within the first 24 hrs.

In fact, when CAC is mixed with water, a small quantity of heat is liberated within minutes. Then no hydration occurs throughout almost 2-3 hrs, which is called as dormant period. After the dormant period, CAC reacts with almost all of the water very rapidly and almost complete hydration is realized within 24 hrs, accompanied by a large amount of heat generation [7]. This summarizes also the distinct property of CAC, slow setting and rapid hardening.

2.5.1 Hydration Mechanism of CAC

The hydration of CAC starts by dissolving of clinker minerals in water as calcium ions, Ca^{2+} , and aluminium hydroxide, $\text{Al}(\text{OH})_4^-$, which continues till the saturation level. Meanwhile, the pH value of liquid phase increases up to 12, particularly 11.2 [13-15]. It is followed by nucleation and precipitation of calcium aluminate hydrate crystals and gibbsite ($\text{Al}_2\text{O}_3 \cdot 3\text{H}_2\text{O}$). These hydrate crystals start to precipitate close to the unreacted clinker surface by forming a gel layer [8, 13-16]. Fujii et al. [13] reported that this layer is permeable to water. Therefore, further hydration of the underlying clinker grains takes place easily as a continuous process as long as enough water for dissolution and hydration is available [8, 13-19].

The hydration and strength development are illustrated in Figure 2.2 [8].

As seen in Figure 2.2, at initial stages, hydration crystals form a gel layer coating the unreacted grains. The mix is still plastic. Depending on the progress in crystal formation as a result of continuous dissolving/precipitation, some bonds take place among clinker grains, resulting in stiffening of the mix. As hydration proceeds further, the mix gets stiffer by gaining strength. Finally, the final stable structure is formed when the water is used up and no further hydration crystal grows [8].

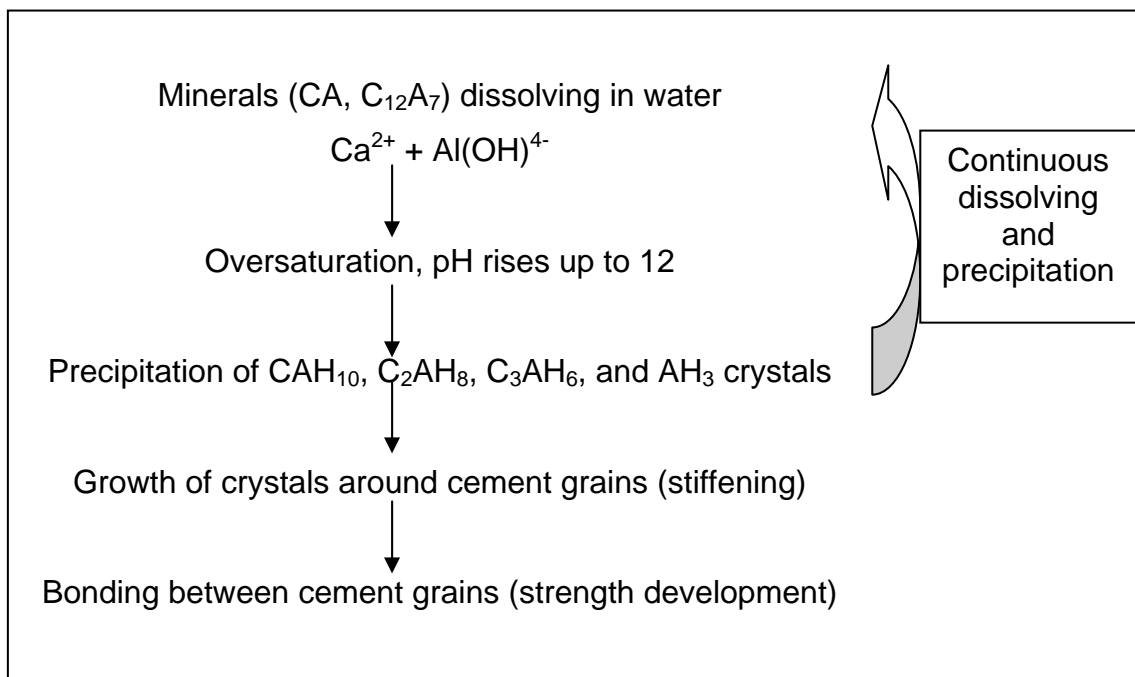


Figure 2.2 Summary of Hydration Mechanism of CAC [8]

As stated previously, the main components of CAC, i.e. $C_{12}A_7$ and particularly CA, dominate the features of the cement. That is why; the hydration of calcium aluminates gives the cement its specific properties. As a result of hydration reactions of mainly CA, different hydration products are created depending particularly on temperature.

There are several known calcium aluminate hydrates, i.e. CAH_{10} , C_2AH_8 , C_3AH_6 , C_4AH_3 , C_4AH_{19} , $C_4A_3H_3$. Nevertheless, principal hydrate forms are CAH_{10} , C_2AH_8 , and C_3AH_6 , together with crystalline AH_3 and/or amorphous AH_3 gel [13,14,20,21]. Since unlike PC, there is no portlandite (CH) in hydration products, a good resistance of CAC to many aggressive agents is assured [2,4].

The physical properties of principal calcium aluminate hydrates are summarized in Table 2.4 [8,13].

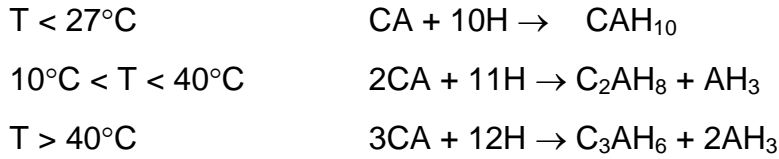
Table 2.4 Physical Properties of Calcium Aluminate Hydrates [8,13]

Hydration Products	Chemical Composition (%)			Crystal Form	Density (g/cm ³)	Volume Ratio of Hydrates to CA
	CaO	Al ₂ O ₃	H ₂ O			
CAH ₁₀	16.6	30.1	53.3	Metastable hexagonal prism	1.72	3.68
C ₂ AH ₈	31.3	28.4	40.3	Metastable hexagonal plates	1.95	2.33
C ₃ AH ₆	44.4	27.0	28.6	Stable cubic trapezohedrals	2.52	1.75
AH ₃	-	65.4	34.8	Stable hexagonal prism	2.42	-

2.5.2 Conversion Mechanism of CAC

During the hydration process of CAC, different types of calcium alumina hydrate, i.e. CAH₁₀, C₂AH₈, and C₃AH₆, may be formed, which mainly depends on temperature, and secondarily on humidity.

The formation of hydration products at different temperatures is as follows:



In fact, at low temperature ($<27^{\circ}\text{C}$) hydration forms the metastable hexagonal hydrates (CAH_{10} and C_2AH_8) and gibbsite (AH_3). CAH_{10} and C_2AH_8 change with time to stable cubic form following the reactions shown in Figure 2.3 [1,2,4,22-24]:

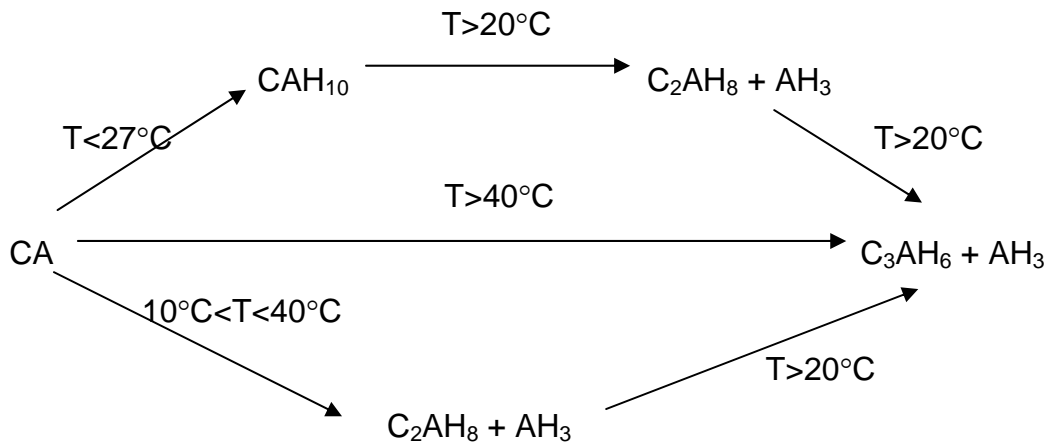


Figure 2.3 Hydration and Conversion Behaviour of CA at Different Temperatures

As seen in Figure 2.3, above 40°C hydration forms directly cubic calcium aluminate hydrate C_3AH_6 and gibbsite, whereas below 10°C sole hydration product is CAH_{10} , and this phase may be formed together with C_2AH_8 and AH_3 up to 27°C . C_3AH_6 and AH_3 are stable hydrates, which do not change, but CAH_{10} and C_2AH_8 are metastable and tend to convert subsequently to

C_3AH_6 , which is the unique stable phase within the C-A-H system. This evolution, known as conversion, is primarily dependent on temperature, and increases steeply as the temperature increases. It also increases with increasing water/cement ratio. An increased temperature during the initial hydration may also accelerate the subsequent rate of conversion [1,2,4,22-24].

As a result of conversion reactions, some of the water bound within the crystal structure of CAH_{10} and C_2AH_8 is liberated resulting in an increase in porosity of CAC matrix and consequently in a decrease in strength. By the way, porosity and strength decrease are also a function of water/cement ratio. Therefore, the water/cement ratio of 0.4 is stated as an upper limit for CAC applications in most of the international standards related with CAC [2,4].

The complete hydration of CA to CAH_{10} phase needs higher amount of water compared with those of CA to C_2AH_8 and to C_3AH_6 . For the formation of CAH_{10} phase, the required water-solid ratio is 1.13, whereas for that of $C_2AH_8 + AH_3$ it is 0.63, and for that of C_3AH_6 it is 0.46. Related with these figures, it can be easily interpreted that conversion of CAH_{10} and C_2AH_8 to C_3AH_6 releases huge amount of water within the hardened cement matrix [1].

The conversion reactions of CAH_{10} and C_2AH_8 to C_3AH_6 are as follows [1,2,4]:



According to the conversion reactions of CAH_{10} to C_3AH_6 given above, 60% of chemically bound water is released causing reduction in the hydrate volume by 53 %. On the other hand, throughout the conversion of C_2AH_8 to C_3AH_6 , 37.5 % of chemically bound water is liberated resulting in a decrease in hydrate volume by 34%. Consequently, these volume changes as a result of release of chemically bound water bring about crystal restructuring and sharp strength decreases [1,8].

2.6 Factors Affecting Conversion

The main factor affecting conversion is temperature. Either the hydration temperature or ambient temperature throughout the service life of CAC primarily determines the rate and amount of conversion reactions of CAH_{10} and C_2AH_8 phases to C_3AH_6 .

Other factors affecting the characteristics of conversion are the initial water-cement ratio and degree of humidity, the CAC matrix is subjected.

2.6.1 Temperature Effect

Different types of calcium aluminate hydrates, i.e. CAH_{10} , C_2AH_8 , and C_3AH_6 may be formed depending particularly on the temperature of hydration. Moreover, the ambient temperature mainly determines the rate and the amount of conversion of initially formed CAH_{10} and C_2AH_8 phases to C_3AH_6 . In other words, the rate of conversion reaction is especially time dependent. As temperature increases, the conversion occurs more rapidly.

The formation of different hydrate phases depending on time at an ambient temperature of 20°C is illustrated in Figure 2.4 [1].

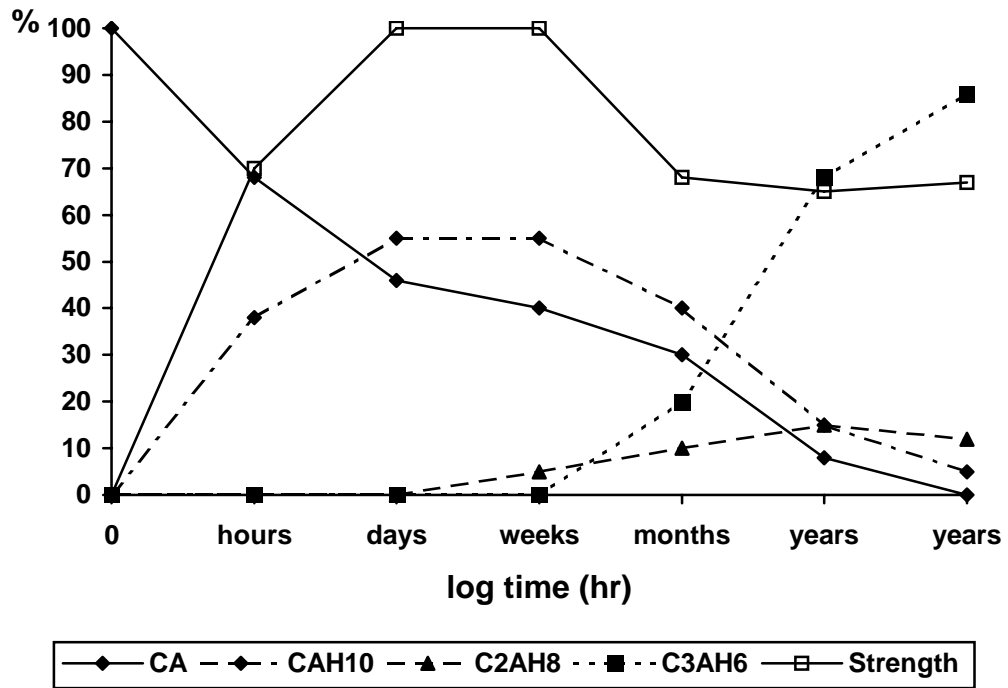


Figure 2.4 The Formation of Different Hydrate Phases Depending on Time at Ambient Temperature of 20°C [1]

As seen in Figure 2.4, during the initial stages of hydration, CAH_{10} and C_2AH_8 are the only hydration products. However, at later stages C_3AH_6 is formed either directly from CA or from CAH_{10} and C_2AH_8 as a result of conversion reactions. It can be clearly seen that complete conversion may take several years at 20°C.

Nevertheless, depending on the increase in either hydration temperature or ambient (or curing) temperature, rate of conversion increases drastically, as shown in Figure 2.5 [4].

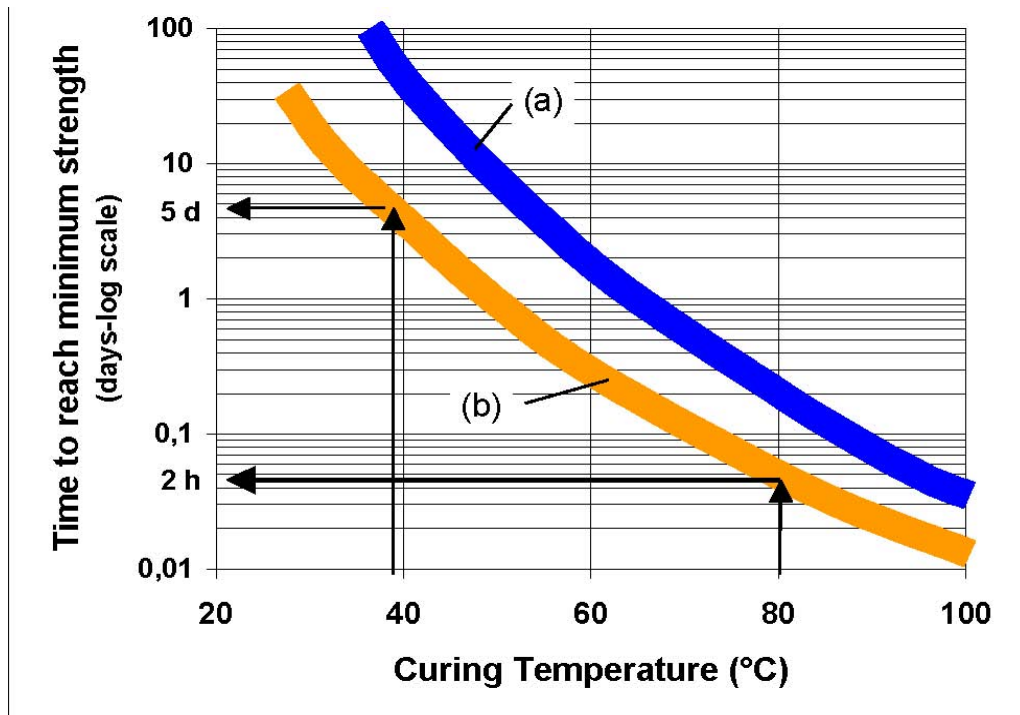


Figure 2.5 Time to Reach Minimum Strength after Conversion at Different Curing Temperatures ((a) Samples were pre-cured for 24 h at 20°C and then cured at the given temperature under water. (b) Samples were placed directly under water (without pre-curing) at the given curing temperature) [4]

Table 2.5 The Rate of Conversion of CAH_{10} and C_2AH_8 to C_3AH_6 Depending on Temperature [1]

Temperature (°C)	CAH_{10}	C_2AH_8
5	>20 years	> 20 years
10	19 years	17 years
20	2 years	21 months
30	75 days	55 days
50	32 hours	21 hours
90	2 minutes	35 seconds

Table 2.5 illustrates the effect of temperature on conversion rate of CAH_{10} and C_2AH_8 to C_3AH_6 [1].

As seen in the Table 2.5, the rate of conversion increases significantly, as the temperature increases. At 5°C the completion of conversion takes more than 20 years and that is why it is not a wrong interpretation that there is no conversion. However, above 50°C the conversion process is almost immediate [1].

2.6.2 Effect of Water-Cement (w/c) Ratio and Humidity

Although the conversion is primarily temperature dependent, w/c ratio and humidity of CAC system throughout its service life play an important role.

According to Robson [6], there is a definite transition temperature at 25°C under which conversion takes place very slowly. It does not matter whether it is wet or dry. However, at higher temperatures humidity is more crucial and therefore the time required for completion of conversion increases greatly as the humidity of CAC matrix is reduced [6]. In other words, conversion occurs more rapidly when the process takes place under humid conditions and the rate of conversion decreases significantly, if the relative humidity drops below saturation level of CAC matrix. This is summarized in Table 2.6 [1].

Table 2.6 Effects of Temperature and Humidity on Conversion [1]

	Low Temperature ($<20^{\circ}\text{C}$)	Elevated Temperature ($>20^{\circ}\text{C}$)
Dry Condition	relative stability	dehydration $\text{CAH}_{10} \rightarrow \text{CAH}_4$ $\text{C}_2\text{AH}_8 \rightarrow \text{C}_2\text{AH}_5$
Humid Condition	slow conversion to $\text{C}_3\text{AH}_6 + \text{AH}_3$	fast conversion to $\text{C}_3\text{AH}_6 + \text{AH}_3$

The rate of conversion also increases with the increase in w/c ratio of CAC matrix [1,3]

2.7 CAC Based Composite Binders

Inorganic cementitious systems with special properties (such as fast setting, rapid hardening, high early strength, rapid drying, shrinkage compensation, etc.) may be obtained by combining calcium aluminate cement with other materials. CAC takes place in such composite cementitious systems either as a main constituent or as a minor addition, usually present in limited amounts [1]. In mixes where CAC is the main constituent, CAC dominates the properties of the composite system, whereas in mixes where CAC is incorporated in limited amounts, CAC is used to modify or to adjust the properties of the composite binder. Such systems may be produced either by premixing the dry constituents or by adding them separately to the wet mix [1].

Main materials, which can be used in CAC based composite binders, are as follows:

- PC
- Gypsum
- Lime
- Fly ash
- GGBFS
- Silica fume
- CaCO_3

- Alkali or ammonium phosphates or polyphosphates (Calcium aluminate phosphate cement)
- Sodium silicate
- PC+gypsum (Type M expansive cement)
- etc.

2.7.1 CAC-PC Combination

Blends of CAC and PC exhibit different setting behaviour and strength development than each of these two binders when used separately [1,25]. According to previous studies [25-30], it is well known that either addition of CAC as a minor constituent to PC or addition of PC as a minor constituent to CAC shortens the setting time of the resultant cement blend significantly [1]. In the range between about 15% and 85% of PC (85%-15% CAC), and a w/c ratio yielding a paste of plastic consistency, the setting time occurs even within few minutes (at ambient temperature). It also enables obtaining measurable strength values in less than an hour, but the final strengths are lower than those attained with PC or CAC alone [1,25].

In CAC-PC blends, when PC is the main constituent, the occurrence of rapid setting and hardening is mainly due to the rapid formation of ettringite and secondarily due to the hydration of CAC. The hydration of calcium silicates has little influence on the setting process, but contributes to strength development at later stages. In such mixes, all phases formed in the hydration of pure PC and CAC are available. In addition to that, straelingite (C_2ASH_8 =a hydration product of gehlenite), i.e. calcium-silica-alumina-hydrate may also be formed throughout the hydration process [1,25].

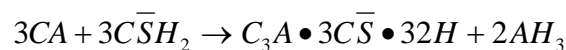
In the case of CAC as the main constituent rapid setting and hardening is due to the rapid formation of CAC hydration, which is mainly owing to the increase of the pH value of the mix, caused by the PC addition [1].

Blends of CAC and PC may be employed in applications in which extremely fast setting and hardening are required. Further acceleration of the setting and hardening process may be achieved by adding small amounts of lithium salts into the system. However, uncontrolled mixing of CAC and PC in normal concrete application may cause unexpected results, such as hardening in the mixing drum or not attaining the required ultimate strength [1,3].

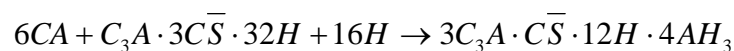
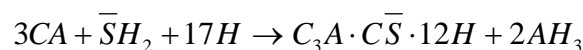
2.7.2 CAC-Gypsum Combination

Gypsum is used in CAC-gypsum system, mainly to modify the expansion properties. To obtain a self-stressing or expansive cement, gypsum, in amounts corresponding to 15-40% SO₃, is combined with CAC. Ettringite and hydrous alumina (amorphous AH₃) are formed as product of hydration [1,31,32]. At lower SO₃ contents in the blend, monosulphate may also be formed, or the primarily formed ettringite may convert to monosulphate [1]. The hydration mechanism at high SO₃ content and at lower SO₃ content is as follows:

At high SO₃ content;



at lower SO₃ content;



In CAC-gypsum combination, as gypsum content is increased, the resulting expansion property increases significantly. It also increases with increasing temperature [1].

Type M expansive cement is a combination of CAC, PC and gypsum, typically in the ratio of 66:20:14. [1,33,34]. Again in such special type of cement the expansion mechanism is dominated mainly by the reaction between CAC and gypsum.

2.7.3 CAC-Lime Combination

The addition of lime to CAC results in mainly fast setting and fast strength development. Like PC addition to CAC, lime addition causes an increase in the pH value, which as a result brings about accelerated hydration. Generally speaking, small amounts of lime are added to CAC mixes to modify setting and hardening properties of the mixes [8].

2.7.4 CAC-GGBFS Combination

Although CAC has a lot of advantages over PC through its rapid strength development and excellent chemical resistance, its initial high strength decreases with time depending mainly on temperature and humidity, which is defined as conversion [35]. In order to compensate this harmful effect, many attempts have been carried out by mixing CAC with other inorganic pozzolonic materials such as fly ash, metakaolin, GGBFS, etc. [35-41]

Most of the research carried out are concentrated mainly on CAC-GGBFS combinations and such blends containing appropriate ratios of CAC to

GGBFS exhibit a steady strength increase without the decline of strength that is common in pure CAC, if hydrated at ambient or moderately elevated temperatures. Generally speaking, the short-term strength of such mixes is lower than that of mixes made with pure CAC, but the long-term strength is higher than that of pure CAC mixes after conversion [1,35,38,39,42,43].

In the hydration of CAC-GGBFS blends, mainly straeltingite (hydration product of gehlenite), which is a stable compound in the C-A-S-H system formed at ambient temperature instead of CAH_{10} and C_2AH_8 , whereas C_3AH_6 is the other important compound formed at elevated temperature. [1,38,44-46]. This stable straeltingite compound forms as a result of the hydration reactions between the calcium aluminate phases and silica of GGBFS [1,35-46].

Following hydration products form in several CAC-GGBFS blends at different temperatures at the end of 90 days [1,46]:

- CAC (%80) + slag (%20)

5°C	CAH_{10}
40°C	$C_3AH_6 + C_2ASH_8$ (little) + AH_3 (little)

- CAC (%50) + slag (%50)

5°C	$C_2ASH_8 + CAH_{10}$ (little)
40°C	$C_2ASH_8 + C_3AH_6$

- CAC (%20) + slag (%80)

5°C	C_2ASH_8
40°C	C_2ASH_8

As seen in the reactions given above, the presence of adequate amounts of GGBFS hinders the conversion of primarily formed CAH_{10} and C_2AH_8 to C_3AH_6 in pure CAC matrix to a high degree. Such a composite binder is suitable not only for applications in which long-lasting service of the structure is required, but also for applications in which excellent chemical resistance to sulphates, seawater, etc. is required [1,38,42].

CHAPTER 3

REVIEW of RESEARCH ON HYDRATION, CONVERSION and STRENGTH DEVELOPMENT of CALCIUM ALUMINATE CEMENT BASED COMPOSITE BINDERS

3.1 General

Since the invention of calcium aluminate cement (CAC), many researches have been carried out to understand its properties. Although the initially produced CAC was aimed to solve the sulphate resistance problem in concrete technology, afterwards it was understood that it possesses also good refractory properties. Later on its slow setting but very rapid hardening property was invented and it became a widely used special cement in construction industry, particularly in precast concrete industry.

The failures occurred in 1960's and 70s in several buildings where CAC was used lead to researches on CAC's stability depending upon time. It was seen that the metastable hydrates initially formed convert to stable hydrate with time resulting in significant decrease in strength. Owing to the conversion reactions, the use of CAC has been limited in load carrying systems in construction industry.

Some precautions have been considered to eliminate or to decrease the harmful effect of conversion. These attempts have focused mainly on blending CAC with other inorganic materials, such as different types of pozzolanic admixtures, particularly ground granulated blast furnace slag.

Building chemistry is another sector where CAC is utilized widely. In the formulations of different types of mortars, such as repair mortars, self levelling compounds, tile adhesives etc., CAC is generally mixed with another inorganic material to obtain the specified properties such as high early strength, self-stressing, etc. In such blended cement based systems, conversion is again of vital importance like in systems where pure CAC is used.

In the following sections, the previous studies on hydration, conversion and strength development of CAC based composite binders are presented.

3.2 Previous Studies on Conversion of Pure CAC and on Factors Affecting Conversion

The hydration mechanism of CAC has already been extensively studied [47-51]. According to these studies, three main stages, which are illustrated in Figure 3.1 are available; (i) dissolution period, (ii) induction period, and (iii) massive precipitation and continuous dissolution/precipitation.

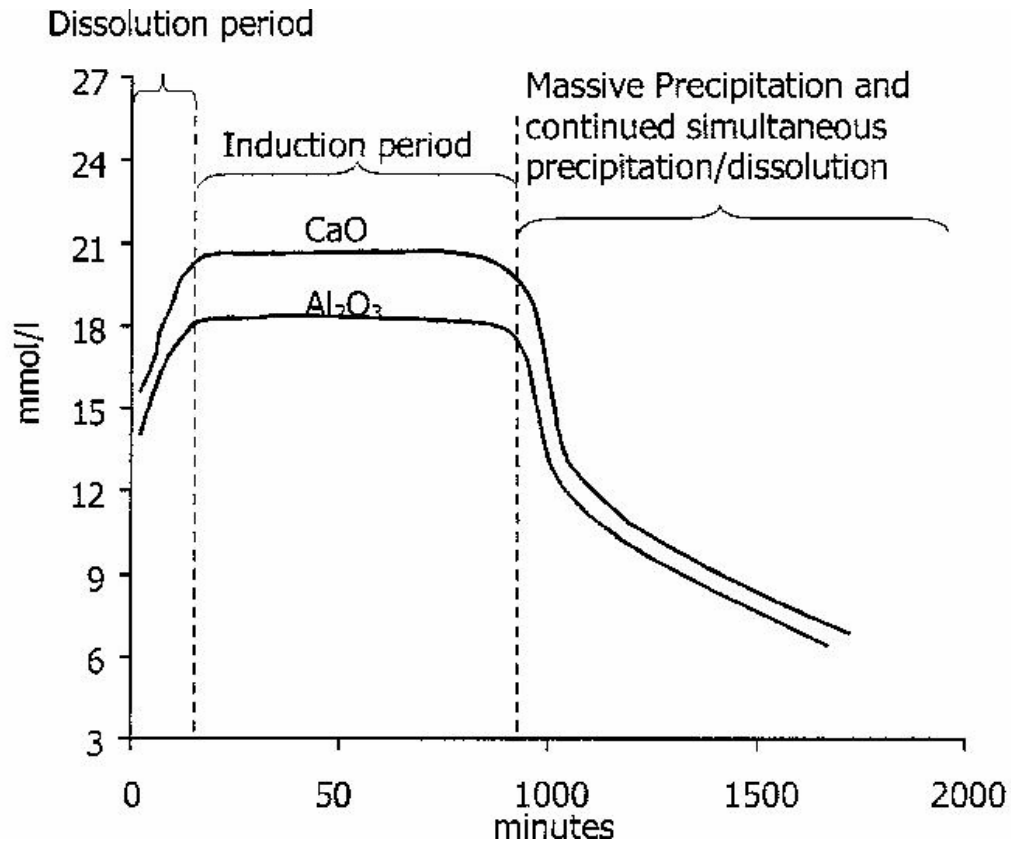


Figure 3.1 Evolution of the Concentration of CaO and Al₂O₃ in Solution During the Hydration of CA [47,52]

Throughout the precipitation period, 3 main calcium aluminate hydrates, CAH₁₀, C₂AH₈, and C₃AH₆, are formed whose relative proportions are dependent mainly on temperature and humidity. Other factors affecting the type of precipitation are water-cement ratio and cement content.

3.2.1 Effects of Temperature on Hydration and Conversion

The effects of temperature, moisture and age on compressive strength of CAC have been the subjects of many studies for over 40 years [3, 53-60].

Smith et al. [59,60] studied the effects of temperature on the type of hydration products of CAC. In this study, 4 different curing temperatures, 5°C, 20°C, 40°C, and 60°C were selected. The CAC (alumina content is approximately 70%) specimens with a constant w/c of 0.33 were subjected to DTA and XRD analysis at different ages up to 5 months. DTA and XRD diagrams are presented in Figure 3.2 and Figure 3.3, respectively, and according to these analyses the types of hydrates at different temperatures from 24 h to 3500 h are listed in Table 3.1 [59,60].

As seen in Table 3.1, at lower temperatures, i.e. 5°C and 20°C, types of hydration products are only CAH_{10} , C_2AH_8 and small amounts of AH_3 , whereas at 40°C and 60°C, C_3AH_6 , AH_3 are formed instead of CAH_{10} and C_2AH_8 . Some of the initially formed C_2AH_8 at 40°C converts to C_3AH_6 with time. On the other hand, at elevated temperatures generally speaking, stable C_3AH_6 forms directly without any conversion reaction. As a result, it can be concluded that the chemical nature of hydrates depends especially on temperature and time. In particular, at 5°C, stable C_3AH_6 does not form during this interval while at 40°C or 60°C C_3AH_6 is detected very early [60,61]. Similar claims were pointed out by Alcocel et al. [61] for a CAC cement of 55% alumina content at temperatures of 5°C and 60°C, as a result of SEM and XRD analysis.

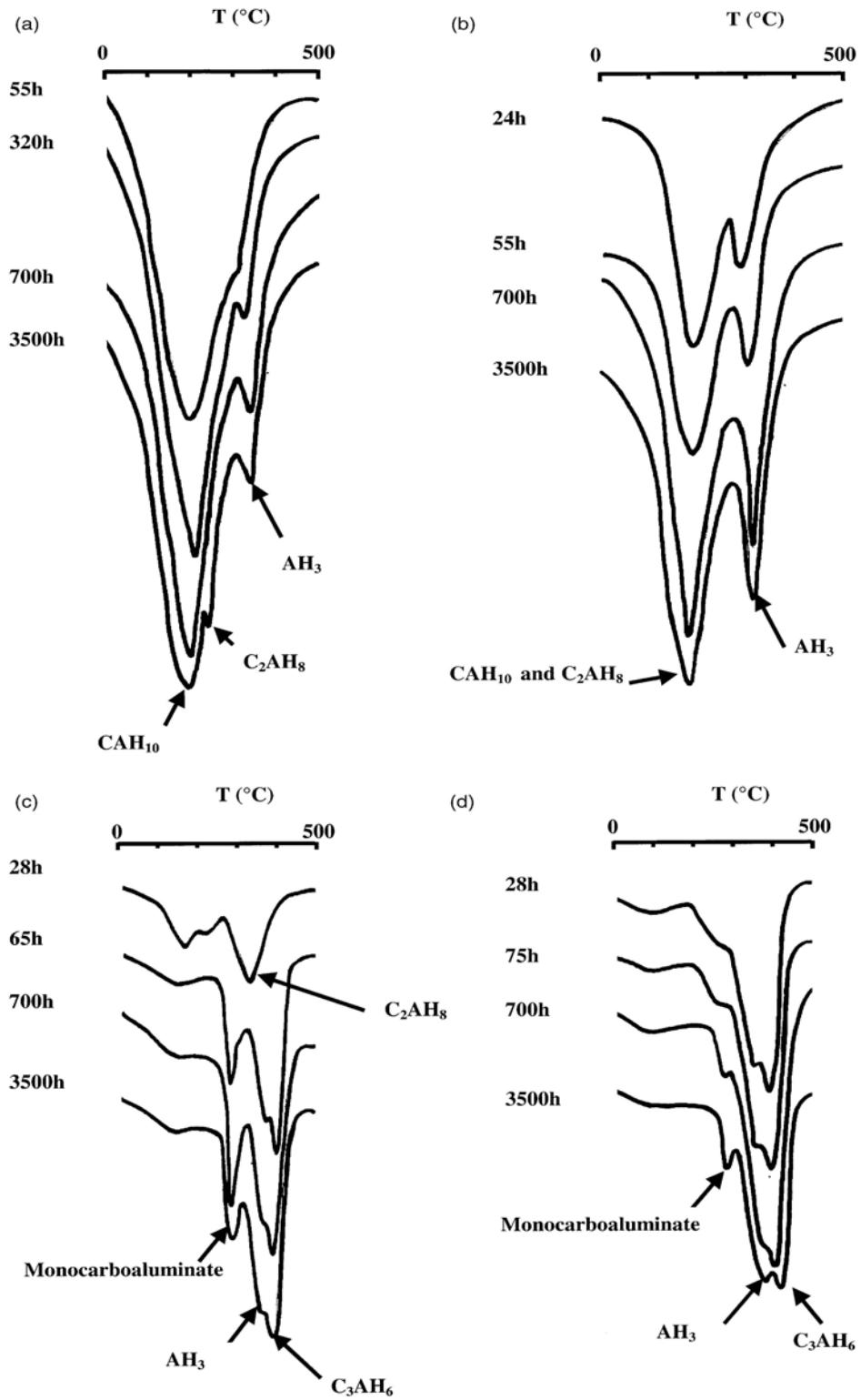


Figure 3.2 DTA Diagrams at Different Temperatures (a) 5°C, (b) 20°C, (c) 40°C, (d) 60°C [59,60]

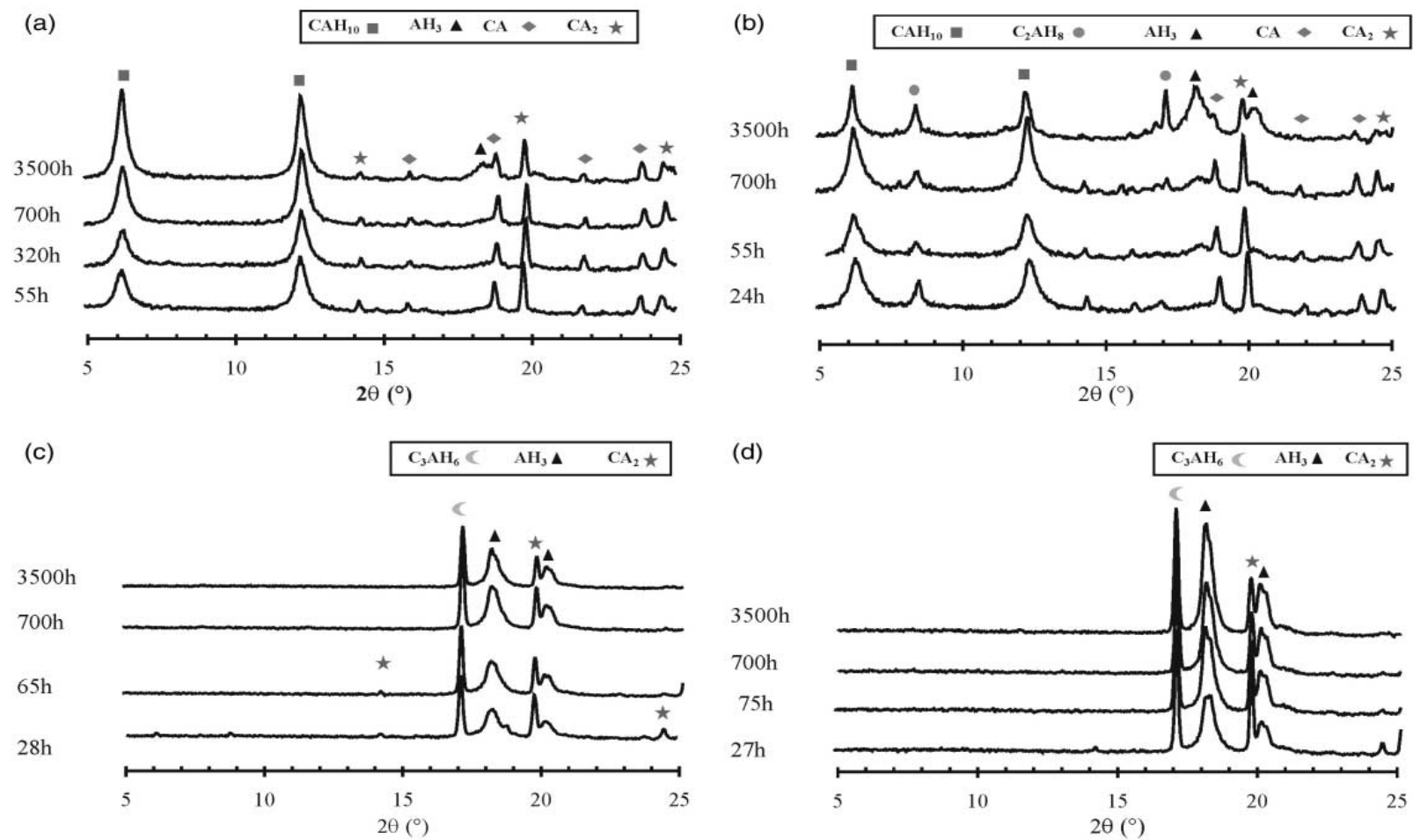


Figure 3.3 XRD Diagrams at Different Temperatures (a) 5°C, (b) 20°C, (c) 40°C, (d) 60°C [59,60]

Table 3.1 Types of Hydrates at Different Temperatures [59,60]

Temperature (°C)	Time after mixing (h)	DTA (amorphous and crystalline phases)	XRD (crystalline phases)
5	55	CAH ₁₀ , AH ₃	CAH ₁₀
	320	CAH ₁₀ , AH ₃	CAH ₁₀
	700	CAH ₁₀ , AH ₃	CAH ₁₀
	3500	CAH ₁₀ , C ₂ AH ₈ , AH ₃	CAH ₁₀ , C ₂ AH ₈
20	24	CAH ₁₀ , C ₂ AH ₈ , AH ₃	CAH ₁₀ , C ₂ AH ₈
	55	CAH ₁₀ , C ₂ AH ₈ , AH ₃	CAH ₁₀ , C ₂ AH ₈
	700	CAH ₁₀ , C ₂ AH ₈ , AH ₃	CAH ₁₀ , C ₂ AH ₈
	3500	CAH ₁₀ , C ₂ AH ₈ , AH ₃	CAH ₁₀ , C ₂ AH ₈ , AH ₃
40	28	C ₂ AH ₈ , C ₃ AH ₆ , AH ₃	C ₂ AH ₈ , C ₃ AH ₆ , AH ₃
	65	C ₃ AH ₆ , AH ₃	C ₃ AH ₆ , AH ₃
	700	C ₃ AH ₆ , AH ₃	C ₃ AH ₆ , AH ₃
	3500	C ₃ AH ₆ , AH ₃	C ₃ AH ₆ , AH ₃
60	28	C ₃ AH ₆ , AH ₃	C ₃ AH ₆ , AH ₃
	75	C ₃ AH ₆ , AH ₃	C ₃ AH ₆ , AH ₃
	700	C ₃ AH ₆ , AH ₃	C ₃ AH ₆ , AH ₃
	3500	C ₃ AH ₆ , AH ₃	C ₃ AH ₆ , AH ₃

Andion et al. performed similar studies by the use of CAC with an alumina content of 40% [62]. In their study, CAC mortars with a w/c ratio of 0.7 were utilized for XRD analysis. XRD spectra at different temperatures and at the ages of 28 days and 120 days are shown in Figure 3.4 and Figure 3.5, respectively [62].

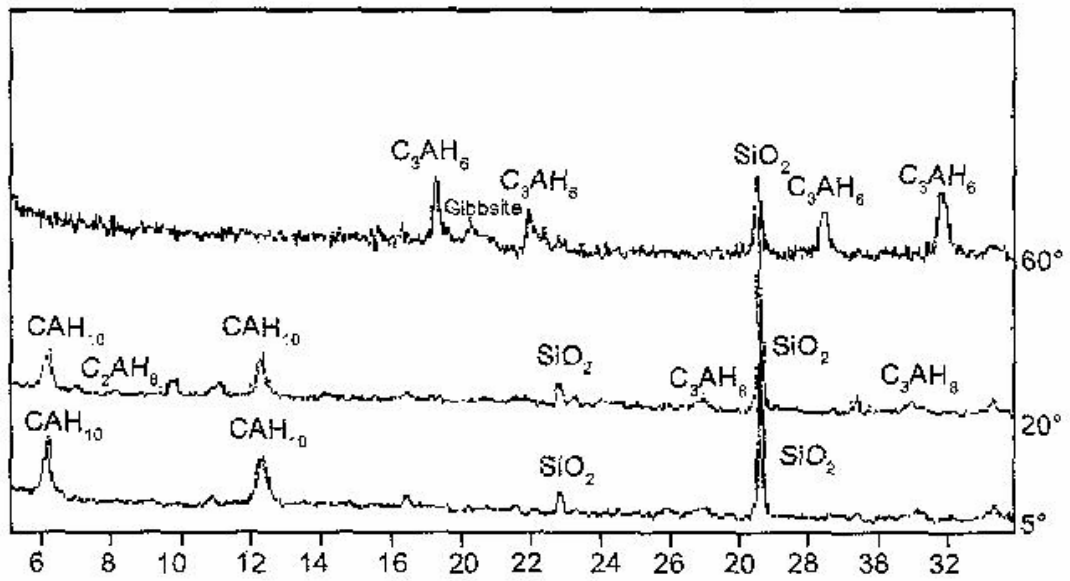


Figure 3.4 28 Days XRD Spectra of CAC Mortars at Different Temperatures [62]

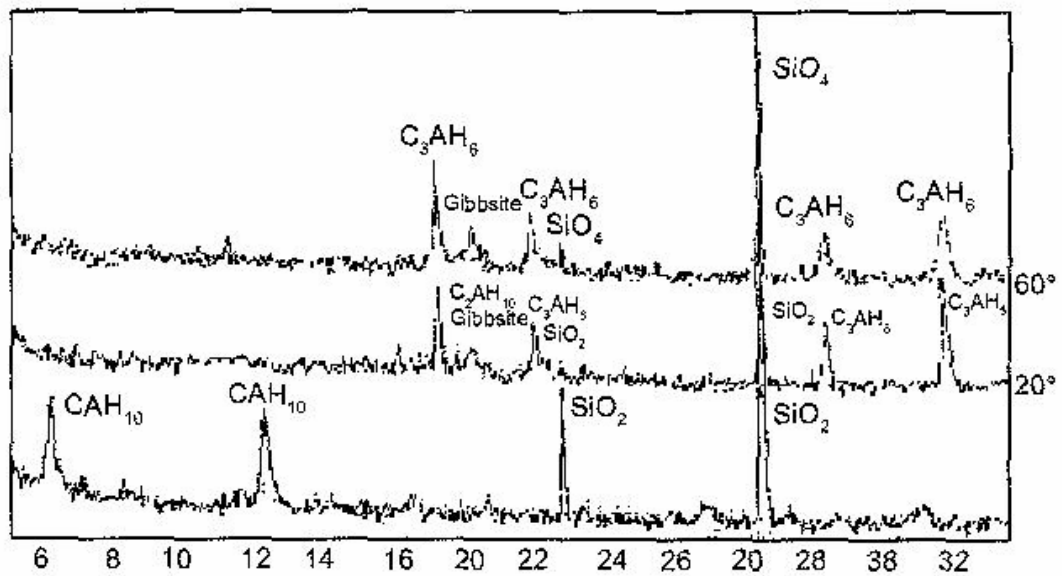


Figure 3.5 120 Days XRD Spectra of CAC Mortars at Different Temperatures [62]

If the curing temperature is 5°C, the predominant phase is hexagonal CAH₁₀. At 20°C the hexagonal phases, CAH₁₀ and C₂AH₈ are still present after 28 days. At longer ages, only the cubic phase, C₃AH₆, and gibbsite, AH₃, appear. If temperature is 60°C for all curing ages, only the cubic phase and the gibbsite appear [62].

3.2.2 Effects of Temperature on Strength

According to Lamour [53] et al., the increase in curing temperature of CAC mortars with an alumina content of 40% causes more stable calcium aluminate hydrate instead of metastable ones, which directly results in a decrease in compressive strength. The test data regarding with this interpretation are summarized in Table 3.2.

Table 3.2 Effects of Curing Temperature on Strength of CAC [53]

Temperature (°C)	Age	Hydrates	Compressive Strength (MPa)
20	7 h	metastable	59.1
	31h	metastable	76.2
	7 d	metastable	84.6
	35 d	metastable	95.8
	90 d	metastable	87.8
38	31 h	metastable	82.9
	8 d	metastable	91.9
	35 d	stable	46.3
	90 d	stable	51.0
70	7 h	stable	32.9
	8 d	stable	44.7

The decrease in compressive strength of CAC mortars depending on the increase in temperature can be explained by two reasons: (i) conversion of CAC causes liberation of chemically bound water of CAH_{10} and C_2AH_8 , and thus porosity of the matrix increases resulting in a reduction in strength [1] (This correlation which is shown in Figure 3.6 was explained in the study of Andion et al, too [62]), (ii) as a less important factor, it is the fact that the bonds of C_3AH_6 and AH_3 are weaker than those of CAH_{10} and C_2AH_8 , even at equal porosity [1,62].

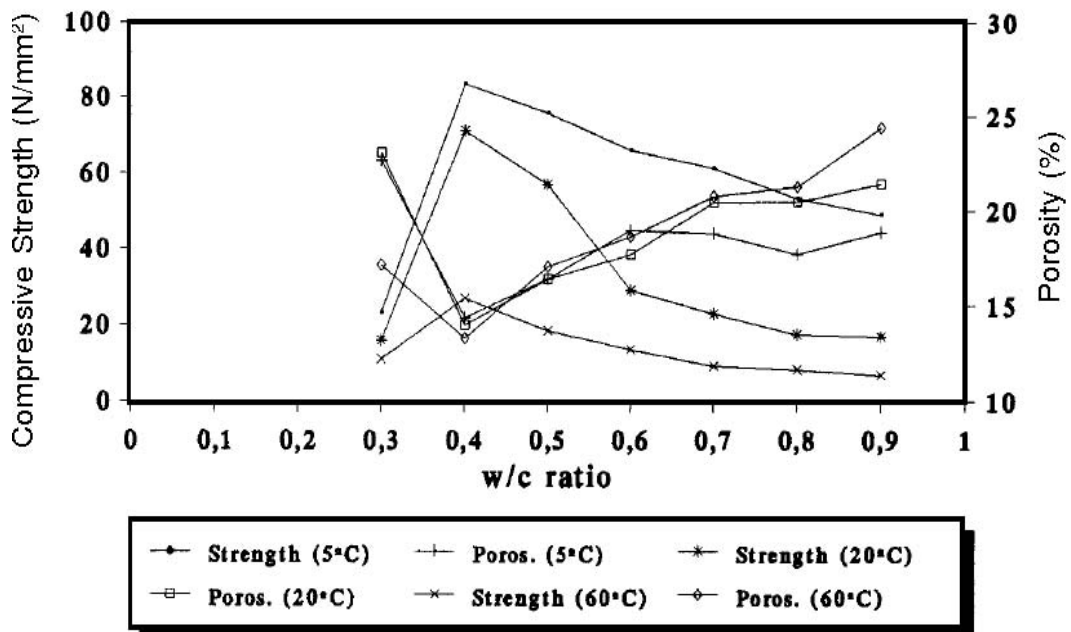


Figure 3.6 Relationship among Compressive Strength, W/C Ratio and Porosity of CAC at 28 Days and Cured at Different Temperatures [62]

Generally speaking, for the same w/c ratio, the strengths of calcium aluminate hydrates formed at low temperatures are better than those of calcium aluminate hydrates formed in hot cure. This is explained by increased porosity depending on the increase in curing temperatures [62].

3.2.3 Effects of Temperature and Water-Cement Ratio on Strength

Andion et al. [62] pointed out in their study the fact that as well as temperature, w/c ratio is another factor affecting the conversion and thus strength development. The relationship among compressive strength, time and w/c ratio was portrayed in Figure 3.7 [62].

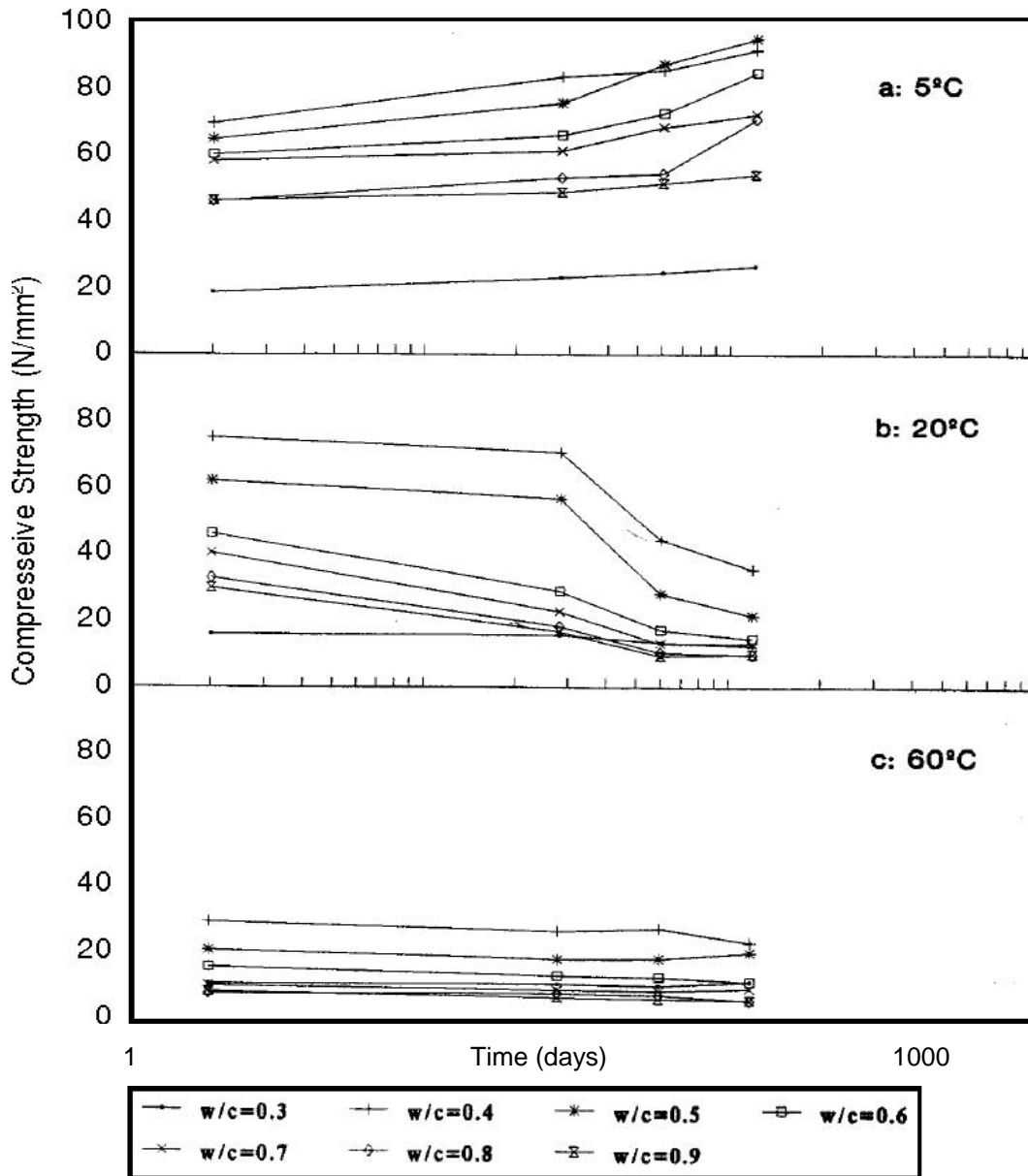


Figure 3.7 Relationship Among Compressive Strength, Time, and W/C Ratio [62]

Similar relations were investigated much earlier by Building Research Establishment in London [3,63]. These relations given in its annual report are shown in Figure 3.8.

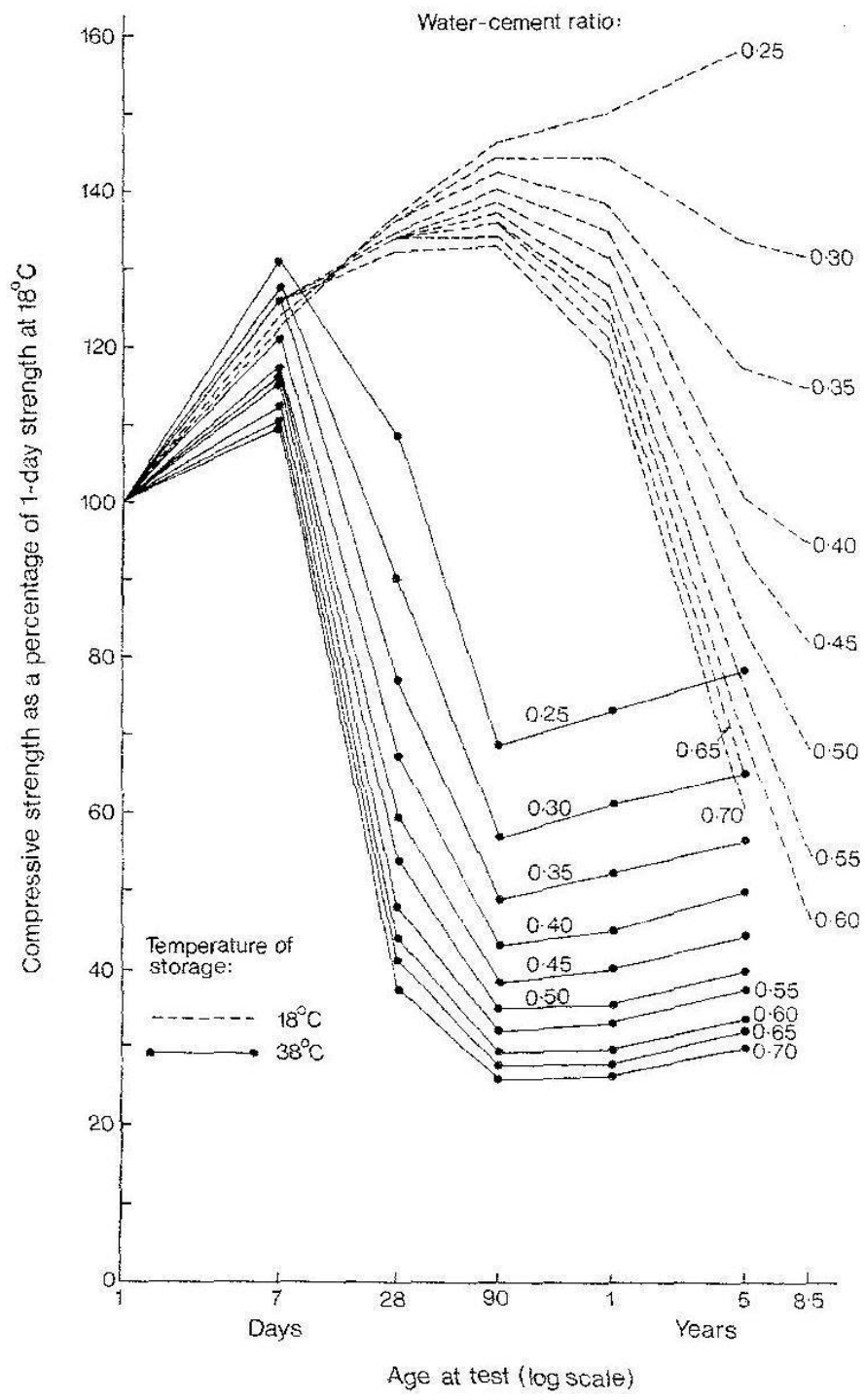


Figure 3.8 Influence of Water-Cement Ratio on the Long-Term Strength of CAC Concrete Stored at 18°C and 38°C [3,63]

In both of the studies shown in Figure 3.7 and Figure 3.8, it is clear that as well as temperature increase, the increase in w/c ratio also speeds up the formation of conversion reactions.

In addition, w/c ratio is of vital importance in the initial strength value, similar to ordinary PC. Providing that full compaction of CAC mix is achieved during placing, a reduction in w/c ratio gives increased strength and thus improved properties in terms of other performance criteria [6].

3.3 Previous Studies on CAC-PC Combinations

In some concrete practices where rapid setting and hardening is required binary cement system of CAC and PC may be used. Particularly, in repair mortars application, some special properties, such as rapid setting and hardening, good adhesion, compatibility with existing structure, volume stability and corrosion resistance are often required. By blending CAC with an ordinary PC, some interesting properties can be obtained. However, even though setting and hardening time is shorter, the strength at specified ages may be lower than the strength obtained by pure CAC or PC. Therefore, the hydration mechanism of CAC-PC combination has to be well understood [28].

Figure 3.9 shows a typical curve of setting time for such binary mixes [9].

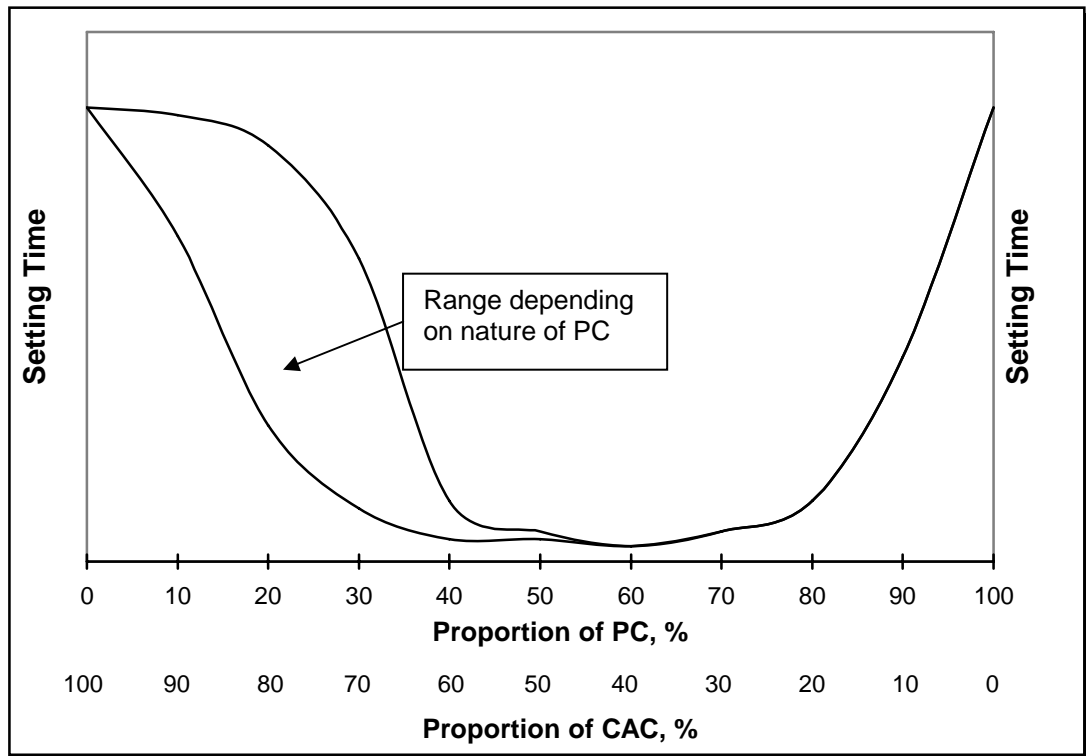


Figure 3.9 Setting Times of CAC-PC Combinations [9]

As seen in Figure 3.9, CAC-PC mixes in different ratios exhibit different setting behaviour than each of these cements separately. The similar relation can be observed in strength behaviour, as seen in Figure 3.10 [7]

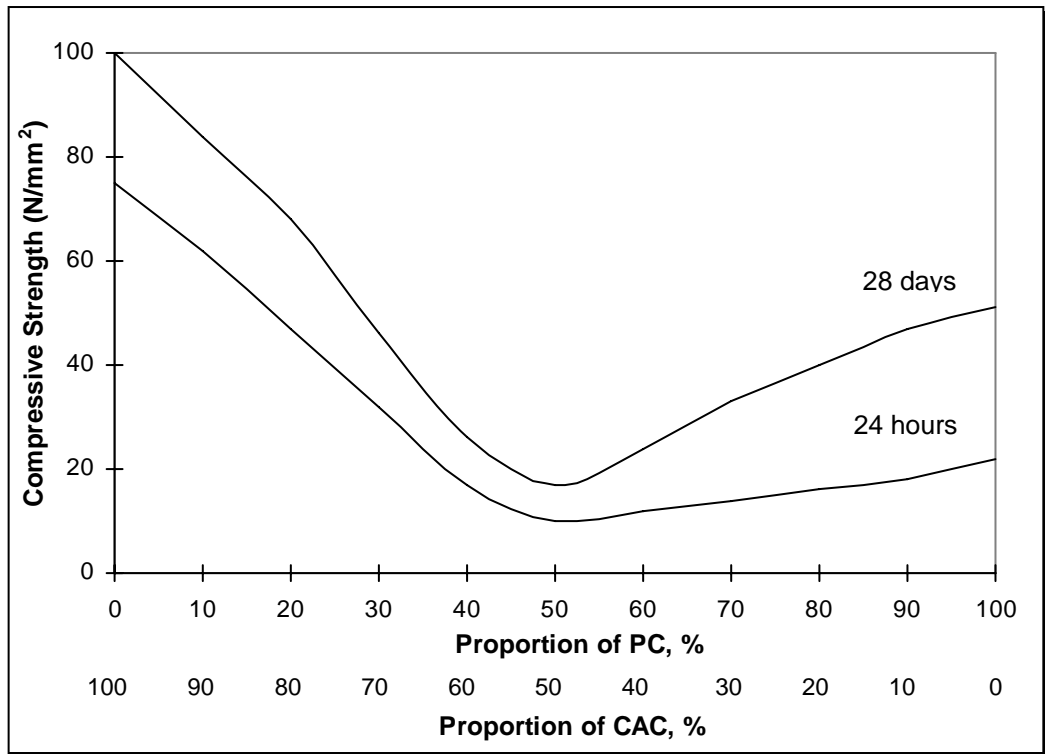


Figure 3.10 Compressive Strength of CAC-PC Combinations [7]

According to Gu et al. [28], many factors influence the strength development of CAC-PC systems. It is clear that the ratio of CAC to PC is critical for hydration mechanism. Factors affecting such a strength development behaviour can be listed as; formation of ettringite, C-S-H, CH, monosulphoaluminate hydrate, and CAH_{10}/C_2AH_8 [28]. Based on the XRD analysis of Gu et al., compounds being formed in CAC-PC mixes at different ratios are summarized in Table 3.3 [28]

Table 3.3 Summary of Compounds Identified by XRD Analysis of CAC-PC Combinations at Different Ages [28]

CAC/PC Ratio	Age				
	1/2 h	4 h	8 h	24 h	48 h
7.5/92.5	gypsum	ettringite, gypsum	ettringite, CH	ettringite, CH	ettringite, CH
20/80	ettringite, gypsum	ettringite, gypsum	ettringite, gypsum	ettringite,	ettringite, CH
80/20	-	-	CAH ₁₀ / C ₂ AH ₈	CAH ₁₀ / C ₂ AH ₈	CAH ₁₀ / C ₂ AH ₈

As seen in Table 3.3, in the mixes where CAC is the minor constituent, rapid formation of needle-like ettringite formation causes primarily quick setting and hardening, whereas in the mixes where CAC is the main constituent, hydration of calcium aluminates governs the quick setting and hardening behaviour [28].

Moreover, Gu et al. [28] claim that the strength decreases in CAC-PC mixes compared to pure PC mix is owing to the delayed hydration of C₃S. That means calcium silicates have little influence on setting process.

Odler stated that in addition to the phases formed in the hydration of pure PC and CAC, straetlingite may also present in the CAC-PC blends at later ages, since formation of straetlingite is slow [1].

There are several studies related with CAC-PC blends in literature conforming to the issues explained [25-30].

3.4 Previous Studies on CAC-Gypsum Combinations

Blends of CAC and gypsum are a special type of binder, which is based upon ettringite formation like blends of CAC and PC explained in the previous section. Ettringite based cements, generally speaking, achieve rapid strength gain as well as self-stressing property [64]. In other words, through blending CAC with gypsum in different ratios, mixes with different setting and hardening times can be produced. In addition, such ettringite formation may compensate shrinkage and hinder early age cracking [9].

In such systems, two basic issues are often questioned; (i) whether presence of ettringite causes durability problems or not, and (ii) whether conversion reactions occur or not [9].

It is well known that delayed ettringite formation causes detrimental results in terms of cracking, as seen during ordinary PC practice. However, in CAC-gypsum combination, whole ettringite formation occurs during the initial hydration reactions. Providing that all calcium sulphate reacts before stiffening of the mix, no harmful expansion will occur [9].

Zhou and Glasser [65] reported that ettringite will not decompose in materials used in the normal range of ambient temperature. Therefore, in

ettringite based binders, such as CAC-gypsum combination, conversion may not occur provided that there is no formation of metastable calcium aluminate hydrates. In such mixes, they will not form until the amount of sulphate is less than that required to combine all the calcium aluminates, which is equal to 13% of calcium sulphate expressed as anhydrite [9,65]

3.5 Previous Studies on CAC-Lime Combinations

Lime is often added to CAC to shorten the setting and hardening period. It mainly increases pH value of such blends. Like little amount of PC addition to CAC, lime addition causes an increase in the pH value, which as a result brings about accelerated hydration. In other words, quick setting and hardening is governed by accelerated hydration of calcium aluminates. That is why, generally speaking, conversion reactions occurred in pure CAC may also be experienced in CAC-lime blends depending on temperature and humidity increase.

3.6 Previous Studies on CAC-GGBFS Combinations

Addition of ground granulated blast furnace slag in CAC system drastically changes the hydration mechanism of pure CAC system. According to the studies carried out till now [35-46], in CAC-GGBFS blends with proper ratios there is no conversion causing strength loss with time depending on mainly temperature and humidity. Quillin et al. [35] reported that the modified chemistry on hydration caused by the high silica content of the GGBFS addition prevents conversion in CAC-GGBFS blends. In fact, calcium aluminates react with amorphous silica coming from GGBFS in

the presence of moisture and form C_2ASH_8 , known as straetlingite or gehlenite hydrate. Due to its high stability, CAC-GGBFS blends do not exhibit the loss of compressive strength that occurs in pure CAC system even though they are kept at elevated temperatures under wet conditions throughout a prolonged period of time [35,39].

Figure 3.11 shows compressive strength development of CAC-GGBFS mixes with time at 20°C. In the blends, the ratio of CAC to GGBFS was 1, and two different w/c ratios were utilized.

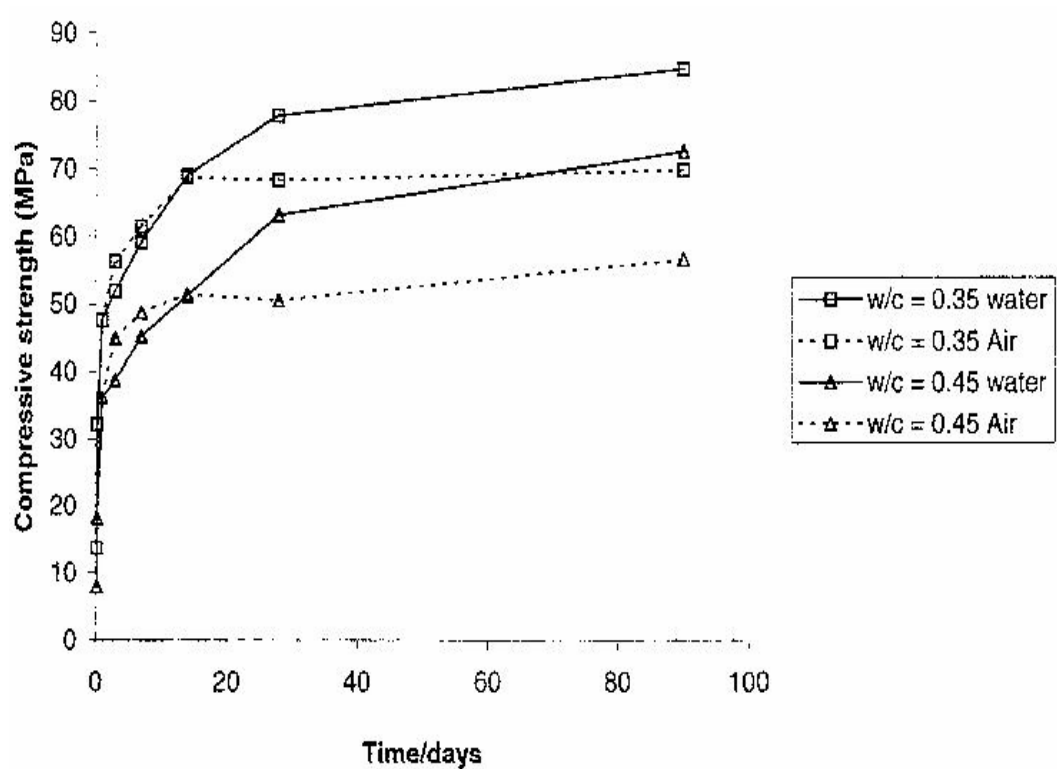


Figure 3.11 Compressive Strength Development of 50% CAC - 50% GGBFS Combination at 20°C [35]

At the same ages, when compressive strength test was conducted, XRD analyses were also performed to understand the mechanism of strength development, which depends particularly on mineralogy [35]. According to the related XRD analysis, Quillin et al. [35] listed the phases present in CAC-GGBFS blends throughout time, which is summarized in Table 3.4.

Table 3.4 Phases Present in CAC-GGBFS Blends [35]

Age	w/c=0.35 air stored	w/c=0.35 water stored	w/c=0.45 air stored	w/c=0.45 water stored
4h	CAH ₁₀ (s)	CAH ₁₀ (s)	CAH ₁₀ (s)	CAH ₁₀ (s)
24h	CAH ₁₀ (s)	CAH ₁₀ (s)	CAH ₁₀ (s)	CAH ₁₀ (s)
3d	CAH ₁₀ (s) C ₂ ASH ₈ (tr)	CAH ₁₀ (s)	CAH ₁₀ (s) C ₂ ASH ₈ (m)	CAH ₁₀ (s) C ₂ ASH ₈ (tr)
7d	CAH ₁₀ (s) C ₂ ASH ₈ (tr)	CAH ₁₀ (s) C ₂ ASH ₈ (m)	CAH ₁₀ (s) C ₂ ASH ₈ (tr)	CAH ₁₀ (s) C ₂ ASH ₈ (s)
14d	CAH ₁₀ (s) C ₂ ASH ₈ (tr)	CAH ₁₀ (s) C ₂ ASH ₈ (s)	CAH ₁₀ (m/w) C ₂ ASH ₈ (s)	CAH ₁₀ (tr) C ₂ ASH ₈ (s)
90d	CAH ₁₀ (m) C ₂ ASH ₈ (w) AH ₃ (tr)	CAH ₁₀ (w) C ₂ ASH ₈ (s)	CAH ₁₀ (w) C ₂ ASH ₈ (s) AH ₃ (tr)	CAH ₁₀ (w) C ₂ ASH ₈ (s) AH ₃ (tr)

s = strong; m = medium peak; w= weak; tr = trace.

As seen in Figure 3.11, there is no decrease in compressive strength whether the samples cured in air or water, or whether the w/c is 0.35 or 0.45. This is owing to the fact that as can be seen in Table 3.4, although initially formed phase is CAH_{10} , which is prone to conversion, stable phase gehlenite hydrate starts to form from the age of 3 days. As time increases, the amount of CAH_{10} decreases by an increase in the amount of C_2ASH_8 in all cases [35].

Quillin et al. [35] also investigated the effects of CAC/GGBFS ratios on strength development at ambient temperature of $20^{\circ}C$. This was portrayed in Table 3.5.

As given in Table 3.5, Quillin reported that particularly 40% CAC to 60% GGBFS blend shows an increase in strength with time, whereas other mixes experience strength losses. This fact was explained by Quillin et al. by considering XRD peak heights at 12.49° and 5.1° for C_2ASH_8 and C_3AH_6 , respectively. Although the analysis is not quantitative, these ratios suggest that the amount of C_2ASH_8 present at both 1 and 5 years increases with the increase in GGBFS amount. This trend is consistent with the strength development shown in Table 3.5 [35,43].

Table 3.5 Some Properties of CAC-GGBFS Blends in Different Mix Ratios [35]

Properties	CAC/GGBFS Ratio			
	100/0	60/40	50/50	40/60
<i>Compressive Strength</i>				
8-9 days	40.8	25.0	31.0	38.0
29-32 days	36.0	26.0	34.0	41.0
180-190 days	36.9	47.5	36.0	47.0
1 year	41.8	32.4	45.2	53.6
5 years	-	32.1	38.0	55.0
<i>Phase at 180 days</i>				
C ₃ AH ₆	strong	strong	medium	trace
C ₂ ASH ₈	not detected	weak	strong	strong
AH ₃	strong	strong	trace	not detected
<i>C₂ASH₈/C₃AH₆ Ratio</i>				
1 year	-	0.03	2.7	7.1
5 year	-	0.3	2.4	7.7

Singh et al. [41] made studies on temperature effect on CAC-GGBFS blend. Throughout their research, they kept the 50% CAC to 50% GGBFS blend for 10 years at 20°C and 38°C. Related compressive strength value vs. time graph is given in Figure 3.12.

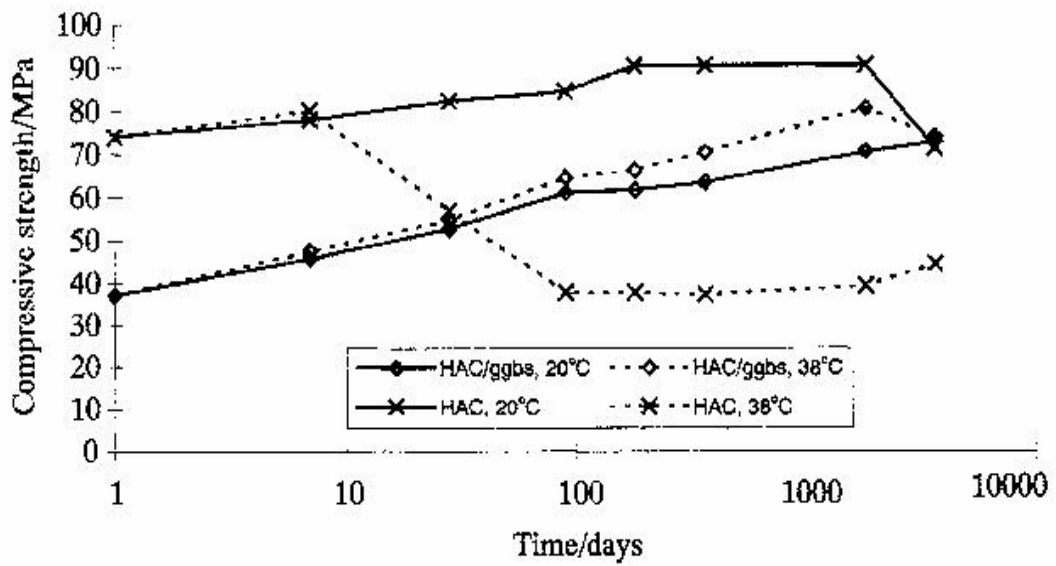


Figure 3.12 Compressive Strength Development of CAC-GGBFS Blend at 20°C and 38°C [41]

Based on the trends shown in compressive strength versus time graph, it is interpreted that increase in curing temperature causes rapid strength losses, as can be seen from the trend line of pure CAC at 38°C. On the other hand, delayed strength losses, particularly after the age of 5 years, are observed in pure CAC mixture cured at 20°C. However, CAC-GGBFS blends show no or very slight decrease in strength at both curing temperatures. This is mainly due to the formation of C_2ASH_8 , stable gehlenite hydrate phase in CAC-GGBFS blends, which cannot form in pure CAC mixes [41].

CHAPTER 4

EXPERIMENTAL STUDY

4.1 Introduction

As stated previously, the objective of this experimental study is to investigate the effects of temperature on calcium aluminate cement (CAC) based composite binders. Therefore, different types of materials were used in producing composite binders. As the name implies, main constituent of such composite binders was CAC, whereas the other constituents were portland cement (PC), gypsum, lime, and ground granulated blast furnace slag (GGBFS). The characteristics of the materials used in this study are given in the following sections.

Several binary binder systems were prepared by mixing the materials mentioned above in different ratios. The mortar or paste samples of these composite binders were then subjected to different curing temperatures, in order to examine their behaviour depending upon temperature. Setting time, heat of hydration, strength development and mineralogical composition were determined throughout this study.

The details of experimental study will be discussed in the following sections.

4.2 Materials

Throughout the study, four different types of binders namely; PC, gypsum, lime, and GGBFS were mixed with CAC. For strength tests, mortars were prepared according to TS-EN 196-1 [66].

CAC (ISIDAÇ 40) and PC (CEM I 42.5 R) were obtained from ÇimSA Cement Production and Trade Co. in Mersin. As the name implies, ISIDAÇ 40 contains 40% of alumina and therefore corresponds to the 4th class CAC in the relevant standard, TS 6271 [5].

Other binders, lime, gypsum, and GGBFS were procured from Erciyes Lime Factory in Kayseri, Alçıbay Gypsum Factory in Ankara, and İskenderun Iron and Steel Plant in Hatay, respectively.

The oxide compositions of the binders as determined by XRF analysis, are shown in Table 4.1.

The fineness of binders as analysed by two methods: determination of specific surface area by Blaine apparatus and determination of median size by Malvern Mastersizer laser granulometer is presented in Table 4.2.

Table 4.1 Chemical Compositions of Binders

Oxides (%)	CAC	PC	GGBFS	Lime	Gypsum
CaO	37.56	63.07	37.16	58.56	32.57
SiO ₂	2.20	19.61	35.94	0.21	0.23
Al ₂ O ₃	40.12	4.89	12.06	0.23	0.09
Fe ₂ O ₃	17.12	2.62	0.64	0.05	0.04
MgO	0.84	2.03	7.59	0.60	0.46
SO ₃	0	2.92	2.29	0.36	43.68
K ₂ O	0.03	0.85	1.16	0.01	0
Na ₂ O	0	0.18	0.40	0	0.03
LOI	0	2.90	0	34.20	18.95

Table 4.2 Fineness of Binders

	Specific Surface Area (cm ² /g)	Median Size (μm)
CAC	3290	17.85
PC	3470	13.09
GGBFS	4420	9.38
Lime	3380	9.79
Gypsum	2860	21.83

The compressive and flexural strengths of CAC and ordinary PC as determined according to the related standards, prEN 14647 [4] and TS-EN196-1 [66], respectively, are given in Table 4.3.

Table 4.3 Compressive and Flexural Strengths of CAC and PC

	Compressive Strength (MPa)	Flexural Strength (MPa)
CAC		
at 6 hours	41.1	5.5
at 24 hours	63.2	8.2
at 28 days	85.1	9.1
PC		
at 2 days	27.6	6.3
at 28 days	47.8	9.4

The mineralogical compositions of inorganic binders were determined qualitatively by X-ray diffraction (XRD) analysis performed by using a Phillips PW-660 diffractometer with a Cu K α radiation. XRD patterns of CAC, PC, GGBFS, lime, and gypsum are displayed in Figures 4.1-4.5, respectively.

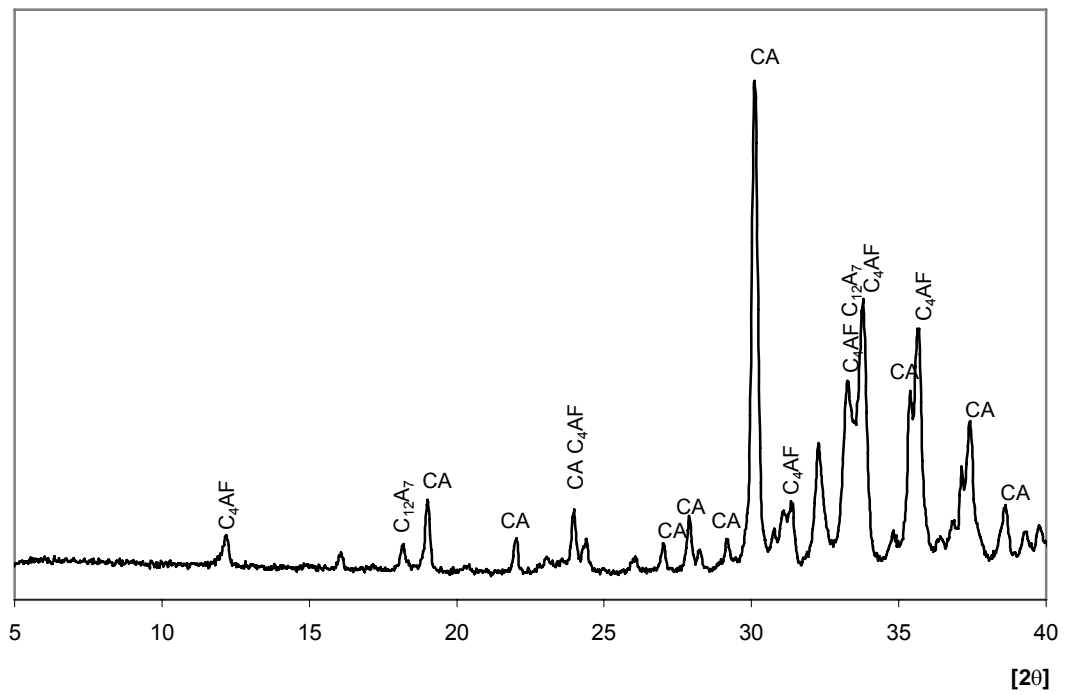


Figure 4.1 XRD Pattern of CAC

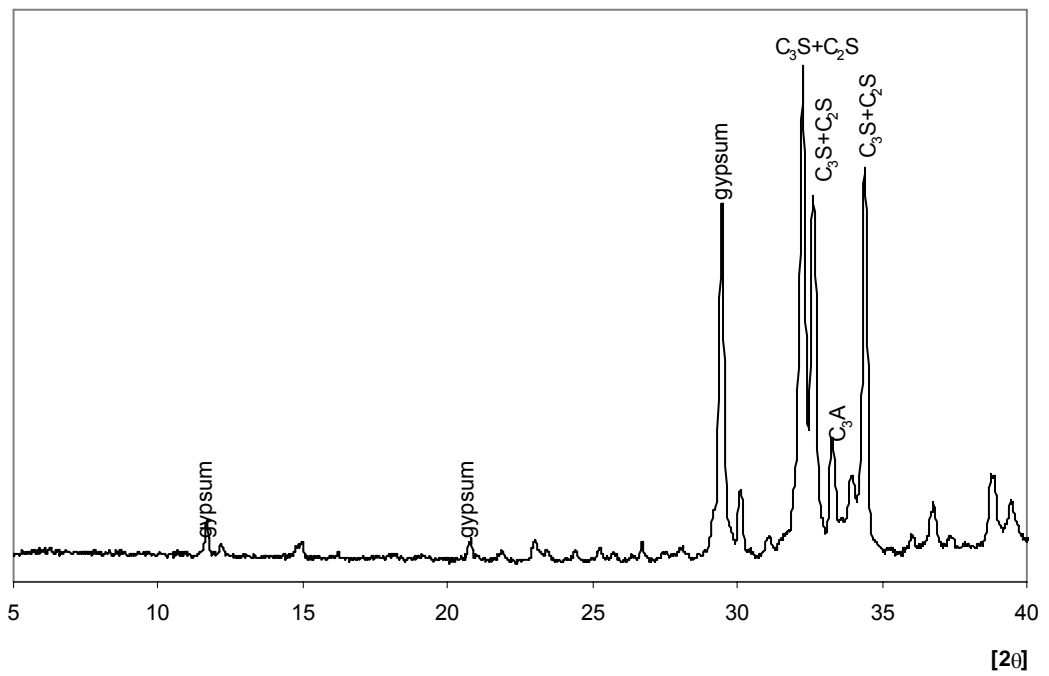


Figure 4.2 XRD Pattern of PC

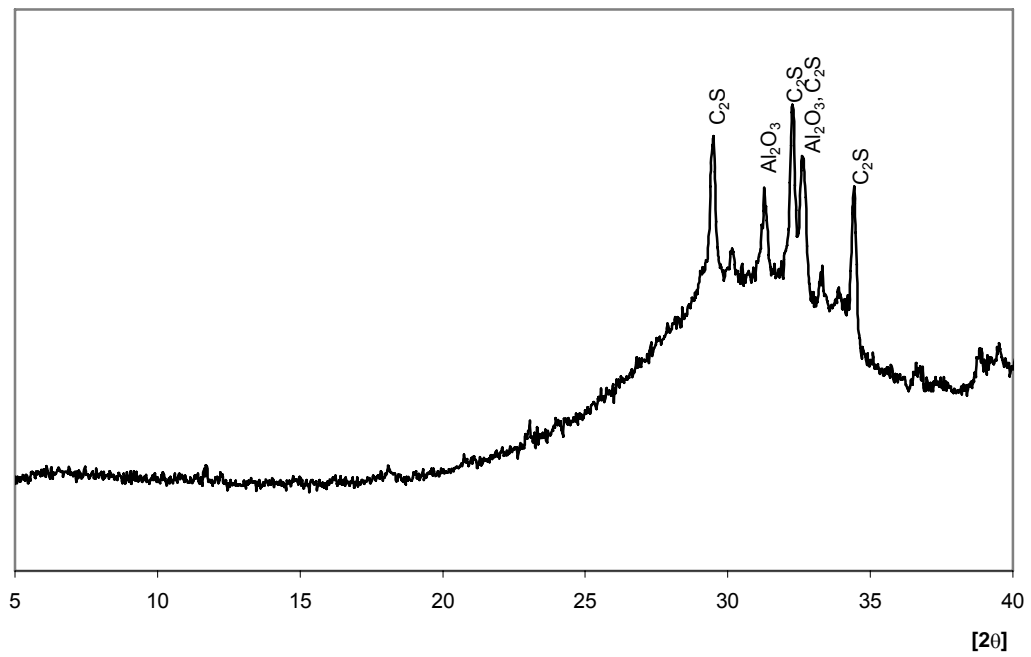


Figure 4.3 XRD Pattern of GGBFS

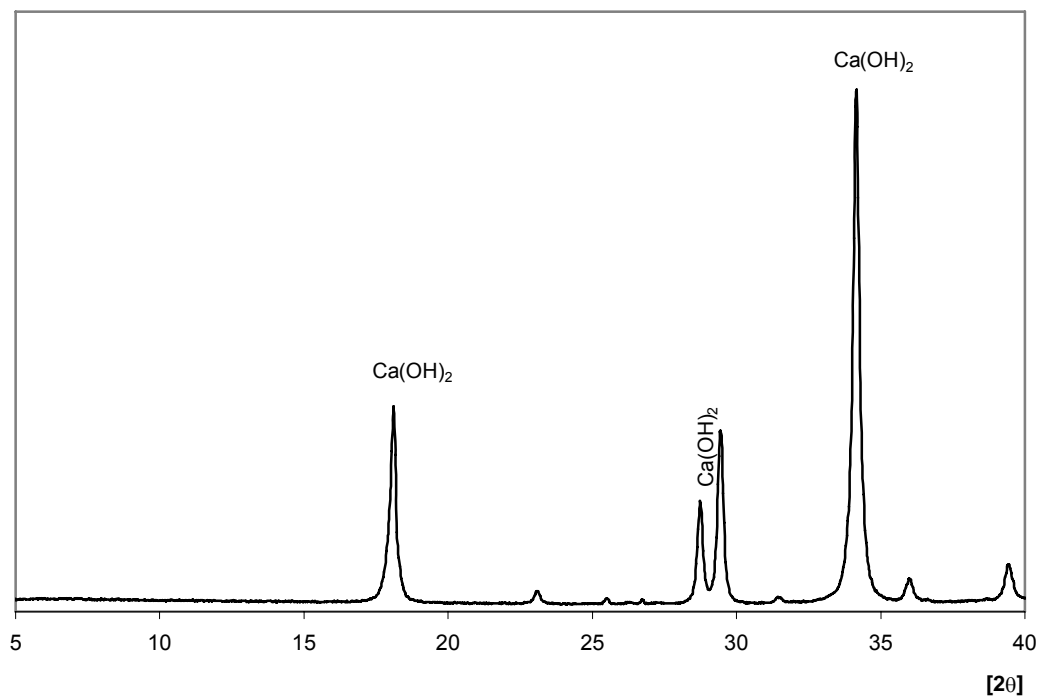


Figure 4.4 XRD Pattern of Lime

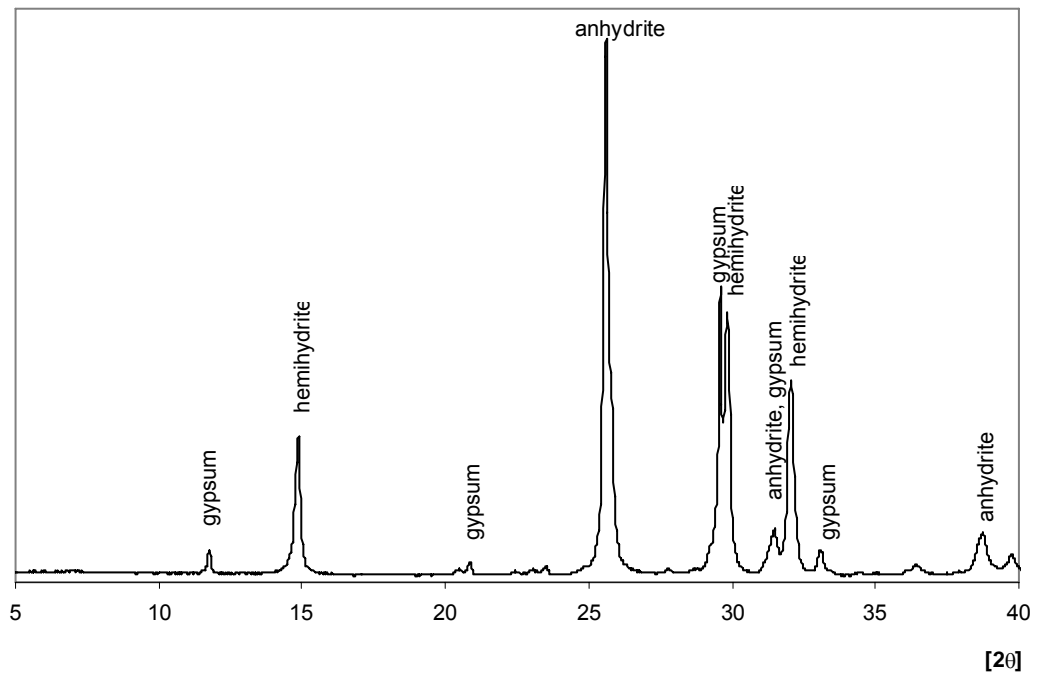


Figure 4.5 XRD Pattern of Gypsum

According to XRD analyses, CAC is composed of mainly CA, $C_{12}A_7$, and C_4AF ; whereas PC contains mainly C_3S , C_2S , and C_3A . On the other hand, $Ca(OH)_2$ is the dominant phase available in lime and $CaSO_4 \cdot 2H_2O$, $CaSO_4 \cdot 1/2H_2O$, and $CaSO_4$ are the dominant phases available in gypsum.

As seen in Figure 4.5, since the amorphous or poorly crystalline structure prevents the identification of existing minerals in GGBFS, peaks in XRD pattern could not be assigned to minerals properly. Thus, only the traces of C_2S and Al_2O_3 can be detected.

4.3 Types of CAC Based Composite Binders

By the use of 5 different binders, i.e. CAC, PC, GGBFS, lime and, gypsum, 17 different CAC based cementitious systems were prepared. All of the prepared mixtures were composed of two different constituents in different ratios, except pure PC and the reference mix, pure CAC. The labelling and the proportions of the CAC based composite binders that were produced throughout the experimental study are as follows:

Pure CAC (reference mix)

100% CAC (designated as IP100=IA100=IK100=IC100)

CAC-PC Combinations (4 mixes)

75% CAC + 25% PC (designated as IP75)

50% CAC + 50% PC (designated as IP50)

25% CAC + 75% PC (designated as IP25)

0% CAC + 100% PC (designated as IP0)

CAC-Gypsum Combinations (4 mixes)

99.5% CAC + 0.5% Gypsum (designated as IA99,5)

98% CAC + 2% Gypsum (designated as IA98)

96% CAC + 4% Gypsum (designated as IA96)

92% CAC + 8% Gypsum (designated as IA92)

CAC-GGBFS Combinations (4 mixes)

80% CAC + 20% GGBFS (designated as IC80)

60% CAC + 40% GGBFS (designated as IC60)

40% CAC + 60% GGBFS (designated as IC40)

20% CAC + 80% GGBFS (designated as IC20)

CAC-Lime Combinations (4 mixes)

99,5% CAC + 0.5% Lime (designated as IK99.5)

99% CAC + 1% Lime (designated as IK99)

98% CAC + 2% Lime (designated as IK98)

96% CAC + 4% Lime (designated as IK96)

The designations “I”, “P”, “C”, “K”, and “A” represent the binders CAC, PC, GGBFS, lime, and gypsum, respectively. On the other hand, the numbers following the designations indicate the percentage of CAC as a main constituent. For instance, “IK98” designates the mixture of CAC and lime, where the percentage of CAC is 98%.

4.4 Experimental Program

The mortar and paste samples for each mixes were prepared with a constant water to binder ratio of 0.5.

The mortar samples for compressive and flexural strength determinations were obtained according to TS-EN 196-1 [66]. In mortar preparation, 450 g of CAC based composite binder, 1350 grams of standard sand according to TS-EN 196-1, and 225 g of water were used. All of the specimens were in size of 4x4x16 cm. At each specified age, three 4x4x16 cm specimens were tested for flexural strength determination and then the broken pieces obtained from flexural strength test were used in compression test. Thus,

six specimens were subjected to compression at each specified age for each curing regime.

The effects of temperature on CAC based composite binders were investigated by applying different curing regimes on the specimens. By the use of climatic chamber as shown in Figure 4.6, all specimens were cured in water at seven different temperatures. The curing regimes were given in Table 4.4. The accuracy of the temperature was $\pm 1^{\circ}\text{C}$

Table 4.4 Curing Regimes Applied

Regime Number	Temperature ($^{\circ}\text{C}$)	Remarks
1	20	Samples were subjected continuously to 20°C .
2	30	Samples were subjected continuously to 30°C .
3	20-30	Samples were subjected to 20°C for a period of 28 days and then to 30°C .
4	40	Samples were subjected continuously to 40°C .
5	20-40	Samples were subjected to 20°C for a period of 28 days and then to 40°C .
6	50	Samples were subjected continuously to 50°C .
7	20-50	Samples were subjected to 20°C for a period of 28 days and then to 50°C .

Compressive strength test of each mixes listed previously was performed at seven different curing temperatures at various ages. The testing ages were determined based on the conversion rate of mixes cured at different temperatures. In fact, as a result of conversion, the ones cured at ambient temperatures experienced strength losses in a long term, whereas others cured at elevated temperatures in a short term. Therefore, mixes cured at elevated temperatures were subjected to strength test at earlier ages and more frequently than mixes cured at ambient temperatures.



Figure 4.6 Climatic Chamber Where Different Curing Regimes Were Applied

Even though the strength tests were performed on each blend listed previously, only the mixes IP100 (=IC100=IK100=IA100), IP75, IP25, IP0, IA96, IC80, IC60, IC40, and IK98 were selected among all CAC based composite binders for XRD and heat of hydration analyses, which were carried out at 28 days and 210 days. According to the previous studies, in CAC-gypsum combinations, rate of strength development is affected mainly by the formation of ettringite [31-34,64,65]. Thus, only a representative mix (IA96) among all CAC-gypsum combinations was selected for XRD analysis. Similarly, the mechanism of strength development of CAC-lime blends is similar to each other although the lime ratio was changed. Strength development of such blends is dominated by pH increase depending on lime inclusion. Therefore, only the mix IK98 was selected for XRD analysis. On the other hand, depending on the ratio of PC and GGBFS in CAC-PC and CAC-GGBFS combinations, respectively, the strength development mechanism differs significantly [25-30,35-46]. That is why, XRD analyses were conducted only on three mixes (IP75, IP25, IP0) of CAC-PC blends and only on three mixes (IC80, IC60, IC40) of CAC-GGBFS blends.

The paste samples for XRD analyses were prepared as follows:

- 5x5x5 cm paste samples of all the CAC based composite binder mixes were prepared and then stored in water at seven different curing temperatures until the time of analysis, i.e. 28 days and 210 days.
- At the specified testing age, the samples were taken out of water, and were crushed and ground by hand until the whole sample passes 90 μm sieve.
- 5 grams of each sample was obtained by quartering method.

- After filling the samples into a circular cup and pressing by screwing a rod onto the cup, pellet specimens were obtained.

After the preparation of a pellet specimen, it was put into the diffractometer and the intensity measurements were performed between 5° and 30° 2θ with an increment of 0.05° , measuring for 6 seconds per step.

Heat of hydration tests were conducted according to ASTM C 186-92 “Standard Test Method for Heat of Hydration of Hydraulic Cement” [67]. For understanding the mechanism of setting behaviour, 17 different CAC based composite binders were subjected to heat of hydration test by the use of a quasi-adiabatic calorimeter device, ToniCAL 7333 with a DCACON 4.04 software. Measuring temperature was 20°C and w/c ratio of 0.50 was used for all heat of hydration specimens.

The ages for the compressive strength tests and XRD analyses for the different curing regimes are shown in Tables 4.5-4.11.

Table 4.5 Ages and Types of Tests Performed on Samples Cured Continuously at 20°C

	Ages and Types of Tests												
	1hr	3hr	6hr	24hr	2d	7d	28d	60d	90d	120d	150d	180d	210d
IP100	S	S	S	S	S	S	S,X	S	S	S	S	S	S,X
IP75	S	S	S	S	S	S	S,X	S	S	S	S	S	S,X
IP50	S	S	S	S	S	S	S	S	S	S	S	S	S
IP25	S	S	S	S	S	S	S,X	S	S	S	S	S	S,X
IP0	S	S	S	S	S	S	S,X	S	S	S	S	S	S,X
IA99.5	S	S	S	S	S	S	S	S	S	S	S	S	S
IA98	S	S	S	S	S	S	S	S	S	S	S	S	S
IA96	S	S	S	S	S	S	S,X	S	S	S	S	S	S,X
IA92	S	S	S	S	S	S	S	S	S	S	S	S	S
IC80	S	S	S	S	S	S	S,X	S	S	S	S	S	S,X
IC60	S	S	S	S	S	S	S,X	S	S	S	S	S	S,X
IC40	S	S	S	S	S	S	S,X	S	S	S	S	S	S,X
IC20	S	S	S	S	S	S	S	S	S	S	S	S	S
IK99.5	S	S	S	S	S	S	S	S	S	S	S	S	S
IK99	S	S	S	S	S	S	S	S	S	S	S	S	S
IK98	S	S	S	S	S	S	S,X	S	S	S	S	S	S,X
IK96	S	S	S	S	S	S	S	S	S	S	S	S	S

S: Compressive strength tests; X: XRD analysis

Table 4.6 Ages and Types of Tests Performed on Samples Cured Continuously at 30°C

	Ages and Types of Tests																							
	1hr	3hr	6hr	24hr	2d	7d	14d	21d	28d	35d	42d	49d	56d	63d	70d	77d	84d	91d	98d	119d	133d	154d	182d	210d
IP100	S	S	S	S	S	S	S	S	S,X	S	S	S	S	S	S	S	S	S	S	S	S	S	S	S,X
IP75	S	S	S	S	S	S	S	S	S,X	S	S	S	S	S	S	S	S	S	S	S	S	S	S	S,X
IP50	S	S	S	S	S	S	S	S	S	S	S	S	S	S	S	S	S	S	S	S	S	S	S	S
IP25	S	S	S	S	S	S	S	S	S,X	S	S	S	S	S	S	S	S	S	S	S	S	S	S	S,X
IP0	S	S	S	S	S	S	S	S	S,X	S	S	S	S	S	S	S	S	S	S	S	S	S	S	S,X
IA99.5	S	S	S	S	S	S	S	S	S	S	S	S	S	S	S	S	S	S	S	S	S	S	S	S
IA98	S	S	S	S	S	S	S	S	S	S	S	S	S	S	S	S	S	S	S	S	S	S	S	S
IA96	S	S	S	S	S	S	S	S	S,X	S	S	S	S	S	S	S	S	S	S	S	S	S	S	S,X
IA92	S	S	S	S	S	S	S	S	S	S	S	S	S	S	S	S	S	S	S	S	S	S	S	S
IC80	S	S	S	S	S	S	S	S	S,X	S	S	S	S	S	S	S	S	S	S	S	S	S	S	S,X
IC60	S	S	S	S	S	S	S	S	S,X	S	S	S	S	S	S	S	S	S	S	S	S	S	S	S,X
IC40	S	S	S	S	S	S	S	S	S,X	S	S	S	S	S	S	S	S	S	S	S	S	S	S	S,X
IC20	S	S	S	S	S	S	S	S	S	S	S	S	S	S	S	S	S	S	S	S	S	S	S	S
IK99.5	S	S	S	S	S	S	S	S	S	S	S	S	S	S	S	S	S	S	S	S	S	S	S	S
IK99	S	S	S	S	S	S	S	S	S	S	S	S	S	S	S	S	S	S	S	S	S	S	S	S
IK98	S	S	S	S	S	S	S	S	S,X	S	S	S	S	S	S	S	S	S	S	S	S	S	S	S,X
IK96	S	S	S	S	S	S	S	S	S	S	S	S	S	S	S	S	S	S	S	S	S	S	S	S

S: Compressive strength tests; X: XRD analysis

Table 4.7 Ages and Types of Tests Performed on Samples Cured 28 days at 20°C then at 30°C

	Ages and Types of Tests																					
	1hr	3hr	6hr	24hr	2d	7d	28d	35d	42d	49d	56d	63d	70d	77d	84d	91d	98d	119d	133d	154d	182d	210d
IP100	S	S	S	S	S	S	S,X	S	S	S	S	S	S	S	S	S	S	S	S	S	S	S,X
IP75	S	S	S	S	S	S	S,X	S	S	S	S	S	S	S	S	S	S	S	S	S	S	S,X
IP50	S	S	S	S	S	S	S	S	S	S	S	S	S	S	S	S	S	S	S	S	S	S
IP25	S	S	S	S	S	S	S,X	S	S	S	S	S	S	S	S	S	S	S	S	S	S	S,X
IP0	S	S	S	S	S	S	S,X	S	S	S	S	S	S	S	S	S	S	S	S	S	S	S,X
IA99.5	S	S	S	S	S	S	S	S	S	S	S	S	S	S	S	S	S	S	S	S	S	S
IA98	S	S	S	S	S	S	S	S	S	S	S	S	S	S	S	S	S	S	S	S	S	S
IA96	S	S	S	S	S	S	S,X	S	S	S	S	S	S	S	S	S	S	S	S	S	S	S,X
IA92	S	S	S	S	S	S	S	S	S	S	S	S	S	S	S	S	S	S	S	S	S	S
IC80	S	S	S	S	S	S	S,X	S	S	S	S	S	S	S	S	S	S	S	S	S	S	S,X
IC60	S	S	S	S	S	S	S,X	S	S	S	S	S	S	S	S	S	S	S	S	S	S	S,X
IC40	S	S	S	S	S	S	S,X	S	S	S	S	S	S	S	S	S	S	S	S	S	S	S,X
IC20	S	S	S	S	S	S	S	S	S	S	S	S	S	S	S	S	S	S	S	S	S	S
IK99.5	S	S	S	S	S	S	S	S	S	S	S	S	S	S	S	S	S	S	S	S	S	S
IK99	S	S	S	S	S	S	S	S	S	S	S	S	S	S	S	S	S	S	S	S	S	S
IK98	S	S	S	S	S	S	S,X	S	S	S	S	S	S	S	S	S	S	S	S	S	S	S,X
IK96	S	S	S	S	S	S	S	S	S	S	S	S	S	S	S	S	S	S	S	S	S	S

S: Compressive strength tests; X: XRD analysis

Table 4.8 Ages and Types of Tests Performed on Samples Cured Continuously at 40°C

	Ages and Types of Tests																						
	1hr	3hr	6hr	24hr	2d	4d	6d	8d	10d	12d	14d	16d	18d	20d	28d	56d	84d	112d	133d	154d	182d	210d	
IP100	S	S	S	S	S	S	S	S	S	S	S	S	S	S	S,X	S	S	S	S	S	S	S	S,X
IP75	S	S	S	S	S	S	S	S	S	S	S	S	S	S	S,X	S	S	S	S	S	S	S	S,X
IP50	S	S	S	S	S	S	S	S	S	S	S	S	S	S	S	S	S	S	S	S	S	S	S
IP25	S	S	S	S	S	S	S	S	S	S	S	S	S	S	S,X	S	S	S	S	S	S	S	S,X
IP0	S	S	S	S	S	S	S	S	S	S	S	S	S	S	S,X	S	S	S	S	S	S	S	S,X
IA99.5	S	S	S	S	S	S	S	S	S	S	S	S	S	S	S	S	S	S	S	S	S	S	S
IA98	S	S	S	S	S	S	S	S	S	S	S	S	S	S	S	S	S	S	S	S	S	S	S
IA96	S	S	S	S	S	S	S	S	S	S	S	S	S	S	S,X	S	S	S	S	S	S	S	S,X
IA92	S	S	S	S	S	S	S	S	S	S	S	S	S	S	S	S	S	S	S	S	S	S	S
IC80	S	S	S	S	S	S	S	S	S	S	S	S	S	S	S,X	S	S	S	S	S	S	S	S,X
IC60	S	S	S	S	S	S	S	S	S	S	S	S	S	S	S,X	S	S	S	S	S	S	S	S,X
IC40	S	S	S	S	S	S	S	S	S	S	S	S	S	S	S,X	S	S	S	S	S	S	S	S,X
IC20	S	S	S	S	S	S	S	S	S	S	S	S	S	S	S	S	S	S	S	S	S	S	S
IK99.5	S	S	S	S	S	S	S	S	S	S	S	S	S	S	S	S	S	S	S	S	S	S	S
IK99	S	S	S	S	S	S	S	S	S	S	S	S	S	S	S	S	S	S	S	S	S	S	S
IK98	S	S	S	S	S	S	S	S	S	S	S	S	S	S	S,X	S	S	S	S	S	S	S	S,X
IK96	S	S	S	S	S	S	S	S	S	S	S	S	S	S	S	S	S	S	S	S	S	S	S

S: Compressive strength tests; X: XRD analysis

Table 4.9 Ages and Types of Tests Performed on Samples Cured 28 days at 20°C then at 40°C

	Ages and Types of Tests																						
	28d	30d	32d	34d	36d	38d	40d	42d	44d	46d	48d	50d	52d	54d	56d	70d	84d	112d	119d	154d	182d	210d	
IP100	S,X	S	S	S	S	S	S	S	S	S	S	S	S	S	S	S	S	S	S	S	S	S	S,X
IP75	S,X	S	S	S	S	S	S	S	S	S	S	S	S	S	S	S	S	S	S	S	S	S	S,X
IP50	S	S	S	S	S	S	S	S	S	S	S	S	S	S	S	S	S	S	S	S	S	S	S
IP25	S,X	S	S	S	S	S	S	S	S	S	S	S	S	S	S	S	S	S	S	S	S	S	S,X
IP0	S,X	S	S	S	S	S	S	S	S	S	S	S	S	S	S	S	S	S	S	S	S	S	S,X
IA99.5	S	S	S	S	S	S	S	S	S	S	S	S	S	S	S	S	S	S	S	S	S	S	S
IA98	S	S	S	S	S	S	S	S	S	S	S	S	S	S	S	S	S	S	S	S	S	S	S
IA96	S,X	S	S	S	S	S	S	S	S	S	S	S	S	S	S	S	S	S	S	S	S	S	S,X
IA92	S	S	S	S	S	S	S	S	S	S	S	S	S	S	S	S	S	S	S	S	S	S	S
IC80	S,X	S	S	S	S	S	S	S	S	S	S	S	S	S	S	S	S	S	S	S	S	S	S,X
IC60	S,X	S	S	S	S	S	S	S	S	S	S	S	S	S	S	S	S	S	S	S	S	S	S,X
IC40	S,X	S	S	S	S	S	S	S	S	S	S	S	S	S	S	S	S	S	S	S	S	S	S,X
IC20	S	S	S	S	S	S	S	S	S	S	S	S	S	S	S	S	S	S	S	S	S	S	S
IK99.5	S	S	S	S	S	S	S	S	S	S	S	S	S	S	S	S	S	S	S	S	S	S	S
IK99	S	S	S	S	S	S	S	S	S	S	S	S	S	S	S	S	S	S	S	S	S	S	S
IK98	S,X	S	S	S	S	S	S	S	S	S	S	S	S	S	S	S	S	S	S	S	S	S	S,X
IK96	S	S	S	S	S	S	S	S	S	S	S	S	S	S	S	S	S	S	S	S	S	S	S

S: Compressive strength tests; X: XRD analysis

Table 4.10 Ages and Types of Tests Performed on Samples Cured Continuously at 50°C

	Ages and Types of Tests																			
	1hr	3hr	6hr	12hr	24hr	1.5d	2d	2.5d	3d	3.5d	4d	4.5d	5d	7d	28d	56d	84d	112d	154d	210d
IP100	S	S	S	S	S	S	S	S	S	S	S	S	S	S	S,X	S	S	S	S	S,X
IP75	S	S	S	S	S	S	S	S	S	S	S	S	S	S	S,X	S	S	S	S	S,X
IP50	S	S	S	S	S	S	S	S	S	S	S	S	S	S	S	S	S	S	S	S
IP25	S	S	S	S	S	S	S	S	S	S	S	S	S	S	S,X	S	S	S	S	S,X
IP0	S	S	S	S	S	S	S	S	S	S	S	S	S	S	S,X	S	S	S	S	S,X
IA99.5	S	S	S	S	S	S	S	S	S	S	S	S	S	S	S	S	S	S	S	S
IA98	S	S	S	S	S	S	S	S	S	S	S	S	S	S	S	S	S	S	S	S
IA96	S	S	S	S	S	S	S	S	S	S	S	S	S	S	S,X	S	S	S	S	S,X
IA92	S	S	S	S	S	S	S	S	S	S	S	S	S	S	S	S	S	S	S	S
IC80	S	S	S	S	S	S	S	S	S	S	S	S	S	S	S,X	S	S	S	S	S,X
IC60	S	S	S	S	S	S	S	S	S	S	S	S	S	S	S,X	S	S	S	S	S,X
IC40	S	S	S	S	S	S	S	S	S	S	S	S	S	S	S,X	S	S	S	S	S,X
IC20	S	S	S	S	S	S	S	S	S	S	S	S	S	S	S	S	S	S	S	S
IK99.5	S	S	S	S	S	S	S	S	S	S	S	S	S	S	S	S	S	S	S	S
IK99	S	S	S	S	S	S	S	S	S	S	S	S	S	S	S	S	S	S	S	S
IK98	S	S	S	S	S	S	S	S	S	S	S	S	S	S	S,X	S	S	S	S	S,X
IK96	S	S	S	S	S	S	S	S	S	S	S	S	S	S	S	S	S	S	S	S

S: Compressive strength tests; X: XRD analysis

Table 4.11 Ages and Types of Tests Performed on Samples Cured 28 days at 20°C then at 50°C

	Ages and Types of Tests																
	28d	28.5d	29d	29.5d	30d	30.5d	31d	31.5d	32d	32.5d	33d	33.5d	56d	84d	112d	154d	210d
IP100	S,X	S	S	S	S	S	S	S	S	S	S	S	S	S	S	S	S,X
IP75	S,X	S	S	S	S	S	S	S	S	S	S	S	S	S	S	S	S,X
IP50	S	S	S	S	S	S	S	S	S	S	S	S	S	S	S	S	S
IP25	S,X	S	S	S	S	S	S	S	S	S	S	S	S	S	S	S	S,X
IP0	S,X	S	S	S	S	S	S	S	S	S	S	S	S	S	S	S	S,X
IA99.5	S	S	S	S	S	S	S	S	S	S	S	S	S	S	S	S	S
IA98	S	S	S	S	S	S	S	S	S	S	S	S	S	S	S	S	S
IA96	S,X	S	S	S	S	S	S	S	S	S	S	S	S	S	S	S	S,X
IA92	S	S	S	S	S	S	S	S	S	S	S	S	S	S	S	S	S
IC80	S,X	S	S	S	S	S	S	S	S	S	S	S	S	S	S	S	S,X
IC60	S,X	S	S	S	S	S	S	S	S	S	S	S	S	S	S	S	S,X
IC40	S,X	S	S	S	S	S	S	S	S	S	S	S	S	S	S	S	S,X
IC20	S	S	S	S	S	S	S	S	S	S	S	S	S	S	S	S	S
IK99.5	S	S	S	S	S	S	S	S	S	S	S	S	S	S	S	S	S
IK99	S	S	S	S	S	S	S	S	S	S	S	S	S	S	S	S	S
IK98	S,X	S	S	S	S	S	S	S	S	S	S	S	S	S	S	S	S,X
IK96	S	S	S	S	S	S	S	S	S	S	S	S	S	S	S	S	S

S: Compressive strength tests; X: XRD analysis

CHAPTER 5

TEST RESULTS AND DISCUSSION

5.1 Determination of Physical Properties of CAC Based Composite Binders

In calcium aluminate cement (CAC) based composite binders, the inclusion of portland cement (PC), ground granulated blast furnace slag (GGBFS), lime and gypsum into CAC may modify the properties of fresh and hardened mortars to a great extent. In order to investigate the effects of addition types and amounts on physical properties of CAC based composite binders, setting time and heat of hydration of 17 different composite binders were determined.

5.1.1 Setting Time

The initial and final setting time of mixes are listed in Table 5.1. In addition, the water requirement for normal consistency, which is essential for setting time determination, was determined according to TS EN 196-3 [68] and listed in the same table.

The effects of replacement ratios of PC, GGBFS, lime, and gypsum with CAC on setting time and on water requirement of CAC-PC, CAC-gypsum, CAC-GGBFS, and CAC-lime mixes are separately given in Figures 5.1-5.4, respectively.

Table 5.1 Setting Times of CAC Based Composite Binders

	Water Requirement for Normal Consistency (%)	Initial Setting Time (min)	Final Setting Time (min)
IP100	21.9	260	300
IP75	26.3	163	203
IP50	35.0	95	180
IP25	32.0	5	12
IP0	28.1	120	160
IA99,5	20.9	118	288
IA98	21.0	21	36
IA96	21.3	25	40
IA92	21.4	16	30
IC80	22.9	275	305
IC60	27.0	280	330
IC40	29.9	169	259
IC20	33.0	157	247
IK99,5	21.7	135	240
IK99	24.3	77	122
IK98	27.4	85	125
IK96	32.9	95	130

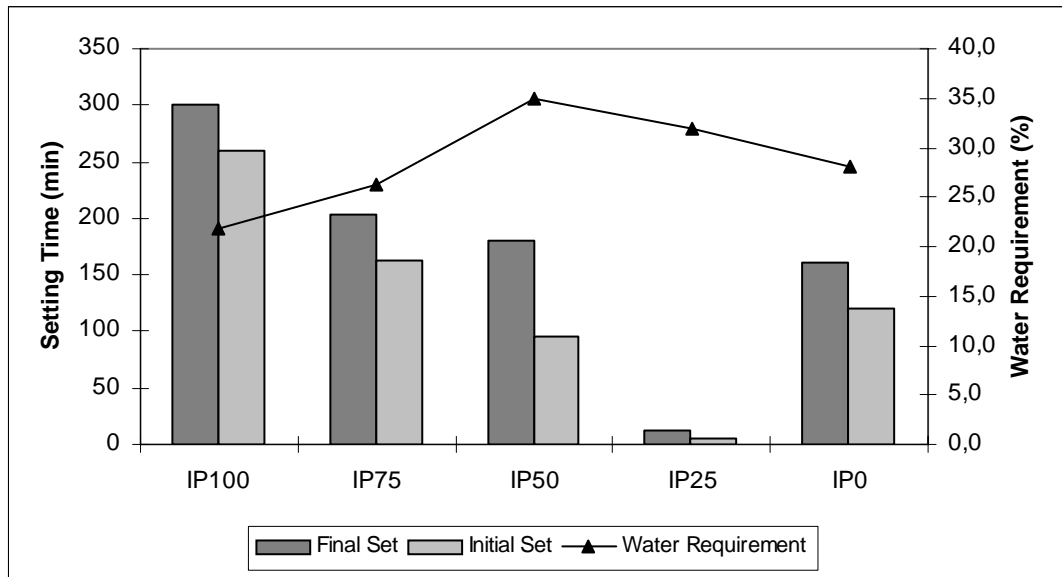


Figure 5.1 Setting Time and Water Requirement of CAC-PC Mixes

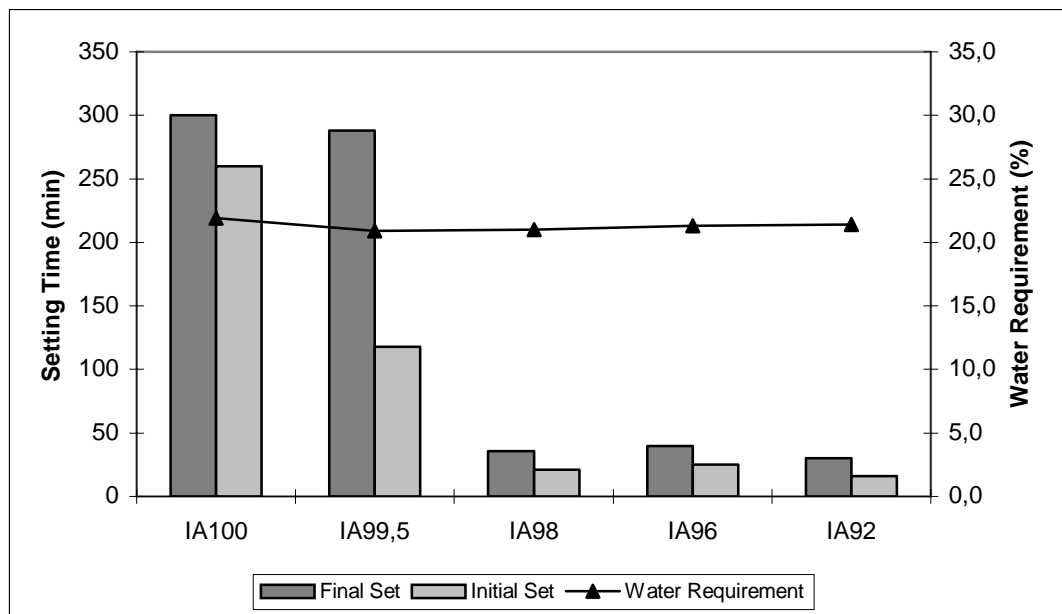


Figure 5.2 Setting Time and Water Requirement of CAC-Gypsum Mixes

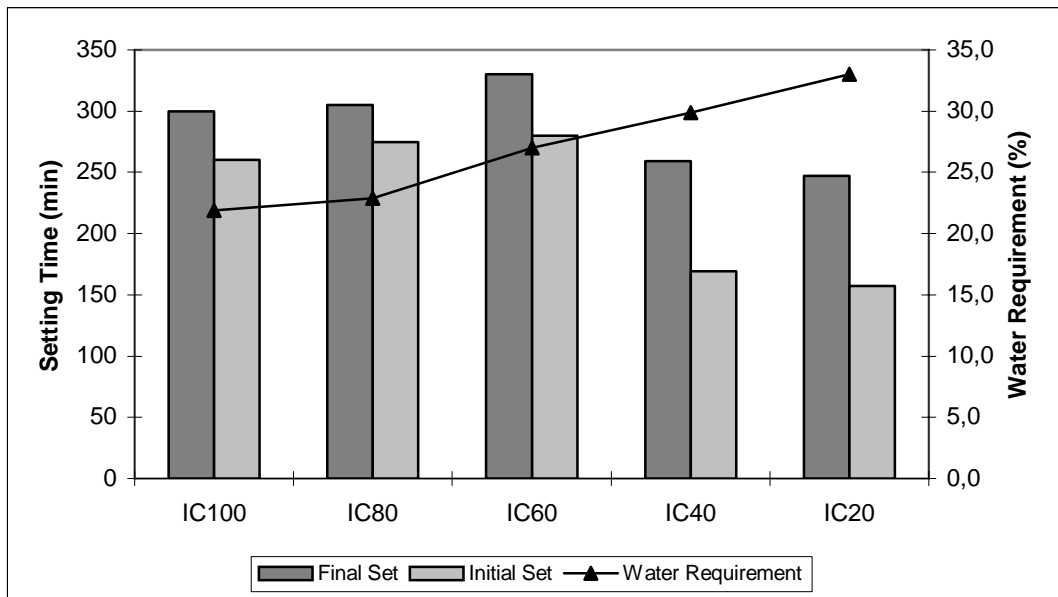


Figure 5.3 Setting Time and Water Requirement of CAC-GGBFS Mixes

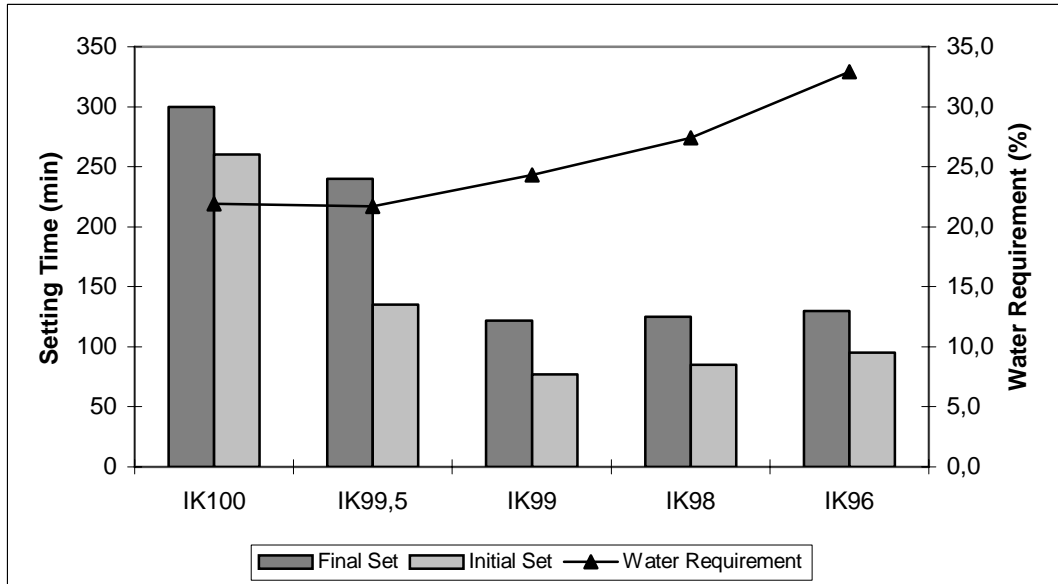


Figure 5.4 Setting Time and Water Requirement of CAC-Lime Mixes

As seen in Figures 5.1-5.4, binary systems of CAC and other inorganic binding materials, i.e. PC, gypsum, GGBFS, and lime exhibited different setting behaviour as compared to pure CAC mix.

Figure 5.1 suggested that all blends of CAC and PC showed shorter setting time than pure CAC mix (IP100), whether PC was the major or minor constituent. In mix IP25 where PC was the main constituent and CAC was the minor constituent, shorter setting times may be mainly due to the ettringite formed by the reaction of calcium aluminates of CAC and sulphates of PC. On the other hand, in the mix IP75, rapid setting may be attributed to the rapid hydration of CA due to increased pH of the medium caused by PC addition. Similar reasoning was made by previous researchers, too [1,25].

The discussions made for CAC-PC mixes are also valid for the mixes of CAC-gypsum and CAC-lime. In the case of gypsum addition to CAC, rapid ettringite formation governed the quick setting behaviour, whereas in the case of CAC-lime mixes, quick setting occurred due to the increased pH of the medium caused by lime addition. These were also claimed by other researchers in the previous studies [1,25].

The setting time of CAC-GGBFS blends were not drastically changed by the inclusion of GGBFS, when compared to that of pure CAC mix (IC100). While IC40 and IC20 exhibited slightly shorter setting time than IC100, IC80 and IC60 showed prolonged setting time. This might be due to the gehlenite hydrate (C_2ASH_8), formed by the reactions of calcium aluminate phases and silica of GGBFS. In fact, its rate of reaction is slower than that of calcium aluminate hydrates, which was also stated in previous studies [35-46].

Except for CAC-gypsum mixes, the water requirements of all CAC based composite binders were higher than that of the reference mix (pure CAC mix, i.e. IP100=IA100=IC100=IK100) (see Figures 5.1-5.4). This was mainly due to higher fineness of PC, GGBFS, and lime compared with CAC. In fact, as given in Table 4.2, the specific surface areas of PC, GGBFS and lime were higher and their median sizes were lower than that of CAC, which caused an increase in water amount necessary for normal consistency of binder pastes. On the other hand, owing to lower fineness of gypsum compared with CAC, CAC-gypsum mixes needed less amount of water than pure CAC mix for normal consistency. Similarly, Glasser [64] reported that even at the same fineness, the water demand of CAC-sulphate binary system is somewhat more than pure CAC mix.

5.1.2 Heat of Hydration

The setting behaviour of CAC based composite binders was also studied by examining their heat of hydration up to 24 hours. The heat of hydration liberated within 24 hours is given in Table 5.2 and the rates of heat evolution of CAC-PC, CAC-gypsum, CAC-GGBFS, and CAC-lime mixes are presented in Figures 5.5-5.8, respectively.

Table 5.2 Heat of Hydration of CAC Based Composite Binders

CAC Based Composite Binders	Heat of Hydration at 24 Hours (J/g)
IP100	33.9
IP75	30.1
IP50	30.3
IP25	17.6
IP0	19.1
IA99,5	34.3
IA98	30.9
IA96	31.3
IA92	30.6
IC80	31.7
IC60	27.2
IC40	20.7
IC20	11.2
IK99,5	34.8
IK99	34.8
IK98	34.7
IK96	34.2

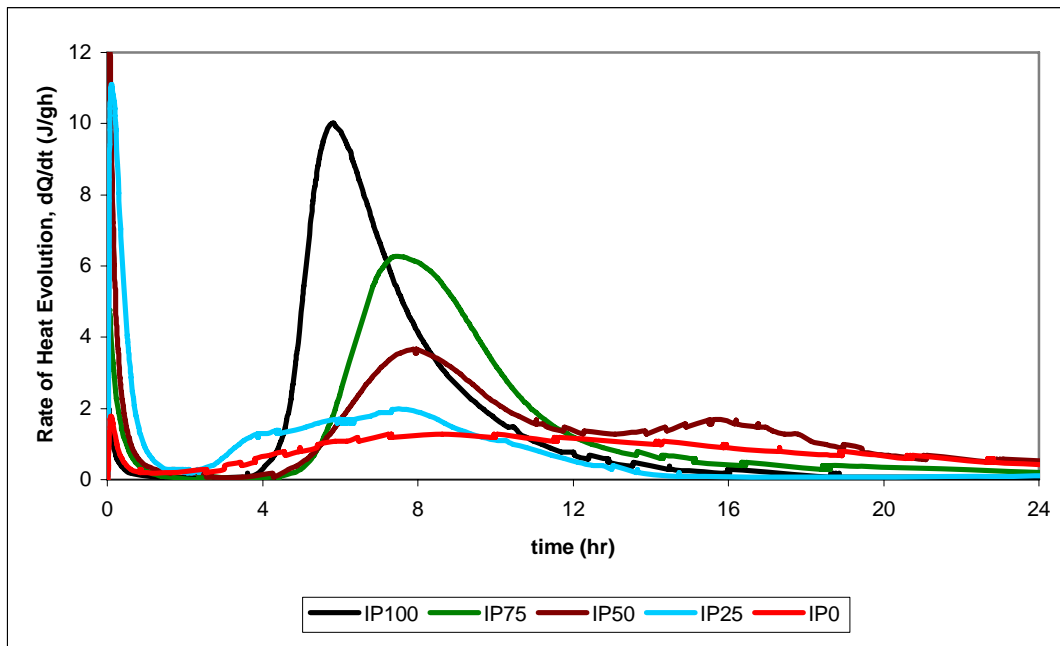


Figure 5.5 Heat Evolution Rates of CAC-PC Mixes

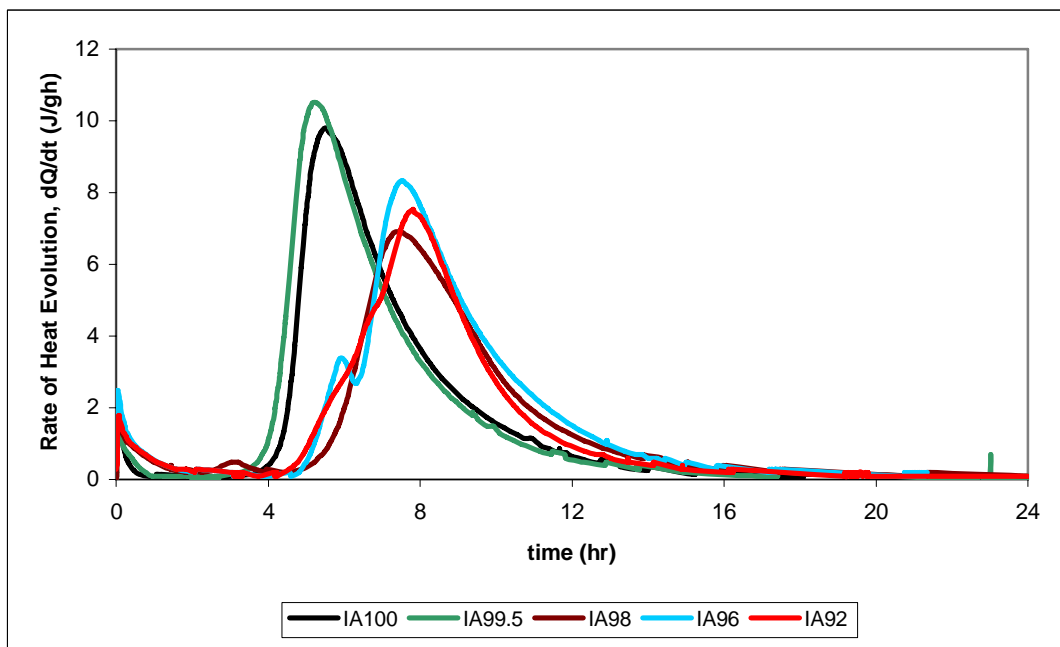


Figure 5.6 Heat Evolution Rates of CAC-Gypsum Mixes

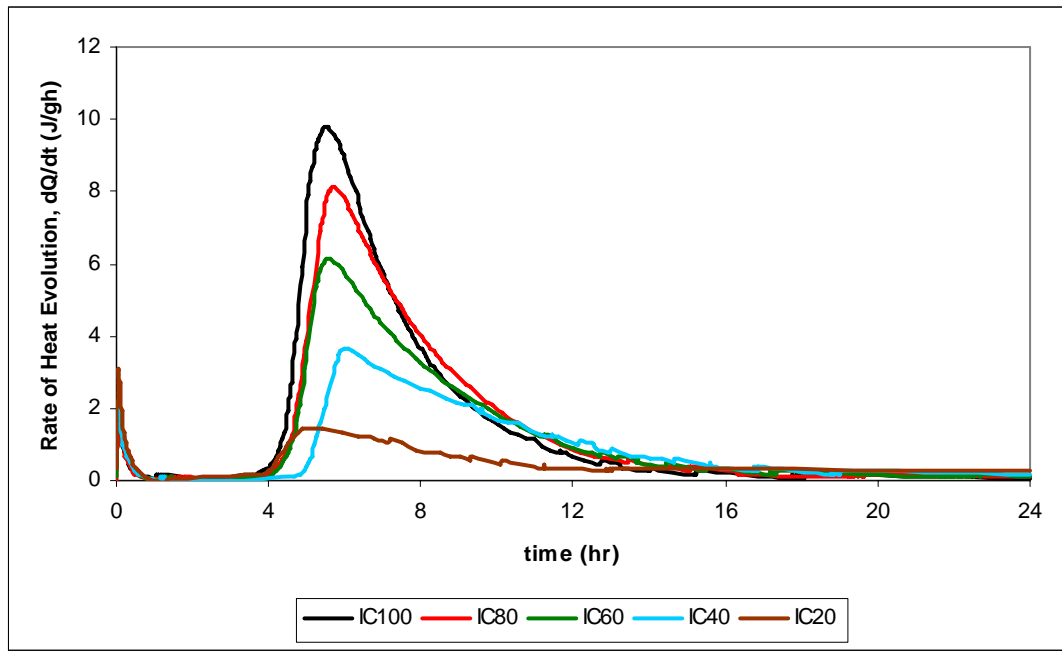


Figure 5.7 Heat Evolution Rates of CAC-GGBFS Mixes

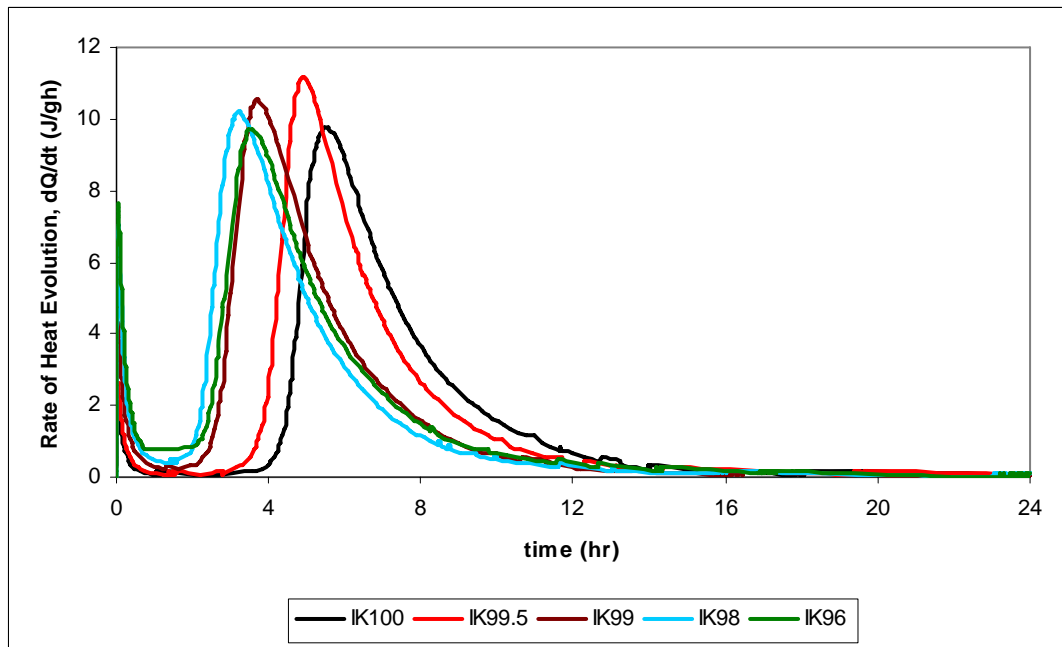


Figure 5.8 Heat Evolution Rates of CAC-Lime Mixes

As seen in Figure 5.5, the rates of heat evolution decreased by the increase in the PC amount of CAC-PC binary system. A peak with a maximum value of rate of heat evolution was experienced at about 6 hours for IP100, whereas a peak was observed at about 8 hours for each of IP75, IP50, IP25 and IP0 mix. The decrease in CAC amount caused a significant delay in the appearance of the main exothermic peak. This was mainly due to the less formation of calcium aluminate hydrates. In fact, the hydration peak at 6 hours for IP100 represented hydration of CA. Lower and much wider peak was observed as the PC amount was increased. This was mainly due to the hydration of calcium silicates of PC. In fact, the hydration of calcium silicates were delayed by the presence of calcium aluminates and by their reactions with sulphates forming ettringite. According to Gu and Beaudoin [28], formation of ettringite causes delay in PC hydration when there is enough calcium aluminates coming from CAC. Ettringite covers the entire surface of unhydrated particles and its semi impermeable state hinders or delay the ongoing hydration reactions of calcium silicates.

The mix IP25 showed the shortest setting time among all IP mixes, as it was mentioned previously in Section 5.1. Steep increase in the rate of heat evolution of IP25, when it contacted with water, was also consistent with its setting time. This was mainly due to the ettringite formed by the reaction of calcium aluminates of CAC and sulphates of PC, whose rate of reaction is too fast.

According to Figure 5.6, it can be claimed that the increase in gypsum amount induced delay in the exothermic hydration peak. While it was observed in the mix IA100 at almost 6 hr, it occurred at 8 hr in mixes IA98, IA96, and IA92. The similar considerations stated for IP mixes are may also be valid for IA mixes. That means, formation of ettringite, which was increased by the increase in gypsum amount, within the first minutes may delay ongoing hydration of calcium aluminates, since ettringite may cover

the whole surface of unhydrated cement particles and its semi impermeable state may delay further hydration reactions of calcium aluminates.

As can be seen in Figure 5.7, increase in GGBFS amount caused decrease in rate of heat evolution. However, there is no delay in the appearance of the main exothermic peak. The decrease in the rate of heat evolution may be related with less formation of calcium aluminate hydrates due to less amount of CAC. In addition, it can also be attributed to slow hydration mechanism of straelingite (i.e. gehlenite hydrate) formed by the hydration reaction of calcium aluminates of CAC and silicates of GGBFS [35-46].

According to Figure 5.8, the increased pH of the medium caused by lime addition governed the quick setting and hydration behaviour. As lime ratio increased, initial rate of heat evolution as soon as the mixes was contact with water got higher and the main exothermic hydration peak occurred earlier. This was also claimed by other researchers in the previous studies [1,25].

5.2 Effect of Temperature on Strength Development of CAC Based Composite Binders

In order to estimate the relationship between the curing temperatures stated previously in Section 4.4 and compressive strength development of 17 different CAC based composite binders, tests were conducted at different ages up to 210 days. Tables 5.3-5.9 show the compressive strengths of CAC based composite binders cured (i) continuously at 20°C, (ii) continuously at 30°C, (iii) 28 days at 20°C then at 30°C, (iv) continuously at 40°C, (v) 28 days at 20°C then at 40°C, (vi) continuously at 50°C, and (vii) 28 days at 20°C then at 50°C, respectively.

Table 5.3 Compressive Strengths of CAC Based Composite Binders Cured Continuously at 20°C

	Compressive Strength (MPa)												
	1hr	3hr	6hr	24hr	2d	7d	28d	2m	3m	4m	5m	6m	7m
IP100	0	5.2	42.1	60.5	65.9	80.4	85.6	78.7	76.3	75.9	79.6	75.9	71.5
IP75	0	0	19.7	35.6	31.4	36.8	39.0	41.4	41.6	39.8	39.1	38.3	36.4
IP50	0	0	10.7	10.8	12.4	16.1	20.4	21.3	18.8	15.1	16.2	15.0	16.8
IP25	1.9	2.8	3.3	3.0	6.8	29.0	36.9	38.0	39.6	40.6	40.2	39.2	39.0
IP0	0	0	0	20.8	28.6	40.0	49.2	51.0	53.9	55.9	57.8	58.4	59.4
IA99.5	0	0	26.0	72.9	83.0	86.1	95.2	83.6	82.4	79.5	83.7	79.1	76.6
IA98	0	0	39.1	54.9	61.0	68.4	79.6	68.9	69.7	68.1	70.2	69.7	68.0
IA96	0	0	18.6	41.3	42.6	41.5	49.9	44.2	39.4	42.8	35.6	36.7	35.2
IA92	0	0	10.0	35.2	41.9	37.2	41.7	35.9	34.8	33.4	29.5	30.9	29.9
IC80	0	0	16.8	58.6	58.8	63.2	73.5	74.3	74.4	64.2	71.2	74.8	73.1
IC60	0	0	15.5	39.3	40.8	39.6	53.6	59.2	66.8	73.7	75.5	76.3	77.5
IC40	0	0	6.6	17.4	17.9	27.3	38.8	53.3	60.1	63.7	67.3	68.2	68.4
IC20	0	0	2.0	3.8	10.0	11.4	25.7	32.2	37.0	43.1	48.6	47.4	51.8
IK99.5	0	3.2	43.2	65.0	73.6	78.6	82.9	77.5	74.2	80.3	73.6	73.3	70.6
IK99	0	17.6	39.0	49.8	51.7	67.2	61.0	57.9	57.8	52.7	57.6	56.8	53.7
IK98	0	14.2	34.1	55.3	51.9	55.1	51.4	49.9	51.2	44.0	44.3	47.7	46.8
IK96	0	13.3	26.2	29.1	36.6	37.7	39.5	36.6	34.5	31.8	40.7	42.4	38.9

Table 5.4 Compressive Strengths of CAC Based Composite Binders Cured Continuously at 30°C

	Compressive Strength (MPa)																							
	1hr	3hr	6hr	24hr	2d	7d	14d	21d	28d	35d	42d	49d	56d	63d	70d	77d	84d	91d	98d	119d	133d	154d	182d	210d
IP100	0,0	0,0	0,0	49.9	38.0	28.3	24.3	23.9	22.9	27.8	28.4	28.9	27.7	25.4	22.7	26.4	25.5	25,0	29,0	25.6	23.8	25.0	24.6	26.2
IP75	0,0	0,0	0,0	29.3	26.1	23.1	19.8	19.5	20.0	21.0	21.9	21.3	21.0	21.8	22.2	22.2	22.1	22.9	22.4	22.2	22.1	21.9	22.5	22.7
IP50	0,0	0,0	0,0	9.0	9.9	8.6	11.0	12.6	12.6	12.2	13.2	13.7	13.6	13.1	13.0	14.2	14.7	14.5	14.1	15.6	15.7	15.4	15.5	16.0
IP25	2.0	2.8	2.6	11.3	20.6	19.8	31.5	36.6	37.4	36.8	37.3	37.7	39.3	38.2	38.3	38.4	38.4	38.6	31.3	35.1	35.4	35.4	34.0	35.0
IP0	0,0	0,0	4.6	26.5	32.4	40.6	43.4	45.3	49.0	49.6	49.4	49.8	51.1	50.3	51.7	51.6	51.8	53.0	51.1	50.9	51.0	51.3	49.8	51.6
IA99.5	0,0	0,0	0,0	44.1	50.3	42.1	47.7	35.1	33.7	32.1	31.2	31.0	30.9	31.9	31.7	31.9	33.3	30.5	32.7	30.1	30.2	30.4	29.1	30.6
IA98	0,0	0,0	28.7	44.4	45.4	42.4	38.8	37.4	34.5	33.4	30.8	28.7	26.1	26.6	26.4	26.7	26.1	25.7	24.8	23.4	24.1	25.2	24.8	25.4
IA96	0,0	6,9	29.2	33.3	33.8	34.4	34.8	31.8	29.5	28.3	27.0	26.5	27.1	26.2	25.2	25.2	24.4	24.1	23.6	22.8	23.5	22.9	23.8	24.7
IA92	0,0	10.4	24.3	25.6	27.8	33.9	29.6	27.8	25.7	24.6	24.6	24.9	24.3	23.7	25.3	24.5	25.2	25.1	24.9	24.8	26.0	26.4	27.6	26.5
IC80	0,0	0,0	20.0	46.6	45.6	49.2	44.4	39.4	46.4	42.7	42.2	36.6	36.1	36.0	36.1	35.2	36.0	36.0	44.2	49.9	50.0	50.7	52.5	52.3
IC60	0,0	0,0	0,0	27.6	27.6	32.8	44.2	49.6	50.8	53.6	54.4	55.1	55.0	57.7	57.6	57.8	60.3	60.5	61.7	57.1	58.5	59.3	60.6	61.0
IC40	0,0	0,0	6.6	13.	15.2	32.9	35.7	42.5	46.0	52.2	56.8	59.1	60.1	60.0	62.1	63.1	63.7	65.1	64.8	65.7	63.2	65.6	67.9	68.2
IC20	0,0	0,0	1.9	6.4	10.3	12.2	24.6	32.8	36.2	39.6	41.2	42.4	42.5	44.2	45.0	45.5	47.7	45.0	44.7	43.6	44.2	45.7	45.6	49.4
IK99.5	0,0	0,0	0,0	42.6	41.9	39.8	27.0	25.0	25.4	25.5	24.9	25.1	25.6	25.2	26.5	27.0	26.1	25.5	24.9	24.4	25.8	24.6	22.9	29.0
IK99	0,0	0,0	27.0	37.9	41.2	23.3	20.7	20.2	20.9	20.0	20.9	19.9	23.3	20.4	20.5	22.6	21.9	21.2	21.1	23.7	24.1	24.4	24.9	25.3
IK98	0,0	18.9	28.9	33.5	32.0	21.5	21.2	19.3	20.8	19.6	21.0	20.6	19.6	19.4	19.8	19.0	20.6	21.2	22.3	23.0	22.6	22.7	22.3	22.1
IK96	0,0	18.5	31.3	28.9	26.0	15.7	16.9	18.8	15.3	17.2	15.9	20.4	18.0	18.6	17.1	19.5	16.0	17.4	19.7	24.1	22.3	21.6	22.5	24.2

Table 5.5 Compressive Strengths of CAC Based Composite Binders Cured 28 days at 20°C then at 30°C

	Compressive Strength (MPa)																					
	1hr	3hr	6hr	24hr	2d	7d	28d	35d	42d	49d	56d	63d	70d	77d	84d	91d	98d	119d	133d	154d	182d	210d
IP100	0,0	5.2	42.1	60.5	65.9	80.4	85.6	79.9	76.7	73.2	70.7	68,3	65,4	66.0	64.6	63.1	62.0	56.8	58.4	46.3	46.8	41.6
IP75	0,0	0,0	19.7	35.6	31.4	36.8	39.0	38.5	37.2	33.9	32.8	32.9	26.1	24.1	22.7	21.0	20.2	19.2	19.6	20.1	21.2	19.9
IP50	0,0	0,0	10.7	10.8	12.4	16.1	20.4	14.2	13.9	13.1	12.8	12.5	12.5	12.0	12.5	12.1	12.7	13.2	13.7	14.0	13.9	13.9
IP25	1.9	2.8	3.3	3.0	6.8	29.0	36.9	39.0	34.1	32.2	28.0	32.9	34.4	32.4	34.7	35.4	35.3	36.0	36.5	36.8	35.5	34.9
IP0	0,0	0,0	0,0	20.8	28.6	40.0	49.2	50.7	52.1	53.4	54.6	52.9	55.0	54.4	55.3	55.9	55.9	58.0	56.4	55.3	55.6	56.7
IA99.5	0,0	0,0	26.0	72.9	83.0	86.1	95.2	90.8	94.4	90.2	86.0	89.6	91.3	83.4	80.1	73.6	74.1	75.0	63.1	52.8	49.0	48.1
IA98	0,0	0,0	39.1	54.9	61.0	68.4	79.6	75.0	75.9	73.2	70.2	69.7	67.3	65.8	63.0	65.6	64.1	61.6	57.8	54.7	52.7	48.4
IA96	0,0	0,0	18.6	41.3	42.6	41.5	49.9	48.3	43.4	39.7	37.7	36.1	36.5	34.5	32.7	32.3	32.1	29.8	29.2	29.2	28.9	26.6
IA92	0,0	0,0	10.0	35.2	41.9	37.2	41.7	39.1	45.5	38.3	30.6	36.1	28.4	30.0	31.6	29.8	30.5	30.1	28.4	26.6	26.7	27.1
IC80	0,0	0,0	16.8	58.6	58.8	63.2	73.5	72.3	67.6	67.6	73.9	63.0	61.1	66.8	58.4	51.4	52.2	39.8	33.8	37.0	35.3	35.7
IC60	0,0	0,0	15.5	39.3	40.8	39.6	53.6	54.1	57.2	62.8	63.3	68.8	69.1	71.0	71.0	70.4	69.5	73.4	69.8	72.9	73.6	74.3
IC40	0,0	0,0	6.6	17.4	17.9	27.3	38.8	48.1	54.2	60.0	60.2	63.2	63.4	65.6	65.6	66.7	67.5	66.5	67.9	68.5	70.3	71.7
IC20	0,0	0,0	2.0	3.8	10.0	11.4	25.7	33.7	38.0	40.5	40.4	43.2	43.9	43.5	47.0	47.3	48.2	44.9	44.4	46.4	50.0	49.5
IK99.5	0,0	3.2	43.2	65.0	73.6	78.6	82.9	77.4	74.3	69.2	65.5	70.7	61.8	58.4	57.3	56.7	55.0	51.1	54.5	49.0	44.7	40.5
IK99	0,0	17.6	39.0	49.8	51.7	67.2	61.0	45.9	42.3	40.0	38.0	36.3	36.4	34.2	34.1	30.9	29.3	31.8	28.6	29.2	26.2	23.2
IK98	0,0	14.2	34.1	55.3	51.9	55.1	51.4	55.4	36.9	42.2	40.9	40.7	33.8	31.0	28.5	27.7	26.1	24.7	22.9	22.0	19.3	19.4
IK96	0,0	13.3	26.2	29.1	36.6	37.7	39.5	31.1	32.6	30.7	26.6	22.4	20.7	21.2	20.1	20.1	21.1	24.5	23.2	24.8	22.6	21.4

Table 5.6 Compressive Strengths of CAC Based Composite Binders Cured Continuously at 40°C

	Compressive Strength (MPa)																					
	1hr	3hr	6hr	24hr	2d	4d	6d	8d	10d	12d	14d	16d	18d	20d	28d	56d	84d	112d	133d	154d	182d	210d
IP100	0,0	0,0	34.1	27.2	25.5	23.7	27.1	26.2	26.7	26.5	27.0	26.9	27.7	25.9	26.3	26.8	27.6	28.1	27.9	27.4	27.9	28.5
IP75	0,0	11.3	22.4	18.4	18.0	17.9	19.1	19.6	19.6	20.3	20.2	20.5	21.1	20.9	20.6	21.7	21.8	22.0	21.9	21.7	22.0	22.2
IP50	0,0	7.1	9.0	9.0	9.5	10.0	10.8	10.6	10.7	11.0	11.3	11.5	11.4	11.3	11.2	11.6	11.7	11.9	12.3	12.3	12.5	12.7
IP25	2.1	2.3	3.2	18.6	23.1	26.3	27.4	27.9	29.2	29.2	29.7	30.4	30.3	30.3	30.4	31.0	30.0	31.1	32.0	30.5	31.7	29.3
IP0	0,0	4.1	10.1	27.7	34.4	37.3	38.6	40.9	40.8	41.9	41.5	42.8	44.5	45.1	45.9	48.7	50.8	49.6	49.5	49.7	48.9	49.9
IA99.5	0,0	0,0	28.5	34.1	28.5	26.3	26.5	27.1	28.4	27.4	28.1	27.9	27.4	27.2	27.6	29.4	30.6	31.6	31.0	30.8	31.3	32.6
IA98	0,0	29.4	27.4	27.8	27.7	25.4	22.1	20.3	20.5	20.5	20.6	21.1	20.7	22.1	24.1	23.6	24.2	24.8	25.1	25.9	26.0	26.5
IA96	0,0	25.3	25.0	25.3	25.0	25.3	22.2	22.2	22.1	21.3	21.2	19.9	19.9	19.6	19.4	19.2	21.0	20.8	21.5	21.9	22.6	23.4
IA92	10.8	21.5	21.7	22.0	23.1	21.0	19.9	19.9	19.4	19.7	20.2	19.8	20.1	19.9	19.6	22.6	23.1	23.8	24.7	26.0	25.8	26.4
IC80	0,0	0,0	15.7	25.1	25.3	27.9	33.7	35.3	38.0	37.5	40.5	39.9	41.5	42.2	45.0	45.6	42.9	48.0	49.8	49.9	49.1	50.2
IC60	0,0	0,0	11.0	19.3	23.1	30.6	32.7	36.1	38.5	38.0	39.4	39.4	41.3	40.3	41.4	44.4	43.5	48.2	49.6	50.3	48.1	49.9
IC40	0,0	0,0	3.7	12.6	18.5	26.0	27.1	28.4	29.5	28.9	31.0	31.3	32.2	31.1	32.9	39.1	40.1	45.0	45.5	48.5	50.1	51.4
IC20	0,0	0,0	0,0	8.2	9.8	12.3	19.9	21.4	23.7	25.2	25.8	27.2	28.1	28.8	30.9	37.4	35.0	41.4	42.6	43.5	43.5	43.9
IK99.5	0,0	0,0	34.0	27.5	23.9	26.2	26.8	26.9	26.4	27.3	26.6	26.3	26.4	27.9	27.0	28.0	29.9	28.9	29.2	29.0	29.2	29.8
IK99	0,0	19.9	29.7	20.4	21.7	22.6	21.5	23.8	21.8	22.8	23.0	21.9	21.6	22.1	22.6	23.9	23.8	24.5	24.9	25.1	25.3	25.9
IK98	0,0	24.5	25.2	16.9	19.8	20.4	21.2	20.1	21.6	21.2	20.8	21.9	21.0	21.4	21.2	24.1	23.7	23.8	23.9	24.2	24.6	24.8
IK96	0,0	26.9	27.4	18.8	20.2	22.8	22.6	22.2	23.4	21.2	22,0	21.4	19.0	22.0	21.8	23.4	22.9	23.5	23.3	23.8	24.2	24.0

Table 5.7 Compressive Strengths of CAC Based Composite Binders Cured 28 days at 20°C then at 40°C

	Compressive Strength (MPa)																					
	28d	30d	32d	34d	36d	38d	40d	42d	44d	46d	48d	50d	52d	54d	56d	70d	84d	112d	119d	154d	182d	210d
IP100	85.6	73.7	65.1	62.0	51.9	46.6	51.1	47.7	40.2	37.4	35.0	29.4	28.5	23.9	18.8	19.7	19.6	20.0	20.4	21.5	22.1	21.4
IP75	39.0	29.4	25.6	21.7	19.9	19.1	20.5	20.0	19.7	19.5	20.0	20.7	20.1	19.3	18.1	18.2	18.6	18.9	18.7	18.5	18.8	18.7
IP50	20.4	11.9	12.4	12.9	11.6	12.0	11.6	11.9	11.8	12.4	12.2	11.9	12.4	12.8	13.2	13.7	14.2	14.4	14.5	14.8	15.0	15.1
IP25	36.9	35.2	36.8	35.0	34.1	33.0	33.8	33.9	33.4	33.7	33.4	34.1	33.8	33.6	33.7	32.6	33.0	32.6	32.0	33.2	32.0	31.0
IP0	49.2	48.1	47.3	48.7	50.1	48.7	49.9	48.0	50.0	52.0	52.6	53.1	53.7	54.1	53.9	53.7	54.0	52.9	54.7	54.6	54.6	54.7
IA99.5	95.2	75.1	64.6	60.4	56.6	55.1	54.5	52.4	48.3	44.6	40.1	36.3	29.0	33.8	28.2	21.2	17.6	17.8	18.5	19.6	20.0	20.2
IA98	79.6	73.1	70.3	74.0	68.7	66.3	60.0	62.4	61.5	61.0	59.5	57.5	53.1	48.0	44.1	19.8	17.9	17.8	17.6	19.5	19.7	20.8
IA96	49.9	37.3	36.4	31.9	29.6	25.5	23.8	22.7	22.4	22.8	21.9	21.8	21.9	21.8	21.7	21.9	22.1	22.5	23.1	23.3	24.2	25.9
IA92	41.7	30.7	29.1	26.2	24.2	23.4	22.8	22.6	23.6	22.9	22.2	22.0	22.1	22.5	22.8	23.6	24.1	25.3	25.8	26.1	26.9	27.5
IC80	73.5	63.0	60.5	49.4	46.3	37.9	33.8	32.6	33.4	32.3	35.6	35.3	35.1	37.2	39.4	41.1	42.9	43.7	43.6	44.2	45.3	43.3
IC60	53.6	50.6	50.5	49.9	51.2	53.9	54.6	58.2	56.4	57.7	61.0	60.2	59.6	61.8	63.4	64.1	63.5	68.2	69.6	71.8	74.9	73.4
IC40	38.8	43.4	48.1	50.2	55.5	55.4	59.7	61.3	60.9	61.3	63.2	62.9	63.0	62.4	64.6	65.0	65.1	66.6	70.2	69.1	69.2	70.2
IC20	25.7	30.9	33.9	35.5	35.9	39.4	41.6	41.3	41.6	43.6	43.4	43.7	43.9	44.5	45.3	45.6	45.0	49.2	46.7	49.9	49.8	57.6
IK99.5	82.9	62.5	53.9	49.5	43.3	39.4	36.1	28.8	26.5	23.8	22.9	19.7	19.7	19.8	19.6	19.8	19.9	20.4	20.9	21.3	21.3	22.5
IK99	61.0	40.5	33.2	25.1	20.8	16.2	16.5	15.7	15.7	15.1	15.1	14.8	15.0	15.2	15.6	16.1	16.7	16.9	17.1	17.6	18.2	18.9
IK98	51.4	38.9	24.8	21.7	19.8	19.7	15.0	14.9	15.4	15.4	15.7	15.7	15.3	15.4	15.1	15.3	15.3	15.9	16.8	17.5	18.0	18.3
IK96	39.5	27.3	21.5	19.1	17.0	16.5	16.7	17.3	15.4	17.6	16.6	17.1	16.5	16.1	15.5	15.8	15.9	16.3	16.8	17.6	18.5	19.3

Table 5.8 Compressive Strengths of CAC Based Composite Binders Cured Continuously at 50°C

	Compressive Strength (MPa)																			
	1hr	3hr	6hr	12hr	24hr	1.5d	2d	2.5d	3d	3.5d	4d	4.5d	5d	7d	28d	56d	84d	112d	154d	210d
IP100	0,0	31.7	26.6	23.2	21.7	24.3	22.8	23.9	23.7	23.7	22.8	23.9	22.0	28.0	27.8	29.1	29.6	30.7	29.7	30.6
IP75	0,0	16.5	16.3	16.2	15.7	16.6	17.0	16.6	16.9	17.5	17.5	17.6	17.2	20.4	20.0	18.8	19.3	19.8	21.3	20.6
IP50	0,0	6.0	7.1	7.8	7.9	8.0	8.9	9.1	9.1	9.1	9.0	9.4	9.6	9.8	10.1	9.5	9.3	9.0	9.6	9.5
IP25	1,8	2.9	7.0	14.4	19.3	20.2	21.8	21.8	22.2	23.2	25.4	23.0	21.8	25.0	26.0	24.1	24.0	24.1	23.8	23.7
IP0	0,0	2.0	14.8	23.9	26.8	29.3	30.7	31.9	32.5	33.5	33.6	34.0	34.6	36.6	40.7	43.5	44.3	45.8	45.1	47.9
IA99.5	0,0	29.6	31.3	27.5	24.1	24.7	24.5	25.5	24.6	26.0	26.4	26.7	23.9	27.4	25.6	29.4	29.3	29.4	29.2	30.5
IA98	0,0	29.2	26.4	27.6	25.8	24.2	20.0	20.8	18.7	19.5	19.9	20.6	20.4	21.0	22.7	25.0	24.7	23.7	24.1	25.4
IA96	0,0	24.6	22.3	22.9	22.2	21.0	18.5	18.6	16.9	18.1	17.0	17.0	16.5	17.5	18.8	19.8	20.5	21.6	24.4	25.6
IA92	0,0	20.8	19.4	20.0	19.7	18.5	17.5	18.4	17.2	17.9	17.5	18.4	17.9	16.8	19.6	19.4	20.9	21.6	23.6	24.3
IC80	0,0	14.0	26.1	21.5	21.9	25.5	26.2	29.6	29.1	32.1	31.2	33.0	32.6	35.8	41.1	42.5	44.0	45.8	44.8	44.9
IC60	0,0	11.2	16.4	16.2	17.5	18.8	19.8	22.9	22.7	25.0	24.3	26.3	26.2	28.2	33.3	34.5	37.1	39.8	39.6	41.7
IC40	0,0	0,0	7.8	9.5	12.5	15.7	14.3	17.4	15.3	17.4	15.5	19.2	18.0	20.3	24.4	29.1	31.8	33.2	35.0	35.1
IC20	0,0	0,0	0.0	5.1	7.8	8.8	8.1	10.6	11.2	12.9	13.7	15.3	17.0	19.1	28.5	33.6	35.2	36.7	38.3	40.1
IK99.5	0,0	30.7	25.7	22.4	22.6	23.0	21.8	23.2	22.8	23.8	24.5	23.8	23.7	25.8	28.0	27.2	27.9	28.2	28.8	28.2
IK99	0,0	23.3	15.4	16.6	18.0	18.8	18.8	20.1	19.3	19.6	19.0	20.3	19.7	20.8	22.2	20.0	22.2	23.6	23.2	25.7
IK98	15.8	17.1	16.1	16.0	17.8	19.0	19.2	20.0	19.9	20.2	19.6	19.3	20.0	21.8	21.4	24.1	22.3	21.1	26.7	23.4
IK96	6.9	15.4	16.7	18.5	18.6	18.4	19.0	19.0	19.7	19.6	19.6	18.7	19.2	20.8	22.7	24.3	24.5	24.9	24.1	25.8

Table 5.9 Compressive Strengths of CAC Based Composite Binders Cured 28 days at 20°C then at 50°C

	Compressive Strength (MPa)																
	28d	28.5d	29d	29.5d	30d	30.5d	31d	31.5d	32d	32.5d	33d	33.5d	56d	84d	112d	154d	210d
IP100	85.6	67.4	62.2	54.9	39.5	29.2	21.2	20.4	18.4	19.3	18.4	18.7	20.7	21.4	22.4	22.8	24.3
IP75	39.0	33.5	28.0	25.0	18.0	19.2	18.4	18.6	18.4	18.6	19.1	19.4	19.4	18.2	19.4	19.6	20.2
IP50	20.4	12.0	11.7	11.6	11.3	11.4	11.5	11.9	11.7	11.8	11.8	11.4	13.9	12.8	12.4	13.6	13.9
IP25	36.9	36.0	35.7	35.0	32.6	33.5	32.0	32.7	31.4	32.7	32.0	32.5	31.1	30.3	30.7	31.2	30.3
IP0	49.2	43.8	44.6	44.4	46.1	46.8	46.8	46.9	47.5	47.8	47.3	49.3	51.2	55.0	54.6	57.1	63.7
IA99.5	95.2	80.1	67.7	63.6	60.8	48.4	41.0	29.8	25.1	21.6	18.2	18.6	19.1	21.4	21.3	23.2	28.4
IA98	79.6	65.7	60.6	56.2	48.0	39.2	31.1	24.6	20.7	20.3	18.5	18.8	19.8	22.1	22.4	22.8	28.7
IA96	49.9	36.0	29.2	26.1	22.9	22.1	21.6	21.9	21.4	22.3	21.3	21.8	21.8	23.6	25.7	26.7	30.4
IA92	41.7	33.8	29.1	26.9	23.4	23.2	23.2	24.0	22.3	23.1	23.1	22.6	22.7	22.7	25.0	26.6	30.8
IC80	73.5	66.1	56.0	45.7	30.7	29.2	28.5	28.8	29.8	30.4	31.5	31.4	44.6	45.2	45.1	45.0	49.2
IC60	53.6	48.0	47.8	47.4	47.6	48.3	47.8	49.7	49.4	50.1	52.5	52.4	64.8	68.0	68.0	69.6	75.7
IC40	38.8	40.2	43.6	44.5	46.1	50.0	50.2	52.4	52.3	52.4	55.9	56.0	63.9	66.7	68.5	72.0	74.7
IC20	25.7	28.2	31.0	31.8	33.1	34.5	35.1	35.1	37.9	37.7	38.7	38.9	42.5	45.6	50.0	48.2	54.2
IK99.5	82.9	69.5	60.4	51.3	44.1	35.3	26.0	26.4	21.9	17.7	17.8	17.3	21.5	21.5	22.9	24.2	24.6
IK99	61.0	42.3	30.5	22.7	14.8	15.6	15.8	14.8	14.3	14.7	14.2	15.0	19.8	21.4	22.9	23.6	22.8
IK98	51.4	36.8	27.4	19.2	15.3	15.8	15.2	14.8	15.7	16.0	15.1	15.0	15.0	16.8	17.8	18.7	19.0
IK96	39.5	24.8	17.5	17.9	15.6	16.5	15.6	16.8	16.5	15.7	15.5	17.0	12.9	14.3	15.7	14.0	15.8

5.2.1 Effect of Temperature on Compressive Strength Development of CAC-PC Mixes

Binary system of CAC and PC may be used in some concrete practices particularly where rapid setting and hardening is required. In addition to that, the conversion reactions of pure CAC mixes can be controlled by PC addition [1,25-30]. In order to investigate the effects of PC addition on strength development of CAC based composite binders depending on curing regimes, compressive strength tests were conducted up to 210 days.

Figures 5.9-5.13 show the compressive strength development of CAC-PC combinations, i.e. IP100, IP75, IP50, IP25, and IP0, respectively, with change in curing temperatures.

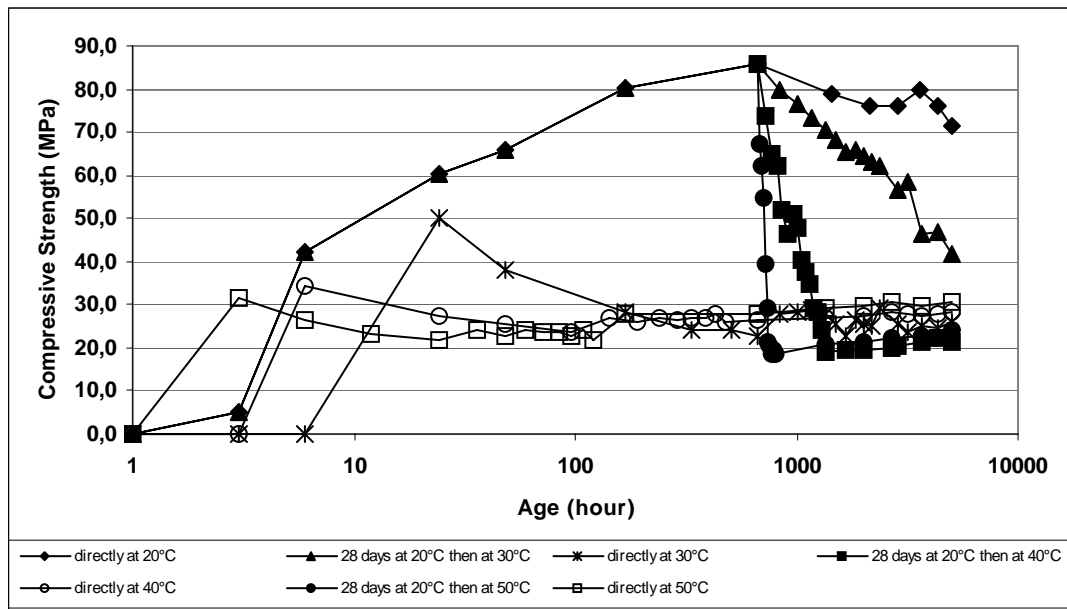


Figure 5.9 Compressive Strength Development of IP100 at Different Curing Temperatures

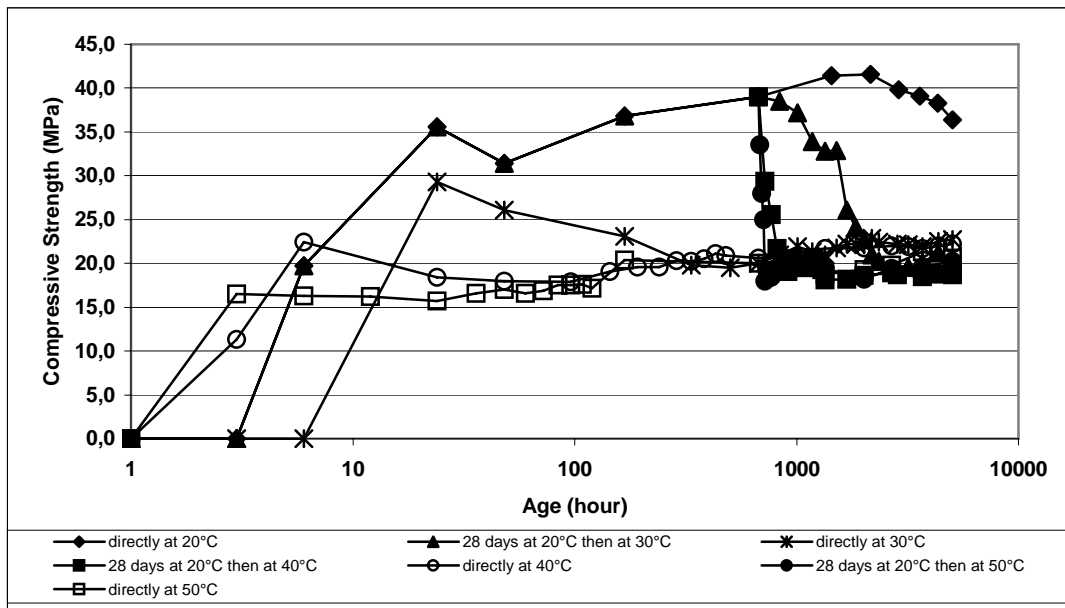


Figure 5.10 Compressive Strength Development of IP75 at Different Curing Temperatures

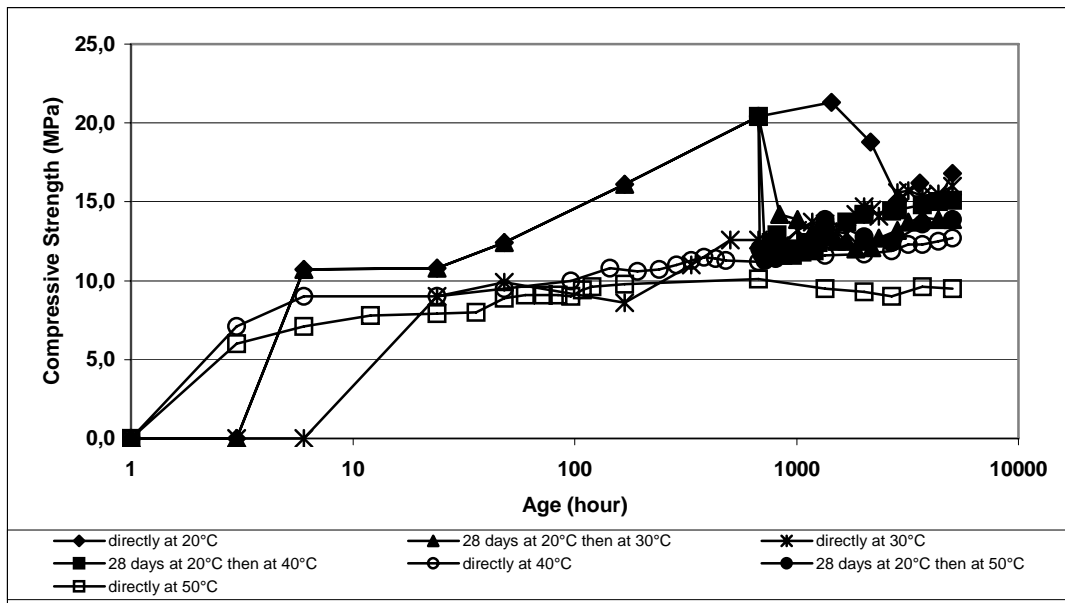


Figure 5.11 Compressive Strength Development of IP50 at Different Curing Temperatures

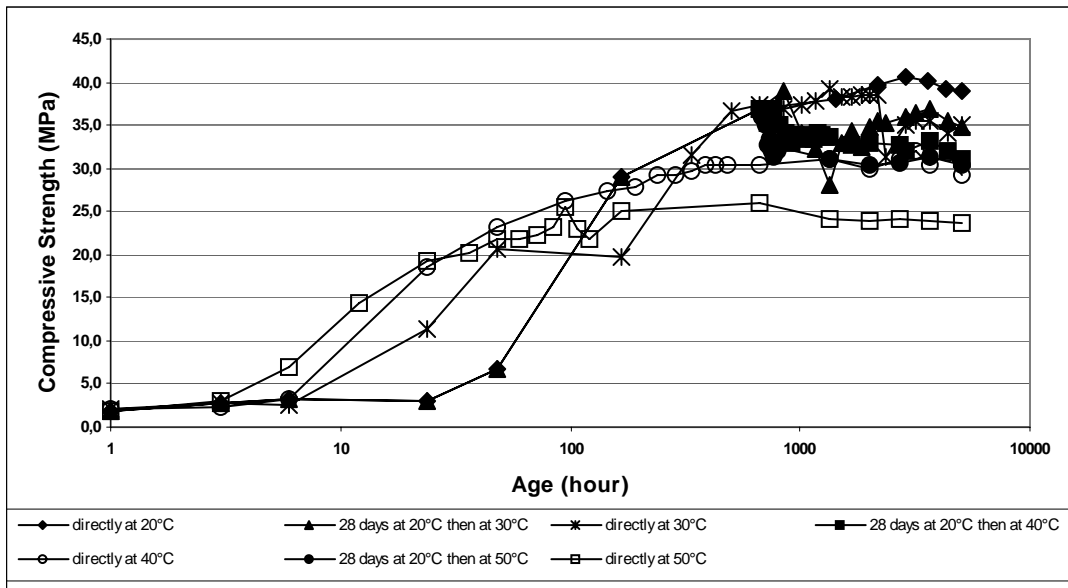


Figure 5.12 Compressive Strength Development of IP25 at Different Curing Temperatures

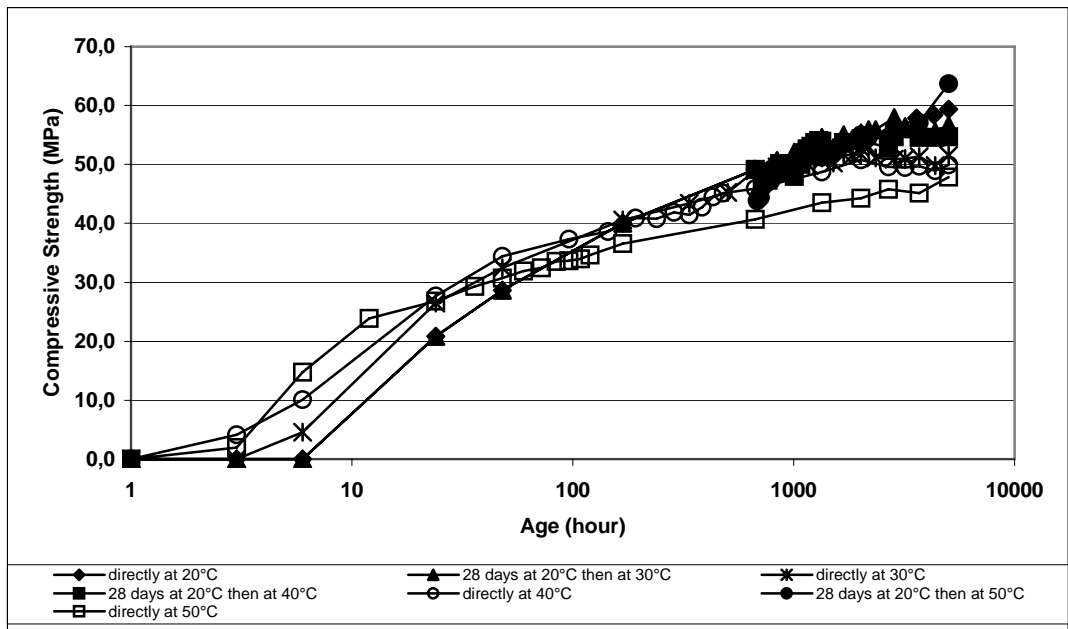


Figure 5.13 Compressive Strength Development of IP0 at Different Curing Temperatures

In order to understand the mechanism of compressive strength development of CAC-PC binary systems, XRD analyses were conducted on paste specimens, as described in Section 4.4. IP100 and IP0 were considered as reference mixes and their XRD patterns obtained at 28 days and at 210 days are given in Figures 5.14-5.17, respectively. On the other hand, XRD analyses of IP75, where CAC was the main constituent, and XRD analyses of IP25 where PC was the main constituent at 28 days and at 210 days are portrayed in Figures 5.18-5.21, respectively.

The designations used for several different phases in XRD analysis are tabulated in Table 5.10.

Table 5.10 The Designations Used for Various Phases in XRD Analysis

Phases		Designations
C_3AH_6	→	☆
C_2AH_8	→	▲
CAH_{10}	→	✦
AH_3	→	a
C_2ASH_8	→	s
CH	→	p
$C_6\bar{A}\bar{S}_3\bar{H}_{32}$	→	e
$C_4\bar{A}\bar{S}\bar{H}_{12}$	→	m

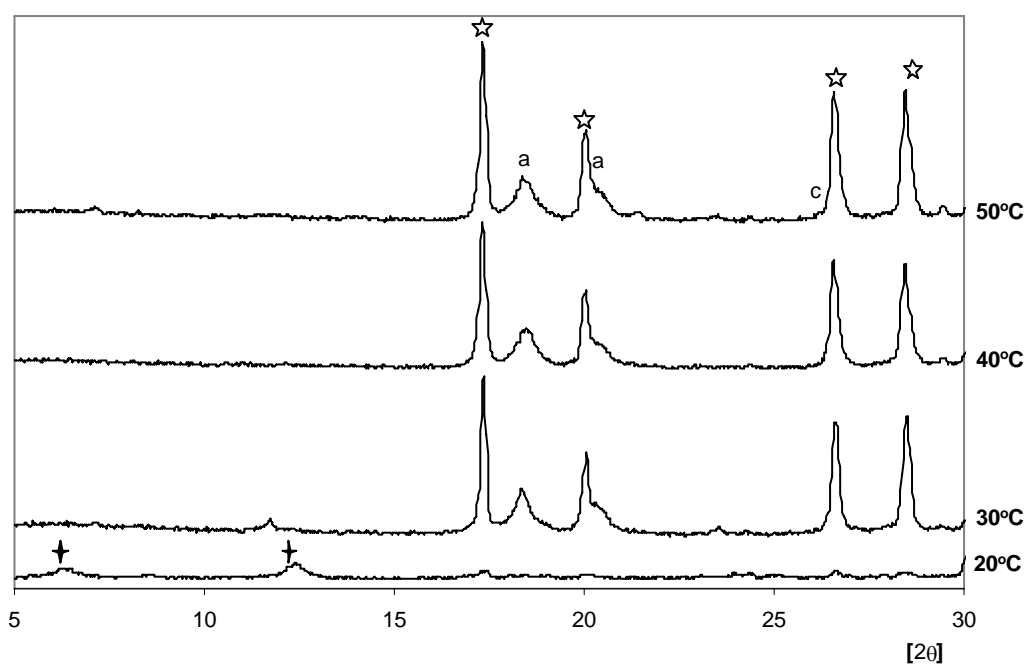


Figure 5.14 XRD Patterns of IP100 at 28 days

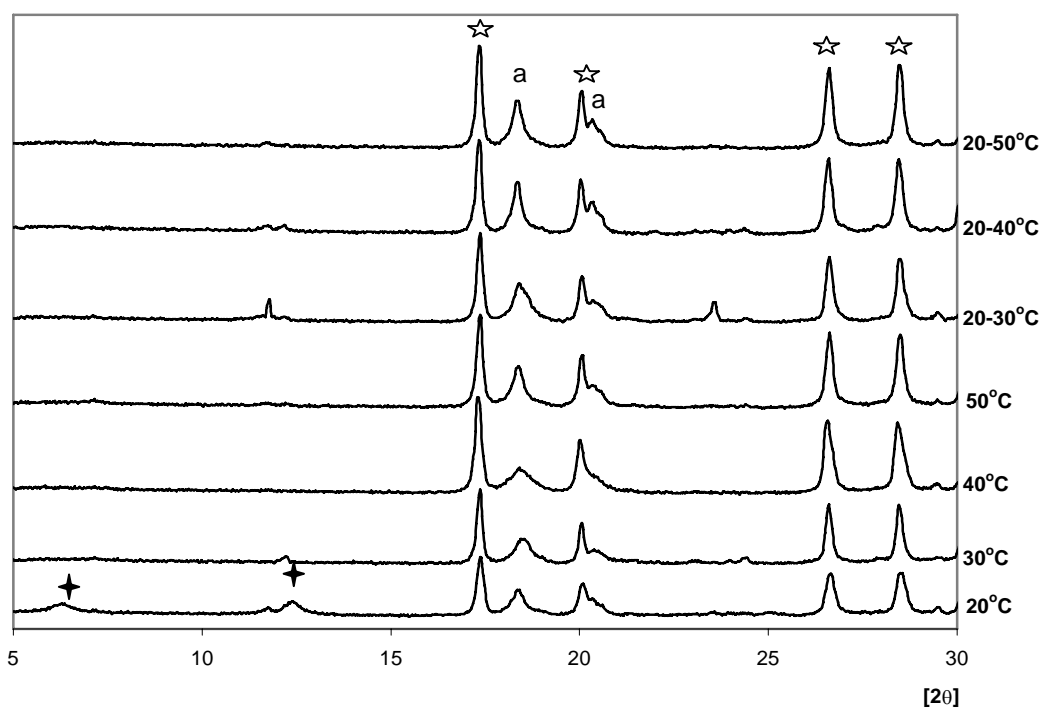


Figure 5.15 XRD Patterns of IP100 at 210 days

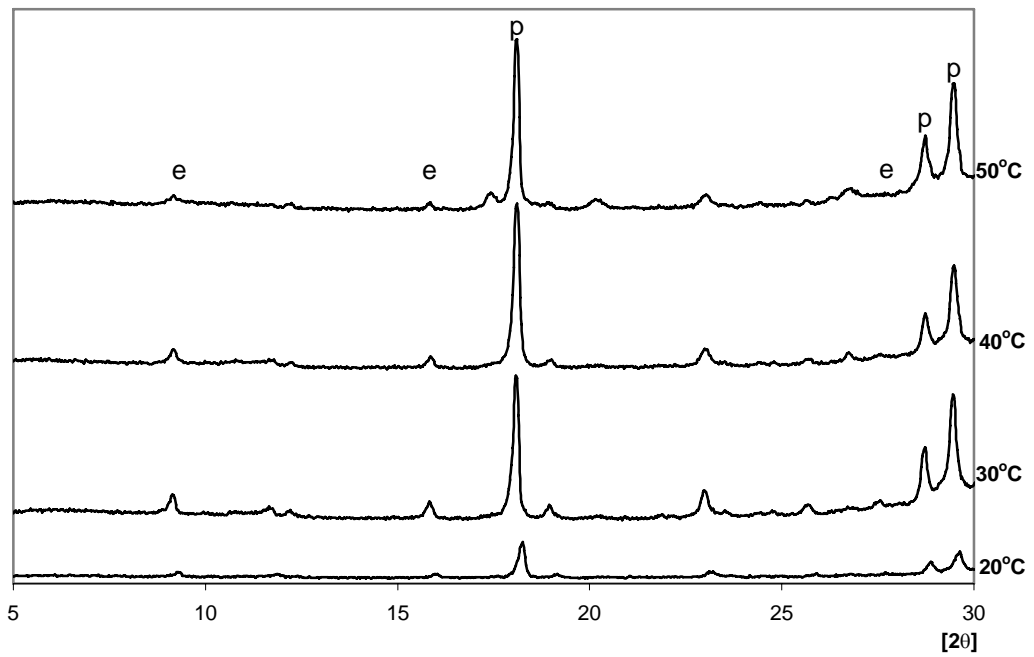


Figure 5.16 XRD Patterns of IP0 at 28 days

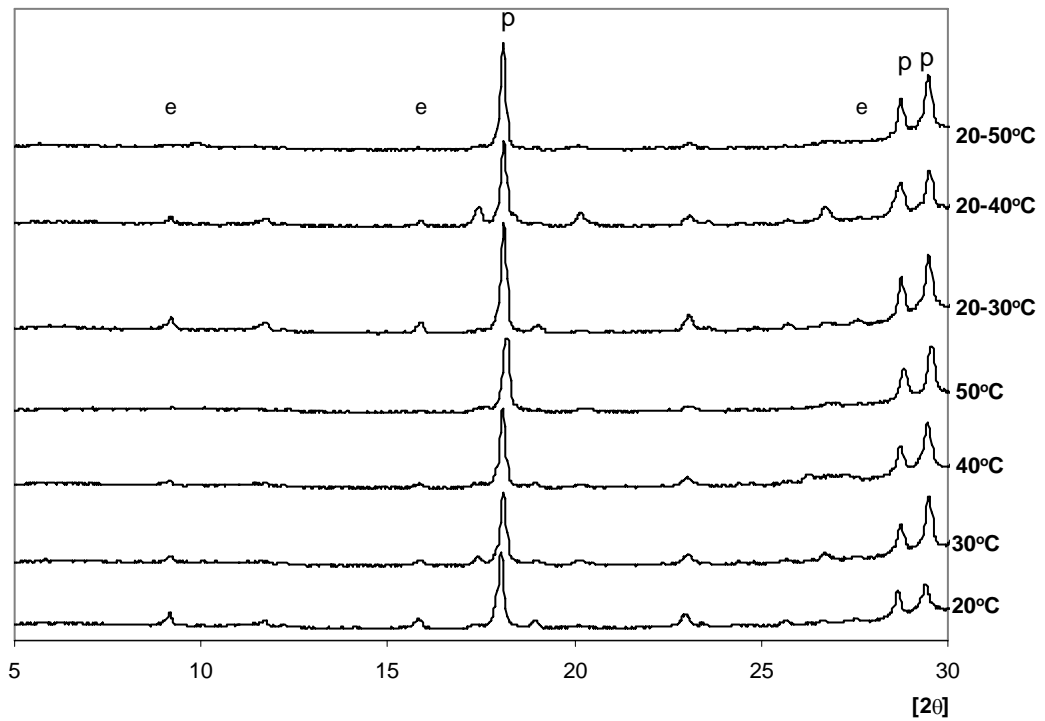


Figure 5.17 XRD Patterns of IP0 at 210 days

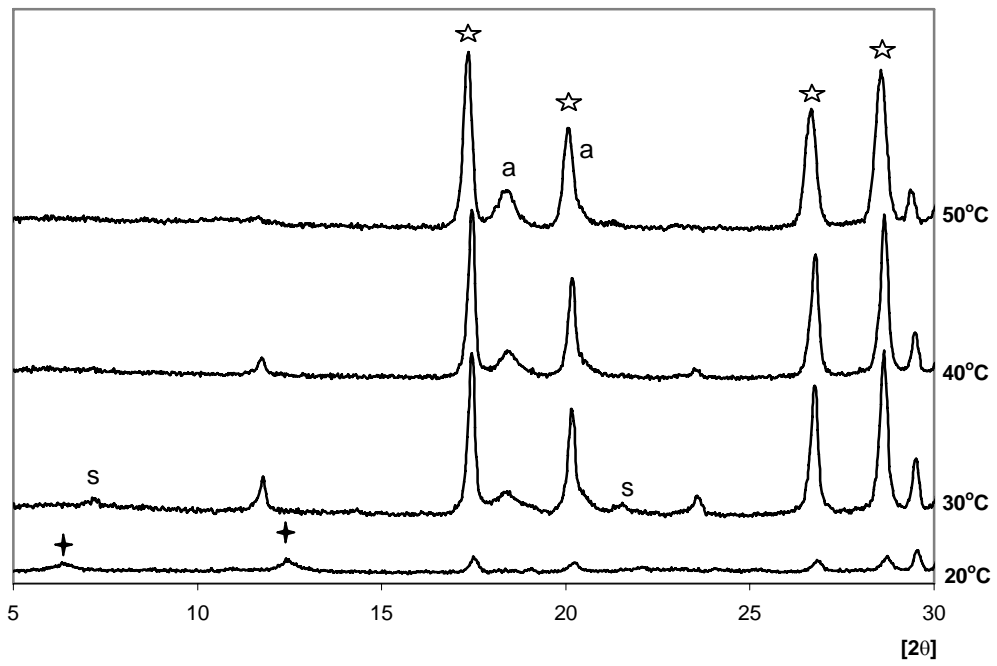


Figure 5.18 XRD Patterns of IP75 at 28 days

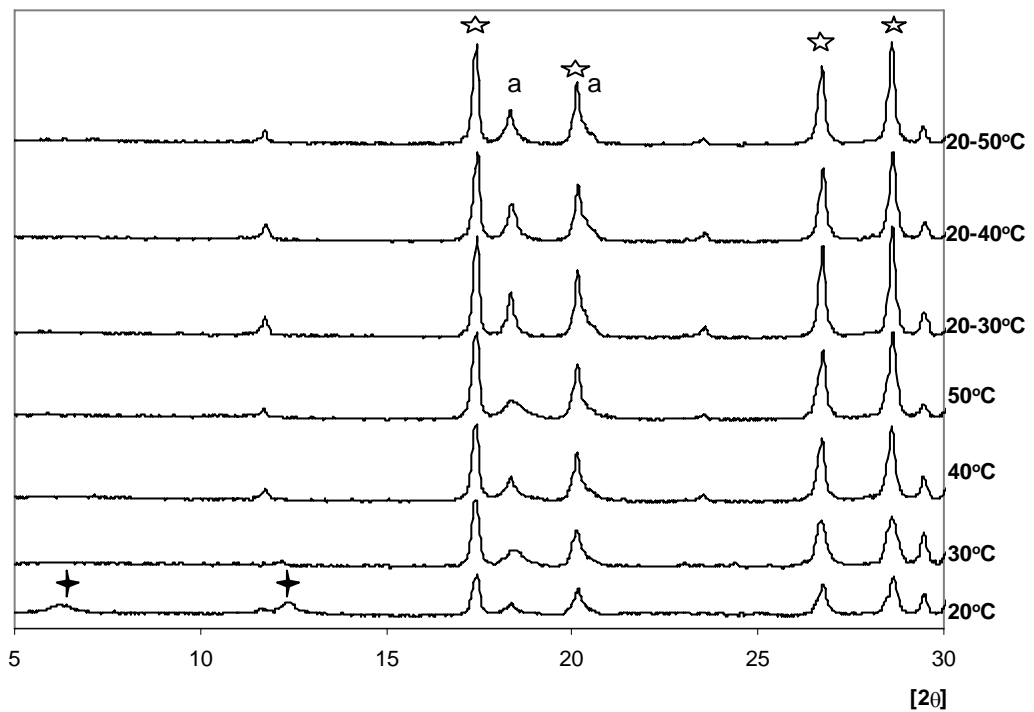


Figure 5.19 XRD Patterns of IP75 at 210 days

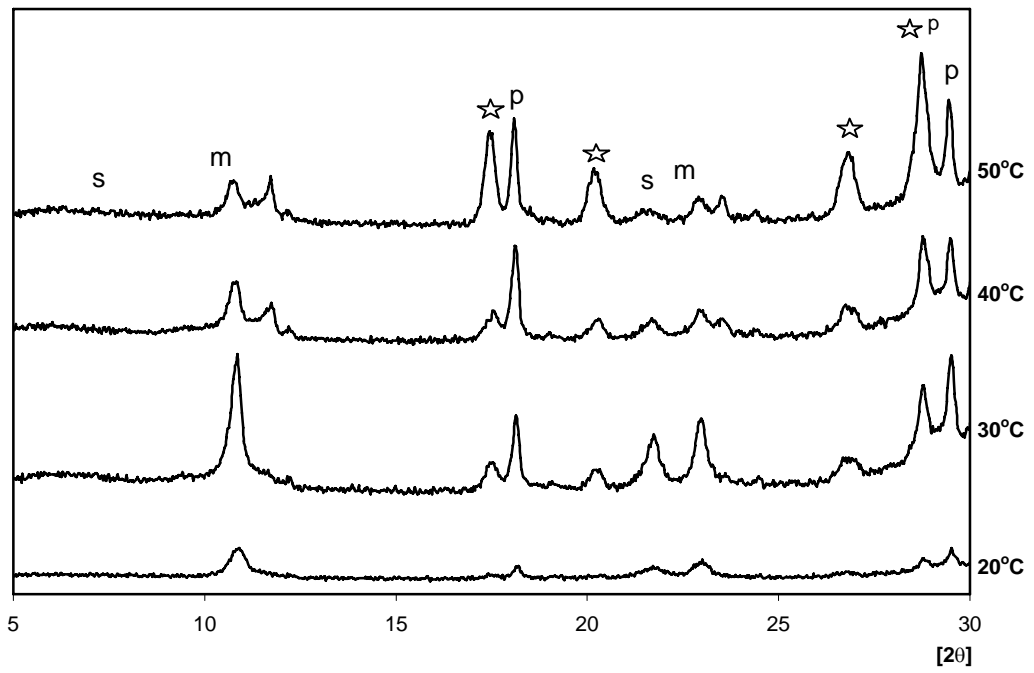


Figure 5.20 XRD Patterns of IP25 at 28 days

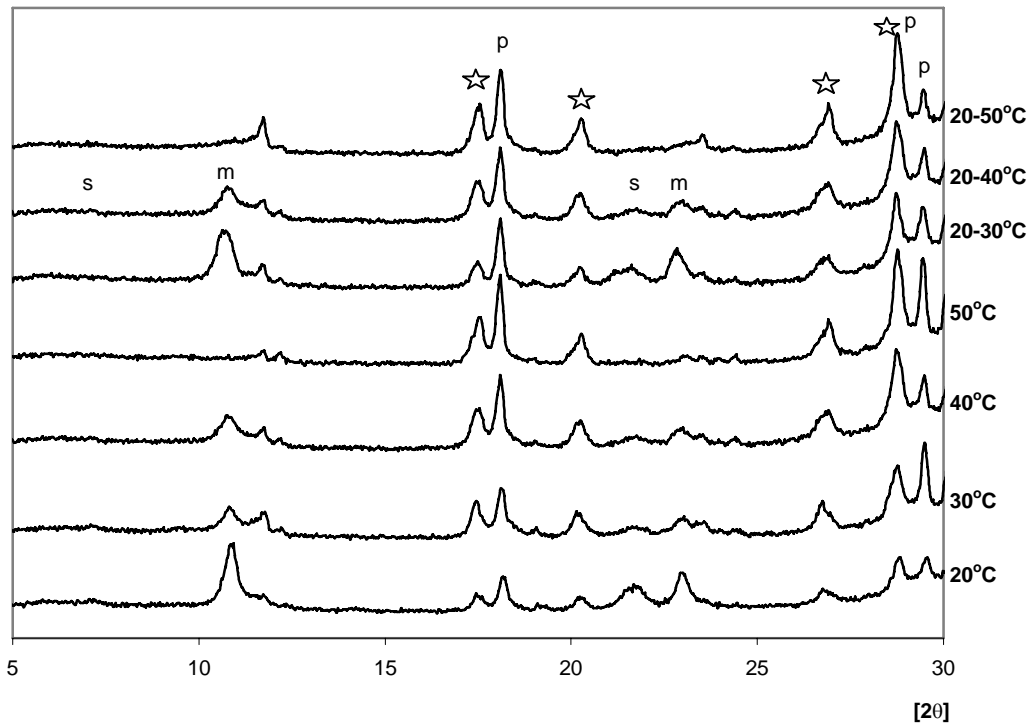


Figure 5.21 XRD Patterns of IP25 at 210 days

XRD analysis is one of the primary techniques used to characterize the phases present. The most common phases obtained throughout this study and their most intense interatomic spacing values (D spacing) and related XRD reflection angles with CuK α radiation between 2 θ values of 5-30° are given in Table 5.11.

Table 5.11 XRD Patterns of Most Common Phases [47,69-73]

Phases	D spacing, Å (Reflection angles, °)
C ₃ AH ₆	5.09 (17.42), 3.30 (26.80), 3.09 (28.89)
C ₂ AH ₈	10.70 (8.26)
CAH ₁₀	7.13 (12.41), 13.92 (6.35)
AH ₃	4.82 (18.41), 4.34 (20.46), 4.30 (20.66)
C ₂ ASH ₈	4.16 (21.36), 12.69 (6.97), 6.20 (14.29)
CH	4.90 (18.10), 3.11(28.71), 3.03 (29.48)
C ₆ A \bar{S} ₃ H ₃₂	9.65 (9.16), 5.58 (15.88), 3.22 (27.70)
C ₃ S ₂ H ₃	3.04 (29.38), 9.67 (9.14), 4.83 (18.37)
C ₄ A \bar{S} H ₁₂	8.13 (10.88), 3.86 (23.04)

In order to observe the change of phases with time, temperature, and type of CAC-PC binary system, semi-quantitatively, the areas under the characteristic peaks were calculated. The peaks at 2 θ =17.42, 8.26, 12.41, 18.41, 21.36, 18.10, 9.16, and 10.88 were selected for C₃AH₆, C₂AH₈,

CAH₁₀, AH₃, C₂ASH₈, CH, C₆A \bar{S} ₃H₃₂, and C₄A \bar{S} H₁₂, respectively. These peaks were chosen according to relative intensities of X-ray patterns of the phases. However, some of them being interfered by the peaks of other phases were not taken into account. The areas under the characteristic peaks were calculated by assuming peaks as a triangle. The calculated peak areas are given in Tables 5.12-15, for IP100, IP75, IP25, and IP0, respectively.

In order to compensate the accuracy problem of area method, the areas were grouped into three as strong (s), medium (m), and weak (w). In other words, the particular phases having peak area less than 25% of the highest value for the same phase observed among all XRD's were quantified as weak, whereas the ones having peak area more than 75% of the highest value for the same phase observed among all XRD's were quantified as strong. The rest were identified quantitatively as medium.

Available crystalline phases and their quantities classified as strong, medium, and weak are listed in Table 5.16 for CAC-PC combinations and for several curing conditions.

Table 5.12 Area under the Peak of the Phases Observed in IP100 at Different Curing Temperatures

Curing Temperature (°C)	Age (day)	Area under the Peak of Phases (unit)		
		C ₃ AH ₆	CAH ₁₀	AH ₃
20	28	86	194	45
	210	1381	180	598
30	28	2021	-	561
	210	2020	-	694
40	28	2043	-	542
	210	2423	-	699
50	28	2361	-	638
	210	2471	-	1094
20-30	210	2129	-	1138
20-40	210	2358	-	1394
20-50	210	2619	-	1251

Table 5.13 Area under the Peak of the Phases Observed in IP75 at Different Curing Temperatures

Curing Temperature (°C)	Age (day)	Area under the Peak of Phases (unit)			
		C ₃ AH ₆	CAH ₁₀	AH ₃	C ₂ ASH ₈
20	28	169	241	-	-
	210	1014	105	175	-
30	28	1529	-	150	55
	210	1774	-	310	-
40	28	1906	-	231	-
	210	2088	-	447	-
50	28	2122	-	394	-
	210	2174	-	358	-
20-30	210	2708	-	904	-
20-40	210	2568	-	795	-
20-50	210	2511	-	598	-

Table 5.14 Area under the Peak of the Phases Observed in IP25 at Different Curing Temperatures

Curing Temperature (°C)	Age (day)	Area under the Peak of Phases (unit)				
		C ₃ AH ₆	C ₂ ASH ₈	C ₄ A \bar{S} H ₁₂	C ₃ S ₂ H ₃	CH
20	28	-	-	301	o. by p	89
	210	154	182	1046	o. by p	245
30	28	203	332	1413	o. by p	368
	210	401	30	399	o. by p	358
40	28	228	91	511	o. by p	416
	210	422	52	434	o. by p	502
50	28	714	44	351	o. by p	513
	210	619	-	-	o. by p	749
20-30	210	316	145	768	o. by p	620
20-40	210	514	80	495	o. by p	502
20-50	210	568	-	-	o. by p	715

not: o. by p means that peaks are overlapped by the peaks of portlandite

Table 5.15 Area under the Peak of the Phases Observed in IP0 at Different Curing Temperatures

Curing Temperature (°C)	Age (day)	Area under the Peak of Phases (unit)		
		$C_6\bar{A}S_3H_{32}$	$C_3S_2H_3$	CH
20	28	37	o. by p	598
	210	202	o. by p	1837
30	28	216	o. by p	2431
	210	139	o. by p	2052
40	28	133	o. by p	3245
	210	93	o. by p	2493
50	28	81	o. by p	3315
	210	-	o. by p	2311
20-30	210	272	o. by p	3087
20-40	210	124	o. by p	2385
20-50	210	25	o. by p	3011

not: o. by p means that peaks are overlapped by the peaks of portlandite

Table 5.16 Phases Formed in the CAC-PC Mixes Depending on Time and Curing Temperatures

Curing Temperature (°C)	Age (day)	Type of Phases Formed in the CAC-PC Mixes			
		IP100	IP75	IP25	IP0
20	28	C ₃ AH ₆ (w)	C ₃ AH ₆ (w)	C ₃ S ₂ H ₃ (?)	C ₆ A \bar{S} ₃ H ₃₂ (w)
		CAH ₁₀ (m)	CAH ₁₀ (s)	CH(w)	C ₃ S ₂ H ₃ (?)
		AH ₃ (w)		C ₄ A \bar{S} H ₁₂ (m)	CH(w)
	210	C ₃ AH ₆ (m)	C ₃ AH ₆ (m)	C ₃ AH ₆ (w)	C ₆ A \bar{S} ₃ H ₃₂ (s)
		CAH ₁₀ (m)	CAH ₁₀ (m)	C ₂ ASH ₈ (w)	C ₃ S ₂ H ₃ (?)
		AH ₃ (m)	AH ₃ (w)	C ₃ S ₂ H ₃ (?) CH(w) C ₄ A \bar{S} H ₁₂ (s)	CH(m)
30	28	C ₃ AH ₆ (s)	C ₃ AH ₆ (m)	C ₃ AH ₆ (w)	C ₆ A \bar{S} ₃ H ₃₂ (s)
		AH ₃ (m)	AH ₃ (w)	C ₂ ASH ₈ (w)	C ₃ S ₂ H ₃ (?)
			C ₂ ASH ₈ (w) CH(m)	C ₃ S ₂ H ₃ (?) C ₄ A \bar{S} H ₁₂ (s)	CH(s)
	210	C ₃ AH ₆ (s)	C ₃ AH ₆ (m)	C ₃ AH ₆ (w)	C ₆ A \bar{S} ₃ H ₃₂ (m)
		AH ₃ (m)	AH ₃ (m)	C ₂ ASH ₈ (w) C ₃ S ₂ H ₃ (?) CH(w) C ₄ A \bar{S} H ₁₂ (m)	C ₃ S ₂ H ₃ (?) CH(m)

Table 5.16 (continued)

Curing Temperature (°C)	Age (day)	Type of Phases Formed in the CAC-PC Mixes			
		IP100	IP75	IP25	IP0
40	28	C ₃ AH ₆ (s)	C ₃ AH ₆ (s)	C ₃ AH ₆ (w)	C ₆ A \bar{S} ₃ H ₃₂ (m)
		AH ₃ (m)	AH ₃ (w)	C ₂ ASH ₈ (w)	C ₃ S ₂ H ₃ (?)
			C ₃ S ₂ H ₃ (?)	CH(s)	
			CH(w)	C ₄ A \bar{S} H ₁₂ (m)	
	210	C ₃ AH ₆ (s)	C ₃ AH ₆ (s)	C ₃ AH ₆ (w)	C ₆ A \bar{S} ₃ H ₃₂ (m)
		AH ₃ (m)	AH ₃ (m)	C ₂ ASH ₈ (w)	C ₃ S ₂ H ₃ (?)
				C ₃ S ₂ H ₃ (?)	CH(s)
				CH(w)	C ₄ A \bar{S} H ₁₂ (m)
50	28	C ₃ AH ₆ (s)	C ₃ AH ₆ (s)	C ₃ AH ₆ (m)	C ₆ A \bar{S} ₃ H ₃₂ (m)
		AH ₃ (m)	AH ₃ (m)	C ₂ ASH ₈ (w)	C ₃ S ₂ H ₃ (?)
			C ₃ S ₂ H ₃ (?)	CH(s)	
			CH(w)	C ₄ A \bar{S} H ₁₂ (m)	
	210	C ₃ AH ₆ (s)	C ₃ AH ₆ (s)	C ₃ AH ₆ (m)	C ₃ S ₂ H ₃ (?)
		AH ₃ (s)	AH ₃ (w)	C ₃ S ₂ H ₃ (?)	CH(m)
				CH(w)	

Table 5.16 (continued)

Curing Temperature (°C)	Age (day)	Type of Phases Formed in the CAC-PC Mixes			
		IP100	IP75	IP25	IP0
20-30	210	C ₃ AH ₆ (s) AH ₃ (s)	C ₃ AH ₆ (s) AH ₃ (m)	C ₃ AH ₆ (w) C ₂ ASH ₈ (w) C ₃ S ₂ H ₃ (?) CH(w) C ₄ A \bar{S} H ₁₂ (m)	C ₆ A \bar{S} ₃ H ₃₂ (s) C ₃ S ₂ H ₃ (?) CH(s)
20-40	210	C ₃ AH ₆ (s) AH ₃ (s)	C ₃ AH ₆ (s) AH ₃ (m)	C ₃ AH ₆ (w) C ₂ ASH ₈ (w) C ₃ S ₂ H ₃ (?) CH(w) C ₄ A \bar{S} H ₁₂ (m)	C ₆ A \bar{S} ₃ H ₃₂ (m) C ₃ S ₂ H ₃ (?) CH(s)
20-50	210	C ₃ AH ₆ (s) AH ₃ (s)	C ₃ AH ₆ (s) AH ₃ (m)	C ₃ AH ₆ (w) C ₃ S ₂ H ₃ (?) CH(w)	C ₆ A \bar{S} ₃ H ₃₂ (w) C ₃ S ₂ H ₃ (?) CH(s)

5.2.1.1 Discussion of the Results for Pure CAC Mix (=IP100=IA100=IC100=IK100)

As seen in Figure 5.9, curing continuously at 20°C caused compressive strength increase up to almost 90 MPa at 28 days. At further ages a slight reduction in strength was observed at the same curing temperature till 210 days. This strength reduction was increased by an increase in curing temperature. In other words, as curing temperatures increased, the strength decreased drastically. Particularly, the ones cured 28 days at 20°C then at 40°C and at 50°C showed significant strength reductions after 28 days, compared to the one cured directly at 20°C and the one cured 28 days at 20°C then at 30°C.

On the other hand, the mixes cured continuously at 30°C, 40°C and 50°C experienced no significant strength reduction. They gained their maximum strengths almost within first 24 hrs and then their strength did not change, significantly. If the strength developments of each IP100 mix at several curing conditions were examined throughout 210 days, it can be clearly seen that almost all strength curves coincided with each other in between the strength values of 20 to 30 MPa or for the mixes (i) cured continuously at 20°C, and (ii) cured 28 days at 20°C and then at 30°C would coincide at later ages.

It can be concluded that the change in strength development depending on time mainly related with curing temperature. This has been pointed out in previous studies over 40 years, too [1-4, 22-24, 53-65,70,74].

As illustrated in Figure 5.9, compressive strength development of pure CAC mix was affected by curing temperature change. This was mainly due to the hydration mechanism occurring differently at different curing temperature.

As it can be clearly seen in Figure 5.14 and 5.15, common phases occurring in CAC matrix at 28 days and at 210 days were C_3AH_6 and AH_3 , whatever the curing temperature was. On the other hand, formation of CAH_{10} was observed only at $20^\circ C$. According to previous studies [1,2,4,22-24], at low temperatures ($<27^\circ C$) the common phases are CAH_{10} , C_2AH_8 , and AH_3 . C_3AH_6 cannot be seen at these temperatures, unless conversion of CAH_{10} and C_2AH_8 to C_3AH_6 occurs over time. As stated previously in Section 2.6.1, the rate of conversion reaction is especially time dependent and complete conversion takes several years, particularly at lower temperatures (i.e. $<20^\circ C$). As temperature goes up, the conversion occurs more rapidly. Therefore, as seen in Table 5.16, at $20^\circ C$ the amounts of C_3AH_6 and AH_3 were the lowest among all curing temperatures. Increase in curing temperature led to an increase in the amount of C_3AH_6 (see Table 5.12), which also means that conversion rate was increased by temperature increase.

Conversion is directly related with strength development, since regard with conversion of unstable CAH_{10} and C_2AH_8 to stable C_3AH_6 , some water was released in hardened matrix, causing an increase in porosity and thereby a decrease in strength [1,8,73].

The increase in AH_3 formation with time depending on the increase in curing temperature, which can be seen in Table 5.12 and Table 5.16, is another indication of conversion, since besides water, AH_3 was also released throughout the conversion reaction of CAH_{10} to C_2AH_8 and C_3AH_6 and of C_2AH_8 to C_3AH_6 .

Coinciding of strength curves of IP100 mixes cured continuously at $40^\circ C$, $50^\circ C$ and cured 28 days at $20^\circ C$ than at $30^\circ C$, at $40^\circ C$, and at $50^\circ C$ at the end of 210 days may be explained by the degree of conversion. As seen

in Table 5.12, the amount C_3AH_6 of mixes cured continuously at 20°C and 30°C were much less than the ones cured at other temperatures. This conclusion coincides with the results of compressive strength tests. At the end of 210 days only these two mixes showed higher strength than the others. That also means that they did not complete conversion reactions. However, their progressive strength decrease trend indicates that at later ages they will also reach the strength level (i.e. between 20 to 30MPa) presented by other mixes.

Similarly, Robson [6] reported that under curing at low temperature (19°C), CAC mix rises to a peak value followed by a strength decrease up to a strength level, which may be called as residual or fully converted strength of this particular mix. In other words, the strength of CAC cannot drop below this residual level at later stages. Likewise, other mixes cured at elevated temperatures reach the same residual strength level. As a result, whether CAC is subjected to high temperature or low temperature curing, even subjected firstly to low temperature curing and then to high temperature curing, it reaches the same residual strength level where conversion occurs completely. Accordingly, the results presented in Figure 5.9 were consistent with these considerations.

The highest strength values among all IP100 mixes at 28 days and at 210 days were 85.6 and 71.5, respectively, observed under curing at 20°C. This was mainly related with the formation of CAH_{10} and this was formed only at 20°C, as seen in Figure 5.14 and Figure 5.15. In addition, even at 210 days there were CAH_{10} , which means that the conversion did not complete in 210 days under curing continuously at 20°C.

Similarly, according to previous studies [1,53,62], the bonds of C_3AH_6 and AH_3 are less stronger than those of CAH_{10} and C_2AH_8 , even at equal

porosity. Therefore, the compressive strengths of pure CAC mix cured at 20°C are the highest due to the presence of CAH_{10} . In addition, as stated previously, increase in porosity caused by water release throughout conversion of CAH_{10} to C_2AH_8 and C_3AH_6 and of C_2AH_8 to C_3AH_6 led to strength reductions in mixes cured at elevated temperatures [1,8,74].

5.2.1.2 Discussion of the Results for Pure PC Mix (=IP0)

Throughout this study, like pure CAC mix IP100, pure PC mix IP0 was considered as reference mix for CAC-PC binary system. Although the object of this study was not focused on PC, it was examined in order to make comparison among CAC-PC binary mixes.

According to Figure 5.13, all IP0 mixes showed progressive strength increase with time. There was no strength reduction with time at any curing temperature, unlike IP100.

The hydration reaction of PC results mainly in formation of calcium silicate hydrate and portlandite (CH). As seen from Figure 5.16 and Figure 5.17, the main phase, as expected, formed in IP0 mixes is CH, i.e. portlandite. The other main phase $C_3S_2H_3$, i.e. tobermorite cannot be detected by X-ray analysis, clearly, since XRD patterns of phases, particularly that of portlandite and tobermorite overlap to each other. Also, the traces of tobermorite cannot be seen clearly due to its poorly crystalline structure.

Another important phase was ettringite ($C_6\bar{A}\bar{S}_3H_{32}$), which formed mainly by the reaction of C_3A coming from PC clinker with SO_3 ions of gypsum added to PC clinker during its production to adjust setting time.

According to the Figures 5.16, 5.17 and Tables 5.15 and 5.16, slight increase was observed in CH formation (that means also formation of $C_3S_2H_3$) with the increase in temperature, particularly at 28 days. On the other hand, at later age, i.e. at 210 days the amount of CH was more or less the same. As a result, the compressive strengths (which is directly proportional with amount of tobermorite formation) of IP0 cured at higher temperature were higher at early ages. On the other hand, as illustrated in Figure 5.13, at later ages, particularly at 210 days, the IP0 mix cured at higher temperature showed slight lower compressive strengths. This may be due to the non-uniform distribution of hydration product occurred within the microstructure at elevated temperature. As stated in previous studies [54,75-78], elevated curing temperatures result in non-uniform distribution of hydration products and also in their high concentration, which limits or even prevents diffusion of ions, thereby reducing further hydration.

5.2.1.3 Discussion of the Results for CAC-PC Binary Mixes (IP75, IP50, IP25)

CAC-PC blends exhibits different setting and hardening behaviour than each of these two binders, separately. Setting behaviour of such mixes was discussed previously in Section 5.1. Similar considerations are also valid for hardening. According to previous studies [1,2,4,6,7,9,25-30], addition of CAC to PC or vice versa shortens setting time, drastically (similar behaviour was observed in this study, too. see Table 5.1 and Figure 5.1), while causing reduction in strength at ultimate ages.

As the strength development curves of IP75, IP50 and IP25 in Figures 5.10-5.12 (respectively) are examined by comparing with those of reference mixes (Figure 5.9 and Figure 5.13), i.e. pure CAC mix IP100 and pure PC mix IP0, it can clearly be seen that the CAC-PC blends

exhibited lower strength than the reference mixes. According to Figures 5.14-5.21 and Tables 5.12-5.16, it can be concluded that formation of less amount of calcium aluminate hydrates and AH_3 in IP75 compared to IP100, mainly due to less amount of CAC and no formation of tobermorite, in spite of the addition of PC, caused decreases in strength. Similar considerations can be drawn for IP25. That means that formation of much less amount of CH (i.e. also much less amount of tobermorite) in IP25 compared to IP0 and much less formation of calcium aluminate hydrates compared to IP100 resulted in lower strength values. Similarly, Gu et al. [28] pointed out that strength decreases in CAC-PC blends compared to pure PC mix is mainly due to the delayed hydration of calcium silicates.

IP75 and IP50 behaved like pure CAC mixes, whereas IP 25 similar to pure PC mixes. In other words, IP 75 and IP50 showed strength decreases after reaching a peak (41.6 and 21.3 MPa, respectively), particularly at 20°C curing, which was similar to the behaviour of IP100. As stated previously, this was mainly due to the conversion reactions. On the other hand, although IP25 exhibited very slight decrease after reaching a peak strength, it would not be wrong to assume that it showed almost progressive increase in strength, like IP0, since main constituent of IP25 was PC. Slight decrease in strength was mainly owing to the availability of calcium aluminate hydrates in restricted amounts compared to pure CAC mix and their conversion, whereas the progressive strength increase was related with progressive formation of CH and tobermorite with time, as it can be seen in Tables 5.12-5.16.

Furthermore, as seen in Tables 5.14 and 5.16, calcium silicate aluminate hydrate, i.e. straetlingite (C_2ASH_8) is another phase formed in IP25. According to previous studies [1,25], formation of straetlingite is a slow process and its contribution to strength may be seen at later ages. This also helps us to explain the mechanism of the progressive strength

increase of IP25 and thus the mechanism of prevention of strength decrease caused by conversion reactions. In other words, in IP25, calcium aluminate hydrates were partially replaced by straetlingite by limiting occurrence of conversion reactions.

As seen in Figures 5.20 and 5.21, and Table 5.14, calcium alumina monosulfo hydrate ($C_4\bar{A}\bar{S}H_{12}$) was detected in IP25, particularly at moderate temperatures. Also, according to these X-ray analyses, there may be a direct proportionality between $C_4\bar{A}\bar{S}H_{12}$ and straetlingite (C_2ASH_8). As the one increased, the other also increased. Both formed much more at moderate temperature than at lower temperature and than at elevated temperature. Evju and Hansen [79-82] reported that insufficient amounts of sulphate in comparison to the equivalent amounts of calcium and aluminium to form ettringite cause formation of monosulfate by consuming the ettringite. In addition, they claimed that due to formation of C_2AH_8 , ettringite is converted to monosulfate. Similarly, in this research the formation of C_2ASH_8 might cause formation of monosulphate instead of ettringite, which also clarifies the direct proportionality between monosulfate and straetlingite. Moreover, insufficient amount of sulphate coming from PC compared to calcium and aluminium may be the reason for formation of monosulfate.

As illustrated in Figures 5.10 and 5.11, IP75 and IP50 behaved like pure CAC mix (IP100). In other words, their strength at 20°C increased till 28 days followed by a decrease until a strength level, which was defined previously in Section 5.2.1.1 as residual strength level (Since conversion proceeded slowly at continuous curing at 20°C, it would probably reach this residual strength value after 210 days, whereas curing at 30°C and 40°C, and 50°C after curing 28 days at 20°C resulted in complete conversion, and thus they reached the residual strength value within 210

days). On the other hand, the IP75 and IP50 mixes cured continuously at 30°C, 40°C, and 50°C did not show a peak strength value, rather they showed a progressive strength increase up to a same residual strength value presented by the mixes cured 28 days at 20°C and then cured at 30°C, 40°C, and 50°C. According to these observations, it can be concluded by taking also into accounts the XRD analysis illustrated in Figures 5.18-5.21 that all mixes cured at different temperatures showed coinciding strength value called as residual strength value. According to related XRD analysis performed in this research and also to previous studies in literature [6,62,83], this residual strength level represents the complete conversion. In other words, all unstable calcium aluminate hydrates (CAH_{10} , C_2AH_8) converted to stable hydrates (C_3AH_6 and AH_3).

5.2.2 Effect of Temperature on Compressive Strength Development of CAC-Gypsum Mixes

The object of gypsum inclusion to CAC is mainly to limit or prevent shrinkage behaviour of CAC. Also, to obtain a self-stressing cement or expansive cement, CAC-gypsum blends can be utilized. In such systems, the expansion is obtained by formation of ettringite between calcium aluminates of CAC and sulphates of gypsum. Ettringite formation also affects the setting and hardening behaviour of such blends [1,6,9,31,32,64,65,70,79,84-86].

Setting behaviour was discussed previously in Section 5.1. The effects of CAC replacements up to 8% (0.5%, 2%, 4%, 8%) by gypsum and temperature effect on compressive strength development of the blends were examined in this section. Accordingly, Figures 5.22-5.25 illustrate the

compressive strength development of CAC-gypsum mixes, IA99.5, IA98, IA96, and IA92, respectively, with respect to curing temperatures.

As stated previously, IA100 implies the reference pure CAC mix for CAC-gypsum blends and its compressive strength development with time with respect to curing temperatures was discussed in Section 5.2.1.1.

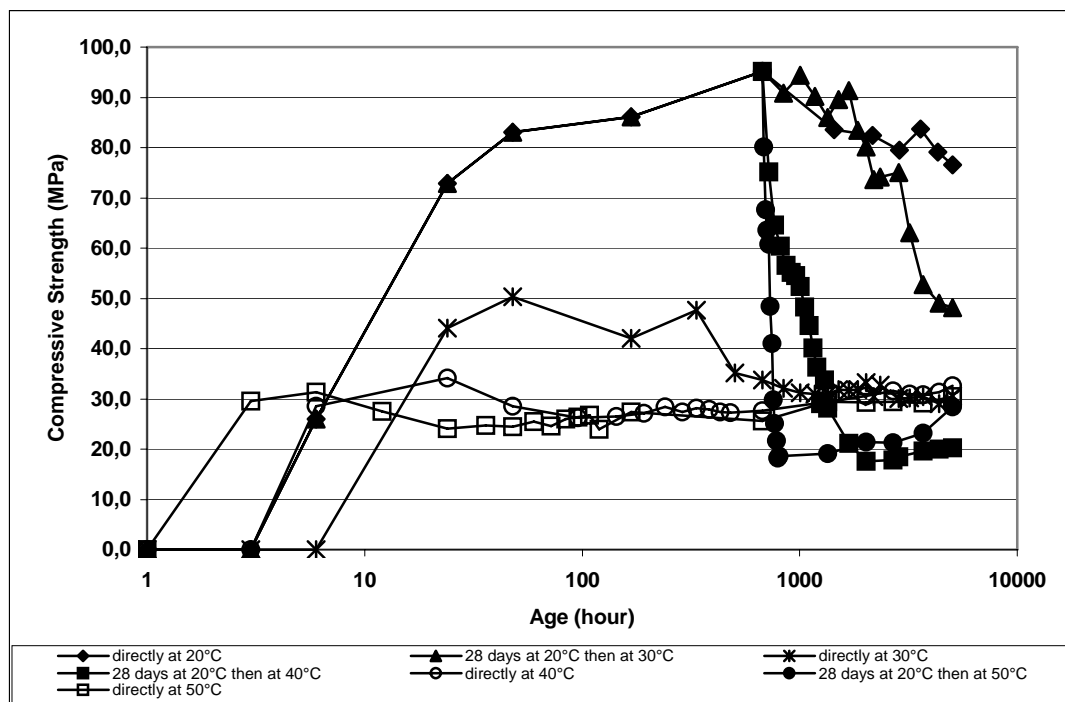


Figure 5.22 Compressive Strength Development of IA99.5 at Different Curing Temperatures

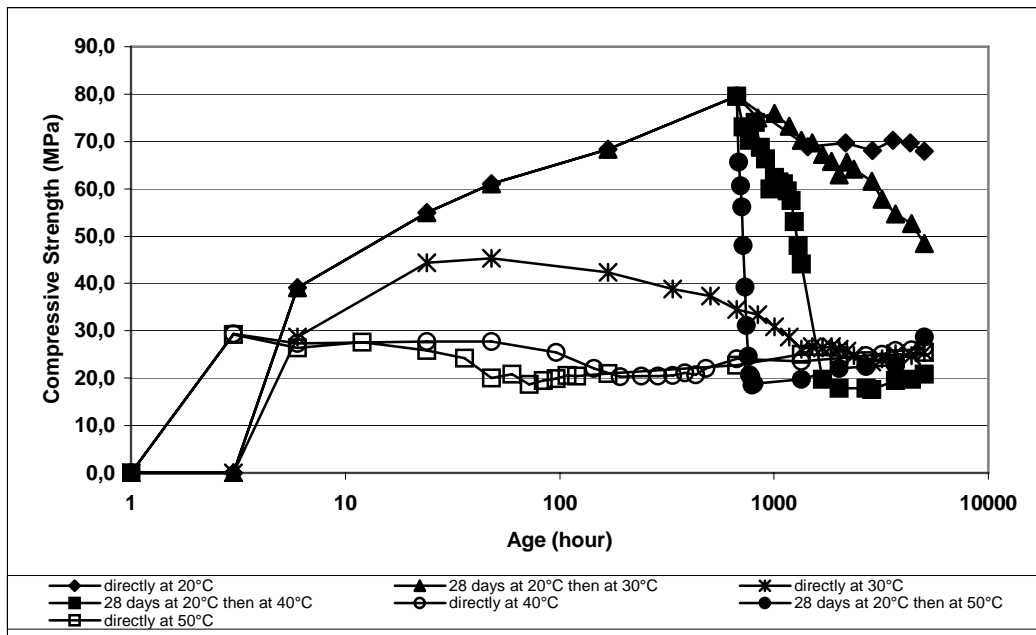


Figure 5.23 Compressive Strength Development of IA98 at Different Curing Temperatures

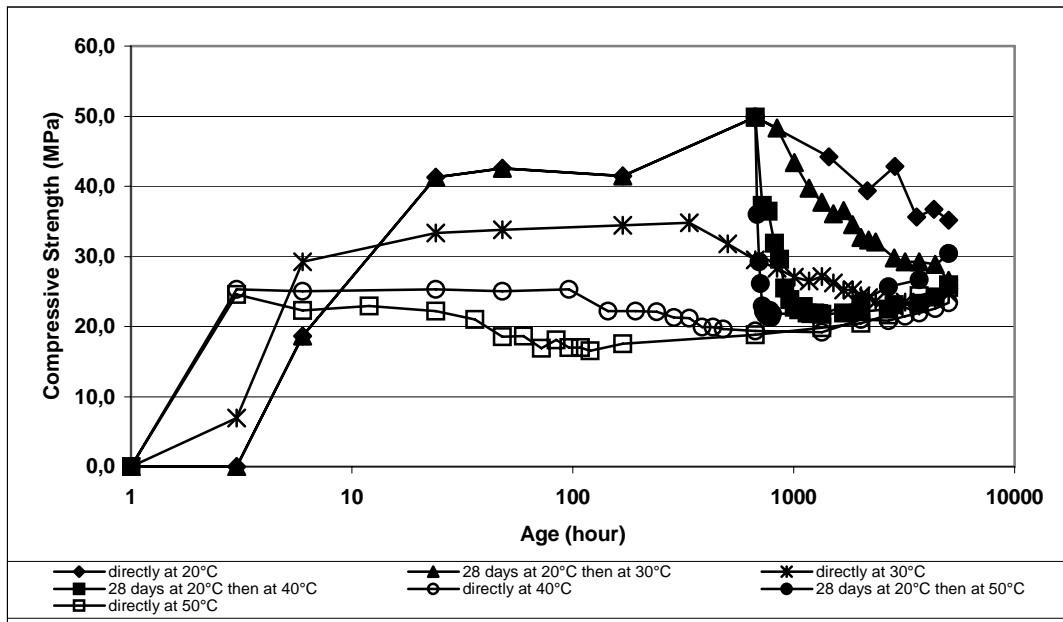


Figure 5.24 Compressive Strength Development of IA96 at Different Curing Temperatures

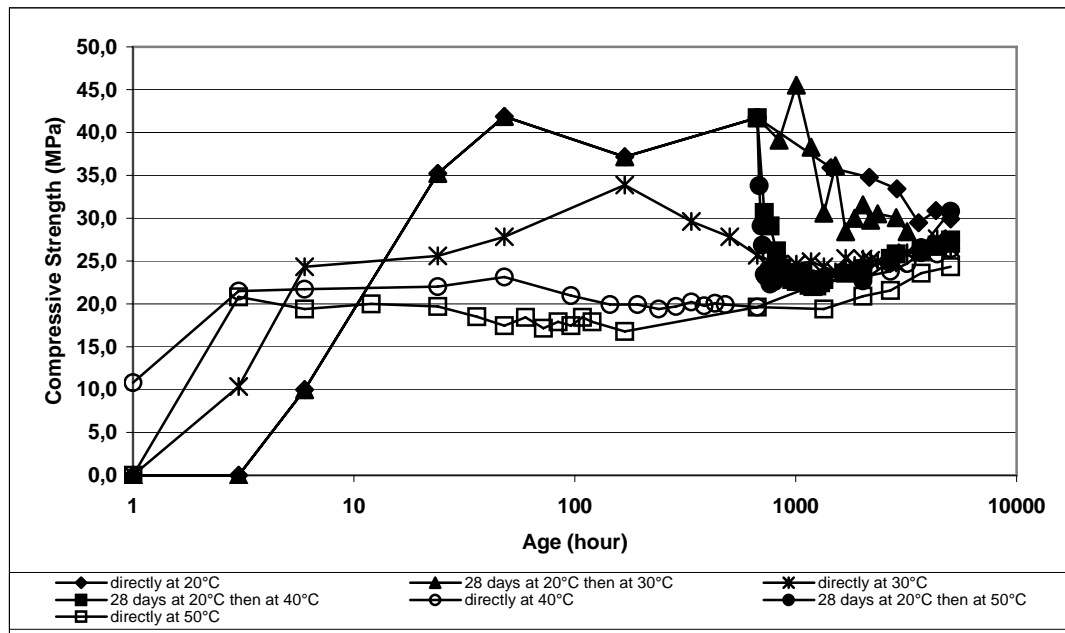


Figure 5.25 Compressive Strength Development of IA92 at Different Curing Temperatures

For understanding the mechanism of compressive strength development of CAC-gypsum blends, XRD analysis was performed only on IP96. According to previous studies [1,6,9,31,32,64,65,70,79,84-86], the behaviour of CAC-gypsum blends at early ages is mainly affected by ettringite formation. Therefore, analysing of one out of four CAC-gypsum blends in terms of XRD may be sufficient.

The XRD patterns of IA 96 at 28 days and at 210 days are given in Figure 5.26 and Figure 5.27, respectively.

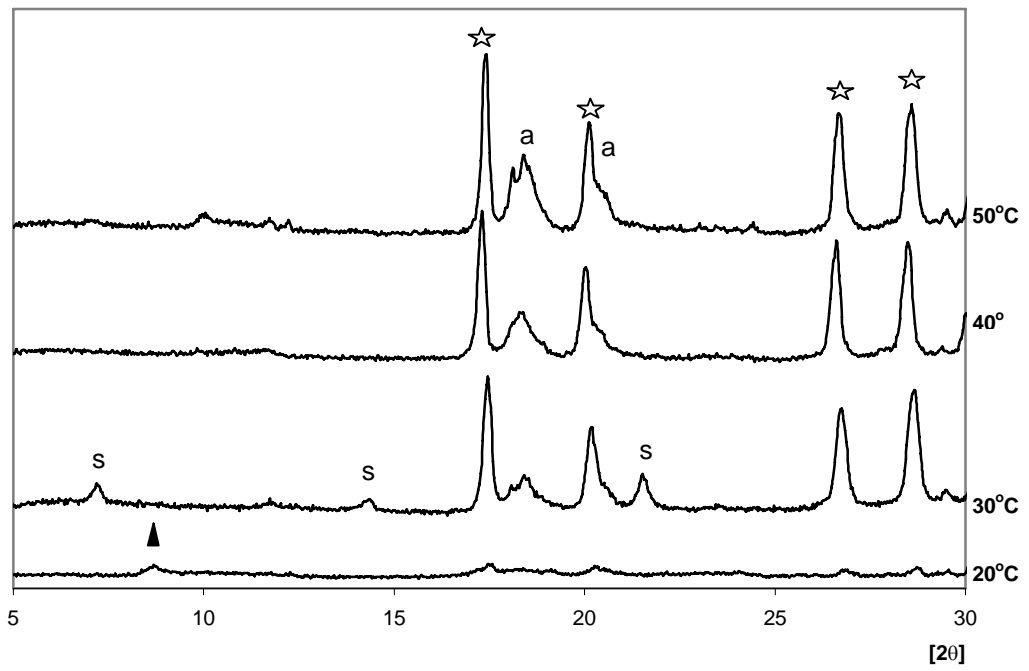


Figure 5.26 XRD Patterns of IA96 at 28 days

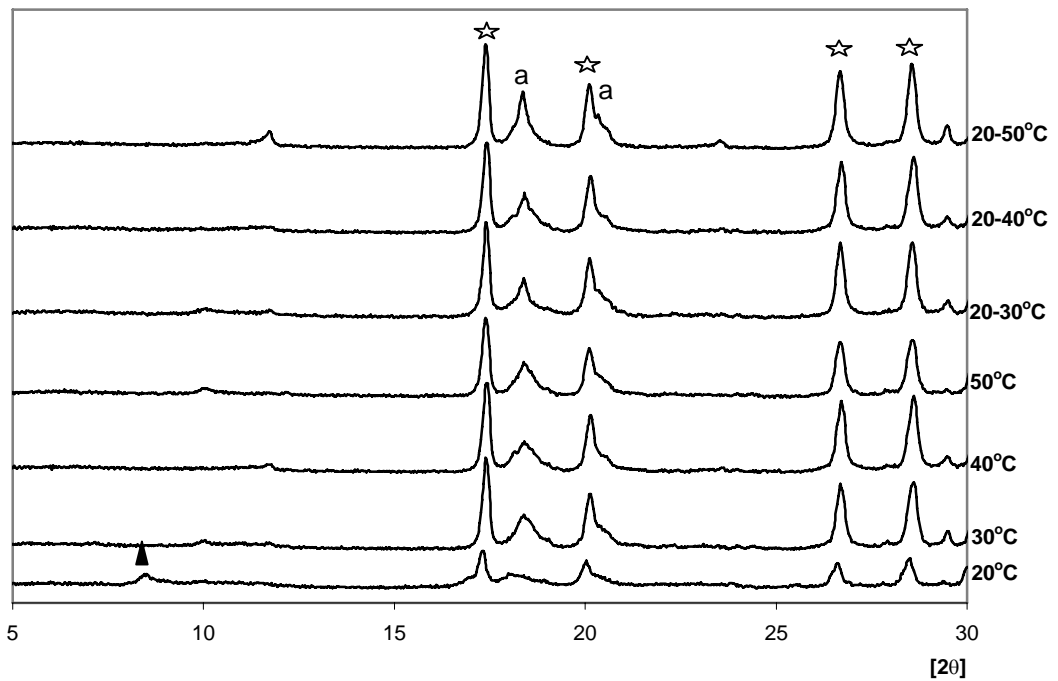


Figure 5.27 XRD Patterns of IA96 at 210 days

The area under the characteristic peaks of available phases observed in Figure 5.26 and Figure 5.27 were calculated and tabulated in Table 5.17. On the other hand, for the sake of illustration, the phases detected in XRD and their semi-quantitative analysis by means of categorization as strong, medium, and weak (whose descriptions were give in Section 5.2.1.1) are listed in Table 5.18.

Table 5.17 Area under the Peak of the Phases Observed in IA96 at Different Curing Temperatures

Curing Temperature (°C)	Age (day)	Area under the Peak of Phases (unit)			
		C ₃ AH ₆	C ₂ AH ₈	AH ₃	C ₂ ASH ₈
20	28	93	128	-	-
	210	887	197	-	-
30	28	1279	-	328	468
	210	1949	-	653	-
40	28	1729	-	425	-
	210	1892	-	701	-
50	28	1818	-	856	-
	210	1945	-	784	-
20-30	210	2181	-	702	-
20-40	210	2057	-	939	-
20-50	210	2191	-	1422	-

Table 5.18 Phases Formed in IA96 Depending on Time and Curing Temperatures

Curing Temperature (°C)	Age (day)	Type of Phases Formed in IA96
20	28	C ₃ AH ₆ (w) C ₂ AH ₈ (m)
	210	C ₃ AH ₆ (m) C ₂ AH ₈ (s)
30	28	C ₃ AH ₆ (m) AH ₃ (w) C ₂ ASH ₈ (w)
	210	C ₃ AH ₆ (m) AH ₃ (m)
40	28	C ₃ AH ₆ (m) AH ₃ (m)
	210	C ₃ AH ₆ (m) AH ₃ (m)
50	28	C ₃ AH ₆ (m) AH ₃ (m)
	210	C ₃ AH ₆ (m) AH ₃ (m)
20-30	210	C ₃ AH ₆ (s) AH ₃ (m)
20-40	210	C ₃ AH ₆ (s) AH ₃ (m)
20-50	210	C ₃ AH ₆ (s) AH ₃ (s)

5.2.2.1 Discussion of the Results for CAC-Gypsum Binary Mixes (IA99.5, IA98, IA96, IA92)

PC paste exhibits a decrease in volume with time, particularly after setting, which is mainly caused by physical and chemical processes. Indeed, the chemical shrinkage called also as autogenous shrinkage is caused by the loss of water throughout hydration reactions, whereas physical shrinkage is caused by the loss of water as a result of drying, and therefore called as drying shrinkage [54,70,79]. Similarly, CAC's experience chemical and physical shrinkage, which causes problems related with volume stability, thereby problems related with mechanical properties in hardened state [6,70,79].

In order to compensate shrinkage in CAC systems, other cementitious materials may be added so that new voluminous hydrates can be formed. Ettringite formed by hydration of calcium aluminate rich materials and calcium sulphates is one of such voluminous hydrate, which eliminates shrinkage problems by its expansive property [70,79, 87].

Blends of CAC-gypsum are mainly used for self-stressing or shrinkage compensation. Moreover, they also exhibit rapid setting and hardening properties. Their setting behaviour was discussed previously in Section 5.1.1. In this section, the strength development of such systems will be examined.

As can be seen in Figures 5.22-5.25, the strength development of CAC-gypsum binary mixes was affected by gypsum inclusion ratio and by the curing temperature applied, drastically.

By examining Figures 5.22-5.25 and also Figure 5.9 (pure CAC mix), it can be concluded that increase in gypsum ratio resulted in reductions in

compressive strength of CAC-gypsum mixes, whatever the curing temperature was. While the compressive strengths of IA100 and IA99.5 were around 90 MPa at 28 days and at curing temperature of 20°C, that of IA98, IA96, and IA 92 were 79.6 MPa, 49.9 MPa, and 41.7 MPa at the same age and at the same curing condition, respectively. On the other hand, the ultimate strengths (at 210 days) of almost all mixes at every curing condition varied within the range of 20 to 30 MPa, except the mixes cured at relatively low temperatures (particularly the one cured continuously at 20°C and the one cured 28 days at 20°C then at 30°C).

The strength developments were mainly affected by the degree of conversion reactions. Depending on the curing temperature, conversion completed at different ages. The mixtures cured at elevated temperatures (over 30°C) were subjected to conversion directly. In other words, at elevated temperatures, stable hydration products (C_3AH_6 and AH_3) formed directly. Therefore, their strength increased progressively without showing a peak value. On the other hand, the ones cured at lower temperatures experienced progressive strength increase up to a peak value and then the strength drastically started to decrease up to a level of strength, which is also the ultimate strength value of the mixes experiencing direct conversion. The same considerations were done previously for CAC-PC mixes.

The degree of conversion affecting the strength development can also be seen in Figure 5.26 and Figure 5.27. In addition, by examining Table 5.17 and 5.18 it can be observed that except the ones cured at 20°C there was no unstable calcium aluminate hydrates (CAH_{10} and C_2AH_8). In other words, the sole hydration products of others were C_3AH_6 and AH_3 , which are the stable converted hydration products of CAC. In addition, their higher amount of C_3AH_6 compared to the mix cured continuously at 20°C proved us the higher degree of conversion.

Another important conclusion, which can be drawn in Figures 5.22-5.25 is that increase in gypsum amount decreased the peak strength at 28 days, particularly at lower temperatures, while decreasing the gap between the peak strength occurred at 28 days and the ultimate strength at 210 days (i.e. residual strength level where conversion completed). This also enables us to claim that increase in inclusion amount of gypsum in CAC-gypsum systems fastened the rate of conversion, even at low temperature, i.e. 20°C.

According to Figures 5.22-5.25 and 5.9, IA100, IA99.5, and IA98 mixes cured (i) continuously at 20°C and (ii) cured 28 days at 20°C and then at 30°C, did not complete conversion within 210 days, while other IA100, IA99.5, and IA98 mixes cured at other temperatures were fully converted. On the other hand, the mix cured continuously at 20°C was the only IA96 mix, which was not fully converted, whereas the rest of IA96 mixes completed the conversion. As IA92 mixes are examined, it can be seen that all mixes including the one cured continuously at 20°C were fully converted (As discussed previously, reaching the residual strength value (which was the range between 20MPa and 30MPa for CAC-gypsum mixes) implies the full conversion of CAC-gypsum mixes). Based upon these observations, it can be interpreted that increase in the amount of gypsum inclusion caused faster conversion, even at low temperatures (i.e. 20°C).

Moreover, particularly at moderate temperature (i.e. 30°C), it may be claimed that gypsum inclusion caused formation of *stratlingite*, as seen in Table 5.17, by hydration reactions between calcium aluminates and calcium silicates or by hydration of *gehlenite* (C_2AS), even though CAC contains both C_2S and C_2AS in little amounts. Similarly, Dunster and Holton [86] reported the formation of *stratlingite* where pure CAC was

subjected to sulphate attack. The partial replacement of low strength stable C_3AH_6 by high strength stable straelingite may also lead to decrease in strength reduction from peak to residual strength (residual strength was previously defined as the strength where conversion is fully completed).

5.2.3 Effects of Temperature on Compressive Strength Development of CAC-Lime Mixes

The main object of lime inclusion to CAC is to shorten setting time of CAC. In addition, it also results in high early strength gain, while decreasing the ultimate strengths.

The effect of lime in CAC-lime binary mixes is related mainly with pH value of the mix. Lime inclusion leads to an increase in pH value, and thus dissolving rate of minerals (mainly CA) increases. Continuous dissolving and precipitation of newly formed calcium aluminate hydrates, accelerated by pH increase, causes decrease in setting time and increase in strength development, particularly at early ages [8].

The effect of lime addition on setting time of CAC-lime binary mixes was discussed previously in Section 5.1.1. On the other hand, the effect of lime addition and its ratio on strength development depending on the curing temperature are examined in this section.

Figures 5.28-5.31 portray the compressive strength development of CAC-lime mixes, i.e. IK99.5, IK99, IK98, and IK96, until 210 days with respect to the curing temperature, respectively.

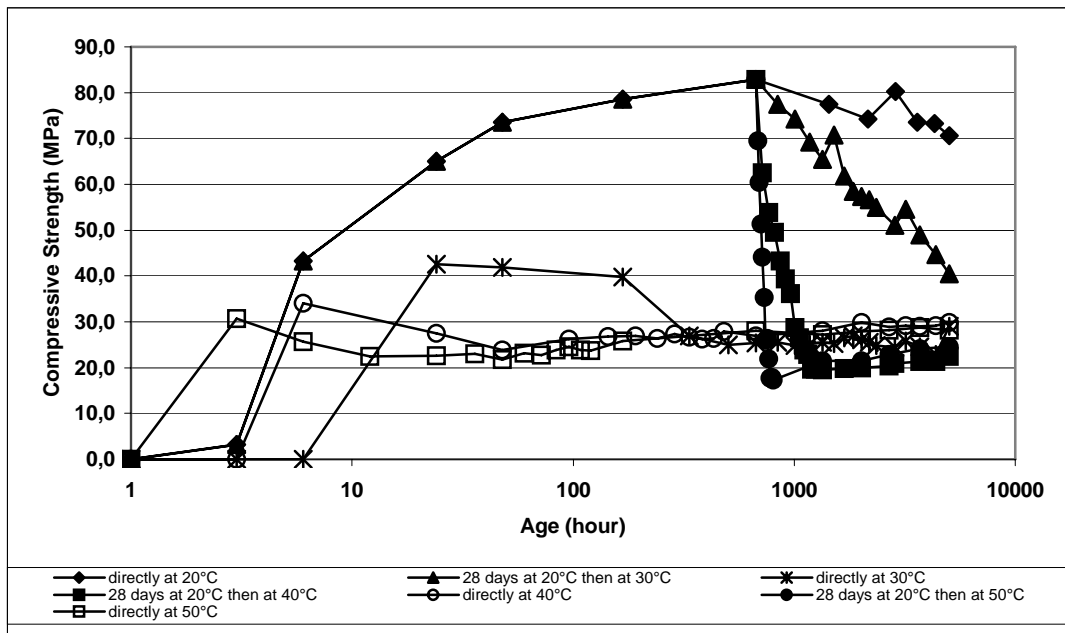


Figure 5.28 Compressive Strength Development of IK99.5 at Different Curing Temperatures

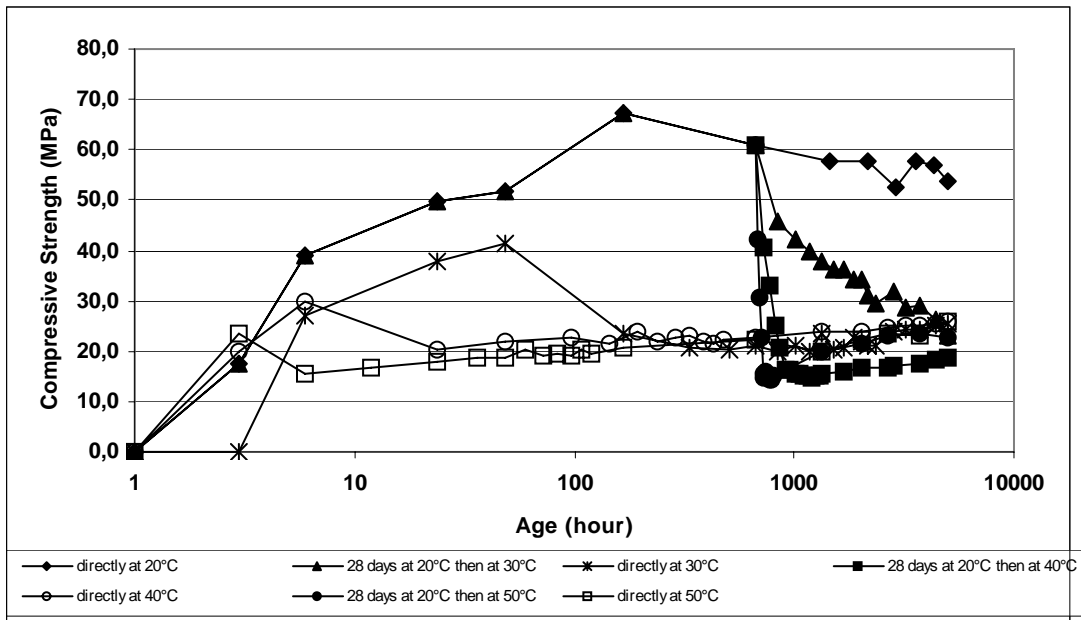


Figure 5.29 Compressive Strength Development of IK99 at Different Curing Temperatures

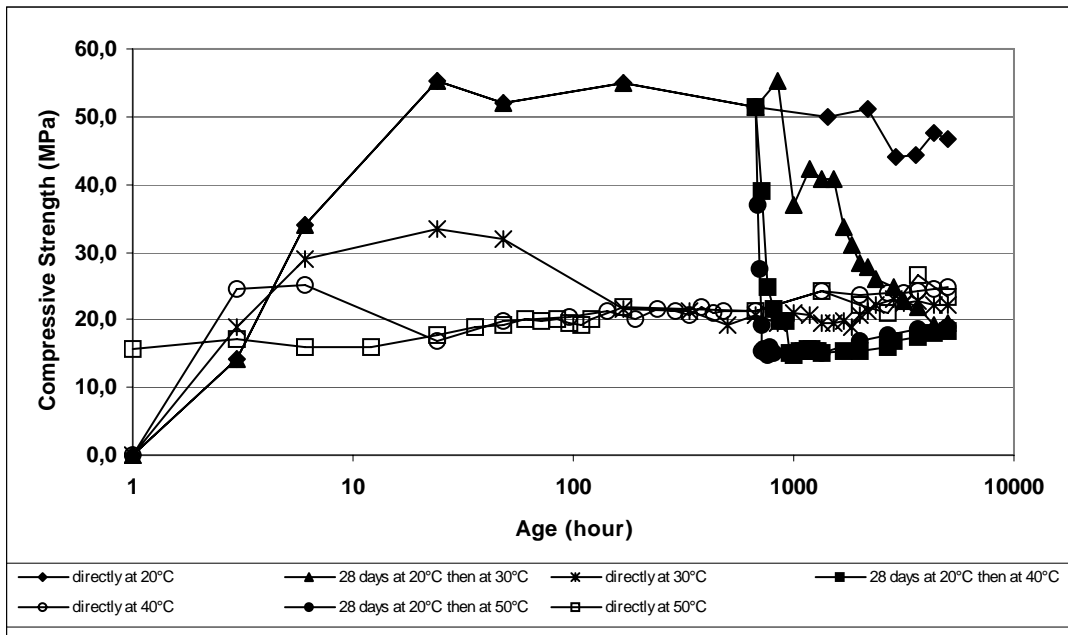


Figure 5.30 Compressive Strength Development of IK98 at Different Curing Temperatures

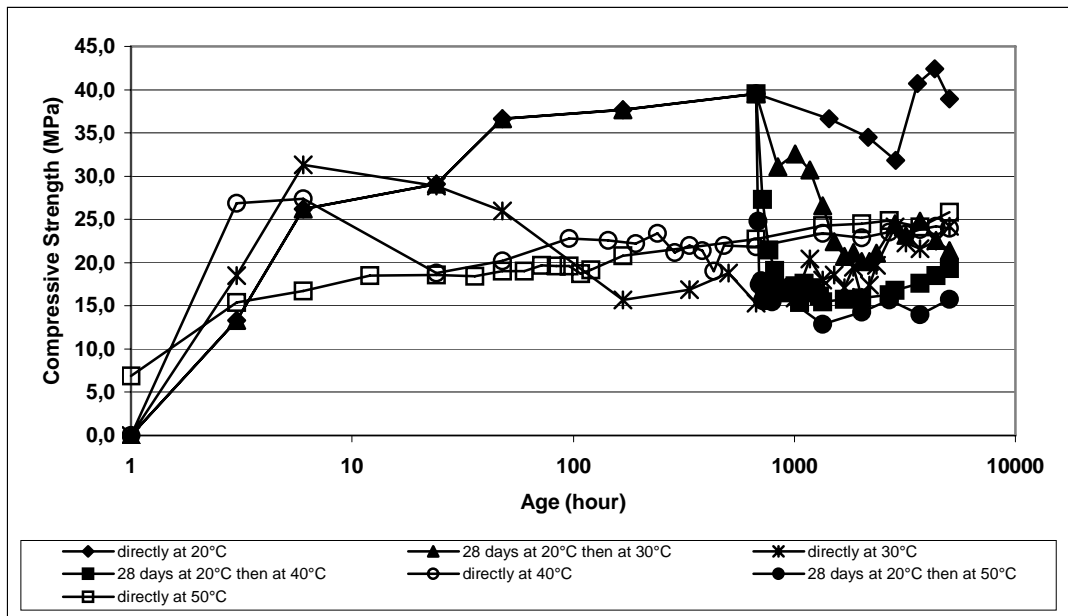


Figure 5.31 Compressive Strength Development of IK96 at Different Curing Temperatures

As mentioned previously, the effect of lime on CAC-lime mixes is related only with pH value. Therefore, regardless of the ratio of lime addition, the mechanism of CAC-lime binary mixes of this research is similar. As a result, IK98 was selected as a representative mix for XRD analysis.

XRD patterns of IK98 at 28 days and at 210 days are given in Figure 5.32 and Figure 5.33, respectively.

Table 5.19 shows the measured areas under the characteristic XRD peak of IK98 at different curing temperatures.

In order to examine the detected phases and their quantities, relatively, the areas were grouped as strong, medium, and weak, as stated previously in 5.2.1. The data are listed in Table 5.20.

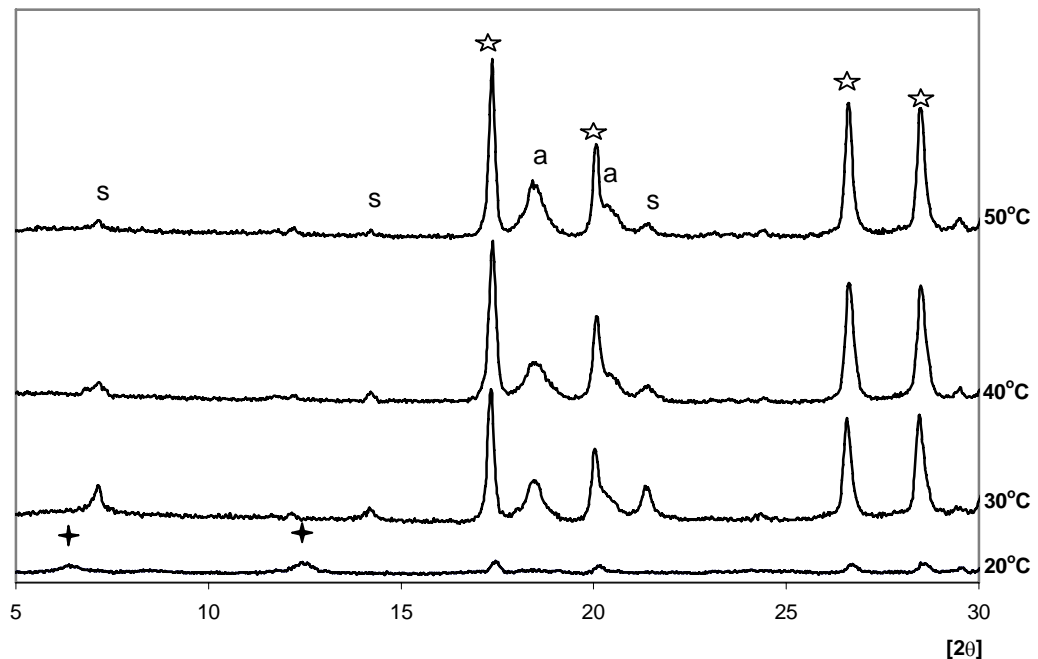


Figure 5.32 XRD Patterns of IK98 at 28 days

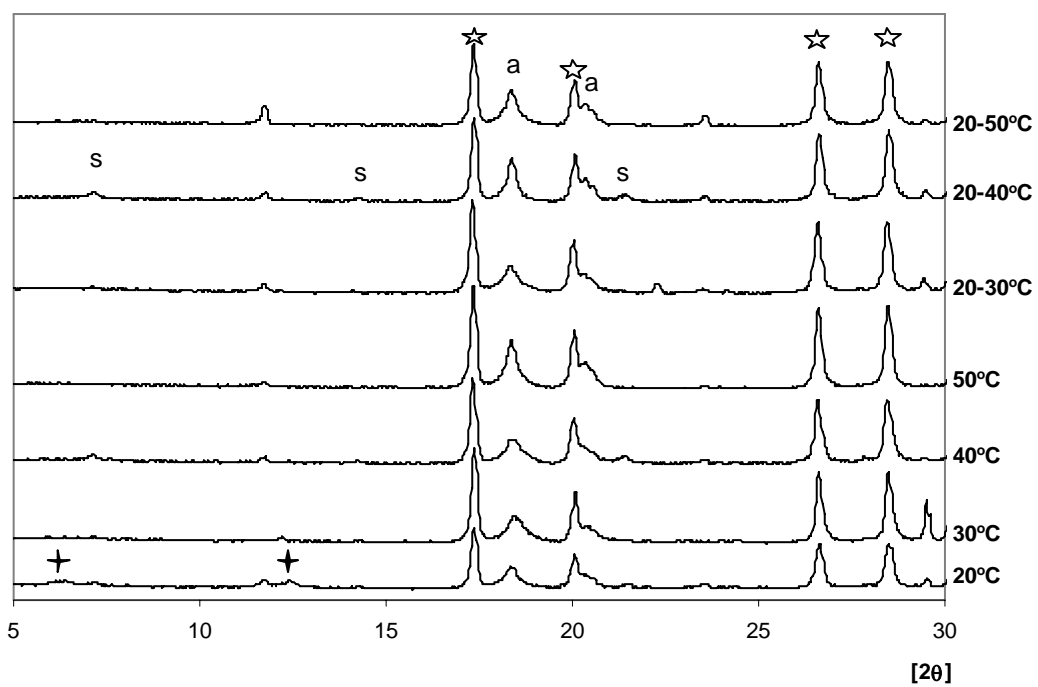


Figure 5.33 XRD Patterns of IK98 at 210 days

Table 5.19 Area under the Peak of the Phases Observed in IK98 at Different Curing Temperatures

Curing Temperature (°C)	Age (day)	Area under the Peak of Phases (unit)			
		C ₃ AH ₆	CAH ₁₀	AH ₃	C ₂ ASH ₈
20	28	99	100	-	-
	210	1715	126	553	-
30	28	1854	-	646	458
	210	2493	-	689	-
40	28	2196	-	443	94
	210	2410	-	794	144
50	28	2313	-	703	61
	210	2714	-	1589	-
20-30	210	2510	-	835	-
20-40	210	2605	-	1556	134
20-50	210	2324	-	1108	-

Table 5.20 Phases Formed in IK98 Depending on Time and Curing Temperatures

Curing Temperature (°C)	Age (day)	Type of Phases Formed in IK98
20	28	C ₃ AH ₆ (w) CAH ₁₀ (m)
	210	C ₃ AH ₆ (m) CAH ₁₀ (m) AH ₃ (m)
30	28	C ₃ AH ₆ (m) AH ₃ (m) C ₂ ASH ₈ (w)
	210	C ₃ AH ₆ (s) AH ₃ (m)
40	28	C ₃ AH ₆ (s) AH ₃ (m) C ₂ ASH ₈ (w)
	210	C ₃ AH ₆ (s) AH ₃ (m) C ₂ ASH ₈ (w)
50	28	C ₃ AH ₆ (s) AH ₃ (m) C ₂ ASH ₈ (w)
	210	C ₃ AH ₆ (s) AH ₃ (s)
20-30	210	C ₃ AH ₆ (s) AH ₃ (m)
20-40	210	C ₃ AH ₆ (s) AH ₃ (s) C ₂ ASH ₈ (w)
20-50	210	C ₃ AH ₆ (s) AH ₃ (s)

5.2.3.1 Discussion of the Results for CAC-Lime Binary Mixes (IK99.5, IK99, IK98, IK96)

Lime is generally used to accelerate the setting time of CAC. Beyond lime's accelerating effect on setting time, it also affects the strength development of CACs.

As stated in Section 5.1.1, lime inclusion shortened the setting time. Generally speaking, the faster the set obtained in CAC mixes, the lower its ultimate strength [6].

Similarly, based on Figures 5.28-5.31, it can be concluded that the higher the amount of lime in CAC-lime binary mixes is, the lower the peak strength obtained at curing at 20°C. The compressive strengths of IK100, IK99.5, IK99, IK98, and IK96 cured at 20°C were 85.6, 82.9, 61.0, 51.4, and 39.5 MPa, respectively.

On the other hand, although curing temperatures and lime ratios in CAC-lime mixes differed from each other, the ultimate strengths of almost all mixes at 210 days were very similar to each other. In fact, except for the one cured continuously at 20°C and the one cured firstly at 20°C then after at 30°C, the compressive strengths at 210 days varied within a range of approximately 20-30 MPa, even though the curing regimes were different. This was consistent with the comments made previously for CAC-PC and CAC-gypsum binary mixes and accordingly the fully converted CAC-lime mixes showed similar strength values at 210 days, whereas at 28 days since conversion was not occurred completely, particularly at low temperatures, the strengths were different depending on the lime ratio and depending on the curing temperature.

Indeed, the main reason for obtaining similar strengths at 210 days and different strengths at earlier ages was related with the degree of conversion, which can be interpreted from Table 5.19 and Table 5.20. Based on these tables, except the mix cured continuously at 20°C, almost all mixes contained similar amounts of C_3AH_6 and AH_3 . In addition to that, CAH_{10} , which is the one of the unconverted types of calcium aluminate hydrates, was only detected in XRD analysis for curing at 20°C. Presence of unstable CAH_{10} and lesser amount of stable C_3AH_6 at 20°C compared to those at other temperatures resulted in higher strengths at 20°C. As stated previously, this was mainly due to the increase in porosity caused by water release as a result of conversion reactions. Another reason may be the higher strength of CAH_{10} compared to C_3AH_6 [1,8,53,62,74].

According to Table 5.19 and 5.20, the temperature increase caused an increase in C_3AH_6 and AH_3 contents. Therefore, it can be claimed that conversion was accelerated by the increase in curing temperature thereby causing strength decreases. This result was consistent with strength development values given in Figures 5.28-5.31, too

Another important conclusion drawn from Figures 5.28-5.31 is that the increase in lime addition brought about a decline in peak strengths. Neunhoeffler [88] reported that the increase in pH of CAC mixes by inclusion of lime results faster conversion, which means also lower strengths. Therefore, the increase in the amount of lime caused an increase in pH, thereby faster conversion and lower peak strengths.

Furthermore, according to Tables 5.19 and 5.20, particularly at moderate temperature, the formation of straelingite as a result of hydration of gehlenite (C_2AS) or of C_2S and CA together was accelerated by the pH increase due to the lime inclusion. On the other hand, as shown in Figures

5.15 and 5.16, straelingite did not formed in pure CAC mix, even though CAC contained CA as a major phase and C_2AS and C_2S as minor phases.

5.2.4 Effect of Temperature on Compressive Strength Development of CAC-GGBFS Mixes

CAC has a lot of advantages over PC particularly through its high early strength development. However, due to conversion reactions it losses its high strength, depending mainly on the curing temperature. Throughout previous studies, many attempts have been carried out to compensate this detrimental effect by adding different types of mineral admixtures such as GGBFS, fly ash, silica fume, metakaolin, etc. [35-41].

Although almost all of them were based on modification of hydration chemistry of pure CAC by replacing calcium aluminate hydrates prone to conversion with stable gehlenite hydrates (straelingite), most of the previous studies have been concentrated on CAC-GGBFS binary system [35-46]. In such systems, focal point of modification of hydration chemistry is related to the formation of straelingite. In fact, straelingite forms by the reaction of calcium aluminates of CAC and amorphous silica of GGBFS in the presence of moisture. Due to its high stability, even at high temperatures, replacement of CAH_{10} , C_2AH_8 and C_3AH_6 by straelingite causes formation of conversion-free binding material [1,35-46].

In this research, different types of CAC-GGBFS binary mixes were examined through replacing CAC with GGBFS by 20%, 40%, 60% and 80%. In addition, the effects of curing temperatures on strength development of various CAC-GGBFS mixes were also investigated. Figures 5.34-5.37 show the compressive strength developments of IC80, IC60, IC40, and IC20, respectively. The strength developments were

examined until the age of 210 days and at 7 different curing temperatures, as described previously in Section 4.4.

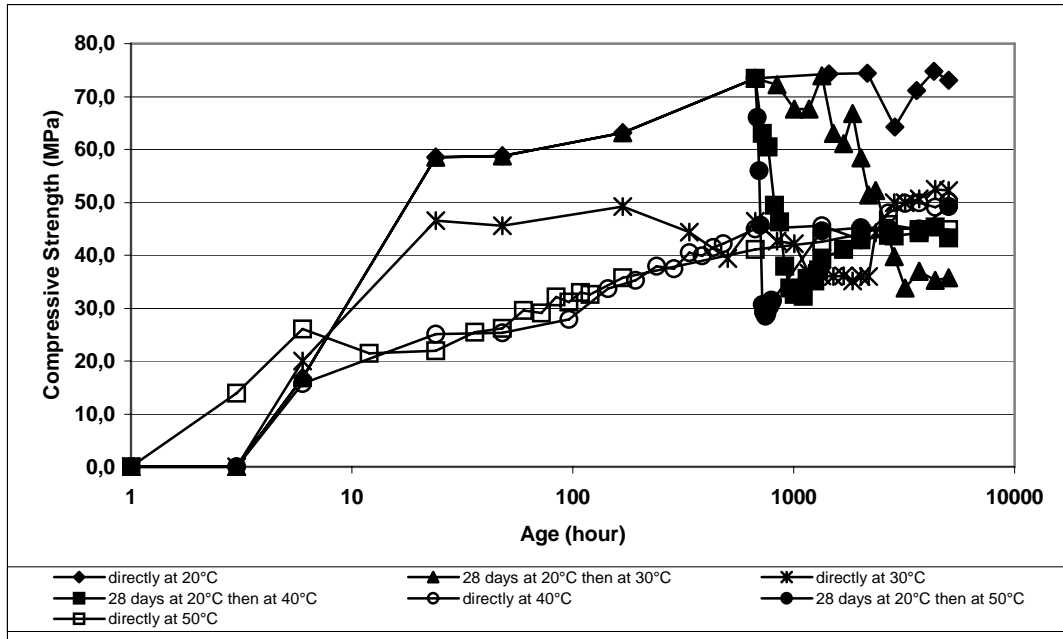


Figure 5.34 Compressive Strength Development of IC80 at Different Curing Temperatures

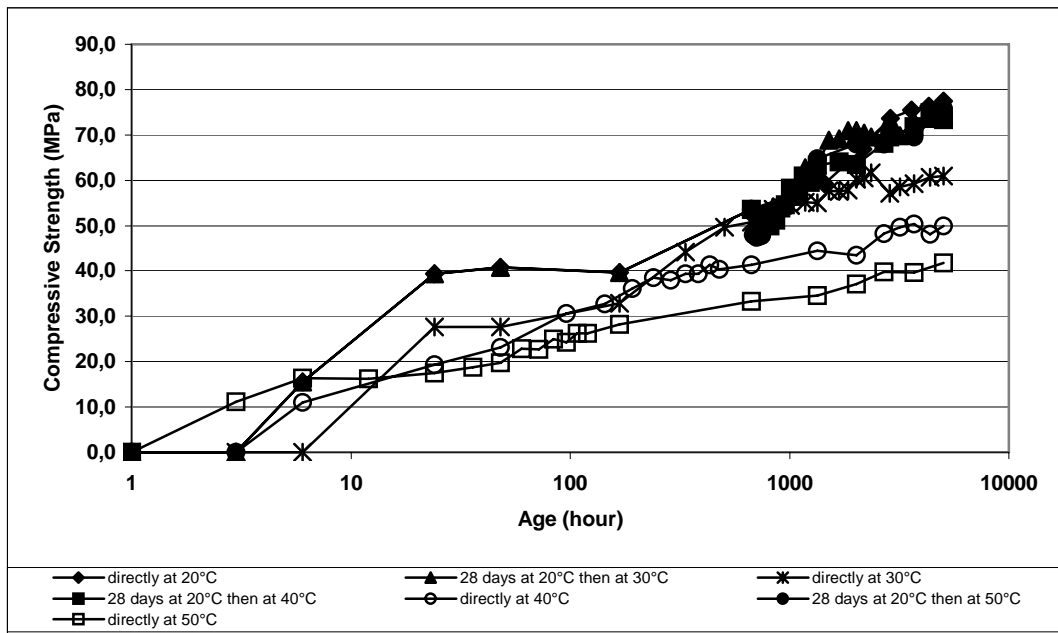


Figure 5.35 Compressive Strength Development of IC60 at Different Curing Temperatures

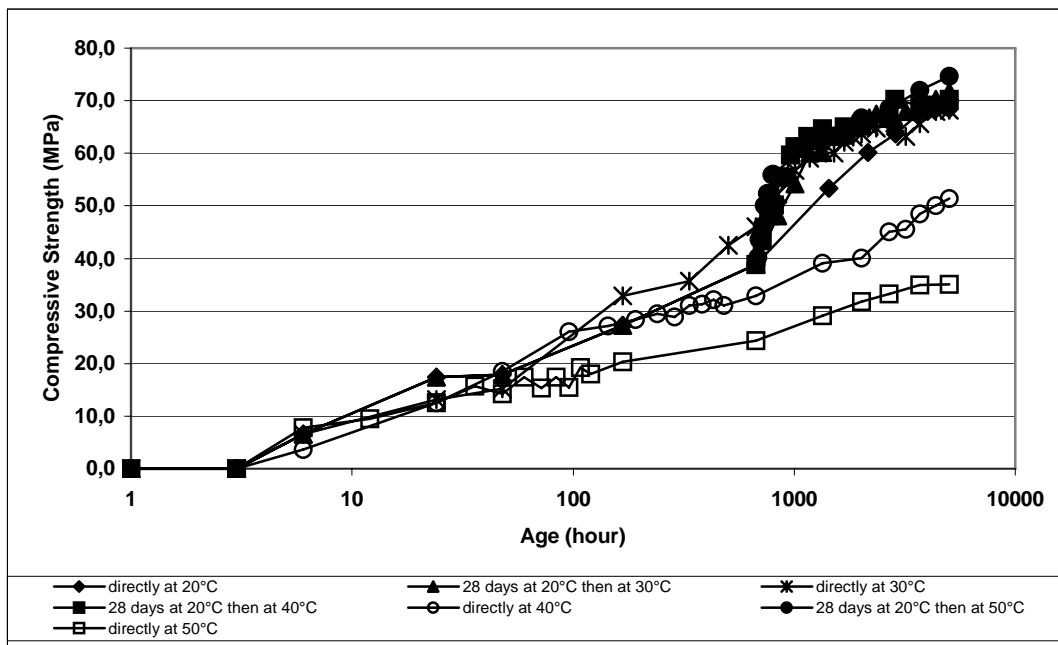


Figure 5.36 Compressive Strength Development of IC40 at Different Curing Temperatures

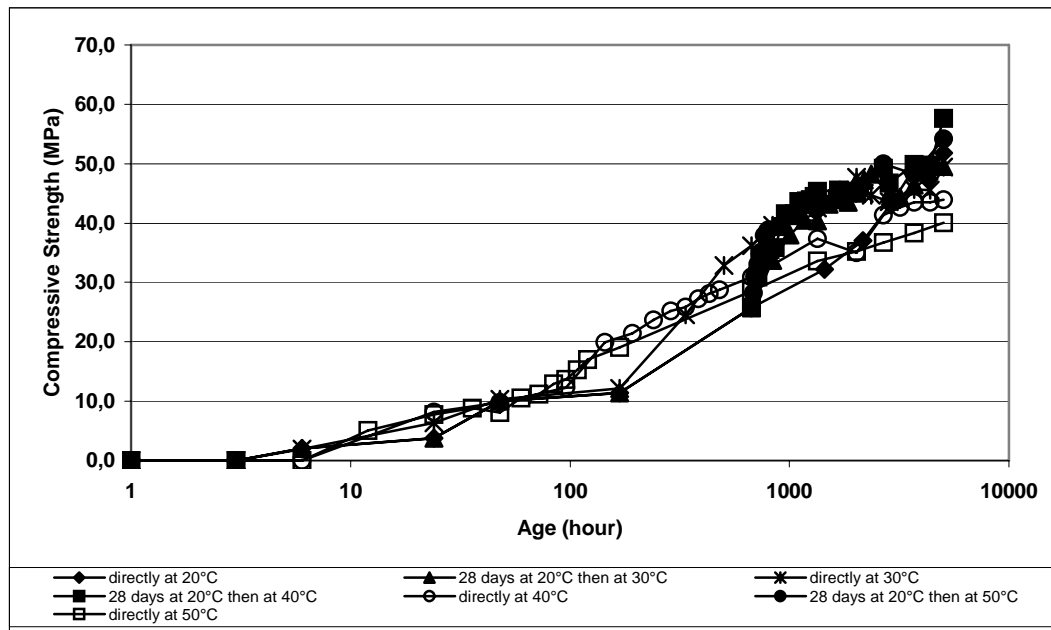


Figure 5.37 Compressive Strength Development of IC20 at Different Curing Temperatures

In order to analyse, the mechanism of the strength development in CAC-GGBFS, XRD analyses were done on IC80, IC60, and IC40 at 28 days and at 210 days. The XRD patterns of IC80, where CAC was the main constituent are given in Figure 5.38 and 5.39, for the ages of 28 days and 210 days, respectively. On the other hand, Figure 5.40 and 5.41 show the XRD patterns of IC60 at 28 days and 210 days, respectively. Finally, XRD patterns of IC40, where GGBFS was the main constituent are illustrated in Figure 5.42 and 5.43, for the ages of 28 days and 210 days, respectively.

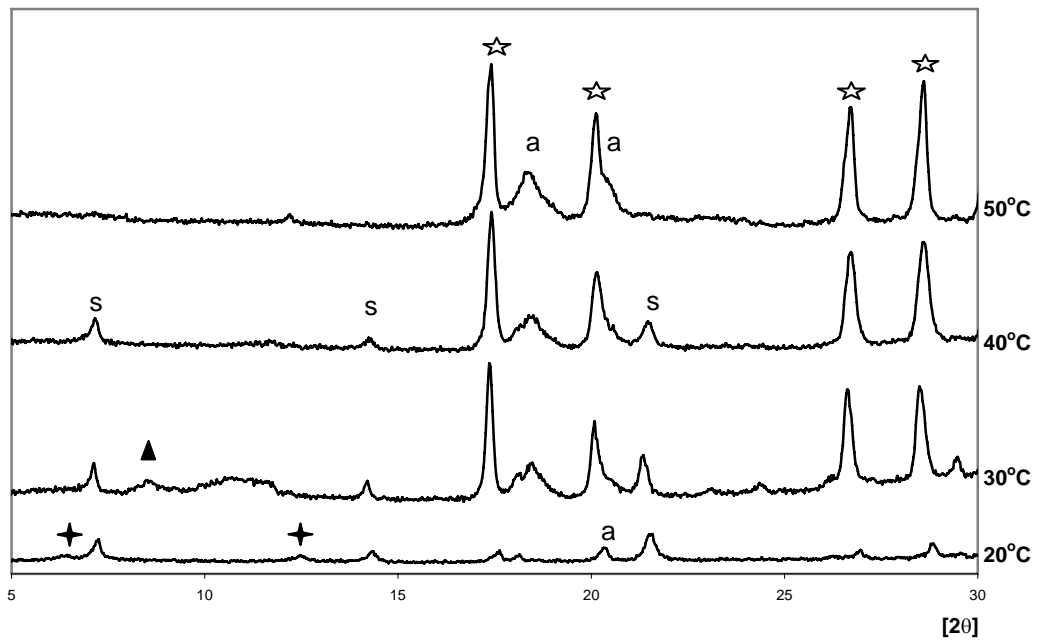


Figure 5.38 XRD Patterns of IC80 at 28 days

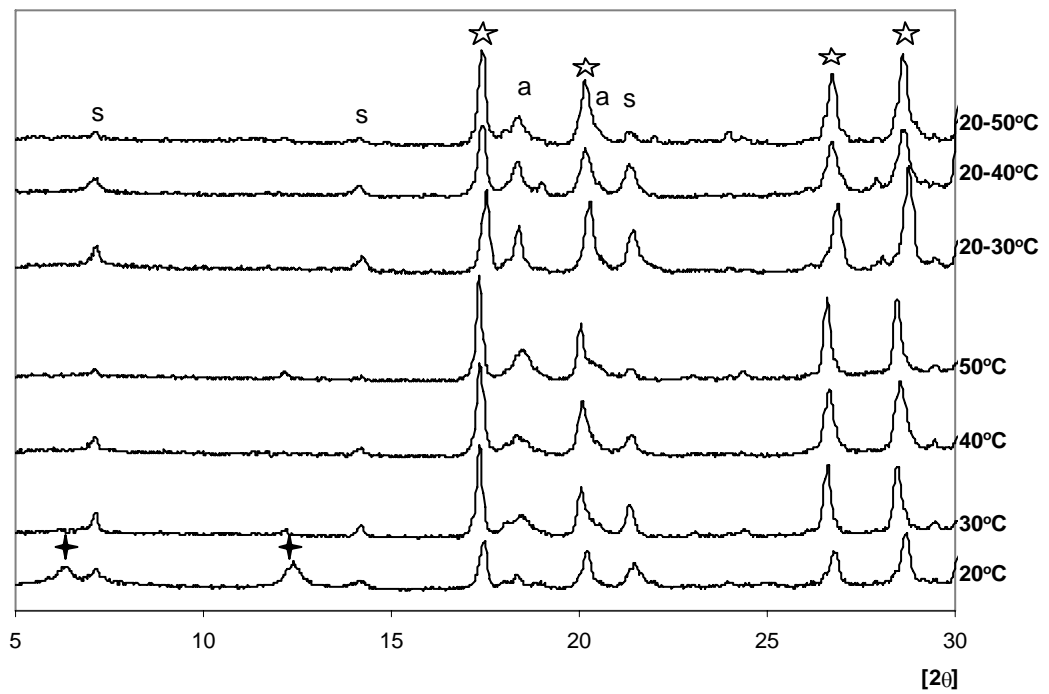


Figure 5.39 XRD Patterns of IC80 at 210 days

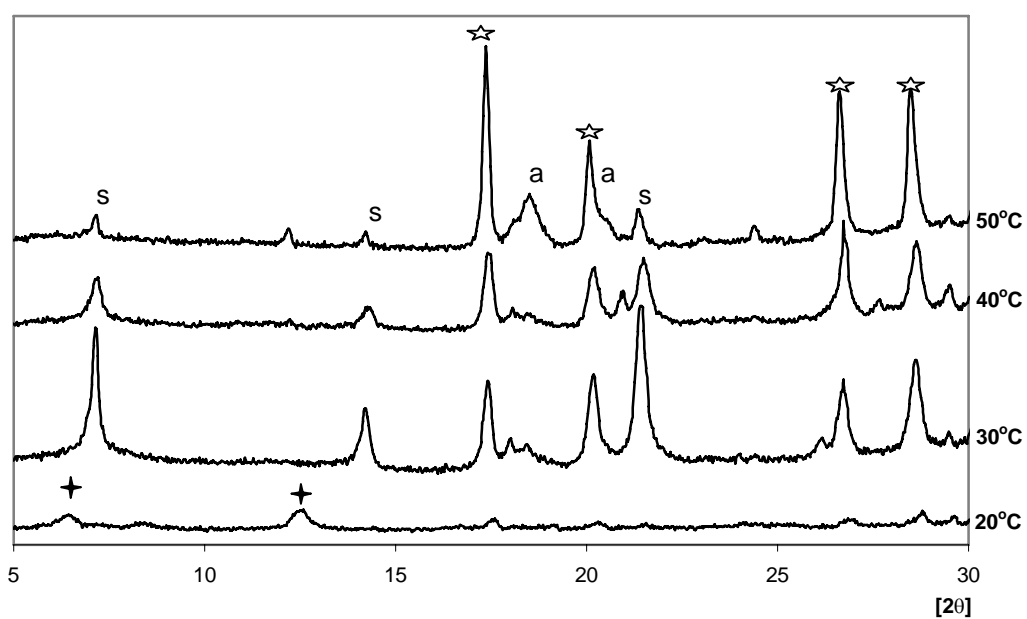


Figure 5.40 XRD Patterns of IC60 at 28 days

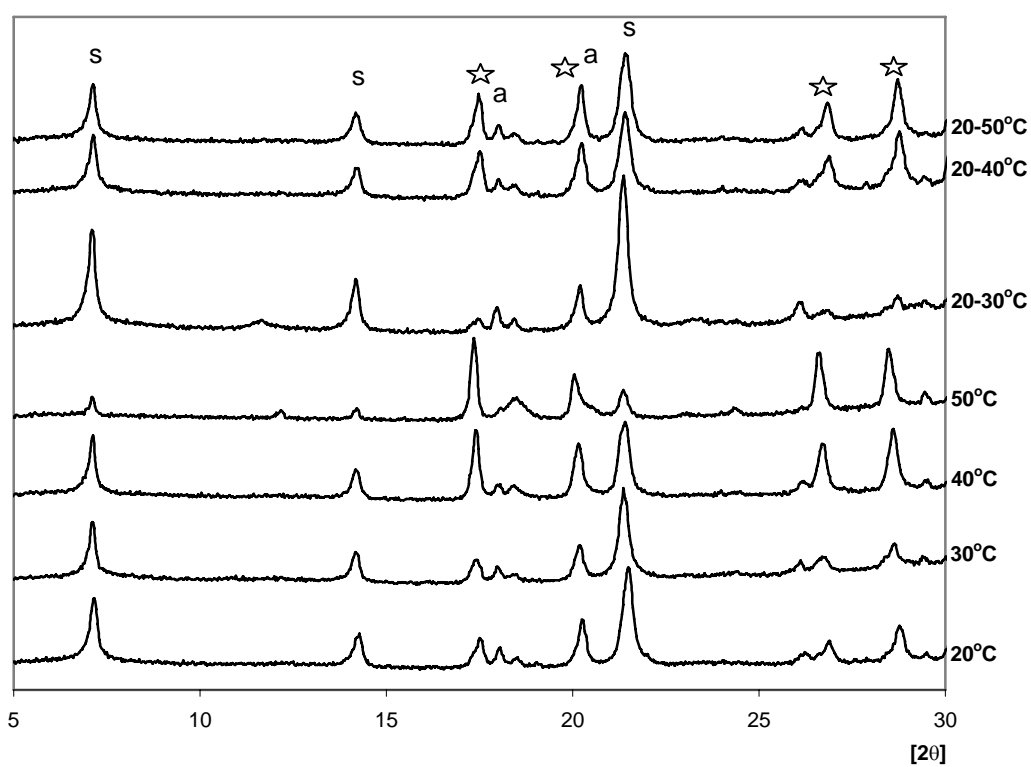


Figure 5.41 XRD Patterns of IC60 at 210 days

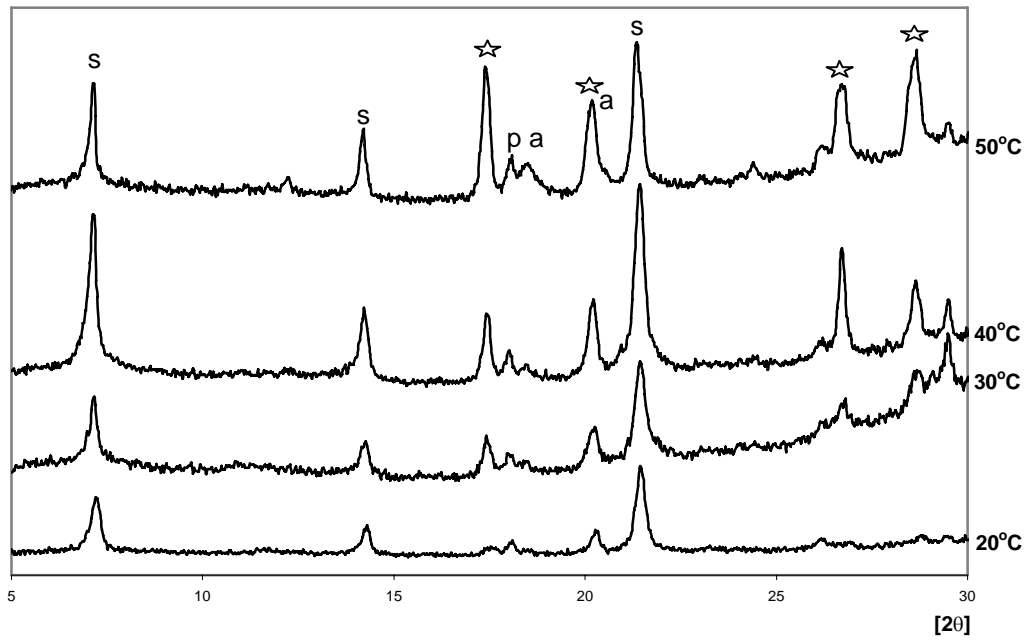


Figure 5.42 XRD Patterns of IC40 at 28 days

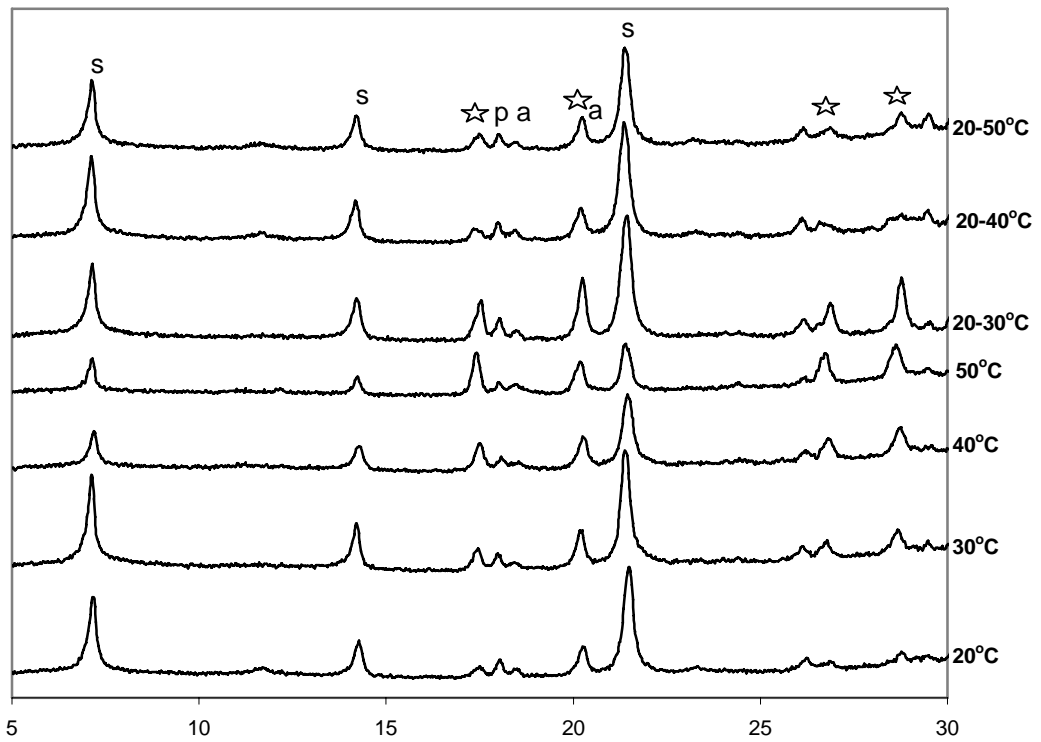


Figure 5.43 XRD Patterns of IC40 at 210 days

Tables 5.21-23 present the detected phases and their area calculated under their characteristic peaks for IC80, IC60, and IC40, respectively. By the use of the area under characteristic peaks, the detected phases are categorized as strong, medium and weak as described previously in Section 5.2.1, semi quantitatively and they were tabulated in Table 5.24.

Table 5.21 Area under the Peak of the Phases Observed in IC80 at Different Curing Temperatures

Curing Temperature (°C)	Age (day)	Area under the Peak of Phases (unit)				
		C ₃ AH ₆	CAH ₁₀	C ₂ AH ₈	AH ₃	C ₂ ASH ₈
20	28	119	51	-	39	296
	210	688	274	-	44	284
30	28	1438	-	87	284	426
	210	1556	-	-	318	431
40	28	1444	-	-	305	273
	210	1564	-	-	316	233
50	28	1878	-	-	314	-
	210	1619	-	-	451	114
20-30	210	1185	-	-	833	677
20-40	210	1091	-	-	585	431
20-50	210	1498	-	-	422	149

Table 5.22 Area under the Peak of the Phases Observed in IC60 at Different Curing Temperatures

Curing Temperature (°C)	Age (day)	Area under the Peak of Phases (unit)			
		C ₃ AH ₆	CAH ₁₀	AH ₃	C ₂ ASH ₈
20	28	53	141	-	-
	210	395	-	38	2129
30	28	646	-	45	1761
	210	350	-	37	1790
40	28	662	-	31	417
	210	1038	-	87	1565
50	28	2272	-	451	207
	210	1318	-	165	276
20-30	210	217	-	65	3163
20-40	210	599	-	26	1803
20-50	210	758	-	46	2040

Table 5.23 Area under the Peak of the Phases Observed in IC40 at Different Curing Temperatures

Curing Temperature (°C)	Age (day)	Area under the Peak of Phases (unit)			
		C ₃ AH ₆	AH ₃	C ₂ ASH ₈	CH
20	28	38	-	675	39
	210	103	25	2366	139
30	28	149	22	753	39
	210	298	35	1643	113
40	28	308	35	1447	90
	210	351	25	1530	84
50	28	614	126	913	147
	210	619	32	861	91
20-30	210	630	63	3037	140
20-40	210	185	68	2574	134
20-50	210	267	41	2200	122

Table 5.24 Phases Formed in the CAC-GGBFS Mixes Depending on Time and Curing Temperatures

Curing Temperature (°C)	Age (day)	Type of Phases Formed in CAC-GGBFS Mixes			
		IC100	IC80	IC60	IC40
20	28	C ₃ AH ₆ (w)	C ₃ AH ₆ (w)	C ₃ AH ₆ (w)	C ₃ AH ₆ (w)
		CAH ₁₀ (m)	CAH ₁₀ (m)	CAH ₁₀ (m)	C ₂ ASH ₈ (w)
	AH ₃ (w)	AH ₃ (w)		CH(w)	
		C ₂ ASH ₈ (w)			
20	210	C ₃ AH ₆ (m)	C ₃ AH ₆ (m)	C ₃ AH ₆ (w)	C ₃ AH ₆ (w)
		CAH ₁₀ (m)	CAH ₁₀ (s)	AH ₃ (w)	AH ₃ (w)
		AH ₃ (m)	AH ₃ (w)	C ₂ ASH ₈ (m)	C ₂ ASH ₈ (m)
			C ₂ ASH ₈ (w)		CH(w)
30	28	C ₃ AH ₆ (s)	C ₃ AH ₆ (m)	C ₃ AH ₆ (w)	C ₃ AH ₆ (w)
		AH ₃ (m)	C ₂ AH ₈ (m)	AH ₃ (w)	AH ₃ (w)
		AH ₃ (w)	C ₂ ASH ₈ (m)	C ₂ ASH ₈ (w)	
		C ₂ ASH ₈ (w)		CH(w)	
30	210	C ₃ AH ₆ (s)	C ₃ AH ₆ (m)	C ₃ AH ₆ (w)	C ₃ AH ₆ (w)
		AH ₃ (m)	AH ₃ (w)	AH ₃ (w)	AH ₃ (w)
			C ₂ ASH ₈ (w)	C ₂ ASH ₈ (m)	C ₂ ASH ₈ (m)
					CH(w)
40	28	C ₃ AH ₆ (s)	C ₃ AH ₆ (m)	C ₃ AH ₆ (w)	C ₃ AH ₆ (w)
		AH ₃ (m)	AH ₃ (w)	AH ₃ (w)	AH ₃ (w)
			C ₂ ASH ₈ (w)	C ₂ ASH ₈ (w)	C ₂ ASH ₈ (m)
					CH(w)

Table 5.24 (continued)

Curing Temperature (°C)	Age (day)	Type of Phases Formed in CAC-GGBFS Mixes			
		IC100	IC80	IC60	IC40
	210	C ₃ AH ₆ (s) AH ₃ (m)	C ₃ AH ₆ (m) AH ₃ (w)	C ₃ AH ₆ (m) AH ₃ (w)	C ₃ AH ₆ (w) AH ₃ (w)
			C ₂ ASH ₈ (w)	C ₂ ASH ₈ (m)	C ₂ ASH ₈ (m) CH(w)
50	28	C ₃ AH ₆ (s) AH ₃ (m)	C ₃ AH ₆ (m) AH ₃ (w)	C ₃ AH ₆ (s) AH ₃ (m)	C ₃ AH ₆ (m) AH ₃ (w)
			C ₂ ASH ₈ (w)	C ₂ ASH ₈ (w)	C ₂ ASH ₈ (m) CH(w)
	210	C ₃ AH ₆ (s) AH ₃ (s)	C ₃ AH ₆ (m) AH ₃ (m)	C ₃ AH ₆ (m) AH ₃ (w)	C ₃ AH ₆ (m) AH ₃ (w)
			C ₂ ASH ₈ (w)	C ₂ ASH ₈ (w)	C ₂ ASH ₈ (m) CH(w)
20-30	210	C ₃ AH ₆ (s) AH ₃ (s)	C ₃ AH ₆ (m) AH ₃ (m)	C ₃ AH ₆ (w) AH ₃ (w)	C ₃ AH ₆ (w) AH ₃ (w)
			C ₂ ASH ₈ (w)	C ₂ ASH ₈ (s)	C ₂ ASH ₈ (s) CH(w)
20-40	210	C ₃ AH ₆ (s) AH ₃ (s)	C ₃ AH ₆ (m) AH ₃ (m)	C ₃ AH ₆ (w) AH ₃ (w)	C ₃ AH ₆ (w) AH ₃ (w)
			C ₂ ASH ₈ (w)	C ₂ ASH ₈ (m)	C ₂ ASH ₈ (s) CH(w)
20-50	210	C ₃ AH ₆ (s) AH ₃ (s)	C ₃ AH ₆ (m) AH ₃ (m)	C ₃ AH ₆ (m) AH ₃ (w)	C ₃ AH ₆ (w) AH ₃ (w)
			C ₂ ASH ₈ (w)	C ₂ ASH ₈ (m)	C ₂ ASH ₈ (m) CH(w)

5.2.4.1 Discussion of the Results for CAC-GGBFS Binary Mixes (IC80, IC60, IC40, IC20)

Inclusion of GGBFS in CAC drastically changes the hydration mechanism of pure CAC. Concrete practices made by the use of pure CAC are prone to loss in compressive strength under particularly hot climatic conditions due to conversion reactions. However, CAC-GGBFS binary mixes exhibit no strength losses, even strength increases under same climatic conditions, as long as proper CAC/GGBFS proportion is chosen [1,35-46].

Throughout this part of the research, several replacement ratios, i.e. 20%, 40%, 60%, 80% for GGBFS in CAC-GGBFS binary system were selected. Moreover, as stated previously in Section 4.4, these mixes were subjected to seven different curing temperatures. The effects of replacement ratios of GGBFS and the curing temperature on the compressive strength development of CAC-GGBFS mixes were investigated. Accordingly, Figures 5.34-5.43 and Tables 5.21-5.24 yielded the followings:

- As illustrated in Figure 5.34, IC 80 behaved like IC100 (pure CAC mix), except the peak strength of IC80 was slightly lower than IC100. This was mainly due to the weak formation of stable straeltingite instead of calcium aluminate hydrates as seen in Tables 5.21 and 5.24, which limited conversion but did not prevent completely due to the weak amount of straeltingite. That is why, although the peak strength of IC80 was lower than IC100, again a compressive strength reduction was observed after 28 days, particularly the mixes cured 28 days at 20°C then cured at 30°C, at 40°C, and at 50°C.

On the other hand, IC80 mixes cured at lower temperature (particularly cured continuously at 20°C) exhibited lower strength losses after 28 days compared to others. This was mainly due to the fact that conversion time at lower temperature is much longer compared to that at higher temperature. Therefore, it may be concluded according to the trend of the mix cured at 20°C that its conversion would probably be completed after 210 days. In addition, as seen in Table 5.21, CAH_{10} formed only at 20°C and the amount of C_3AH_6 at 20°C was the lowest among all other mixes. This is the main indication that conversion was not completed at 20°C and therefore its strength was higher than the others.

IC80 cured continuously at 30°C experienced a slight strength decrease after 7 days. This was an indication of a slight conversion, which can be seen in Table 5.21, too. Accordingly, the unstable calcium aluminate hydrate, C_2AH_8 formed at 28 days but it converted to C_3AH_6 at the end of 210 days.

IC80 cured continuously at 40°C, and at 50°C exhibited direct conversion. According to Table 5.21, there were no unstable hydration products at 28 days and at 210 days. Therefore, almost no strength decreases were observed throughout their life up to 210 days for these curing temperatures.

Whatever the curing temperature was, the ultimate strengths of all mixes except for the one cured continuously at 20°C coincided to each other. As discussed previously for pure CAC mix, the coinciding ultimate strengths of IC100 at 210 days varied within a range of 20 to 30 MPa, whereas those of IC80 were higher, i.e. almost between 30-50 MPa. This can be explained by the formation

of straeltingite in the case of IC80, even though it was in a small amount (see Table 5.24)

As a result, IC80 mixes could not hinder the conversion reactions completely. That means that GGBFS replacement ratio of 20% was not sufficient for preventing the strength losses occurred due to the conversion reactions, completely.

- According to Figures 5.35-5.37, IC60, IC40, and IC20 exhibited a progressive strength increase with time. At every curing temperature, they did not experience any strength losses throughout 210 days. According to their trends, the strength also continued to increase progressively after 210 days. This was mainly due to the formation of stable straeltingite instead of calcium aluminate hydrates. As seen in Tables 5.21-5.24, the increase in GGBFS amount caused an increase in straeltingite amount and thereby a decrease in calcium aluminate hydrates amount. This was completely consistent with the compressive strength developments as shown in Figures 5.35-5.37.

Although IC60 cured at 20°C had CAH₁₀ at 28 days, it converted partially to C₃AH₆ but mostly to straeltingite up to 210 days and there was no CAH₁₀ at that age. Therefore, the strength reduction due to the conversion of CAH₁₀ to C₃AH₆, was compensated by straeltingite at later ages, and so the strength continued to increase progressively.

The formation of straeltingite was a slow process, which can be seen in Tables 5.22 and 5.23, clearly. For instance, although there was no straeltingite in IC60 cured at 20°C at 28 days, quite strong

straetlingite was observed at the end of 210 days. This was somewhat similar to that in other mixes and at other temperatures.

Another important conclusion related with straetlingite, which can be interpreted from XRD analyses and from the strength development curves is that the formation of straetlingite and its replacement with C_3AH_6 was faster at moderate temperatures. The higher the curing temperature was, the lower the straetlingite and the higher C_3AH_6 . In other words, particularly at $50^\circ C$, the formation of C_3AH_6 was faster than that of straetlingite and therefore C_3AH_6 could not be replaced by straetlingite, completely. This was also consistent with the strength development curves. As it can be seen in Figures 5.35-5.37, the lowest strengths were observed under continuous curing at $50^\circ C$ (for IC60, IC40 and IC20), since conversion itself (or formation of C_3AH_6) causes an increase in porosity, and thus a strength decrease. Also, the strength of C_3AH_6 is less than other calcium aluminate hydrates and straetlingite, even at equal porosity [1,53,62].

- The increase in GGBFS ratio between 40% and 80% brought about a slight strength decrease at 210 days. In other words, IC60, IC40, and IC20 had 210 days strengths up to almost 80 MPa, 70 MPa, and 60 MPa, respectively. This may be due to the slow hydration rate of straetlingite.
- GGBFS replacement ratios over than 40% in CAC-GGBFS binary mixes limited or eliminated the conversion reactions, so that no strength decrease could be observed. The strength development curves and related XRD analyses are consistent to each other.

- The main disadvantage of GGBFS inclusion in CAC-GGBFS was the fact that the increase in GGBFS ratio caused decreases in early age strength compared to pure CAC, although the ultimate strengths at 210 days were much higher than pure CAC, particularly as long as conversion was completed.
- Whether the curing temperature was high or not, CAC-GGBFS mixes, where GGBFS ratio was over 40% experienced no strength loss, even the strength increased progressively.

5.3 Statistical Assessment of Temperature Effect on Strength Development of CAC Based Composite Binders

As discussed previously, compressive strength development of CAC and CAC based composite binders is affected by several factors. Some of the factors affecting the strength development are binder content, water-cement ratio, curing temperature, the type and amount of addition in CAC based binder system, etc.

Throughout this research, the effects of curing temperature and the type and amount of various inorganic binders (PC, GGBFS, lime, and gypsum) in CAC based binder systems were investigated. The results and their discussions were previously summarized in Section 5.1 and 5.2.

In order to draw meaningful conclusions from the collected data, statistical tools were also utilized throughout this study. By the use of the statistical software Minitab 14, relationships among several variables were drawn. Through this statistical study, compressive strengths and the amount of mineral phases (C_3AH_6 , CAH_{10} , C_2AH_8 , C_2ASH_8 , AH_3 which formed as

hydration products) measured as area under their characteristic peaks were examined as outputs or responds. On the other hand, the curing temperature, time, and the type and amount of various inorganic binders in CAC based composite binders were the variables or factors influencing the listed responds.

The main statistical tool of Minitab used in this research was “design of experiments” (DOE). Although as the name implies this tool is generally utilized for designing and planning the experiments for minimizing the effort to find out the significant variables of related responds, it is also used for analysing the relationship between responds and variables and for constructing empirical formulations and relations [89,90].

Throughout this statistical study, “response surface design” was utilized as DOE tool. In fact, when response variable is a non-linear function of factors involved, response surface design is the most convenient tool for constructing empirical relationship between them [89,90].

The “response surface design” was utilized only for exploration of empirical regression from the available data collected throughout the experimental part of this study. In other words, it was not used for designing the experimental program; rather it was used for drawing non-linear empirical relations between responds and factors involved in this study.

Throughout statistical analysis, a confidence interval (CI) of 95% was selected. In other words, in t-test and analysis of variance (ANOVA), level of significance, i.e. the probability of error occurrence (α) was selected as 0.05. That means, p values less than 0.05 in t-test and ANOVA implies statistically significant effect.

As stated above, three different variables (factors) were examined and their low and high settings according to experimental study are given in Table 5.25. These limits were used in response surface design, which means that the drawn relations were based upon these ranges and they are significant within these ranges.

Table 5.25 Variables and Their Low and High-Settings

Variables	Low Settings	High Settings
Curing Temperature (°C)	20	50
Time (hr)	0	5040
Amount of Addition (%)		
PC	0	100
GGBFS	0	80
Gypsum	0	8
Lime	0	4

5.3.1 Statistical Assessment for CAC-PC Mixes

5.3.1.1 Statistical Analysis of Compressive Strength

According to the response surface regression analysis performed by Minitab 14, the estimated regression coefficients for compressive strength of CAC-PC mixes are given in Table 5.26. It also includes p values of variables, which were used for determining the significance of variables

with respect to responds (i.e. compressive strength). (The whole response surface design analysis is given in Table A.1 in Appendix).

Table 5.26 Regression Coefficients and p-Values of Variables in CAC-PC Systems According to Response Surface Regression Analysis

Term	Coefficient	p value
Constant	55.7880	0.000
time (hr)	0.0159	0.000
PC ratio (%)	-0.9668	0.000
Temp (°C)	-1.4779	0.001
time (hr)*time (hr)	-0.0000	0.000
PC ratio (%)*PC ratio (%)	0.0075	0.000
Temp (°C)*Temp (°C)	0.0157	0.009
time (hr)*PC ratio (%)	0.0000	0.000
time (hr)*Temp (°C)	-0.0001	0.000
PC ratio (%)*Temp (°C)	0.0066	0.000

The regression analysis yielded a regression coefficients of $R^2 = 53.0\%$ and $R^2_{\text{adjusted}} = 52.0\%$. It also represents a correlation coefficient of about 72%. R^2_{adjusted} is very similar to R^2 , which means statistically that the variation within each variable was quite low. In addition, R^2_{adjusted} is a modified R^2 that has been adjusted for the number of terms in the model. If

you include unnecessary terms, R^2 can be artificially high, whereas R^2_{adjusted} may get smaller as unnecessary terms are included to the model [90].

The ANOVA for compressive strength of CAC-PC mixes is given in Table 5.27, where the level of significance (p value) for linear, square, and interaction type of regression can be seen.

Table 5.27 Analysis of Variance for Regression between Compressive Strength and Variables of CAC-PC Mixes

Source	Degrees of Freedom	F value	p value
Regression	9	50.73	0.000
Linear	3	76.79	0.000
Square	3	81.60	0.000
Interaction	3	15.55	0.000

According to Table 5.27, the fact that the p-values lower than 0.05 in linear, square, and interaction regression implies there is a non-linear relation between the respond (compressive strength) and factors (time, temperature, and ratio of PC). Thus, the regression coefficients given in Table 5.26 are meaningful.

By using the coefficients in Table 5.26, an equation representing the relation between compressive strength and factors (time, temperature, and PC ratio) was constructed and it is given in Equation 1.

$$\sigma = 55.79 + 0.02t - 0.97r - 1.48T - 2.08 \times 10^{-6}t^2 + 0.01r^2 + 0.02T^2 + 4.33 \times 10^{-5}tr - 1.49 \times 10^{-4}tT + 0.01rT \quad (1)$$

where; σ : Compressive strength, MPa
 t : time, hr
 T : temperature, °C
 r : PC ratio, %

Using the contour plots and surface plots of the compressive strength given in Figure A.1 in Appendix, the relation among compressive strength, time, temperature, and PC ratio of CAC-PC mixes can be examined.

The following conclusions can be drawn according to Table A.1, and Figure A.1 in Appendix;

- The factors (time, temperature, and PC ratio) alone are not sufficient to identify the compressive strength development of CAC-PC mixes. In other words, there are missing variables influencing the strength development, which are embedded in the constant term of the expression. The p-value of constant term in the expression is less than 0.05 and therefore is statistically significant. That means other variables not involved in the expression are represented by this constant. In addition, R^2 of 53.0% is an indication for this.

- Even though the R^2 is not so high, regression still gives meaningful information about the compressive strength development as affected by time, temperature, and PC ratio.
- According to the derived equation, the increase in PC inclusion causes bell type behaviour in compressive strength (as seen in Figure A.1 in Appendix). In other words, up to a level of PC inclusion rate, strength drops, then after it starts to increase. This is consistent with the observation seen in Section 5.2.
- Increase in the temperature causes decreases in strength, particularly at ultimate age, which was previously explained by conversion. The higher the temperature, the faster is the conversion, and thus the lower is the strength.
- Time is another effective factor in compressive strength of CAC-PC mixes. The strength increases with time up to a peak level after which it starts to drop due to the conversion reactions till the strength level where full conversion is accomplished. This behaviour can also be extracted from Figure A.1 in Appendix.

5.3.1.2 Statistical Analyses of Hydration Products

As stated previously, strength development of CAC-PC mixes is directly related with type and amount of hydration products. In this part of the study, a statistical analysis was performed on the amounts of hydration products, C_3AH_6 , CAH_{10} , AH_3 , and CH .

The measured area under the characteristic peaks of formed phases in XRD analyses given in Tables 5.12-5.15 were utilized in the regression

analysis. The hydration products were taken as responds, whereas time, temperature, and PC ratio were taken as factors.

The response surface regression analysis and ANOVA for regressions are given in Tables A.2-A.5 in Appendix for C_3AH_6 , CAH_{10} , AH_3 , and CH, respectively.

The R^2 values of C_3AH_6 , CAH_{10} , AH_3 , and CH are 75.0%, 26.0%, 80.7%, and 53.4%, respectively.

The surface and contour plots of C_3AH_6 , CAH_{10} , AH_3 , and CH are given in Figures A.2-A.5 in Appendix, respectively.

According to Tables A.2-A.5 and Figures A.2-A.5 in Appendix, the followings can be interpreted:

- The factors time, temperature, and PC ratio are effective on C_3AH_6 formation. Their interactions and squares are also statistically significant. C_3AH_6 formation can be estimated by observing the change of these factors, quite accurately, since R^2 is quite high. However, other factors also influence its formation, which can be interpreted from the p value of the constant term involved in the empirical formula (since the constant is statistically significant). Generally speaking, the increase in time and temperature, and the decrease in PC ratio cause an increase in C_3AH_6 formation. This is consistent with the mechanism of conversion and formation of C_3AH_6 . Similar considerations are also valid for formation of AH_3 , and those can be interpreted from Figure A.4 in Appendix. Due to higher R^2 of AH_3 regression, this conclusion is more reliable. As discussed in previous sections, the formation of C_3AH_6 induces the formation of AH_3 , which is consistent with the statistical evaluation.

- Even though the R^2 of CAH_{10} is quite low, it can be concluded from its response surface regression that it is highly temperature dependent rather than time. Time is not a significant factor affecting the formation of CAH_{10} . On the other hand, the increase in the temperature causes a drastic reduction in CAH_{10} formation. PC ratio is another important factor. Another important conclusion, which can be drawn from Table A.3 in Appendix, is that there are other factors influencing formation of CAH_{10} , which did not take part in the regression analysis. One of them may be the water-cement ratio, which is a major factor for hydration of CAC according to previous studies [3,6,62,63].
- In CAC-PC systems, CH formation is directly related with time and PC ratio. As they increase, CH increases, too.

5.3.2 Statistical Assessment for CAC-Gypsum Combinations

The response surface regression performed for the compressive strength of CAC-gypsum mixes yields quite satisfactory relationship, where each factor analysed takes part in the empirical formulation. The R^2 of the derived regression equation is 43.4% and the whole statistical analyse is given in Table B.1 in Appendix, including the regression coefficients of variables involved.

Equation 2 shows the relationship between compressive strength and factors (time, temperature, and gypsum ratio) involved.

$$\sigma = 119.26 + 0.01t - 4.67r - 4.62T - 9.32 \times 10^{-7}t^2 + 0.05T^2 - 1.05 \times 10^{-4}tT + 0.09rT \quad (2)$$

where; σ : Compressive strength, MPa
 t : time, hr
 T : temperature, °C
 r : gypsum ratio, %

The contour and surface plots of compressive strength of CAC-gypsum mixes according to the results of surface regression analysis are illustrated in Figure B.1 in Appendix.

According to Table B.1 and Figure B.1 in Appendix, it can be concluded that the temperature increase leads to a drastic reduction in strength. The strength reduction owing to a temperature increase is more evident especially for lower gypsum ratio. In other words, the increase in gypsum ratio causes a decline in strength reduction rate resulted by a temperature increase. Indeed, as discussed previously, the increase in gypsum ratio brings about direct conversion reactions, and thereby leads to reach the ultimate residual strength level, where conversion is completed, in an easy manner. This can be clearly seen in contour plot, too.

As stated previously, the R^2 of the regression equation is not so high. That means that the variables (time, temperature, and gypsum ratio) are not sufficient to model the compressive strength development, completely. There is a need to include other parameters inside the expression. The level of significance (p-value) of the constant term in the equation implies the same conclusion. On the other hand, as discussed above, parameters involved give quite satisfactory information about the behaviour of compressive strength development.

5.3.3 Statistical Assessment for CAC-Lime Mixes

Table C.1 in Appendix shows the results of the response surface design analysis performed for compressive strength of CAC-lime mixes.

Figure C.1 in Appendix illustrates the contour and surface plots of compressive strength of CAC-lime mixes, which was derived from the response surface regression.

The regression equation yields an R^2 value of 47.9%, which is very similar to that of CAC-gypsum mixes. Likewise, there is a non-linear relationship between the compressive strength and the variables (time, temperature, lime ratio). The regression equation is given in Equation 3.

$$\sigma = 128.22 + 0.01t - 8.34r - 5.29T - 6.14 \times 10^{-7}t^2 + 0.06T^2 - 8.09 \times 10^{-5}tT + 0.17rT \quad (3)$$

where; σ : Compressive strength, MPa
 t : time, hr
 T : temperature, °C
 r : lime ratio, %

Similar considerations, which were mentioned for CAC-gypsum mixes, are also valid for CAC-lime mixes. In fact, as the contour and surface plots of both CAC-gypsum and CAC-lime mixes are examined, it can be clearly seen that the variables (time, temperature, and addition inclusion rate) affect the compressive strength development in similar manner.

5.3.4 Statistical Assessment for CAC-GGBFS Mixes

5.3.4.1 Statistical Analysis of Compressive Strength

The results of response surface design performed for compressive strength of CAC-GGBFS mixes are shown in Table 5.28 and 5.29. As shown in Table 5.29, the derived regression analysis yielded a non-linear relationship between compressive strength and the variables (time, temperature, GGBFS ratio) involved.

The whole response surface design done by Minitab 14 is also given in Table D.1 in Appendix.

Table 5.28 Regression Coefficients and p-Values of Variables in CAC-GGBFS Systems According to Response Surface Regression Analysis

Term	Coefficient	p value
Constant	73.1339	0.000
time (hr)	0.0159	0.000
GGBFS ratio (%)	-0.4175	0.000
Temp (°C)	-1.9296	0.000
time (hr)*time (hr)	-0.0000	0.000
Temp (°C)*Temp (°C)	0.0170	0.016
time (hr)*GGBFS ratio (%)	0.0001	0.000
GGBFS ratio (%)*Temp (°C)	0.0065	0.005

Table 5.29 Analysis of Variance for Regression between Compressive Strength and Variables of CAC-GGBFS Mixes

Source	Degrees of Freedom	F value	p value
Regression	7	70.88	0,000
Linear	3	44.67	0,000
Square	2	36.26	0,000
Interaction	2	15.47	0,000

The response surface regression yields the following relation shown in Equation 4.

$$\sigma = 73.13 + 0.02t - 0.42r - 1.93T - 2.81 \times 10^{-6}t^2 + 0.02T^2 + 8.20 \times 10^{-5}tr + 0.01rT \quad (4)$$

where; σ : Compressive strength, MPa
 t : time, hr
 T : temperature, °C
 r : GGBFS ratio, %

According to the response surface regression, R^2 and R^2_{adjusted} are 56.2% and 55.4%, respectively. The difference between R^2 and R^2_{adjusted} is too small, which means that the variation within variables is too low.

Although the R^2 is 56.2%, the correlation coefficient R is almost 75.0%, which is quite satisfactory. However, according to the level of significance (p-value) of the constant term in the equation, there should be other factors influencing the compressive strength, since the constant term is statistically significant (its p-value is less than 0.05) and it may represent other factors, which were not taken into account throughout the statistical analysis. According to previous studies [3,6,62,63], water-cement ratio might be an effective factor influencing the compressive strength.

Figure D.1 in Appendix shows the contour and surface plots, through which the applied response surface design can be interpreted.

According to Table D.1 and Figure D.1 in Appendix, followings can be concluded:

- As GGBFS ratio increases, the strength decline due to conversion reactions decreases drastically.
- As time increases, compressive strength shows a continuous strength increase up to a level after which a strength decrease is experienced. This trend is more evident in low temperatures.
- As the temperature increases, the strength decreases drastically, particularly at low GGBFS ratio. This is mainly owing to the fact that conversion causing strength decrease is faster at higher temperatures. Contrarily, at higher GGBFS ratio, due to the formation of straeltingite and due to less amount of C_3AH_6 , the temperature increase does not cause a drastic strength reduction. These conclusions are consistent with the results and discussions mentioned in Section 5.2.

5.3.4.2 Statistical Analysis of Hydration Products

The strength development of CAC-GGBFS mixes is directly related with the hydration behaviour. Type and amount of hydration products are two main factors affecting the strength development, drastically.

In the hydration of CAC-GGBFS mixes, various hydration products are formed, such as C_3AH_6 , CAH_{10} , AH_3 , C_2ASH_8 , etc. The formation of the hydration products and their semi-quantitative evaluation were observed by XRD analyses and they were previously illustrated in Figures 5.38-5.43. Regard with these XRD analyses, semi-quantitative evaluations of hydration products were performed by measuring area under their particular characteristic peaks. They were previously shown in Tables 5.21-5.25.

In statistical evaluation, the hydration products (i.e. C_3AH_6 , CAH_{10} , AH_3 , and C_2ASH_8) were taken as responds, whereas time, temperature, and GGBFS ratio were selected as variables affecting these responds. In this way, the relationship between these responds and variables (time, temperature, and GGBFS ratio) were constructed by the use of statistical tools of Minitab 14.

The response surface design of C_3AH_6 , AH_3 , CAH_{10} and C_2ASH_8 are given in Tables D.2-D.5 in Appendix, respectively. Accordingly, their R^2 are 84.1%, 89.2%, 62.5%, and 77.8%, respectively.

In order to show the relationships more clearly, the regressions are illustrated as contour and surface plots in Figures D.2-D.5 in Appendix for C_3AH_6 , AH_3 , CAH_{10} , and C_2ASH_8 , respectively.

According to Tables D.2-D.5 and Figures D.2-D.5 in Appendix, the following are concluded:

- Due to the high R^2 values, the regressions derived are quite reliable. By means of variables (time, temperature, and GGBFS ratio), the type and amount (semi-quantitatively) of hydration products influencing compressive strength development can be modelled in an empirical formulation, in a reliable manner.
- C_3AH_6 , AH_3 , and C_2ASH_8 are time, temperature, and GGBFS ratio dependent, whereas CAH_{10} is time-independent. Rather it is temperature and GGBFS ratio dependent. Similar results were drawn throughout the statistical analysis of CAC-PC mixes, which were mentioned in Section 5.3.1.
- The relationship between hydration products and variables (time, temperature, GGBFS ratio) are consistent with the behaviour of compressive strength modelled in Section 5.4.1.
- As the temperature increases, the amount of C_3AH_6 and AH_3 increases, whereas CAH_{10} decreases. This is mainly owing to the fact that conversion is faster at higher temperatures. Conversion means higher amounts of C_3AH_6 and AH_3 and less amount of CAH_{10} . On the other hand, the formation of C_2ASH_8 is much more at intermediate temperatures compared to at high and low temperatures.
- As time increases, generally speaking, the formation of C_3AH_6 , AH_3 , and C_2ASH_8 increases, too. On the other hand, due to the fact that

the formation of CAH_{10} is time-independent, there is no significant change in the amount of CAH_{10} with time.

- As the GGBFS ratio is increased, the formation of C_2ASH_8 also increases. However, the formation of C_3AH_6 , AH_3 , and CAH_{10} are hindered due to the inclusion of GGBFS into the CAC-GGBFS system. This is mainly due to the inclusion of amorphous silica of GGBFS into the system, which causes formation of C_2ASH_8 instead of calcium aluminate hydrates and AH_3 .
- All considerations asserted above are consistent with the results and discussions given previously in Section 5.2.

CHAPTER 6

CONCLUSIONS

CAC has several advantages over PC through its (i) high early strength within 6 hour, (ii) high durability against corrosion, (iii) high resistance to sulphate attack, (iv) high resistance to acid attack, (v) high abrasion resistance, and (vi) high heat resistance, while its setting property is very similar to PC. However, its main drawback limiting its usage in construction industry is the fact that its high early strength inducing hydration products (i.e. CAH_{10} and C_2AH_8) convert to stable hydration product (C_3AH_6) by causing drastical decreases in strength. These conversion reactions may last several days or many years depending mainly on temperature, humidity, initial water-cement ratio, cement content, and etc.

In this study, the effect of temperature on compressive strength development of CAC based composite binder was investigated by focusing on the formation of hydration products dependent mainly on time and temperature. In addition, another objective of this research was to examine the effects of the type and amount of inorganic binders (PC, gypsum, lime, and GGBFS) in CAC based binary system on strength development and thereby hydration and conversion.

According to the results of this investigation, the following conclusions are derived:

1. Pure CAC mix cured at 20°C experiences a continuous strength increase up to a peak strength level followed by a strength decrease till the residual strength level, where conversion is completed. At higher temperatures, it shows a steady strength increase up to the residual strength level, without experiencing a peak strength. Therefore it is observed that the ones cured at elevated temperatures exhibit direct conversion.
2. The residual compressive strengths of all pure CAC mixes coincide within the same range of 20-30 MPa, even though each of them is cured at different temperatures. Whether conversion lasted few days or few months, the strengths at converted case are similar.
3. The conversion time of pure CAC mixes at low temperatures is longer than that of mixes cured at elevated temperatures. In addition, initial low temperature curing followed by high temperature curing results in longer conversion time when compared with curing continuously at elevated temperatures.
4. The strength of pure CAC mixes cured at 20°C or above depends on the amounts of CAH_{10} and C_2AH_8 . Besides, conversion rate of these compounds into C_3AH_6 , which is directly proportional with temperature determines the strength reduction rate.
5. CAC-PC binary mixes behave very similar to pure CAC when PC amount is low. On the other hand, high PC content results in a behaviour similar to pure PC. Increasing the amount of PC in CAC-PC mixes results in less CAH_{10} and C_2AH_8 formation and consequently

less conversion of these to C_3AH_6 . Therefore, when compared with pure CAC, CAC-PC mixes neither show high strengths nor serious amounts of conversion. The presence of C_2S and C_3S in CAC-PC mixes leads to C-S-H and C_2ASH_8 formation.

6. The strength developments of CAC-gypsum and CAC-lime mixes regard with temperature are similar to each other, although their hydration mechanisms are different. Early setting and hydration of CAC-lime mixes are induced by the increase in pH, whereas those of CAC-gypsum are caused by the ettringite formation.
7. PC (except where it is the main constituent), lime, and gypsum inclusion in CAC did not induce conversion-free CAC binary system. However, they lead to direct conversion by expediting rapid formation of stable C_3AH_6 compound instead of metastable, high strength inducing compounds of CAH_{10} and C_2AH_8 . On the other hand, in CAC-GGBFS binary mixes, particularly where GGBFS ratio is higher than 40%, the formation of stable straetlingite (C_2ASH_8) instead of calcium aluminate hydrates hinders the conversion reactions. Therefore, such CAC-GGBFS mixes do not exhibit strength reduction, rather they show continuous strength increase.
8. The formation of stable straetlingite instead of calcium aluminate hydrates occurs quicker at lower temperatures. On the other hand, temperatures higher than $40^\circ C$ induces a partial replacement of straetlingite with C_3AH_6 , causing strength reduction eventually.
9. Statistical evaluation of the experimental study reveals that strength development of each CAC based binary mix is a function of time, temperature, and type and amount of additions. There are strong relationships between them. However, according to the response

surface design analysis, there should be other variables influencing the strength development. According to previous studies, the water-cement ratio and humidity may be other variables, which were not investigated in this study.

CHAPTER 7

RECOMMENDATIONS

Based on this investigation, the followings are recommended for further studies:

- According to the statistical study performed in this investigation, R^2 's in response surface regressions of compressive strength varied almost between 40 to 60%. In addition, the level of significance (p-value) of constants in empirical formulations of compressive strength (which was less than 0.05, i.e. it was statistically significant) revealed that there should be another factor or factors influencing compressive strength development. Based on previous studies, water-cement ratio, humidity, and binder content may affect strength development. Therefore, they should be investigated in further studies.
- Temperature effect was analysed between 20°C and 50°C. In further studies, it is suggested to investigate the strength development of CAC based composite binders at temperature, particularly lower than 20°C.
- According to this study, GGBFS inclusion to CAC limited or eliminated conversion reactions, thereby compensated strength decreases due to conversion reactions. This was enabled by reacting amorphous silica

coming from GGBFS with calcium aluminates of CAC. In further studies, different types of mineral admixtures, such as silica fume, fly ash, zeolite, etc. containing amorphous silica instead of GGBFS are recommended to investigate.

- Throughout this study, only the setting and strength development of CAC based composite binders were evaluated. Particularly, the CAC-GGBFS mixes, where conversion was limited or eliminated without causing strength decrease, should be analysed in terms of different hardened state properties. The advantages of CAC based systems over other binders are through its high durability and abrasion properties. Therefore, CAC-GGBFS mixes should also be evaluated in further researches regard with these factors.

REFERENCES

- [1] Odler, I., *Special Inorganic Cements*, E and FN Spon Publication, New York, 2000
- [2] CEN/TC 51 N 645, *Report of CEN/TC 51 WG 6 TG1: Calcium Aluminate Cement*, Krakow, 2000
- [3] Neville, A., *High Alumina Cement Concrete*, John Wiley and Sons Publications, New York, 1975.
- [4] CEN/TC 51 N802, *prEN 14647 Calcium Aluminate Cement: Composition, Specifications and Conformity Criteria*, Lisbon, 2004.
- [5] TS 6271, *Alüminalı Çimentolar-Refrakter Olarak Kullanılan*, Türk Standardları Enstitüsü, Türkiye, 1988.
- [6] Robson, T.D., *High Alumina Cement and Concretes*, John Wiley and Sons Publ., New York, 1962
- [7] "High Alumina Cement", *Betoniek*, Heidelberger Zement AG, September 1998.
- [8] Garsel, D.V., *High Alumina Cements and Chemical Binders*, Seminar Given by Alcoa Industrial Chemicals Europe at Institute of Refractories Engineering, South Africa, 1996.
- [9] Scrivener, K.L., "Historical and Present Day Applications of Calcium Aluminate Cements", *Proceedings of the International Conference on CAC*, Edinburgh, UK, pp. 3-23, 2001
- [10] Chatterjee, A.K., "An Update on the Binary Calcium Aluminates Appearing in Aluminous Cement", *Proceedings of the International Conference on CAC*, Edinburgh, UK, pp. 37-64, 2001.
- [11] Heller, L., *The Structure of Calcium Aluminate and Dicalcium Silicate α Hydrate*, Ph. D. Thesis, University of London, 1951.

- [12] Dougile, M.W., "Crystal Structure of Monocalcium Aluminate", *Nature*, 180 (4580), 1957.
- [13] Gülgün, M.A., *Processing and Microstructure of Standard and Modified Macro-Defect Free Cement*, Ph. D. Thesis, University of Illinois at Urbana-Campaign, Illinois, 1996.
- [14] George, C.M., *Industrial Aluminous Cement in Structure and Performance of Cements*, ed. P. Barnes, Appl. Sc. Publ., London, 1983.
- [15] Fujii, K., Kondo, W., Ueno, H., "Kinetics of Hydration of Monocalcium Aluminate", *Journal of American Ceramic Society*, Vol. 69 [4], pp. 623-635, 1990.
- [16] Rodger, S.A., Brooks, S.A., Sinclair, W., Groves, G.W., Double, D.D., "High Strength Cement Pastes: Part 2 Reactions During Setting", *Journal of Material Science*, Vol. 20, pp. 2853-2860, 1985.
- [17] Bushnell-Watson, S.M., Sharp, J.H., "The Effects of Temperature upon the Setting Behaviour of Refractory Calcium Aluminate Cements", *Cement and Concrete Research*, Vol. 16, pp. 875-884, 1986.
- [18] Bushnell-Watson, S.M., Sharp, J.H., "Further Studies of the Effect of Temperature upon the Setting Behaviour of Refractory Calcium Aluminate Cements", *Cement and Concrete Research*, Vol. 20, pp. 623-635, 1990.
- [19] Bushnell-Watson, S.M., Sharp, J.H., "On the Cause of the Anomalous Setting Behaviour with Respect to Temperature of Calcium Aluminate Cements", *Cement and Concrete Research*, Vol. 20, pp 677-686, 1990.
- [20] Johnson, B.R., *Calcium Aluminate Cement*, AFOSR 1st Year Internal Report, University of Illinois at Urbana-Campaign, 1995.
- [21] "Annual Mineral Review", *American Ceramic Society Bulletin*, Vol. 73, pp. 90-91, 1994.
- [22] Müller, D., "Progress in the Al MAS NMR Spectroscopy Monitoring the Hydration of Calcium Aluminate Cements", *Proceedings of 9th ICCG*, New Delhi, Vol. 6, pp.148-154, 1992.

- [23] Rettel, A., Damidot, D., Scrivener, K., "Study of the Hydration of mixtures of CA and α -Al₂O₃ at different Temperatures", *Proceedings of 10th ICCC*, paper, 2ii026, Göteborg, 1997.
- [24] Rashid, S., "Conversion of Calcium Aluminate Cement Hydrates Conversion Re-examined with Synchrotron Energy Dispersive Diffraction", *Journal of Materials Science Letters* 13, pp. 1232-1234, 1994.
- [25] Gu, P., Yan, F., Ping, X., Beaudoin, J.J., "A Study of the Hydration and Setting Behaviour of Ordinary Portland Cement High Alumina Cement Pastes", *Cement and Concrete Research*, Vol. 24 (4), pp. 682-694, 1994.
- [26] Amathieu, L., Bier, T.A., Scrivener, K.L., "Mechanism of Set Acceleration of Portland Cement Through CAC Addition", *Proceedings of the International Conference on CAC*, Edinburgh, UK, pp. 303-317, 2001.
- [27] Scrivener, K.L., Campas, A., "Calcium Aluminate Cements", *Lea's Chemistry of Cement and Concrete*, 4th edition, pp. 709-778.
- [28] Gu, P., Beaudoin, J.J., Quinn, E.G., Myers, R.E., "Early Strength Development and Hydration of Ordinary Portland Cement Calcium Aluminate Cement Pastes", *Advanced Cement Based Materials*, Vol. 6, pp. 53-58, 1997.
- [29] Gu, P., Beaudoin, J.J., "Lithium Salt Based Additives for Early Strength Enhancement of Ordinary Portland Cement High Alumina Cement Paste", *Journal of Materials Science Letters*, Vol. 16, pp. 696-698, 1997.
- [30] Garces, P., Alcocel, E.G., Andreu, C.G., "Hydration Characteristic of High Alumina Cement/Portland Cement Mixtures", *Zement Kalk Gips International*, Vol. 11, pp. 646-649, 1998.
- [31] Xue, J. et al., "Study of High Self-Stress Aluminate Cement", *Proceedings of 8th ICCC*, Vol. 4, pp. 305-311, Rio de Janeiro, 1986.
- [32] Bayoux, P.A., Testud, M., Esponasa, B., "Thermodynamic Approach to Understand the CaO-Al₂O₃-SO₃ system", *Proceedings of 9th ICCC*, Vol. 4, pp. 164-169, New Delhi, 1992.

- [33] Mikhailov, V.V., "Stressing Cement and the Mechanism Self-Stressing Concrete Regulation", *Proceedings of 4th ICCO*, Washington, Vol. 2, pp. 927-955, 1960.
- [34] Budnikov, P.B., Kravchenko, I.V., "Expansive Cements", *Proceedings of 5th ICCO*, Tokyo, Vol. 5, pp. 319-329, 1968.
- [35] Quillin, K.C., Osborne, G., Majumdar, A., Singh, B., "Effects of W/C Ratio and Curing Conditions on Strength Development in BRECEM Concretes", *Cement and Concrete Research*, Vol. 31 pp. 627-632, 2001.
- [36] Majumdar, A.J., Singh, B., "Properties of Some Blended High Alumina Cements", *Cement and Concrete Research*, Vol.22, pp.1101-, 1992.
- [37] Majumdar, A.J., Singh, B., *UK Patent GB 2211 182 B*, 1991.
- [38] Majumdar A.J., Singh, B., Edmonds, R.N., "Hydration of Mixtures of Cement Fondue Aluminous Cement and Granulated Blast Furnace Slag", *Cement and Concrete Research*, Vol. 20, pp. 197-208, 1990.
- [39] Osborne, G.J., Singh, B., "The Durability of Concretes Made with BRECEM Cement Comprised of Blends of CAC and GGBFS", *Proceedings of the 5th CANMET/ACI International Conference on Fly Ash, Silica Fume, Slag and Natural Pozzolans in Concrete*, Milwaukee, Vol. 2, pp 885-909, 1995.
- [40] Collepardi, M., Monosi, P., Piccioli, P., "The Influence of Pozzolanic Materials on the Mechanical Stability of Aluminous Cement", *Cement and Concrete Research*, Vol. 25, pp. 961-, 1995.
- [41] Singh, B., Majumdar, A.J., Quillin, "Properties of BRECEM-10 Year Results", *Cement and Concrete Research*, Vol. 29, pp. 429-433, 1999.
- [42] Quillin, K.C., "Blended High Alumina Cements", *Materials World*, Vol. 1, pp. 103-105, 1993.
- [43] Quillin, K.C., Majumdar, A.J., "Phase Equilibria in the CaO-Al₂O₃-SiO₂-H₂O System at 5°C, 20°C and 38°C", *Advances in Cement Research*, Vol. 6, pp. 47-56, 1994.
- [44] Fentiman, C.H. et al., "The Effect of Curing Conditions on the Hydration and Strength Development in Fondu: Slag", *Proceedings of the International Symposium on CAC*, London, pp. 272, 1990.

- [45] Richardson, I.G., Groves, G.W., "The Microstructure of Blast Furnace Slag/High Alumina Cement Pastes", *Proceedings of the International Symposium on CAC*, London, pp. 282-290, 1990.
- [46] Romero, L., et al., "Activation of Blast Furnace Slag/High Alumina Cement Pastes, Mechanical and Microstructural Evolution", *Proceedings of 10th ICCO*, paper 3ii096, Göteborg, 1997.
- [47] Lamour, V.H.R., Monteiro, P.J.M., Scrivener, K.L., Fryda, H., "Microscopic Studies of the Early Hydration of Calcium Aluminate Cement", *Proceedings of the International Conference on CAC*, Edinburgh, UK, pp. 169-180, 2001.
- [48] Cottin, B., "Etude au Microscope, Électronique de Pâtes de Ciments Alumineux Hydratées en C_2AH_8 et en CAH_{10} ", *Cement and Concrete Research*, Vol. 1, pp.177-86, 1971
- [49] Scrivener, K.L., Taylor, H.F.W., "Microstructural Development in Pastes of a Calcium Aluminate Cement", *In Calcium Aluminate Cements, Proceedings of the International Symposium*, University of London, London, R. J. Mangabhai, ed., E.&F.N.Spon, pp. 41-51, July 1990.
- [50] Poon, C.S., Groves, G.W., "TEM Observations of High Alumina Cement Paste", *Journal of Materials Science Letters*, Vol. 7, pp. 243-244, 1988.
- [51] Edmonds, R.N., Majumdar, A.J., "The Hydration of Monocalcium Aluminate at Different Temperatures", *Cement and Concrete Research*, Vol. 18, pp. 311-320, 1988.
- [52] Barret, P., Bertrandie, D., "Hydration of Aluminate Cements", *In Advances in Cement and Concrete, Proceedings of the Engineering Foundation Conference*, Durham, Grutzeck and Sarkar, eds., pp. 132-174, 1994.
- [53] Lamour, V.H.R., Monteiro, P.J.M., Scrivener, K.L., Fryda, H., "Mechanical Properties of Calcium Aluminate Cement Concretes", *Proceedings of the International Conference on CAC*, Edinburgh, UK, pp. 199-213, 2001.
- [54] Neville, A.M., *Properties of Concrete*, 4th ed., Prentice Hall, 1996.
- [55] Midgley, H.G., Midgley, A. "The Conversion of High Alumina Cement", *Magazine of Concrete Research*, Vol. 27, pp. 59-77, 1975.

- [56] Collins, R.J., Gutt, W., "Research on Long-Term Properties of High Alumina Cement Concrete", *Magazine of Concrete Research*, Vol. 40, pp. 195-208, 1988.
- [57] Teychenne, D.C., "Long-Term Research into the Characteristics of High Alumina Cement Concrete", *Magazine of Concrete Research*, Vol. 27, pp. 78-102, 1975.
- [58] French, P.J., Montgomery, R.G.J., Robson, T.D., "High Strength Concrete Within the Hour", *Concrete* 5, Vol. 8, pp. 253-8, 1971.
- [59] Smith, A., Chotard, T., Gimet-Breart, N., Fargeot, D., "Correlation Between Hydration Mechanism and Ultrasonic Measurements in an Aluminous Cement: Effect of Setting Time and Temperature on the Early Hydration", *Journal of the European Ceramic Society*, Vol. 22, pp. 1947-1958, 2002.
- [60] Smith, A., Chotard, T., Gimet-Breart, N., Fargeot, D., "Ultrasonic Measurements as an in Situ Tool for Characterising the Ageing of an Aluminous Cement at Different Temperatures", *Journal of the European Ceramic Society*, Vol. 22, pp. 2261-2268, 2002.
- [61] Alcocel, E.G., Garces, P., Chinchon, S., "General Study of Alkaline Hydrolysis in Calcium Aluminate Cement Mortars under a Broad Range of Experimental Conditions", *Cement and Concrete Research*, Vol. 30, pp. 1689-1699, 2000.
- [62] Andion, L.G., Garces, P., Cases, P., Andreu, C.G., Galao, O., "Metallic Corrosion of Steel Embedded in Calcium Aluminate Cement Mortars", *Proceedings of the International Conference on CAC*, Edinburgh, UK, pp. 405-421, 2001.
- [63] Building Research Establishment, *Annual Report*, London, pp. 15-16, 1973.
- [64] Glasser, F.P., Zhang, L., Zhou, Q., "Reactions of Aluminate Cement with Calcium Sulphate", *Proceedings of the International Conference on CAC*, Edinburgh, UK, pp. 551-564, 2001.
- [65] Zhou, Q., Glasser, F.P., "Kinetics and Mechanism of the Carbonation of Ettringite", *Advanced Cement Research*, Vol. 12, pp. 131-136, 2000.
- [66] TS EN 196-1, *Methods of Testing Cement-Part 1: Determination of Strength*, Turkish Standard Institute, March 2002.

- [67] ASTM C 186-92 "Standard Test Method for Heat of Hydration of Hydraulic Cement", *Annual Book of ASTM Standards*, Vol. 04.01, 1993.
- [68] TS EN 196-1, *Methods of Testing Cement-Part 3: Determination of Setting Time and Soundness*, Turkish Standard Institute, March 2002.
- [69] Barthelmy, David, *X-Ray Spacing*, www.webmineral.com/X-Ray.shtml, March 2006.
- [70] Evju, C., Hansen, S., "Expansive Properties of Ettringite in a Mixture of Calcium Aluminate Cement, Portland Cement and β -Calcium Sulphate Hemihydrate", *Cement and Concrete Research*, Vol. 31, pp. 257-261, 2001.
- [71] Goni, S., Guerrero, A., "Stability of Friedel's Salt in Calcium Aluminate Cement Paste Seven Years Old at 40°C", *Proceedings of the International Conference on CAC*, Edinburgh, UK, pp. 385-394, 2001.
- [72] Gatzanaga, M.T., Goni, S., Guerrero, A., "Accelerated Carbonation of Calcium aluminate Cement Paste", *Proceedings of the International Conference on CAC*, Edinburgh, UK, pp. 349-359, 2001.
- [73] Kurdowski, W., Duszak, S., Sorrentino, F., "Corrosion of Gehlenite Hydrate in Strong Chloride Solution", *Proceedings of the International Conference on CAC*, Edinburgh, UK, pp. 371-378
- [74] Fryda, H., Scrivener, K.L., Chanvillard, G., Feron, C., "Relevance of Laboratory Tests to Field Applications of Calcium Aluminate Cement Concretes", *Proceedings of the International Conference on CAC*, Edinburgh, UK, pp. 227-246.
- [75] Verbeck, G.J. Helmuth, R.H., "Structures and Physical Properties of Cement Pastes", *Proceeding of the 5th International Congress on the Chemistry of Cement*, Tokyo, 1968.
- [76] Kim, J.K., Moon, Y.H., Eo, S.H., "Compressive Strength Development of Concrete with Different Curing Time and Temperature", *Cement and Concrete Research*, Vol 28, 1998
- [77] Kjellsen, K.O., Reaction Kinetics of Portland Cement Mortars Hydrated at Different Temperatures. *Cement and Concrete Research*, Vol 22, 1992

- [78] Kırca, Ö., Şahin, M., Erdem, T.K., “Compressive Strength Development of Concrete at Early Ages“, *Proceedings of 5th International Congress on Advances in Civil Engineering*, Vol. 2, pp. 835-844, Istanbul-Turkey, 25-27 September 2002.
- [79] Evju, C., Hansen, S., “Dilatation and Phase Development in Pastes of Aluminate Cement, Portland Cement, and β -Calcium Sulphate Hemihydrate“, *Proceedings of the 21st International Conference on Cement Microscopy*, International Cement Microscopy Association, pp. 124-130, 1999.
- [80] Taylor, H.F.W., *Cement Chemistry*, Academic Pres, London, 1990.
- [81] Brown, P.W., Lacroix, P., “The Kinetics of Ettringite Formation“, *Cement and Concrete Research*, Vol. 19, pp.879-884, 1989.
- [82] Brown, P.W., “Kinetics of Tricalcium Aluminate and Tetracalcium Aluminoferrite Hydration in the Presence of Calcium Sulphate“, *Journal of American Ceramic Society*, Vol. 76, pp. 2971-2976, 1993.
- [83] Garces, P., Alcocel, E.G., Chinchon, S., Andreu, C.G., Alcaide, J., “Effect of Curing Temperature in Some Hydration Characteristic of Calcium Aluminate Cement Compared with Those of Portland Cement“, *Cement and Concrete Research*, Vol. 27, pp.1343-1355, 1997.
- [84] Amathieu, L., Bier T.A., Scrivener, K.L., “Mechanism of Set Acceleration of Portland Cement through CAC Addition“, *Proceedings of the International Conference on CAC*, Edinburgh, UK, pp. 303-317, 2001.
- [85] Bier, T.A., Estienne, F., Amathieu, L., “Shrinkage and Shrinkage Compensation in Binders Containing Calcium Aluminate Cement“, *Proceedings of the International Conference on CAC*, Edinburgh, UK, pp. 215-226, 2001.
- [86] Dunster, A., Holton, I., “A laboratory Study of the Resistance of CAC Concretes to Chemical Attack by Sulphate and Alkali Carbonate Solutions“, *Proceedings of the International Conference on CAC*, Edinburgh, UK, pp. 333-348, 2001.
- [87] Mehta, P.K., Lesnikof, G., “Hydration Characteristic and Properties of Shrinkage Compensating Cements“, *Proceedings of the 6th International Congress on the Chemistry of Cement*, Moscow, pp. 89-115, 1976.

- [88] Schmid, M., Goetz-Neunhoeffler, F., Neubauer, J., "Effect of $\text{Ca}(\text{OH})_2$ on Hydration Behaviour of Synthetic Calcium Aluminate Cements", *Proceedings of the 11th International Congress on Chemistry of Cement*, G. Grieves & G. Owens Editions, Durban, pp. 645-654, 2003.
- [89] Sung, H.P. *Six Sigma for Quality and Productivity Promotion*, Productivity Series 32, Asian Productivity Organization, Tokyo, 2003.
- [90] Minitab Inc., *MINITAB Statistical Software*, Release 14 for Windows, State College, Pennsylvania, 2003

APPENDIX A

STATISTICAL ANALYSIS OF CAC-PC MIXES

Table A.1 Response Surface Regression of CAC-PC Combinations:
Compressive Strength (MPa) versus time (hr); PC ratio (%);
Temperature (°C)

The analysis was done using uncoded units.

Estimated Regression Coefficients for C.Strength (MPa)

Term	Coef	SE Coef	T	P
Constant	55,7880	8,15233	6,843	0,000
time (hr)	0,0159	0,00187	8,474	0,000
PC ratio (%)	-0,9668	0,08270	-11,690	0,000
Temp (oC)	-1,4779	0,44113	-3,350	0,001
time (hr)*time (hr)	-0,0000	0,00000	-7,320	0,000
PC ratio (%)*PC ratio (%)	0,0075	0,00054	13,751	0,000
Temp (oC)*Temp (oC)	0,0157	0,00596	2,632	0,009
time (hr)*PC ratio (%)	0,0000	0,00001	4,059	0,000
time (hr)*Temp (oC)	-0,0001	0,00004	-4,214	0,000
PC ratio (%)*Temp (oC)	0,0066	0,00157	4,179	0,000

S = 11,57 R-Sq = 53,0% R-Sq(adj) = 52,0%

Analysis of Variance for C.Strength (MPa)

Source	DF	Seq SS	Adj SS	Adj MS	F	P
Regression	9	61114	61114,2	6790,5	50,73	0,000
Linear	3	22063	30832,4	10277,5	76,79	0,000
Square	3	32806	32766,1	10922,0	81,60	0,000
Interaction	3	6245	6244,7	2081,6	15,55	0,000
Residual Error	405	54207	54207,0	133,8		
Total	414	115321				

Figure A.1 Contour and Surface Plots of Response Surface Regression of CAC-PC Combinations: Compressive Strength (MPa) versus time (hr); PC ratio (%); Temperature (°C)

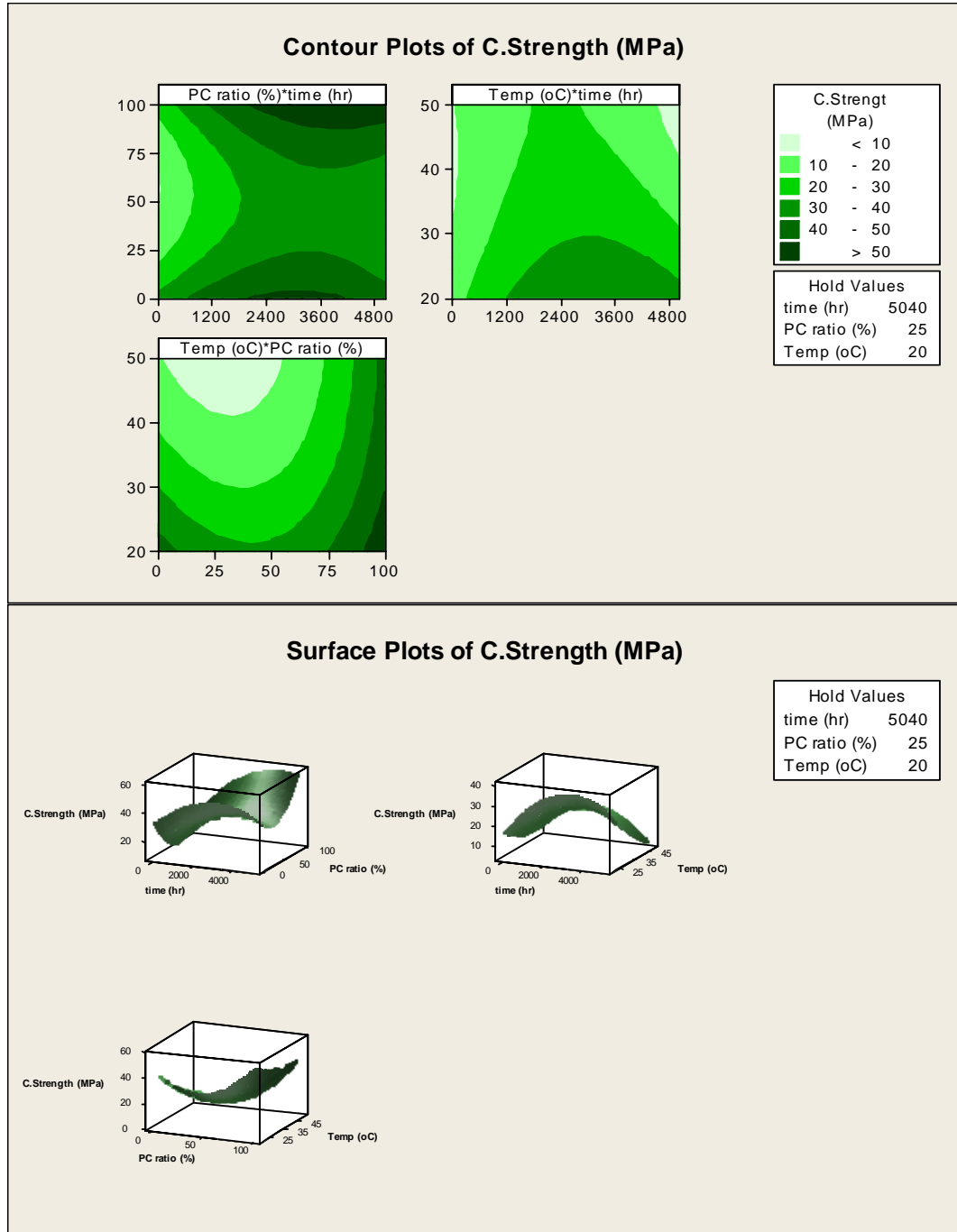


Table A.2 Response Surface Regression of CAC-PC Combinations:
 C_3AH_6 (unit) versus time (hr); PC ratio (%); Temperature ($^{\circ}C$)

The analysis was done using uncoded units.

Estimated Regression Coefficients for C_3AH_6 (unit)

Term	Coef	SE Coef	T	P
Constant	-638,211	245,934	-2,595	0,011
time (hr)	0,566	0,089	6,354	0,000
PC ratio (%)	5,166	2,951	1,750	0,083
Temp ($^{\circ}C$)	35,437	6,477	5,472	0,000
time (hr)*time (hr)	-0,000	0,000	-3,129	0,002
time (hr)*PC ratio (%)	-0,004	0,000	-7,892	0,000
PC ratio (%)*Temp ($^{\circ}C$)	-0,342	0,077	-4,453	0,000

S = 324,7 R-Sq = 75,0% R-Sq(adj) = 73,7%

Analysis of Variance for C_3AH_6 (unit)

Source	DF	Seq SS	Adj SS	Adj MS	F	P
Regression	6	36604496	36604496	6100749	57,86	0,000
Linear	3	28104586	10544275	3514758	33,33	0,000
Square	1	63966	1032238	1032238	9,79	0,002
Interaction	2	8435944	8435944	4217972	40,00	0,000
Residual Error	116	12231428	12231428	105443		
Total	122	48835923				

Table A.3 Response Surface Regression of CAC-PC Combinations:
CAH₁₀ (unit) versus time (hr); PC ratio (%); Temperature (°C)

The analysis was done using uncoded units.

Estimated Regression Coefficients for CAH₁₀(unit)

Term	Coef	SE Coef	T	P
Constant	187,385	25,2421	7,424	0,000
PC ratio (%)	-1,002	0,1598	-6,272	0,000
Temp (oC)	-8,039	1,3186	-6,097	0,000
Temp (oC)*Temp (oC)	0,081	0,0173	4,693	0,000
PC ratio (%)*Temp (oC)	0,024	0,0043	5,615	0,000

S = 22,76 R-Sq = 26,0% R-Sq(adj) = 24,5%

Analysis of Variance for CAH₁₀(unit)

Source	DF	Seq SS	Adj SS	Adj MS	F	P
Regression	4	35503	35503	8875,7	17,13	0,000
Linear	2	10406	29563	14781,6	28,53	0,000
Square	1	8762	11415	11414,9	22,03	0,000
Interaction	1	16335	16335	16334,7	31,52	0,000
Residual Error	195	101047	101047	518,2		
Lack-of-Fit	15	48436	48436	3229,1	11,05	0,000
Pure Error	180	52611	52611	292,3		
Total	199	136550				

Table A.4 Response Surface Regression of CAC-PC Combinations:
 AH₃(unit) versus time (hr); PC ratio (%); Temperature (°C)

The analysis was done using uncoded units.

Estimated Regression Coefficients for AH₃(unit)

Term	Coef	SE Coef	T	P
Constant	-90,9994	47,8884	-1,900	0,059
time (hr)	0,0984	0,0064	15,365	0,000
PC ratio (%)	-3,2160	0,8248	-3,899	0,000
Temp (oC)	8,4102	1,2278	6,850	0,000
PC ratio (%)*PC ratio (%)	0,0471	0,0052	9,039	0,000
time (hr)*PC ratio (%)	-0,0011	0,0001	-13,423	0,000
PC ratio (%)*Temp (oC)	-0,0953	0,0151	-6,309	0,000

S = 64,07 R-Sq = 80,7% R-Sq(adj) = 80,1%

Analysis of Variance for AH₃(unit)

Source	DF	Seq SS	Adj SS	Adj MS	F	P
Regression	6	3212536	3212536	535423	130,45	0,000
Linear	3	1892422	2103598	701199	170,84	0,000
Square	1	450621	335373	335373	81,71	0,000
Interaction	2	869492	869492	434746	105,92	0,000
Residual Error	187	767510	767510	4104		
Total	193	3980046				

Table A.5 Response Surface Regression of CAC-PC Combinations:
CH (unit) versus time (hr); PC ratio (%); Temperature (°C)

The analysis was done using uncoded units.

Estimated Regression Coefficients for CH(unit)

Term	Coef	SE Coef	T	P
Constant	-13,9207	39,5600	-0,352	0,725
time (hr)	0,0335	0,0145	2,312	0,022
PC ratio (%)	-8,4511	2,4776	-3,411	0,001
PC ratio (%)*PC ratio (%)	0,2106	0,0266	7,929	0,000

S = 329,0 R-Sq = 53,4% R-Sq(adj) = 52,7%

Analysis of Variance for CH(unit)

Source	DF	Seq SS	Adj SS	Adj MS	F	P
Regression	3	23564550	23564550	7854850	72,55	0,000
Linear	2	16758387	1887371	943685	8,72	0,000
Square	1	6806163	6806163	6806163	62,86	0,000
Residual Error	190	20570957	20570957	108268		
Lack-of-Fit	95	15226836	15226836	160282	2,85	0,000
Pure Error	95	5344121	5344121	56254		
Total	193	44135507				

Figure A.2 Contour and Surface Plots of Response Surface Regression of CAC-PC Combinations: Katoite ($=C_3AH_6$) (unit) versus time (hr); PC ratio (%); Temperature ($^{\circ}C$)

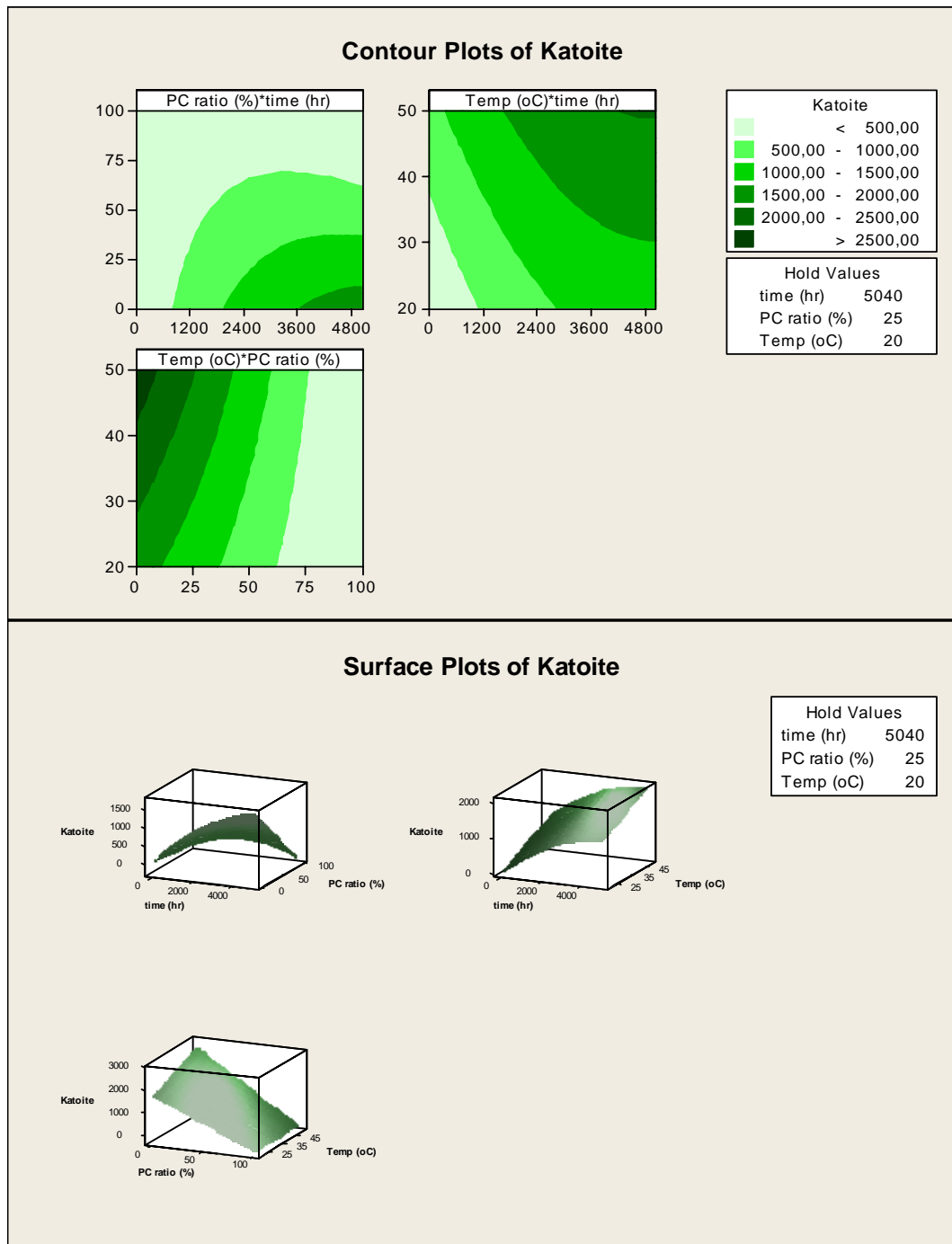


Figure A.3 Contour and Surface Plots of Response Surface Regression of CAC-PC Combinations: CAH₁₀ (unit) versus PC ratio (%); Temperature (°C)

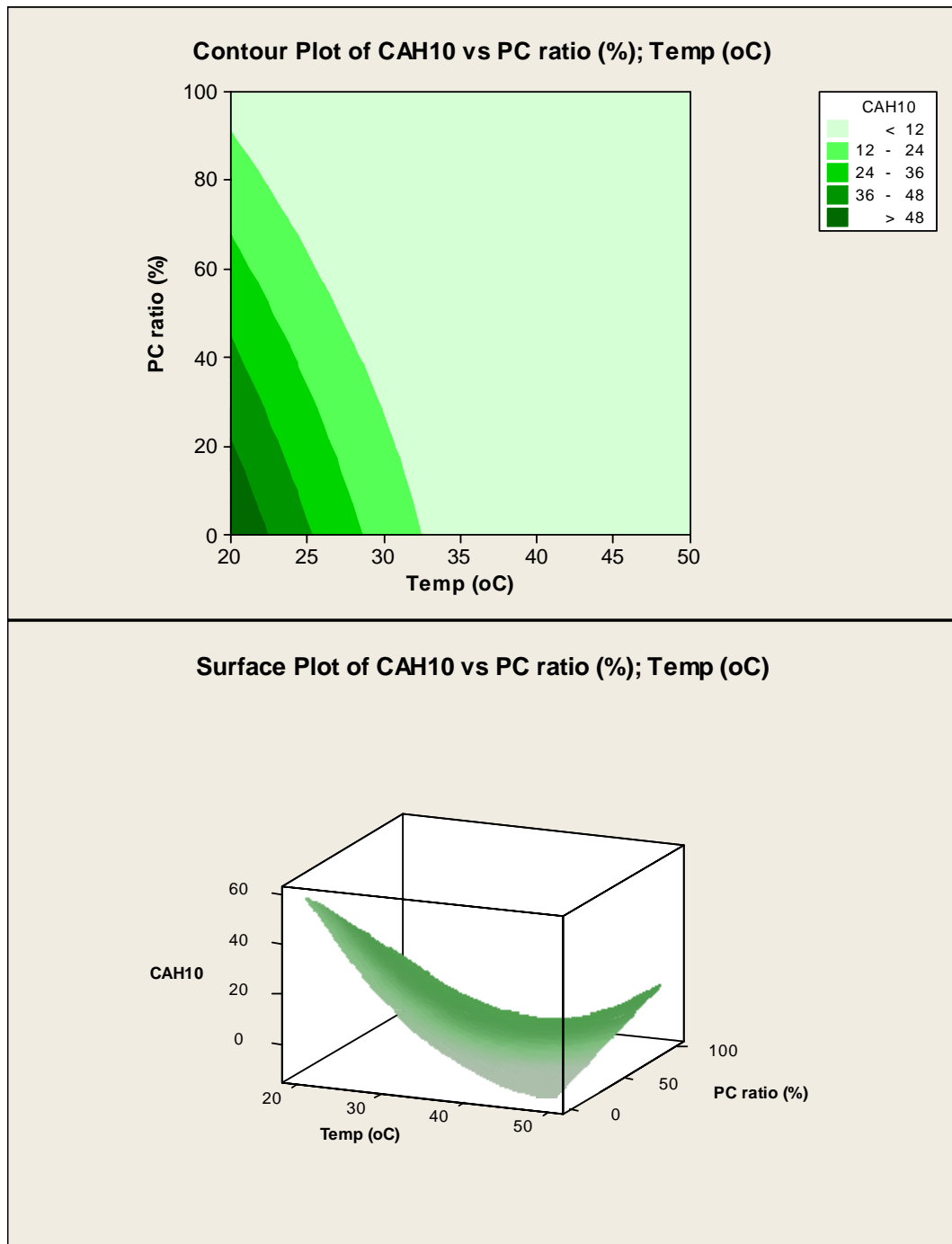


Figure A.4 Contour and Surface Plots of Response Surface Regression of CAC-PC Combinations: AH₃ (unit) versus time (hr); PC ratio (%); Temperature (°C)

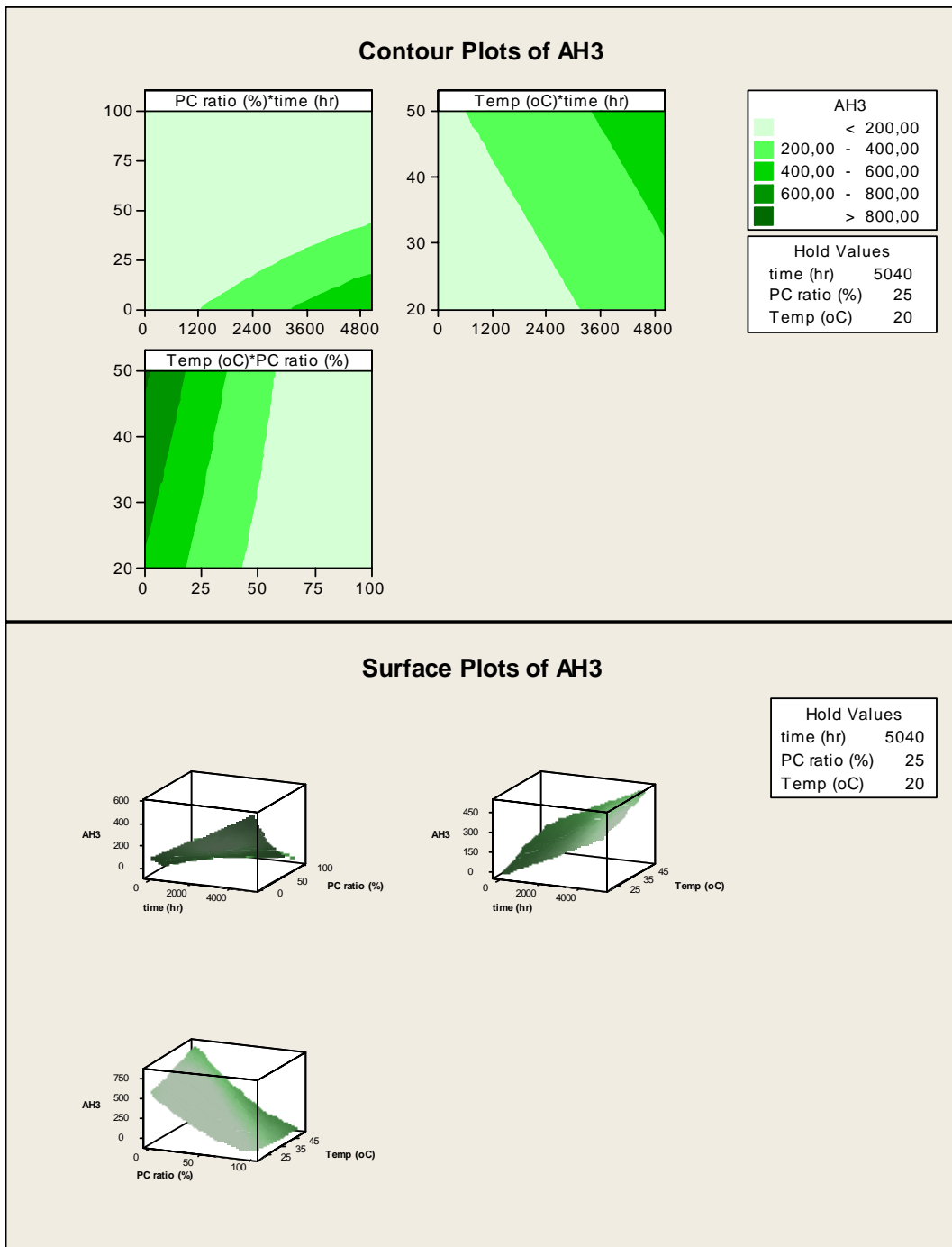
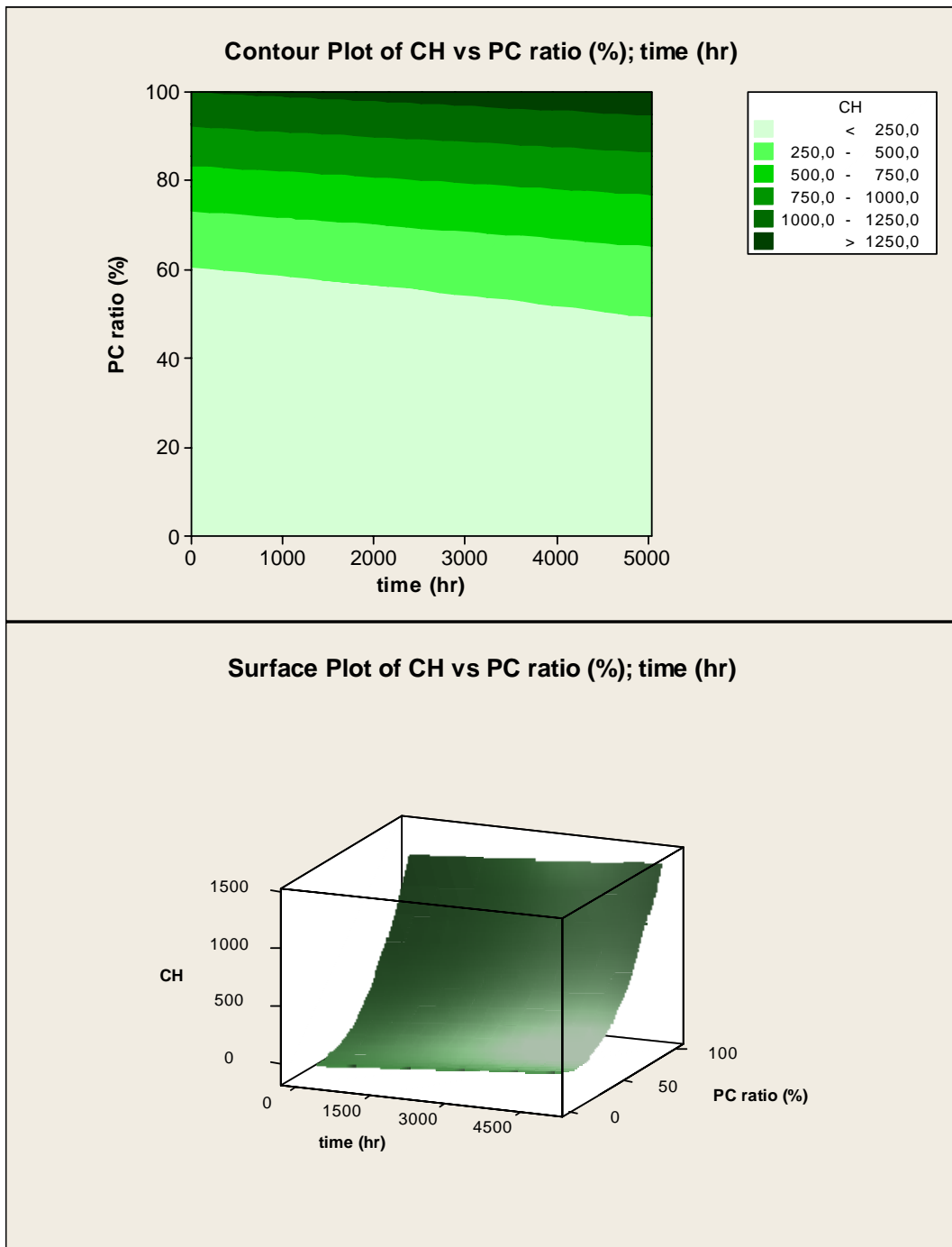


Figure A.5 Contour and Surface Plots of Response Surface Regression of CAC-PC Combinations: CH (unit) versus time (hr); PC ratio (%)



APPENDIX B

STATISTICAL ANALYSIS of CAC-GYPSUM MIXES

Table B.1 Response Surface Regression of CAC-Gypsum Combinations: Compressive Strength (MPa) versus time (hr); Gypsum ratio (%); Temperature (°C)

The analysis was done using uncoded units.

Estimated Regression Coefficients for C.Strength (MPa)

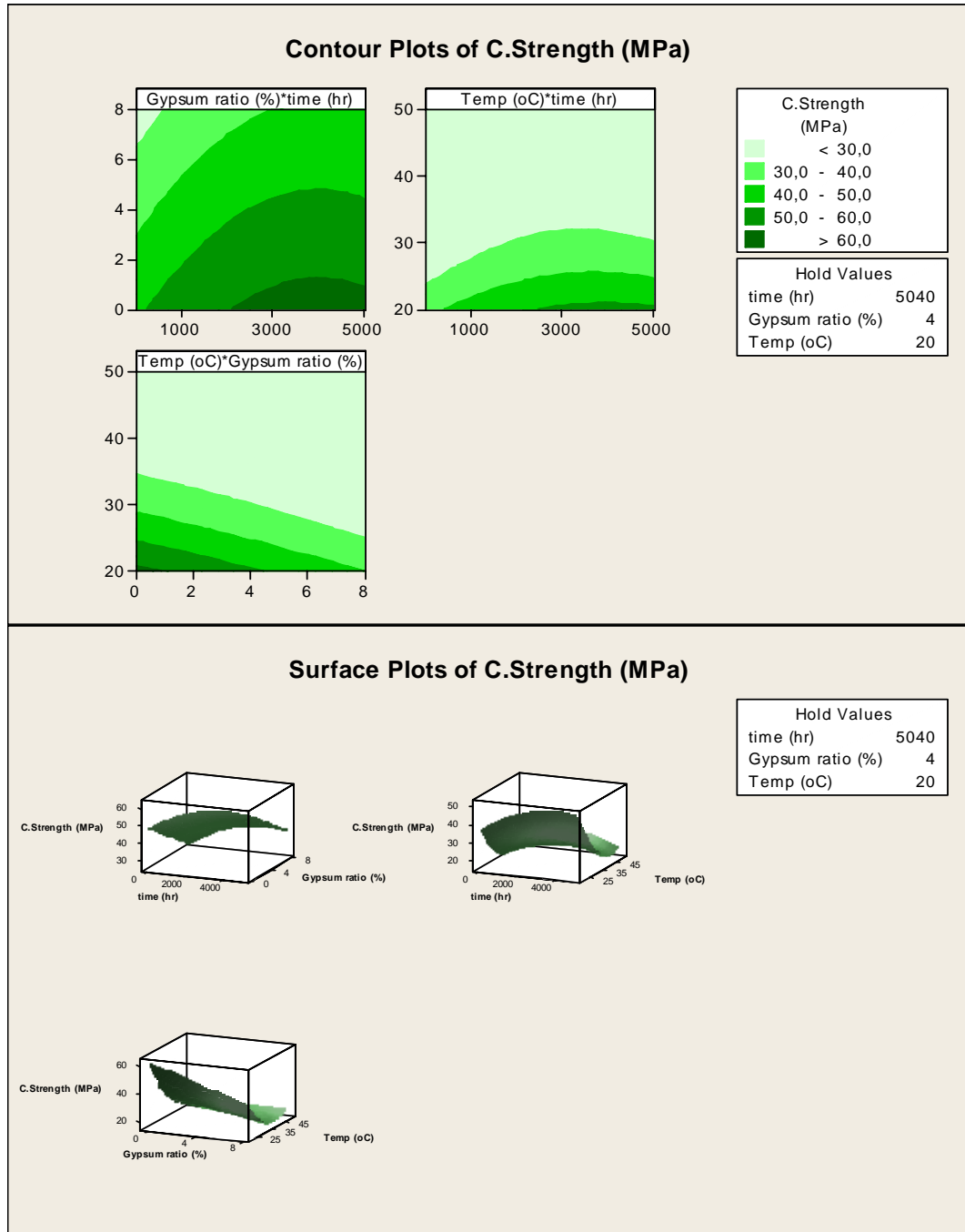
Term	Coef	SE Coef	T	P
Constant	119,257	8,74129	13,643	0,000
time (hr)	0,010	0,00200	4,827	0,000
Gypsum ratio (%)	-4,674	0,78874	-5,926	0,000
Temp (oC)	-4,620	0,48875	-9,453	0,000
time (hr)*time (hr)	-0,000	0,00000	-2,987	0,003
Temp (oC)*Temp (oC)	0,054	0,00663	8,073	0,000
time (hr)*Temp (oC)	-0,000	0,00004	-2,700	0,007
Gypsum ratio (%)*Temp (oC)	0,093	0,02095	4,448	0,000

S = 12,52 R-Sq = 43,4% R-Sq(adj) = 42,4%

Analysis of Variance for C.Strength (MPa)

Source	DF	Seq SS	Adj SS	Adj MS	F	P
Regression	7	46469	46468,6	6638,37	42,37	0,000
Linear	3	30534	22130,5	7376,84	47,08	0,000
Square	2	11692	10665,3	5332,66	34,04	0,000
Interaction	2	4242	4242,3	2121,17	13,54	0,000
Residual Error	387	60633	60633,0	156,67		
Total	394	107102				

Figure B.1 Contour and Surface Plots of Response Surface Regression of CAC-Gypsum Combinations: Compressive Strength (MPa) versus time (hr); Gypsum ratio (%); Temperature (°C)



APPENDIX C

STATISTICAL ANALYSIS of CAC-LIME MIXES

Table C.1 Response Surface Regression of CAC-Lime Combinations: Compressive Strength (MPa) versus time (hr); Lime ratio (%); Temperature (°C)

The analysis was done using uncoded units.

Estimated Regression Coefficients for C.Strength (MPa)

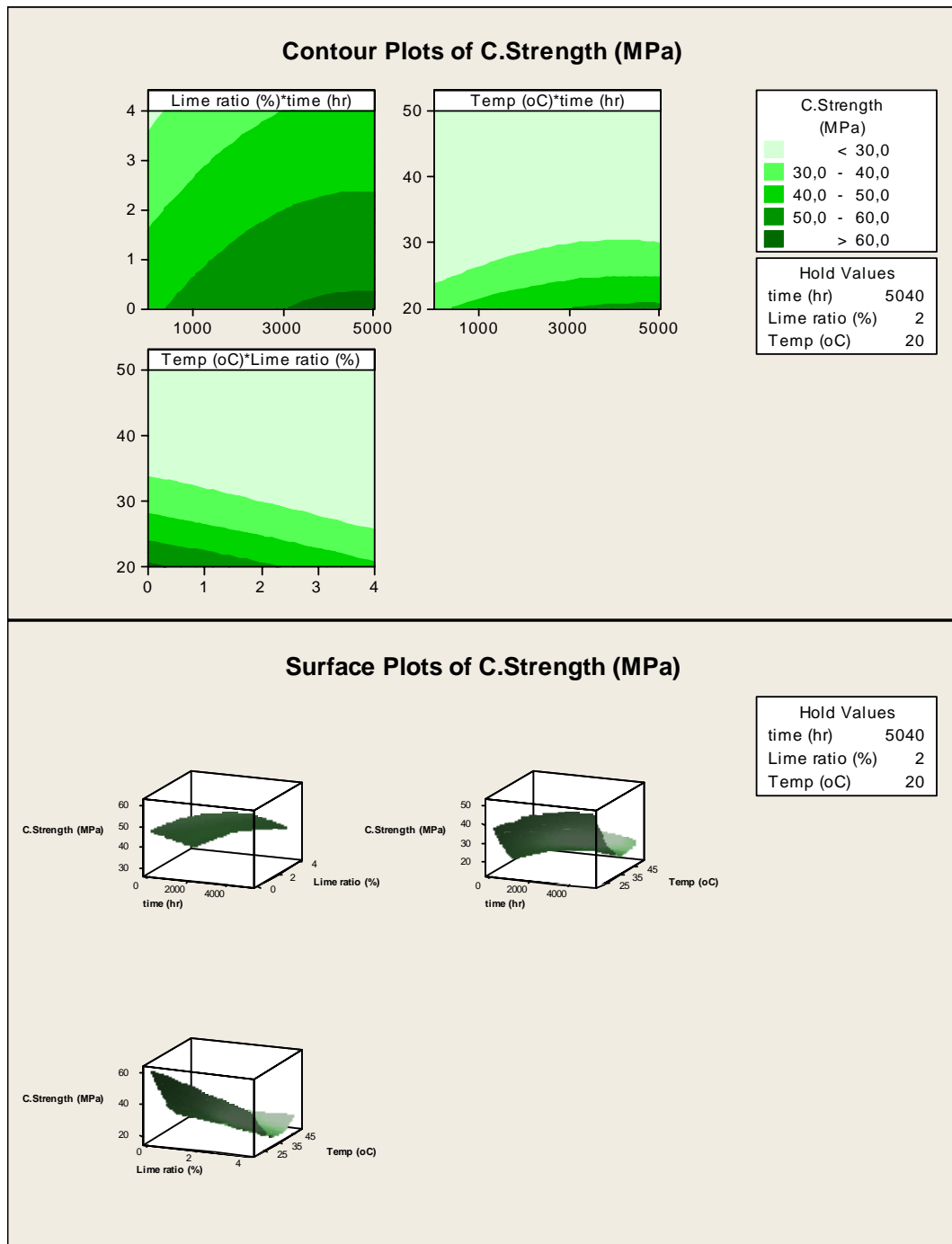
Term	Coef	SE Coef	T	P
Constant	128,219	7,83338	16,368	0,000
time (hr)	0,007	0,00178	4,192	0,000
Lime ratio (%)	-8,339	1,44562	-5,768	0,000
Temp (oC)	-5,291	0,43650	-12,123	0,000
time (hr)*time (hr)	-0,000	0,00000	-2,206	0,028
Temp (oC)*Temp (oC)	0,063	0,00592	10,703	0,000
time (hr)*Temp (oC)	-0,000	0,00003	-2,322	0,021
Lime ratio (%)*Temp (oC)	0,170	0,03839	4,425	0,000

S = 11,17 R-Sq = 47,9% R-Sq(adj) = 46,9%

Analysis of Variance for C.Strength (MPa)

Source	DF	Seq SS	Adj SS	Adj MS	F	P
Regression	7	44338,1	44338,1	6334,02	50,79	0,000
Linear	3	25808,8	23543,9	7847,96	62,93	0,000
Square	2	15415,2	14317,1	7158,54	57,40	0,000
Interaction	2	3114,1	3114,1	1557,05	12,48	0,000
Residual Error	387	48265,5	48265,5	124,72		
Total	394	92603,6				

Figure C.1 Contour and Surface Plots of Response Surface Regression of CAC-Lime Combinations: Compressive Strength (MPa) versus time (hr); Lime ratio (%); Temperature (°C)



APPENDIX D

STATISTICAL ANALYSIS OF CAC-GGBFS MIXES

Table D.1 Response Surface Regression of CAC-GGBFS Combinations: Compressive Strength (MPa) versus time (hr); GGBFS ratio (%); Temperature (°C)

The analysis was done using uncoded units.

Estimated Regression Coefficients for C.Strength (MPa)

Term	Coef	SE Coef	T	P
Constant	73,1339	9,26229	7,896	0,000
time (hr)	0,0159	0,00162	9,807	0,000
GGBFS ratio (%)	-0,4175	0,09325	-4,477	0,000
Temp (oC)	-1,9296	0,51156	-3,772	0,000
time (hr)*time (hr)	-0,0000	0,00000	-8,455	0,000
Temp (oC)*Temp (oC)	0,0170	0,00700	2,431	0,016
time (hr)*GGBFS ratio (%)	0,0001	0,00002	5,246	0,000
GGBFS ratio (%)*Temp (oC)	0,0065	0,00233	2,798	0,005

S = 13,33 R-Sq = 56,2% R-Sq(adj) = 55,4%

Analysis of Variance for C.Strength (MPa)

Source	DF	Seq SS	Adj SS	Adj MS	F	P
Regression	7	88137	88136,6	12590,94	70,88	0,000
Linear	3	69756	23804,7	7934,90	44,67	0,000
Square	2	12884	12884,2	6442,10	36,26	0,000
Interaction	2	5496	5496,1	2748,07	15,47	0,000
Residual Error	387	68749	68748,7	177,65		
Total	394	156885				

Figure D.1 Contour and Surface Plots of Response Surface Regression of CAC-GGBFS Combinations: Compressive Strength (MPa) versus time (hr); GGBFS ratio (%); Temperature (°C)

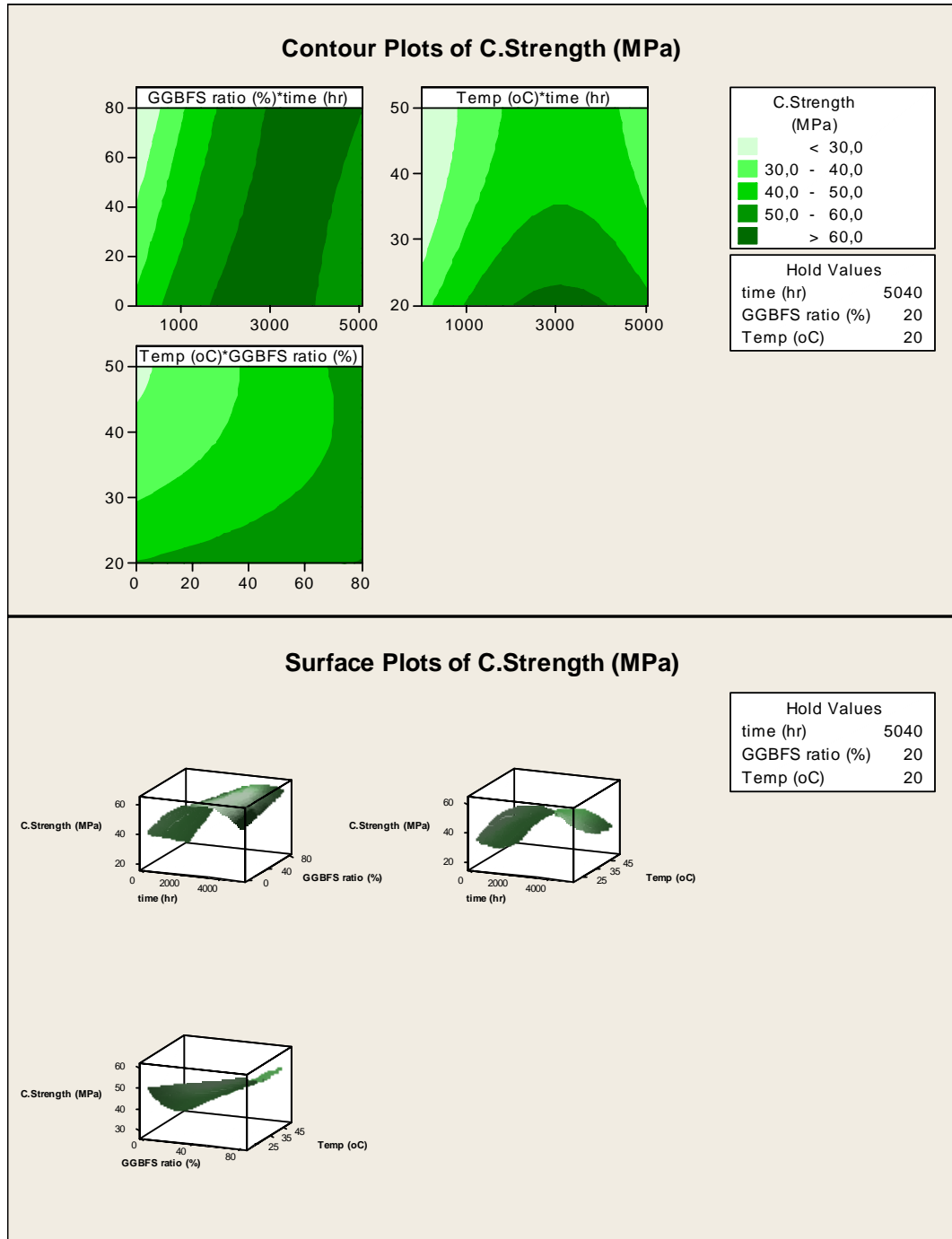


Table D.2 Response Surface Regression of CAC-GGBFS Combinations: C₃AH₆ (unit) versus time (hr); GGBFS ratio (%); Temperature (°C)

The analysis was done using uncoded units.

Estimated Regression Coefficients for C₃AH₆ (unit)

Term	Coef	SE Coef	T	P
Constant	-250,736	338,706	-0,740	0,465
time (hr)	0,212	0,091	2,339	0,027
GGBFS ratio (%)	-24,457	2,557	-9,565	0,000
Temp (oC)	56,850	8,955	6,349	0,000
time (hr)*Temp (oC)	-0,005	0,002	-2,211	0,035

S = 344,3 R-Sq = 84,1% R-Sq(adj) = 81,9%

Analysis of Variance for C₃AH₆ (unit)

Source	DF	Seq SS	Adj SS	Adj MS	F	P
Regression	4	17589945	17589945	4397486	37,10	0,000
Linear	3	17010390	17019016	5673005	47,86	0,000
Interaction	1	579555	579555	579555	4,89	0,035
Residual Error	28	3318682	3318682	118524		
Total	32	20908627				

Table D.3 Response Surface Regression of CAC-GGBFS Combinations: AH₃ (unit) versus time (hr); GGBFS ratio (%); Temperature (°C)

The analysis was done using uncoded units.

Estimated Regression Coefficients for AH₃ (unit)

Term	Coef	SE Coef	T	P
Constant	-113,056	103,973	-1,087	0,287
time (hr)	0,056	0,014	4,088	0,000
GGBFS ratio (%)	-8,756	3,080	-2,843	0,009
Temp (oC)	15,938	2,642	6,032	0,000
GGBFS ratio (%)*GGBFS ratio (%)	0,179	0,037	4,804	0,000
time (hr)*GGBFS ratio (%)	-0,001	0,000	-3,573	0,001
GGBFS ratio (%)*Temp (oC)	-0,218	0,068	-3,227	0,003

S = 101,5 R-Sq = 89,2% R-Sq(adj) = 86,7%

Analysis of Variance for AH₃ (unit)

Source	DF	Seq SS	Adj SS	Adj MS	F	P
Regression	6	2219407	2219407	369901	35,89	0,000
Linear	3	1835202	1239844	413281	40,10	0,000
Square	1	121193	237838	237838	23,08	0,000
Interaction	2	263012	263012	131506	12,76	0,000
Residual Error	26	267951	267951	10306		
Total	32	2487358				

Table D.4 Response Surface Regression of CAC-GGBFS Combinations: CAH₁₀ (unit) versus time (hr); GGBFS ratio (%); Temperature (°C)

The analysis was done using uncoded units.

Estimated Regression Coefficients for CAH₁₀ (unit)

Term	Coef	SE Coef	T	P
Constant	539,343	94,2911	5,720	0,000
GGBFS ratio (%)	-4,001	1,0941	-3,657	0,001
Temp (oC)	-23,748	5,5043	-4,315	0,000
Temp (oC)*Temp (oC)	0,255	0,0775	3,290	0,003
GGBFS ratio (%)*Temp (oC)	0,089	0,0283	3,135	0,004

S = 44,27 R-Sq = 62,5% R-Sq(adj) = 57,1%

Analysis of Variance for CAH₁₀ (unit)

Source	DF	Seq SS	Adj SS	Adj MS	F	P
Regression	4	91334	91334	22833	11,65	0,000
Linear	2	47946	56604	28302	14,44	0,000
Square	1	24130	21216	21216	10,82	0,003
Interaction	1	19257	19257	19257	9,83	0,004
Residual Error	28	54878	54878	1960		
Lack-of-Fit	12	19975	19975	1665	0,76	0,678
Pure Error	16	34903	34903	2181		
Total	32	146212				

Table D.5 Response Surface Regression of CAC-GGBFS Combinations: C₂ASH₈ (unit) versus time (hr); GGBFS ratio (%); Temperature (°C)

The analysis was done using uncoded units.

Estimated Regression Coefficients for C₂ASH₈ (unit)

Term	Coef	SE Coef	T	P
Constant	-2582,49	908,230	-2,843	0,009
time (hr)	0,25	0,113	2,223	0,036
GGBFS ratio (%)	33,97	10,478	3,243	0,003
Temp (oC)	136,47	50,798	2,687	0,013
Temp (oC)*Temp (oC)	-1,65	0,708	-2,323	0,029
time (hr)*GGBFS ratio (%)	0,00	0,001	2,250	0,034
time (hr)*Temp (oC)	-0,01	0,003	-2,535	0,018
GGBFS ratio (%)*Temp (oC)	-0,58	0,263	-2,192	0,038

S = 404,3 R-Sq = 77,8% R-Sq(adj) = 71,6%

Analysis of Variance for C₂ASH₈ (unit)

Source	DF	Seq SS	Adj SS	Adj MS	F	P
Regression	7	14343662	14343662	2049095	12,54	0,000
Linear	3	10851934	3224202	1074734	6,58	0,002
Square	1	974260	881829	881829	5,39	0,029
Interaction	3	2517468	2517468	839156	5,13	0,007
Residual Error	25	4086334	4086334	163453		
Total	32	18429997				

Figure D.2 Contour and Surface Plots of Response Surface Regression of CAC-GGBFS Combinations: Katoite ($=C_3AH_6$) (unit) versus time (hr); GGBFS ratio (%); Temperature ($^{\circ}C$)

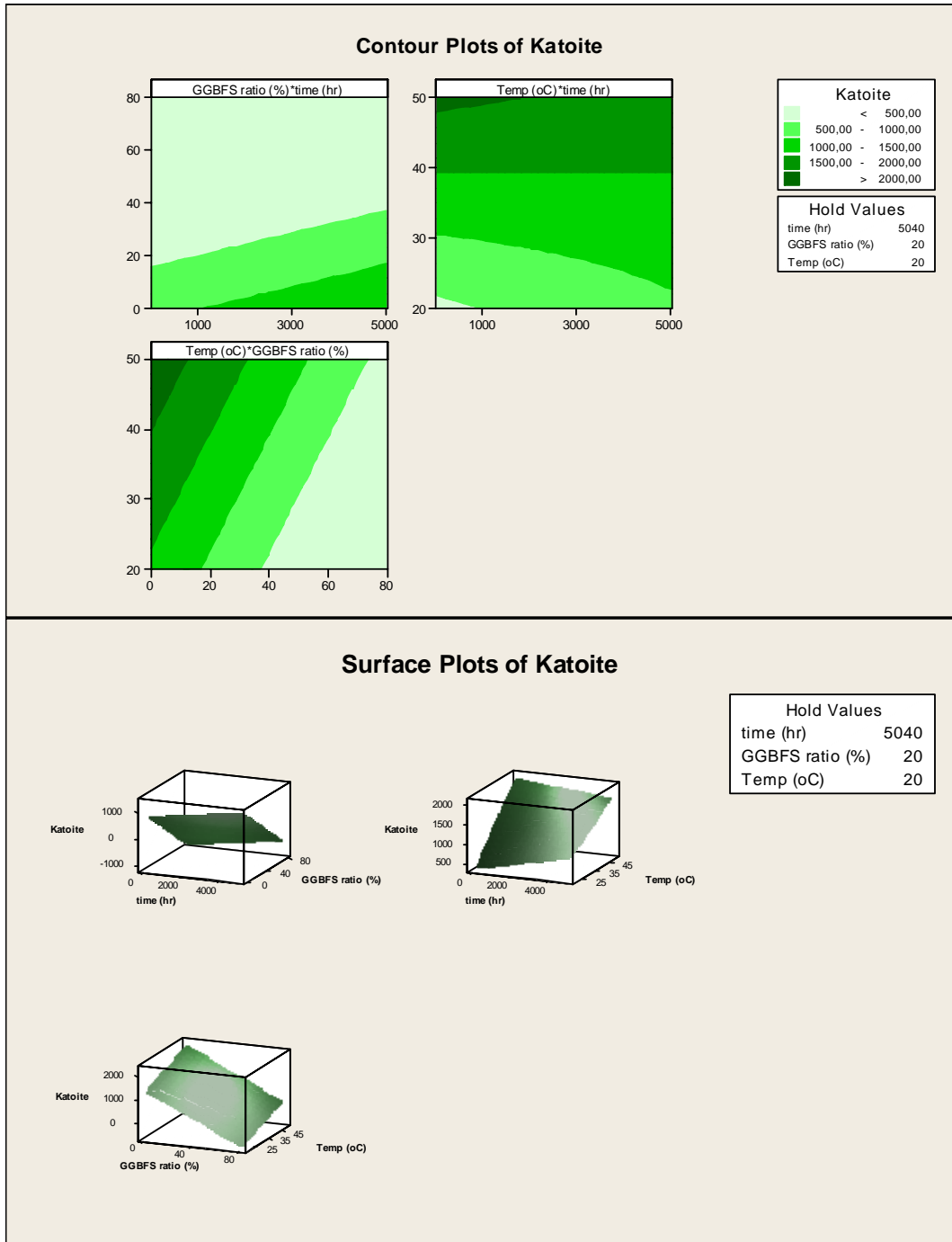


Figure D.3 Contour and Surface Plots of Response Surface Regression of CAC-GGBFS Combinations: AH_3 (unit) versus time (hr); GGBFS ratio (%); Temperature ($^{\circ}C$)

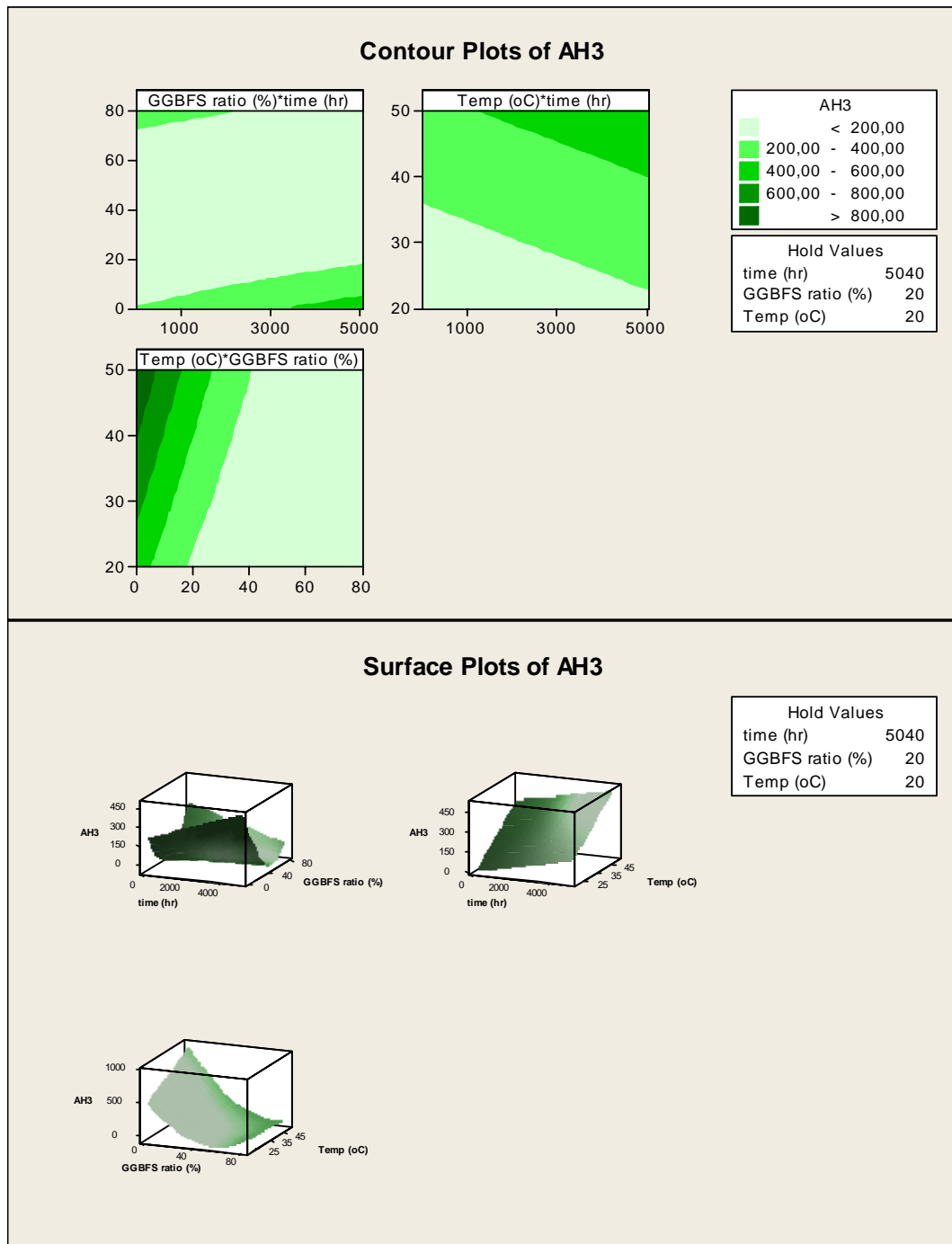


Figure D.4 Contour and Surface Plots of Response Surface Regression of CAC-GGBFS Combinations: CAH₁₀ (unit) versus GGBFS ratio (%); Temperature (°C)

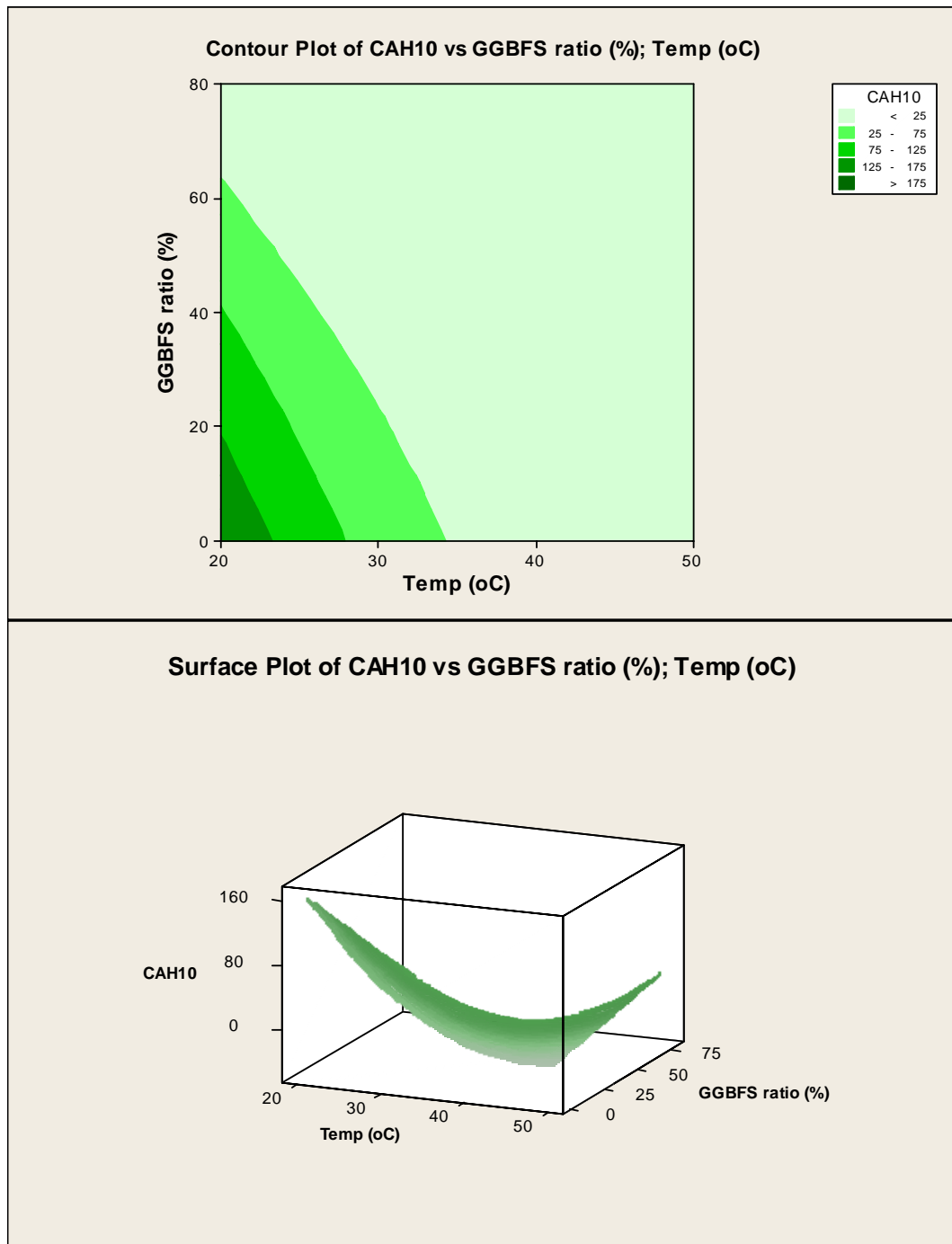
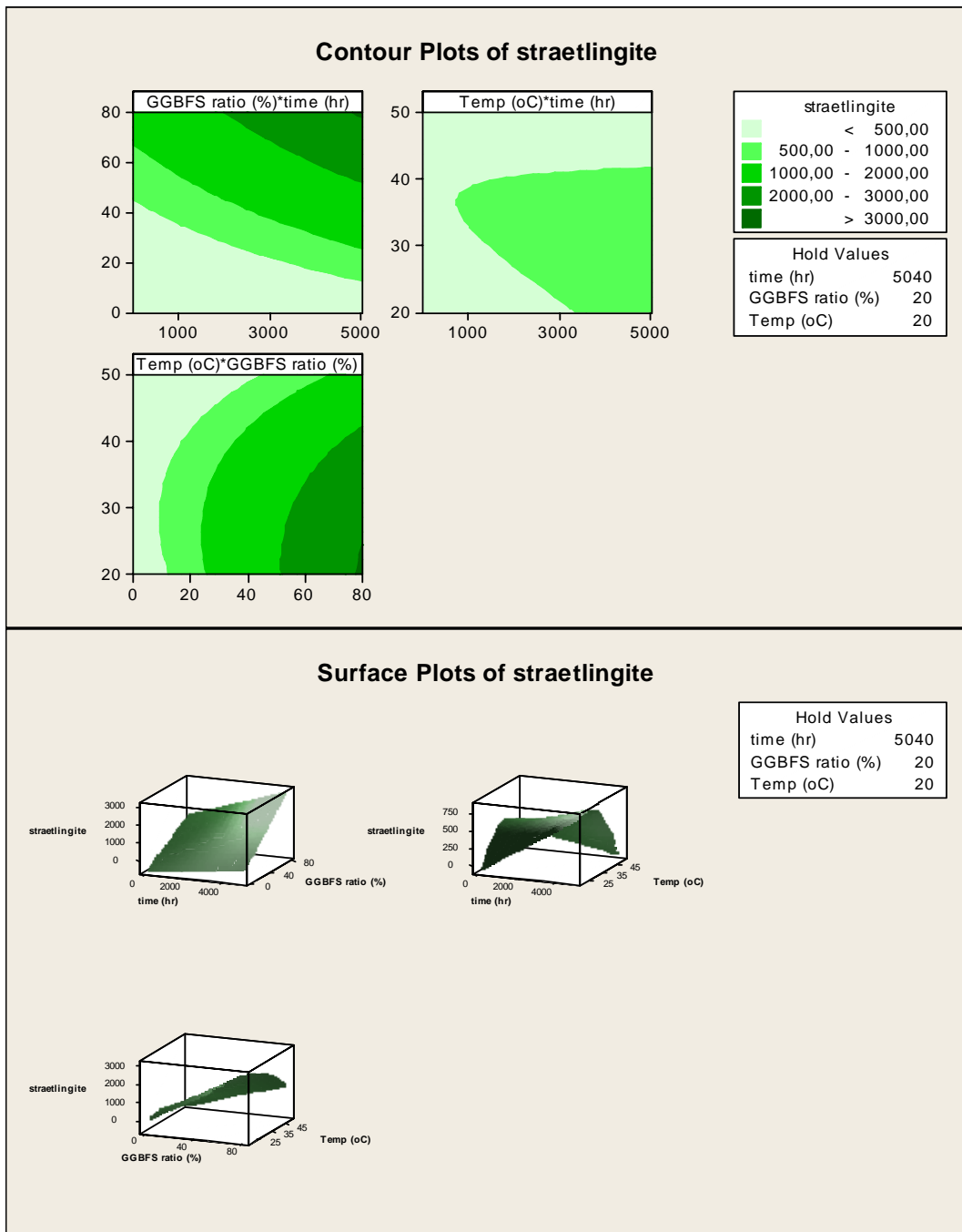


Figure D.5 Contour and Surface Plots of Response Surface Regression of CAC-GGBFS Combinations: Straetlingite (=C₂ASH₈) (unit) versus GGBFS ratio (%); Temperature (°C)



CURRICULUM VITAE

PERSONAL INFORMATION

Surname, Name: Kırca, Önder
Nationality: Turkish (TR)
Date and Place of Birth: 4th of March 1975, Erzurum
Marital Status: Married
Phone: +90 324 454 00 60
Fax: +90 324 454 00 75
e-mail: o.kirca@cimsa.com.tr

EDUCATION

Degree	Institution	Year of Graduation
MS	METU Civil Engineering	2000
BS	METU Civil Engineering	1998
High School	Ankara Anadolu High School, Ankara	1993

TEACHING EXPERIENCE

Year	Place	Enrolment
2003- Present	Mersin University - Department of Architecture	Part-time Lecturer
1998-2000	METU Department of Civil Engineering	Research Assistant

WORK EXPERIENCE

Year	Place	Enrolment
2002- Present	Çimsa Cement Production and Trade Company	R&D Assistant Manager
2000-2002	Çimsa Cement Production and Trade Company	Research Engineer

FOREIGN LANGUAGES

Advanced English, Fluent German

PUBLICATIONS

1. Kırca, Ö., Şahin, M., "Hazır Beyaz Beton ve Uygulamaları", *THBB Hazır Beton Dergisi*, No 73, sayfa 46-50, Ocak-Şubat 2006.
2. Kırca, Ö., Şahin, M., Erdem T.K., "Beyaz Portland Çimentosu, Metakaolen ve Öğütülmüş Pomzanın Yüksek Dayanımlı Betonda Beraber Kullanımı", *6. Ulusal Beton Kongresi: Yüksek Performanslı Betonlar Bildiri Kitabı*, pp. 219-227, İstanbul, 16-18 November 2005.
3. Kırca, Ö., Şahin, M., "Kalsiyum Alüminatlı Çimento Klinkerinin Refrakter Agregası Olarak Kullanımı", *12. Uluslararası Metalurji-Malzeme Kongresi Bildiriler Kitabı*, 28 September-02 October 2005.
4. Kırca, Ö., Şahin, M., "Kalsiyum Alüminatlı Çimentoların Refrakterlik Özellikleri", *12. Uluslararası Metalurji-Malzeme Kongresi Bildiriler Kitabı*, 28 September-02 October 2005.
5. Kırca, Ö., Şahin, M., "The Use of White Cement in Architecture", *22nd World Congress of Architecture: UIA 2005*, İstanbul, 3-7 July 2005. (poster)
6. Kırca, Ö., Şahin, M., "Beton Prefabrikasyonunda Beyaz Çimentonun Yeri", *11. Beton Prefabrikasyon Sempozyumu*, Türkiye Prefabrik Birliği, İzmir, 20 November 2004.
7. Kırca, Ö., "Ancient Binding Materials, Mortars and Concrete Technology: History and Durability Aspects", *Proceedings of 4th International Seminar on Structural Analysis of Historical Constructions*, Vol.1, pp. 87-94, Padova-Italy, 10-13 November 2004.
8. Kırca, Ö., Erdem T.K., "An Experimental Study on the Construction Materials of the Ankara Citadel", *Proceedings of 4th International Seminar on Structural Analysis of Historical Constructions*, Vol.1, pp. 223-229, Padova-Italy, 10-13 November 2004.
9. Kırca, Ö., Şahin, M., Erdem T.K., "Corrosion Resistance of White Portland Cement: The Effects of Pozzolanic Admixtures", *Proceedings of 9th International Corrosion Symposium*, pp. 432-440, Ankara, 22-24 September 2004.
10. Kırca, Ö., Erdem T.K., "Durability of High Performance Concrete", *Proceedings of 9th International Corrosion Symposium*, pp. 256-263, Ankara, 22-24 September 2004.

11. Kırca, Ö., Şahin, M., "Hazır Beyaz Beton ve Uygulamaları", *Beton 2004 Kongresi Bildiriler Kitabı*, pp. 554-563, İstanbul, 10-12 June 2004.
12. Şahin, M., Türkyener, C., Kırca, Ö., "Tamir Harçlarında Kalsiyum Alüminatlı Çimento Kullanımı", *Yapı Malzemeleri Kurultayı*, İstanbul, 8-9 December 2003.
13. Kırca, Ö., Şahin, M., "Polipropilen Lif Kullanımının Beyaz Beton Dayanıklılığına Etkisi", *İnşaat Mühendisleri Odası 5. Ulusal Beton Kongresi Bildiriler Kitabı*, pp. 375-382, İstanbul, 1-3 October 2003.
14. Şahin, M., Kırca, Ö., "The Use of White Cement in City Furniture, *2nd International City Furniture Symposium*, İstanbul, 24-26 April 2003.
15. Kırca, Ö., Şahin, M., Erdem T.K., "Erken Yaşlarda Betonun Basınç Dayanımındaki Gelişim", *Türkiye Prefabrik Birliği Beton Prefabrikasyon Dergisi*, No. 65-66, pp 5-10, 2003.
16. Kırca, Ö., Şahin, M., Erdem T.K., "Compressive Strength Development of Concrete at Early Ages", *Proceedings of 5th International Congress on Advances in Civil Engineering*, Vol.2, pp. 835-844, İstanbul, 25-27 September 2002.
17. Kırca, Ö., Şahin, M., "Effects of Water-Reducing and Set-Retarding Admixtures on Slump Loss of White Portland Cement Concrete", *Proceedings of 5th International Congress on Advances in Civil Engineering*, Vol.2, pp. 855-864, İstanbul, 25-27 September 2002.
18. Kırca, Ö., Turanlı L., Erdoğan, T.Y., "Effects of Retempering on Consistency and Compressive Strength of Concrete Subjected to Prolonged Mixing", *Cement and Concrete Research*, Vol. 32, pp. 441-445, 2002.
19. Kırca, Ö., Erdem, T.K., Uslu, H.B., Bakırcı, Ö., "Estimation of the In-Situ Mechanical Properties of the Construction Materials in a Medieval Anatolian Building, Sahip Ata Hanikah in Konya", *Proceedings of 2nd International Congress on Studies in Ancient Structure*, Vol. 2, pp. 691-701, İstanbul, 5-9 July 2001.
20. Erdoğan, T.Y., Turanlı L., Kırca, Ö., "Effects of Prolonged Mixing and Delivery Time on Slump Loss of Ready-Mixed Concrete and on Strength of Retempered Concrete", *Proceedings of 4th International Congress on Advances in Civil Engineering*, Vol. 4, pp. 1569-1575, Gazi Magosa, 1-3 November 2000.
21. Kırca, Ö., "Effects of Prolonged Mixing and Retempering on Properties of Ready-Mixed Concrete", M.Sc. Thesis, METU, Ankara, August 2000.